CHALMERS

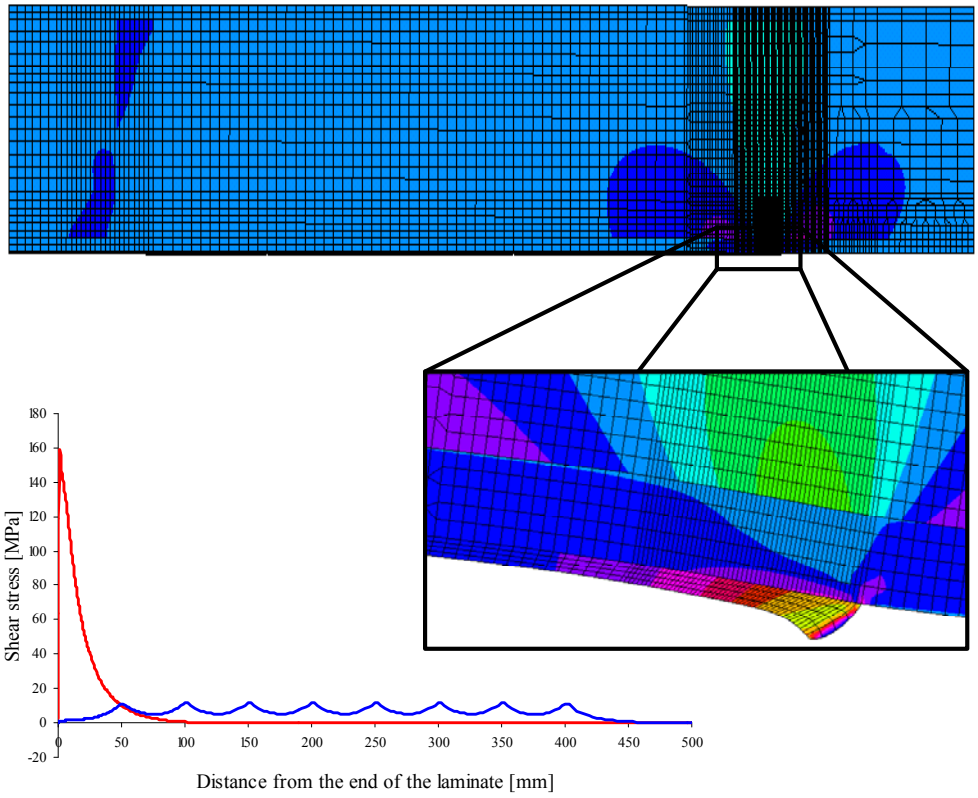

Strengthening of steel structures with bonded prestressed laminates

Numerical analyses of alternative techniques for reducing the interfacial stresses

Master's Thesis in the International Master's Programme Structural Engineering

ANNA BJÖRKLUND

JOAKIM HÖGLIND

Department of Civil and Environmental Engineering
Division of Structural Engineering
Steel and Timber Structures
CHALMERS UNIVERSITY OF TECHNOLOGY
Göteborg, Sweden 2007
Master's Thesis 2007:80

MASTER'S THESIS 2007:80

Strengthening of steel structures with bonded prestressed laminates

Numerical analyses of alternative techniques for reducing the interfacial stresses

Master's Thesis in the *International Master's Programme Structural Engineering*

ANNA BJÖRKLUND

JOAKIM HÖGLIND

Department of Civil and Environmental Engineering
Division of Structural Engineering
Steel and Timber Structures
CHALMERS UNIVERSITY OF TECHNOLOGY
Göteborg, Sweden 2007

Strengthening of steel structures with bonded prestressed lamiantes
Numerical analyses of alternative techniques for reducing the interfacial stresses
Master's Thesis in the *International Master's Programme Structural Engineering*
ANNA BJÖRKLUND
JOAKIM HÖGLIND

Master's Thesis 2007:80
Department of Civil and Environmental Engineering
Division of Structural Engineering
Steel and Timber Structures
Chalmers University of Technology
SE-412 96 Göteborg
Sweden
Telephone: + 46 (0)31-772 10 00

Cover:
Finite Element model of a steel beam strengthened with bonded prestressed laminate

Chalmers Reproservice / Department of Civil and Environmental Engineering
Göteborg, Sweden 2007

Strengthening of steel structures with bonded prestressed lamiantes
Numerical analyses of alternative techniques for reducing the interfacial stresses
Master's Thesis in the *International Master's Programme Structural Engineering*
ANNA BJÖRKLUND
JOAKIM HÖGLIND
Department of Civil and Environmental Engineering
Division of Structural Engineering
Steel and Timber Structures
Chalmers University of Technology

ABSTRACT

Many existing steel structures have insufficient load bearing capacity. This is due to a number of reasons such as corrosion, aging, and deficient structural design. Therefore, there is an increased interest of using CFRP (Carbon Fibre Reinforced Polymers) to strengthening existing steel structures. CFRP-laminate offers a variety of advantages such as high strength to weight ratio, resistance to corrosion, and unlimited delivery lengths. By prestressing the laminate the high strength of the CFRP can be utilized better and the behaviour of the structure is improved in the elastic state. However, if the laminate is prestressed and attached to the steel structure by adhesive bond, high stresses will appear in the adhesive at the ends of the laminate. These stresses may exceed the strength of the adhesive and cause premature failure. Hence, by investigating the effect of different parameters and introduce new methods to lower the interfacial stresses a smart bonding can be achieved. Different parameters and techniques have been investigated by using finite element analyses.

A steel beam was modelled and used to investigate the effect of different parameters and techniques. The model was verified by comparing the results with simplified analytical solutions. The parameters that were investigated were; the level of prestressing, external loading, elastic modulus of adhesive and laminate, and the effects of elastic-plastic behaviour of the adhesive. The techniques analysed were leaving the ends of the laminate unprestressed, step-releasing and gradual prestressing, and different tapers at the ends of the laminate.

In conclusion, the results show that the elastic modulus of the laminate and the adhesive have a large effect on the interfacial stresses. When it comes to different techniques, the results were somewhat surprising. As long as the taper in thickness is shorter than approximately 7 times the thickness the peeling stresses will increase. No decrease of interfacial stresses was observed for tapering in width. What, on the other hand, showed excellent results were leaving the end unprestressed and also step releasing and gradual prestressing. Step releasing and gradual prestressing reduced the maximum shear stress from 165 MPa to 1.2 MPa and the maximum peeling stress from 159 MPa to 12 MPa. Further studies are needed to find a way to take care of the high interfacial stresses in provisional anchorage and prestressing device.

Key words: FE-analysis, CFRP, Laminate, Prestressing, Pre-stress, Interfacial stress, Shear stress, Peel stress, Normal stress, Steel, Beam, Structure, Anchorage, Bond, Adhesive, Strengthening, Taper.

Förstärkning av stålkonstruktioner med pålimmade förspända laminat

Numeriska analyser av metoder för reducering av spänningarna i limmet
Examensarbete inom Konstruktion och mekanik
ANNA BJÖRKLUND
JOAKIM HÖGLIND
Institutionen för bygg- och miljöteknik
Avdelningen för Konstruktionsteknik
Stål- och träbyggnad
Chalmers tekniska högskola

SAMMANFATTNING

Många befintliga stålkonstruktioner behöver förstärkas eller repareras. Detta beror på en rad olika faktorer som tillexempel korrosion, utmattning och dålig detaljutformning. Det finns därför ett ökat intresse att använda CFRP (kolfiberarmerade polymerer) till att förstärka stålkonstruktioner. CFRP-laminat erbjuder en rad fördelar så som hög hållfasthet, låg vikt och resistans mot korrosion och de kan levereras i obegränsade längder. Om laminaten förspänns innan de limmas på, så utnyttjas kolfiberlaminaten bättre och stålkonstruktionen får ett bättre beteende i brukgränstillstånd. Detta kommer dock att medföra att höga spänningar uppkommer i limmet vid ändarna av laminatet. Dessa spänningar kan komma att överskrida limmets styrka vilket kan medföra att brott uppträder tidigare än beräknat. Genom att undersöka olika parametrar och införa nya tekniker för att minska spänningarna i limfogen så kan en smartare fastsättning av laminat åstadkommas.

För att analysera effekten av de olika parametrarna och teknikerna användes en Finita Element-modell av en stålbalk. De parametrar som analyserades var storleken av förspänningskraften, påverkan av yttre last, limmets och laminatets elasticitetsmodul samt limmets elastiskt-plastiska beteende. De tekniker som analyserades var: att lämna ändan av att laminatet oförspänt, släppa förspänningskraften stegvis och att förspänna stegvis. Dessutom undersöktes olika geometrier vid laminatändan.

Resultaten visade att elasticitetsmodulerna för limmet och laminatet påverkar spänningarna i limmet avsevärt. När det gäller olika geometrier så var resultatet något förvånande. Minskning av laminatets tjocklek vid ändan av laminatet visade att normalspänningarna i limmet ökade och att ändringen av tjockleken måste göras över en sträcka längre än ungefär 7 gånger den ursprungliga tjockleken för att normalspänningarna skall minska. När det gäller att minska bredden av laminatet mot slutet kunde ingen positiv effekt erhållas. Vad som visade utmärkta resultat var att lämna ändan av laminatet oförspänt, släppa förspänningskraften stegvis och att förspänna stegvis. Att släppa förspänningskraften stegvis eller förspänna stegvis minskade de maximala skjuvspänningarna i laminatet från 159 MPa till 12 MPa och de maximala normalspänningarna från 165 MPa till 1,2 MPa. Fortsatta studier är nödvändiga för att minska de höga spänningar som uppkommer i de tillfälliga anordningar som behövs vid användningen av ovanstående förspänningstekniker.

Nyckelord: FE-analys, CFRP, Laminat, Förspänning, Skjuvspänningar, Normalspänningar, Stål, Balk, Konstruktion, Förankring, Limfog, Lim, Fasning.

Contents

Preface

In this Master's project the interfacial stresses in steel structures strengthened with laminate were studied. The study took place during the months of September 2006 through February 2007. The project was done within the International Master's programme in Structural Engineering at the department of Civil and Environmental Engineering, Structural Engineering – Steel and Timber Structures at Chalmers University of Technology in Gothenburg, Sweden.

First of all we would like to extend our greatest thanks to our supervisor and examiner of this Master's Thesis Assistant Professor Mohammad Al-Emrani for all the support and valuable discussions during this study. We would also like to express our thanks to the Ph.D student M.Sc. Reza Haghani Dogaheh and Lic. Eng. Dag Linghoff who have contributed to our project by sharing their knowledge and for being available for first-class discussions. Furthermore, we would also like to thank our opponents of this Mater's Thesis Amjad Hussain Mohammed and Arshad Abosh for their comments and ideas. Last but not least, many thanks to our families and friends for all the support and understanding.

Göteborg, February 2007

Anna Björklund & Joakim Höglind

Notations

Roman upper case letters

A_l	Cross-sectional area of laminate
A_s	Cross-sectional area of steel beam
C_1	Constant
C_2	Constant
E_l	Elastic modulus of laminate
E_s	Elastic modulus of steel beam
F	Prestressing force introduced to beam
F_l	Axial force in laminate
G_a	Shear modulus of adhesive
I_s	Moment of inertia of steel section
I_{eff}	Effective moment of inertia
L	Length of laminate
L_P	Distance between the concentrated load and the support
M_l	Moment due to loading
M_s	Bending moment in beam due to prestressing
$M_{yielding}$	Yielding moment
P	Load
P_0	Initial prestressing force in laminate
P_l	Prestressing force in laminate after bonding and releasing
P_s	Axial force in beam due to prestressing
ΔT	Temperature load

Roman lower case letters

b_l	Width of laminate
b_a	Width of adhesive
b_f	Width of flange
e	Distance from gravity centre of beam section to centre of laminate
h	Height of beam
h_w	Height of web
t_a	Thickness of adhesive layer
t_f	Thickness of flange
t_l	Thickness of laminate
t_{end}	Thickness of the end of laminate
$y_{G.C}$	Distance from gravity centre
$y_{G.C,uf}$	Distance between gravity centre and to outmost fibre in upper flange

$y_{N.A}$	Distance from neutral axis
$y_{N.A,uf}$	Distance between gravity centre and outmost fibre in upper flange

Greek lower case letters

α	Thermal expansion coefficient
δ_l	Displacement of laminate
δ_s	Displacement of steel
ε_0	Initial strain
ε_l	Strain in laminate
ε_s	Strain in steel
σ_F	Stresses in cross-section due to prestressing
σ_M	Stresses in cross-section due to moment caused by prestressing
σ_{M_l}	Stresses in cross-section due to loading
σ_0	Initial stress
$\sigma_{yielding}$	Yielding stress of stel
τ	Shear stress
υ	Poisson's ratio
ω	Constant

1 Introduction

1.1 Background

In a modern society, it is of great importance to have a well organised and widely spread infrastructure. As a part of this process, structural engineers have designed millions of bridges around the world throughout the years. Unfortunately, many of these bridges do not have sufficient load bearing capacity and serviceability. In the USA alone, 122 000 out of their 615 000 bridges need some kind of improvement. Europe has a large number of old bridges as well, of which up to 66 % are 50 years or older. At the same time, new bridges are planned to improve the existing infrastructure [7] [8].

The need for strengthening and repair is not only a result of aging and insufficient structural design. The loads applied to many of the bridges have changed during the years. More traffic and heavier vehicles increase the magnitude and the intensity of the applied load. At the same time there is an increased use of de-icing salt, which in combination with poor maintenance enhances the risk of corrosion and decreases the strength of the bridges [2].

When a structure cannot be restored by maintenance and local repair, it must be strengthened or replaced. It is often more advantageous to strengthen a structure due to the fact that strengthening is, in most cases, less expensive than replacement. Strengthening would be especially favourable if the method used is fast, effective, and simple. For some structures, such as bridges of historical importance, replacement is not an alternative [6].

The traditional strengthening method of adding steel plates to the tensioned part of the structure has proven to be a good technique. By bolting or welding steel plates to the existing structure, the moment of inertia of the cross-section increases. However, this method has several disadvantages, such as the risk of corrosion, fatigue, and difficulties related to the material properties [2] [6]. A more effective way of strengthening, without greater influence on the traffic flow and without adding a heavy dead load to the structure, is to use Carbon Fibre Reinforced Polymer, CFRP [10] [18]. CFRP has low density, excellent mechanical properties and is resistant to corrosion. It also has high strength-to-weight ratio, high stiffness-to weight ratio and good fatigue and creep properties [1].

If the laminates are prestressed before they are bonded by adhesive to a structure, both the properties of the CFRP and the cross-section of the strengthened structure will be better utilized. However, there are some problems related to prestressing, such as the high shear and peeling stresses that appear in the adhesive at the zones closest to the ends of the laminates [7].

In this thesis, several techniques for reducing the interfacial stresses at the ends of prestressed laminates will be investigated. Some of these techniques have been suggested before, but need to be studied in more detail, others are new and are treated for the first time.

1.2 Aim and objective

Earlier studies have shown that beams strengthened with CFRP will mainly increase the ultimate load bearing capacity. In order to increase the load for which the beam starts yielding, and in order to utilize the maximum strength of the CFRP-laminate, the laminate can be prestressed before bonding to the steel beam. Strengthening structures using CFRP-laminates is a fast and sufficient method. The problem encountered by prestressing is the high interfacial stresses that appear at the end of the laminate.

The aim of this project is to numerically analyse parameters and techniques that influence the interfacial stresses that appears in the adhesive at the end of prestressed laminates bonded to steel structures. The result should be a base for further research within the area.

The main objective of this project was to study a steel beam strengthen with prestressed CFRP. The beam is a 2 meter long and has a HEA-180 cross-section.

1.3 Limitations

The analyses regarding interfacial stresses will be carried out for a simply-supported beam strengthened with a prestressed laminate bonded to the tension flange.

The study is mainly limited to the investigation of shear and peeling stresses at the ends of prestressed laminates bonded to strengthened steel beams. Numerical analysis using the Finite Element method is used in the study and only the interfacial stresses in the middle of the adhesive at the end of the laminate are analysed.

1.4 Method/Scientific approach

The first step was to conduct a literature study in order to find out what has been previously studied concerning structures prestressed with CFRP-laminates. The second step was to find parameters and techniques that can be used to reduce the high interfacial stresses. Different methods were discussed and promising alternatives were chosen. Finally, the parameters and techniques were numerically analysed. To determine the credibility of the results from the numerical analyses, the same model was analysed analytically to confirm the results of the numerical analysis.

1.4.1 Literature study

The first part of the project is a literature study. During this part, earlier research and practical applications were studied.

An extensive literature study was performed to gather information about the strengthening technique. Relevant information is considered not only from the field of

steel structures strengthened with prestressed CFRP-laminates, but also from other fields such as strengthening of concrete structures and strengthening of steel structures with unprestressed laminates.

The material has been collected from data bases on the Internet, the Department of Civil and Environmental Engineering's library, Chalmers Library, and personal collections.

1.4.2 Reflection

The next step was to come up with ideas on how the interfacial stresses could be decreased. Different parameters and techniques were discussed and analysed. Different methods were discussed and promising alternatives were chosen.

1.4.3 Analysis tools

The last step was to create a FE-model and analyse the influence of different parameters and techniques that were chosen earlier. Many different software tools were used in this master thesis. For FE-analysis I-deas and Abaqus were used. I-deas was used, both as a modelling tool and as a solving tool. Abaqus was only used as a solving tool. When Abaqus was used, the model was created in I-deas. Microsoft Office Excel was used to organize information from the numerical analyses. Microsoft Office Excel was also used to illustrate the results graphically. To write the master thesis Microsoft Office Word was used. To create illustrations AutoCAD and Microsoft Office Visio were used.

1.5 Structure of the report/Outline

Chapter 2 and Chapter 3 are related to the literature study. In Chapter 2 the different materials used in the strengthening technique are presented and the behaviour of a prestressed steel beam is explained. Also theory of interfacial stresses is discussed in Chapter 2. In Chapter 3 earlier executed laboratory tests and field applications are presented.

With help of Chapter 2, Chapter 3, and analytically analyses, different parameters and techniques were discussed. In Chapter 4, promising parameters, and techniques are studied in more detail.

In Chapter 5 the structural model is presented and in Chapter 6 the FE-model is presented.

In Chapter 7 the results from numerical analyses are presented. The first step was to analyse how laminates with different modulus of elasticity influence the global behaviour of the beam. This was investigated for both unprestressed and prestressed laminates. The next step was the analysis of different parameters to reduce the high

shear and peeling stresses. Finally, analyses of alternative techniques were analysed with the purpose of reducing the high interfacial stresses.

In Chapter 8 a summery of the results and suggestions on field applications are presented.

Finally, in Chapter 9, conclusions and suggestions on further research are presented.

2 CFRP-Strengthened Structures

Today, CFRP strengthened bridges are more common for concrete structures than for steel structures. This is due to the fact that steel structures have a different and a more difficult set of problems. One of the problems is the risk of instability. Another is the high strength and stiffness of steel, which makes it more difficult to strengthen, especially since the CFRP, used in civil engineering, has a lower modulus of elasticity than the CFRP used in other sectors. This implies that for a given allowable strain the CFRP will work at a lower stress than steel and the substantial load transfer can only take place after the steel has started to yield. However, if the CFRP is strengthened an improved behaviour can be obtaine. Finally, the bond between the CFRP and the steel, which is often the weakest link, will in many cases control the mode of failure [9].

Because of the fact that strengthening by using CFRP is widely used in concrete structures makes it interesting to study applications in this field and try to apply the knowledge on steel structures.

2.1 Materials

To understand the behaviour of a structure strengthened with prestressed CFRP-laminates, the materials included in the strengthening system need to be studied.

2.1.1 Carbon fibre reinforced polymer, CFRP

Fibre reinforced polymer, FRP, is a composite material, which consists of two or more constituent materials with significantly different physical and chemical properties. However, the materials remain separate and distinct within the composite. The properties of the resulting composite material have combined characteristics of the constituent materials. Moreover, the mechanical and material properties of the composite material are superior the constituent materials separately [3].

The materials in a fibre-reinforced polymer are divided into two groups: the reinforcement and the matrix. Reinforcement is harder and stronger, and the matrix works as a protective layer that holds the reinforcement together and transfers forces between them [3].

Some examples of reinforcements are E-glass, Carbon, and Aramid, which all have a relatively high modulus of elasticity and high strength, see Table 2.1. In civil engineering carbon fibre is the dominating reinforcement, even though glass fibres have been used in some applications [3] [4].

Table 2.1 Material parameters of E-glass, Carbon, and Aramid [5].

	Carbon fibre			Aramid fibre	E-glass fibre
	High strength (HS)	High modulus (HM)	Ultra-high modulus (UHM)		
Modulus of elasticity [Gpa]	230-240	295-390	440-640	125-130	70-85
Strength [Mpa]	4300-4900	2740-5940	2600-4020	3200-3600	2460-2580
Strain to failure [%]	1.9-2.1	0.7-1.9	0.4-0.8	2.4	3.5
Density [kg/m³]	1800	1730-1810	1910-2120	1390-1470	2600

Carbon fibre is the dominating reinforcement in FRP laminates used in civil engineering because of its good material properties. Carbon fibre has a strong and stable bond at the atom level, is rigid and strong, resistant to many chemical aggressive environments, has low density and is available. However, the material is brittle [1].

There are a number of factors, such as fibre length, amount of fibres, fibre orientation and different materials that contribute to the mechanical performance of the composite [3] [4]. The orientation of the fibres in the composite sheets can be arranged to provide a quasi-isotropic or an anisotropic composite material. If the fibres are arranged with equal proportions in multiple directions, for example 0º, 30º, 45º, 90º, then the material is quasi-isotropic. If the fibres are arranged in the same direction, the material is unidirectional and anisotropic [3].

The matrix can consist of a polymer material such as Epoxy, Polyester, Phenolic, or Polyurethane, see Table 2.2 [5].

Table 2.2 Material parameters of Epoxy, Polyester, Phenolic, and Polyurethane[5].

	Epoxy	Polyester	Phenolic	Polyurethane
Modulus of elasticity [GPa]	2.6-3.8	3.1-4.6	3.0-4.0	0.5
Strength [MPa]	60-85	50-75	60-80	15-25
Strain to failure [%]	1.5-8.0	1.0-2.5	1.0-1.8	10
Poisson's ratio	0.3-0.4	0.35-0.38	not available	0.4
Coefficient of thermal expansion (parallel to fibre) [10^{-6}/ºC]	30-70	30-70	80	40
Density [kg/m³]	1110-1200	1110-1250	1000-1250	1150-1200

The polymer matrix contributes to the composite's transverse strength and modulus and also the shear strength and modulus. Another contribution is the thermal resistance and expansion [4].

Carbon fibres are often combined with the polymer material epoxy as the matrix and is then called carbon fibre reinforced polymer, CFRP. CFRP is resistant to many chemical aggressive environments and corrosion. Furthermore, CFRP has good fatigue and creep properties, high strength-to-weight ratio and high stiffness-to-weight ratio [1].

CFRP-laminates are divided into different grades depending on the manufacturing process, for example high strength (HS), high modulus (HM) and ultra-high modulus (UHM), see Table 2.3 [5].

Table 2.3 Material properties of high strength, high modulus, and ultra-high modulus CFRP-laminates from Sika® Carbodur [6].

	Sika® Carbodur HS	Sika® Carbodur HM	Sika® Carbodur UHM
Strength [MPa]	2800	2400	1300
Modulus of elasticity [GPa]	165	210	300

CFRP is around ten times more expensive than mild steel. However, the cost of materials is often only 20 % of the total cost of a strengthening project and advantages such as the easy handling of the CFRP leads often to a more economical strengthening [1].

2.1.2 Adhesive

The CFRP is applied to the existing structure by using a separate structural adhesive. The adhesive is often applied as a paste to the CFRP and the existing structure. The paste can fill the irregularities on the surface of the substrate much better than other adhesive bonding methods such as film, which is often used in the aerospace sector. If adhesive films are used, a more rigorous surface preparation will usually be required [5].

The same polymers used as matrix in composite materials, se Section 2.1.1 can also be used to bond the CFRP to the existing structure. Two component epoxies are the most common structural adhesives. The pot life for the two component epoxies is 20-45 minutes and the application must therefore be carefully planned and carried out fast [5].

The strength of the adhesive depends on some material factors such as [5]:

- Variation in the thickness of the adhesive
- The extents of voids, disbands and other defects

2.2 Behaviour of externally prestressed beams

Prestressing is a construction technique widely used for bridges and buildings today. The concept of prestressing in structural engineering is to apply a compressive force externally or internally to a structure in order to introduce initial compressive and tensile stresses. The initial stresses are applied before the structure is loaded and counteract the stresses developed by the external load [19].

Strengthening using unprestressed CFRP-laminate will only increase the effective moment of inertia and thereby increase the ultimate load carrying capacity. This will just have a minor effect on the load for which the outmost fibre in the upper flange starts yielding.

By prestressing the CFRP-laminate, the material is used more efficiently, since a greater part of its tensile capacity is used. If a structure is prestressed, the serviceability can be improved and the deflection is reduced. Furthermore, the risk of fatigue failure in steel structures is reduced by inducing compressive stresses at critical details subjected to tensile stress range. In concrete structures, the compressive stresses induced by the prestressing will unload the steel reinforcement, decrease the crack width of existing cracks, and also delay the onset of new cracks [7] [11]. However, the technique with prestressed laminate attached to a steel beam with

adhesive will bring in new factors that have to be taken into account. One of these factors is the high stress concentrations that appear at the end of the laminate.

2.2.1 Behaviour of a prestressed steel beam

When a steel beam is strengthened with prestressed CFRP-laminate the behaviour will be different compared to an unstrengthened beam or a beam strengthened with unprestressed laminates.

In order to introduce a prestressing force into the beam, the CFRP-laminate is elongated and attached to the lower flange of the beam. Due to the elongation, the laminate wants to contract after the prestressing force has been released. The adhesive and the steel beam counteract this deformation, which will result in a compressive prestressing force, F, acting on the steel beam, see Figure 2.1. The force will act with an eccentricity e. e is the distance from the gravity centre of the steel beam to the centre of the laminate.

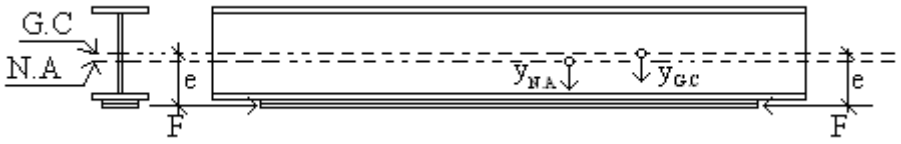

Figure 2.1 Beam with a prestressed laminate bonded to lower flange [19].

The prestressing force, F, will create compressive stresses in the lower flange and tensile stresses in the upper flange, see Figure 2.2. The stress distribution over the cross-section is a combination of two things. The first thing is the force F that will act over the steel area and create compressive stresses over the cross-section, see equation (2.1). The second thing is the moment, M, which is a result of the eccentricity, e, of the force. This moment will create tensile stresses in the upper flange and compressive stresses in the lower flange, see equation (2.2).

$$\sigma_F = -\frac{F}{A_s} \tag{2.1}$$

$$\sigma_M(y_{G.C}) = -\frac{F \cdot e}{I_s} \cdot y_{G.C} \tag{2.2}$$

where

A_s is the cross-sectional area of the steel section
F is the prestressing force introduced to the steel beam
I_s is the moment of inertia of steel section
e is the distance from the gravity centre of the steel beam to the centre of the laminate
$y_{G.C}$ is the distance from the gravity centre of the steel beam, positive downwards

σ_F is the stresses in the steel cross-section due to prestressing

σ_M is the stresses in the steel cross-section due to moment caused by prestressing

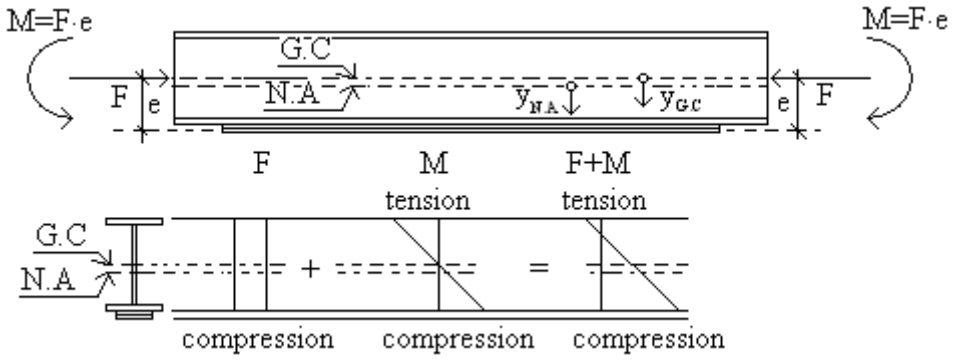

Figure 2.2 Beam with a prestressed laminate bonded to lower flange. Force and moment that influence the beam [19].

After the beam has been prestressed, the upper flange may be in tension and the lower flange will be in compression. When the steel beam is loaded, the initial stresses will counteract the stresses from the load, see Figure 2.3. However, the initial force, F, will introduce compressive stresses that have a negative effect on the load capacity for which the outmost fibre in the upper flange is yielding. The initial moment, M, on the other hand has a positive effect. In order to increase the yielding load the positive effect from the moment, M, most be greater than the negative effect from the compressive force, F.

The tensile stresses in the upper flange will delay yielding of the outmost fibre in the upper flange. This is the main improvement of the behaviour compared to a beam strengthened by unprestressed laminates. If the load is applied gradually, the tensile stresses in the upper flange will decrease and later on compressive stresses will appear. A similar behaviour will appear in the lower flange where the compressive stresses will decrease. The stress distribution in the cross-section due to loading can be expressed by equation (2.3)

$$\sigma_{M_l}(y_{N.A}) = \frac{M_l}{I_{eff}} \cdot y_{N.A} \tag{2.3}$$

where

I_{eff} is the effective moment of inertia

M_l is the moment due to loading

$y_{N.A}$ is the distance from neutral axis, positive downwards

σ_{M_l} is the stresses in cross-section due to loading

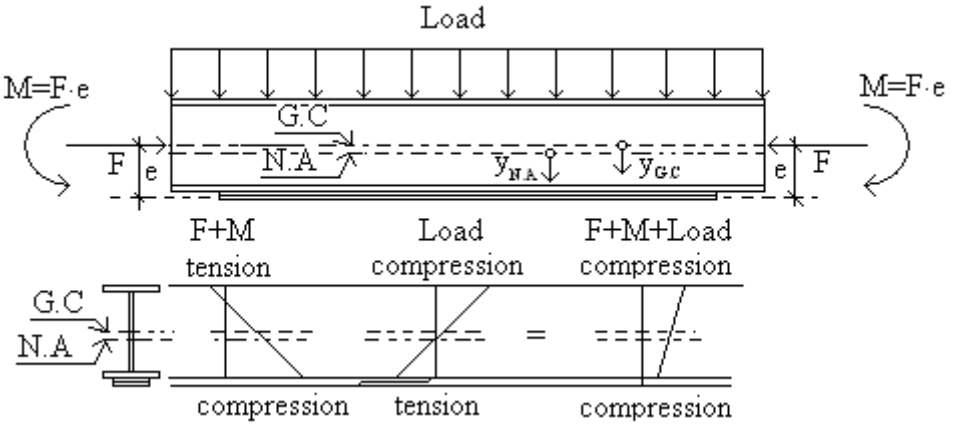

Figure 2.3 Loaded beam with a prestressed laminate bonded to lower flange. Forces and moment that influence the beam [19].

For a beam strengthened with unprestressed laminate the increase of load for which the outmost fibre in the upper flange starts yielding is due to the increased moment of inertia. The stresses in the cross-section due to loading can be expressed by equation (2.3). For an unstrengthened beam the stresses in the cross-section due to loading can be expressed with equation (2.4).

$$\sigma_{M_l}(y_{G.C}) = \frac{M_l}{I_s} \cdot y_{G.C} \tag{2.4}$$

At a certain load, the outmost fibre in the upper flange will start yielding and with further loading yielding will slowly be spread throughout the cross-section. This will affect the neutral axis, which successively moves closer to the laminate. When almost the entire steel beam has yielded in compression, the ultimate capacity of the composite beam has been reached, and additional loading will cause failure. For an unstrengthened beam with a symmetrical cross-section, half the cross-section will yield in tension and half the cross-section will yield in compression.

2.2.2 Failure modes of prestressed CFRP strengthened steel structure

For metallic structures strengthened with CFRP-laminates, which are bonded to the structure using adhesive, there are several possible failure modes. Which mode governs the failure of the structural element will depend on several geometrical properties, physical and mechanical properties as well as on the durability of steel, CFRP and adhesive. The possible failure modes include [5]:

- Tensile rupture of the CFRP material
- Tensile rupture or yielding of the strengthened material
- Adhesion failure in the adhesive joint in areas with stress concentrations
- Adhesion failure at a crack or any discontinuity at the surface of the strengthened material
- Global buckling of the strengthened structure

- Local buckling of the strengthened structure
- Compressive failure of the strengthened structure
- Long term fatigue failure in the metallic material, the CFRP, or the adhesive interface (in fatigue loaded structures)
- Long term creep failure of the adhesive joint
- Failure due to loss of prestressing as a result of creep of the adhesive
- Accidental damage of the CFRP or the adhesive as a result of impact or fire

Of all the failure modes mentioned above, the weakest link in a steel structure strengthened with CFRP is the adhesive bond between the steel and the CFRP [9].

The typical way of attaching prestressed CFRP-laminates is to bond them to the strengthened structure by adhesive. Results from parametric studies, Finite Element studies, and laboratory tests show that areas with stress concentrations in form of high shear stresses and peeling stresses exist in the adhesive joint between the CFRP-laminates and the strengthened structure. These shear and peeling stresses are discussed in detail in Section 2.2.3 below. Theses stresses reach their maximum values at the end of the laminates, and can cause failure due to debonding of the laminate [7] [17].

2.2.3 Interfacial stresses

When a CFRP-laminate is prestressed and bonded to a structural element, high stress concentrations will appear, at the end of the laminate. These stress concentrations will appear in the adhesive between the surface of the laminate and steel and are called interfacial stresses. The interfacial stresses consist of shear stresses and normal stresses. The normal stresses are also called peeling stresses, see Figure 2.4.

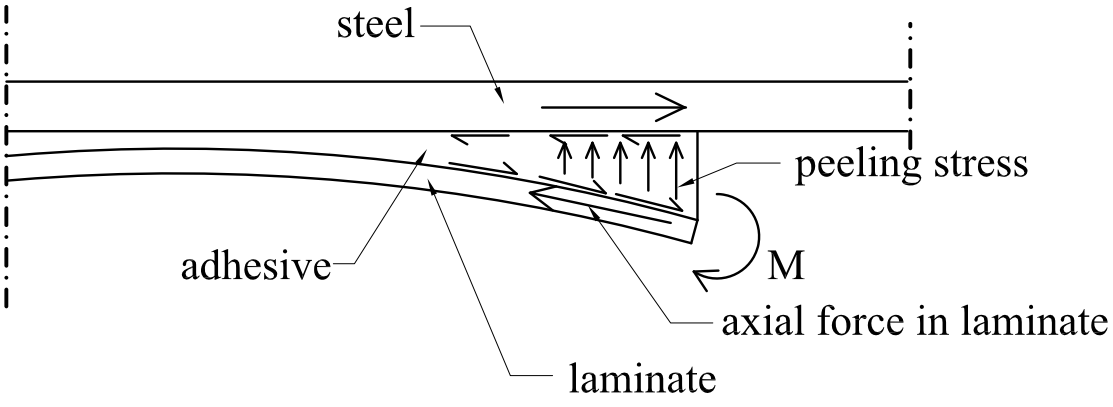

Figure 2.4 Schematic figure of the interfacial stresses.

Shear stresses

The shear stresses in the adhesive are related to the difference in deformation between the steel and the laminate, see Figure 2.5. The shear stresses are derived in Appendix

B. A simplified expression of the shear stresses, in the middle of the adhesive, can be expressed by means of equation (2.5) [7].

$$\tau(x) = \frac{G_a}{t_a}(\delta_l(x) - \delta_s(x)) \tag{2.5}$$

where

G_a is the shear modulus of the adhesive

t_a is the thickness of the adhesive layer

δ_l is the displacement of the laminate

δ_s is the displacement of the outermost fibres in the steel beam's lower flange

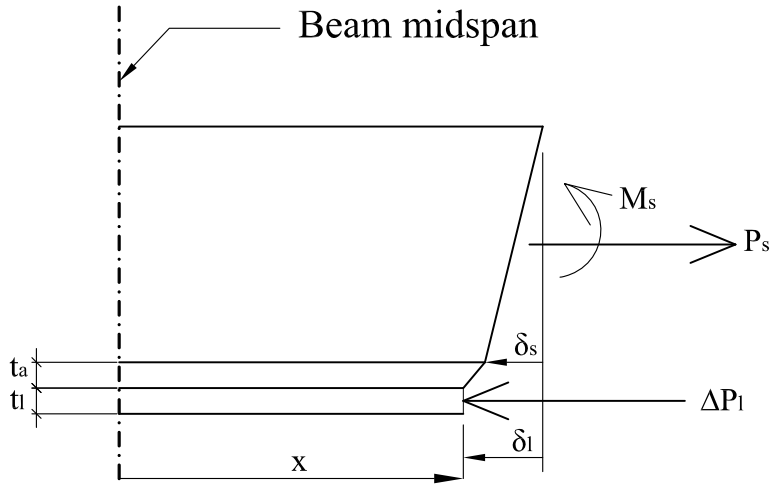

Figure 2.5 Deformations and forces at the distance x from the mid-span of the beam [9].

The distribution of the shear stresses in the adhesive layer along the bond line can be expressed by equation (2.6), where x is the distance from the mid-span of the beam.

$$\tau(x) = \frac{G_a \cdot P_0}{t_a \cdot A_l \cdot E_l} \cdot \frac{\sinh(\omega \cdot x)}{\omega \cdot \cos\left(\frac{\omega \cdot L}{2}\right)} \tag{2.6}$$

where

$$\omega^2 = \frac{G_a}{t_a}\left(\frac{b_l}{A_l \cdot E_l} + \frac{b_l}{A_s \cdot E_s} + \frac{b_l \cdot h^2}{4 \cdot I_s \cdot E_s}\right)$$

A_l is the cross-sectional area of the laminate

A_s is the cross-sectional area of the steel beam

E_l is the elastic modulus of the laminate

E_s is the elastic modulus of the steel beam

L is the length of the beam

P_0 is the initial prestressing force in the laminate

b_l is the width of the laminate

h is the height of the steel beam

τ is the shear stress in the adhesive layer

The axial force in the laminate can be expressed by equation (2.7).

$$P_l(x) = \frac{P_0}{A_l \cdot E_l} \cdot \left[1 - \frac{\cosh(\omega \cdot x)}{\cosh\left(\frac{\omega \cdot L}{2}\right)} \right] \cdot \frac{1}{\left(\frac{1}{A_l \cdot E_l} + \frac{1}{A_s \cdot E_s} + \frac{h^2}{4 \cdot E_s \cdot I_s} \right)} \tag{2.7}$$

where

I_s is the moment of inertia of the steel beam

P_l is the Prestressing force in the laminate after bonding and releasing

The distribution of bending moment due to prestressing along the strengthened length of the beam can be expressed by equation (2.8).

$$M_s(x) = -P_0 \cdot \frac{h}{2} \cdot \frac{\left[1 - \frac{\cosh(\omega \cdot x)}{\cosh\left(\frac{\omega \cdot L}{2}\right)} \right]}{\left(1 + \frac{A_L \cdot E_L}{A_s \cdot E_s} + \frac{A_L \cdot E_L \cdot h^2}{4 \cdot E_s \cdot I_s} \right)} \tag{2.8}$$

where

M_s is the bending moment in the steel beam due to prestressing

These formulas are applicable to any beam with arbitrary cross-section and material properties and are based on the assumptions that the bending stiffness of the laminate is neglected, the stresses are assumed to be constant through the thickness of the adhesive and that the materials have linear-elastic behaviour. This requires that the laminate is relatively flexible and that the layer of adhesive is thin [7].

Peeling stresses

The eccentricity of the axial force in the laminate compared to the force in the steel will create a bending moment, see Figure 2.6. The bending moment wants to bend the laminate but this is restricted by the adhesive. This will result in peeling stresses in the adhesive. The bending moment depends on the axial force at the end of the laminate and the lever arm of the axial force. The peeling stresses depend on the value of the bending moment, the stiffness of the laminate and the stiffness of the adhesive.

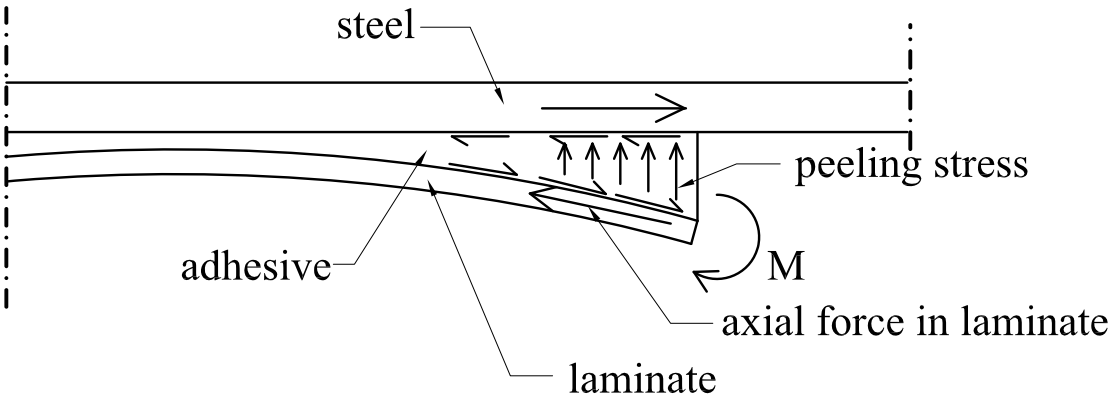

Figure 2.6 Moment due to the eccentricity of the axial force in the laminate.

2.2.4 Parameters that influence the magnitude of the interfacial stresses

Debonding of the CFRP-laminate is common in prestressed structures due to the high shear and peeling stresses in the adhesive. There are a number of factors that influence the distribution and the maximum shear and peeling stresses in these composite elements. It is interesting to study these parameters to understand the behaviour of the structure and especially the areas where the stress raisers exist.

The prestressing force in the laminate is build up gradually over the length of the laminate, see Figure 2.7. The force has a development length before the full prestressing force is achieved. It is in this area the prestressing force is transferred in to the beam and the shear and peeling stresses are high and can cause debonding of the CFRP-laminate.

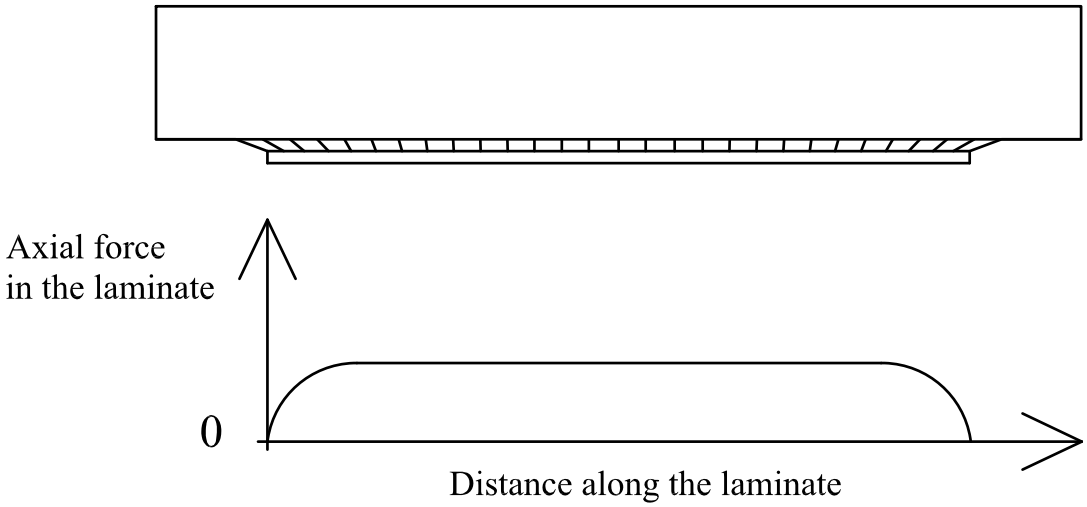

Figure 2.7 Schematic figure of the axial force in a prestressed laminate

Effect of the elastic modulus of the laminate

If the laminate is prestressed, it is preferable to use a very stiff one. Assuming a constant *prestressing force*, a stiffer laminate will experience lower strain levels and thus lower initial deformation. The shear stress in the adhesive layer is related to the difference in the deformation between the CFRP-laminate and the steel beam to which the laminate is bonded according to equation (2.5) in Section 2.2.3. Therefore, the maximum shear stress decreases when the axial elastic modulus of the CFRP-laminate is increased. The strain levels in the laminate needed to achieve one specific prestressing force are smaller for a laminate with higher elastic modulus [7].

Effect of the elastic modulus of the adhesive

By decreasing the stiffness (i.e. the shear modulus) of the adhesive, the shear stresses generated by a specific prestressing force will also decrease. This can be seen by considering the equations (2.5) and (2.6) which can be found in Section 2.2.3. The effective transfer length of the axial force in the laminate is increased. An increased effective transfer length will result in a more gradual transfer of the prestressing force to the steel structure. By introducing a more gradually transfer of the prestressing force the shear stresses are more uniformly distributed and the maximum shear stresses will be decreased [7].

Effect of the geometry of the laminate

If the initial prestressing *force* is kept constant, the value of the interfacial stresses will decrease when the cross-section area of the CFRP-laminate is increased. An increase of the cross-section can be obtained by increasing the thickness and/or the width of the laminate. By increasing the cross-sectional area, the normal stresses in the laminate will decrease. However, if the initial *stress* is kept constant, the maximum

interfacial stresses will decrease if the thickness of the CFRP-laminate is reduced and the width of the laminate is increased. This means that using a wider but thinner laminate will be beneficial concerning the magnitude of maximum shear and peeling stress at the ends of the laminate [7].

Deng J et al. [15] have investigated the influence of tapering the ends of an unprestressed laminate sheet using Finite Element analysis. The laminate that was analysed had a thickness of 12 millimetres and the adhesive used was two millimetres thick. By changing the length of the taper, a, and the thickness of the tapered end, t_{end}, the influence of the two parameters could be examined, see Figure 2.8.

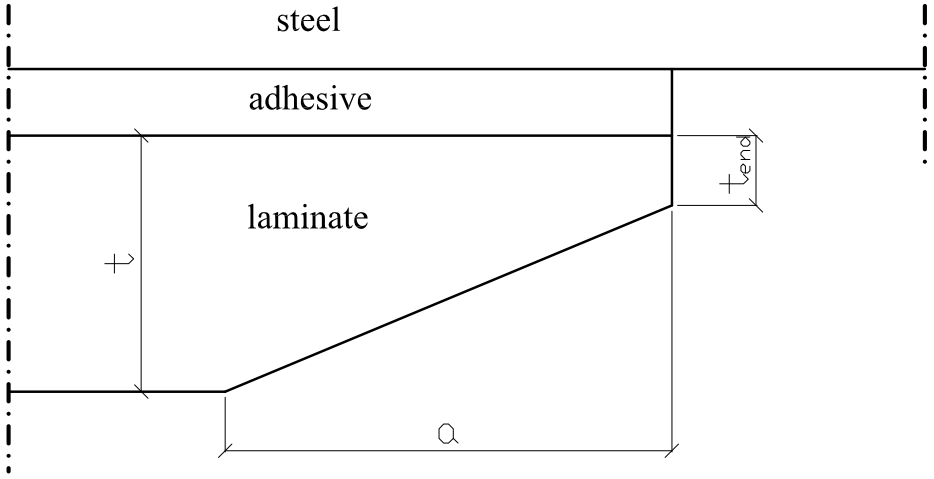

Figure 2.8 Geometrical parameters of taper.

The result of the study shown that a thinner tapered end, t_{end}, decreases the magnitude of the shear and peeling stress. The maximum shear and peeling stress were also dependent on the length of the taper, a. The conclusion was that the most favourable effect is received with a long taper and a thin end of the taper, t_{end}. However, no improvements of the result could be observed with lengths over 500 millimetres [15].

According to the guideline "Strengthening metallic structures using externally bonded fibre-reinforced polymers" the interfacial stresses at the end of the laminate can be greatly reduced by tapering the end of the laminate in width or thickness [5].

Effect of the adhesive thickness

The thickness of the adhesive also influences the interfacial stresses. By increasing the thickness of the adhesive, the maximum interfacial stress is decreased according to the equations (2.5) and (2.6) as can be found in Section 2.2.3 [7].

3 Prestressed CFRP for strengthening and repair- Literature review

3.1 External prestressing techniques

Several systems have been developed to cause the prestressing effect in order to strengthen existing structures. There are mainly three different methods to receive the prestressing effect: cambered beam system, tensioning against an independent beam, and tensioning against the strengthened beam [11].

3.1.1 Cambered beam system

With help of external forces, the self weight of the structure is counteracted. The release of strain when the structure is unloaded can then be used to prestress the laminate which is first bonded to one side of the structure. An example of this system is to use a hydraulic jack to lift the mid-span of a beam upwards, see Figure 3.1. The laminate is then bonded to the bottom of the beam and when the adhesive has been cured, the external force is released and the structure is externally prestressed. The prestressing force that is introduced with this method is relatively low and the uplifting force can damage the structure [11].

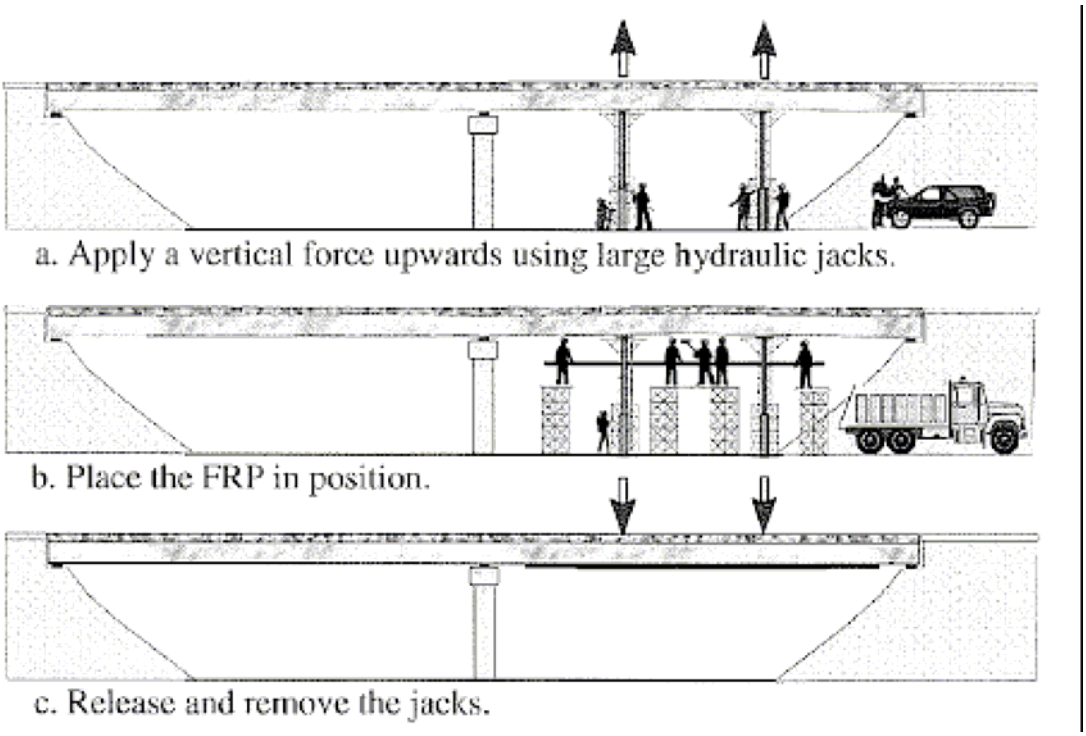

Figure 3.1 Cambered beam system [11].

3.1.2 Tensioning against an independent beam system

Tensioning against an independent beam system is another method to stress CFRP-laminates. In order to introduce the prestressing force into the laminate, an external prestressing device is used. After the laminate has been prestressed it will be bonded to the girder with adhesive. When the adhesive has cured, the external prestressing device can be removed, see Figure 3.2 [11].

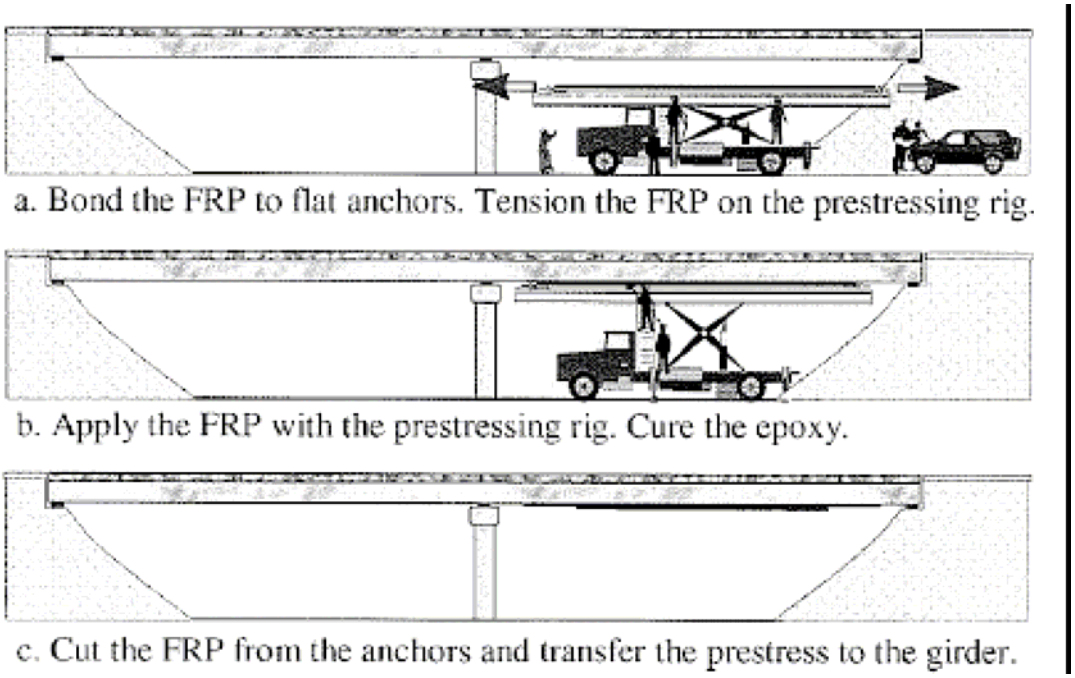

Figure 3.2 Tensioning against an independent beam system [11].

3.1.3 Tensioning against the strengthened beam

In the last method, tensioning against the strengthened beam, the laminate is prestressed by a prestressing device attached to the strengthened structure. The sheet is anchored to the prestressing device and with help of, for example, a horse-shoe jack, the laminate can be prestressed. For this method, a permanent anchorage is an important part of the system, see Figure 3.3 [11].

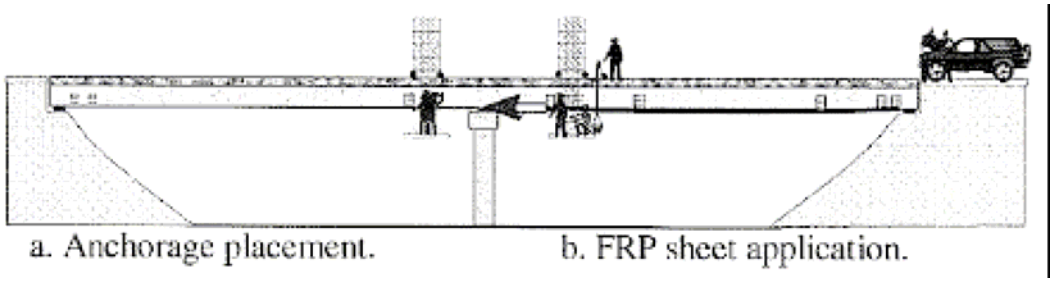

Figure 3.3 Tensioning against the strengthen beam [11].

3.2 Surface preparation

To ensure good performance of the CFRP-laminate, surface preparation of the steel and the CFRP must be executed in order to improve the bonding strength between the steel, the CFRP, and the adhesive. Bad surface preparation can result in bond defects that can give stress concentrations and cause peel-off of the CFRP-laminate before the theoretical ultimate load is reached [12].

Most surface treatments involve cleaning followed by removal of weak layers and re-cleaning. Degreasing is necessary to remove oil and other contaminants [13].

3.2.1 Surface preparation of steel

Surface grinding or sandblasting is a good way to remove rust, paint and other impurities from the steel surface. The next step is a chemical treatment of the surface with acetone or other appropriate substances [13].

The last step is to pre-treat the bare steel surface with either an adhesion promoter or a primer/conditioner. This leaves a thin layer attached to the metal oxide surface. The pre-treating should be chosen with consideration to the adhesive. This to ensure that maximum bond will be developed between the steel and the adhesive [12].

3.2.2 Surface preparation of carbon fibre reinforced polymer, CFRP

The preparation of the CFRP-laminate at site depends on how the laminate was prepared before delivery. Sometimes the manufacturer prepares the CFRP for the bonding. Otherwise some preparation needs to be done.

Voids and unevenness in the steel or the CFRP will be filled with putty. If the filling and the application of the adhesive are executed at the same time, so called wet in wet, there is no need to roughen and clean the putty [12].

The side of the CFRP that will face the steel surface may be prepared by using medium grit sandpaper or a sandblaster to increase the surface roughness and then cleaned by acetone. Too much surface preparation of the CFRP-laminate can cause galvanic corrosion if the laminate is placed in direct contact with the steel surface [12].

3.3 Anchorage systems

In order to take care of the high shear and peeling stresses at the end of the laminate, a large number of studies have been done. Most of them consider concrete structures with unprestressed laminates, but some consider steel structures as well. Not until recently has a larger interest for using prestressed CFRP-laminates to strengthen steel structures been developed.

In this chapter, the studies found from the review of existing literature are summarized.

3.3.1 Test of different anchorage geometries

Due to severe stress conditions at the anchorages, tests with different shapes of the anchorage zone were carried out. The geometries tested were a round bar, an ellipse-shaped bar and a flat plate. The round bar had a diameter of 32 mm, see Figure 3.4; the ellipse bar had dimensions of 67.5 x 47 mm, where 20 mm were flat along the long side of the ellipse, see Figure 3.5; the flat plate had a 100 mm long anchorage zone, see Figure 3.6 [16].

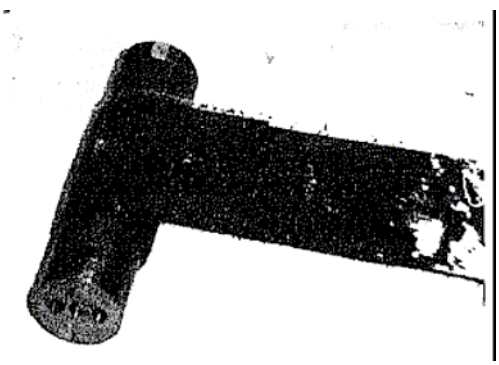

Figure 3.4 Round bar [16].

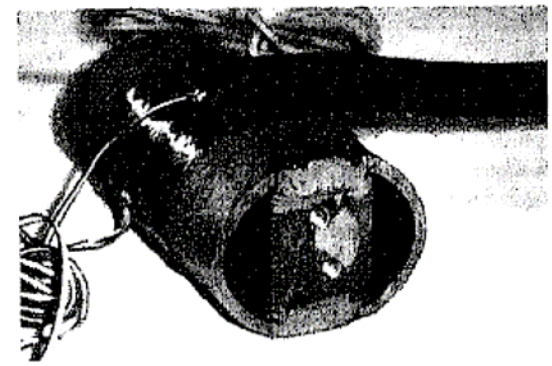

Figure 3.5 Ellipse bar [16].

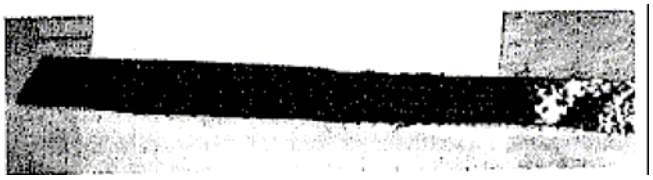

Figure 3.6 Flat plate [16].

For the flat plate, one, two, and three layers of continuous laminates were considered. For some of the specimens a 200 mm long additional layer of laminate was used at the anchorage zone. How the anchorage zone for the flat plate was established can be seen in Figure 3.7 [16].

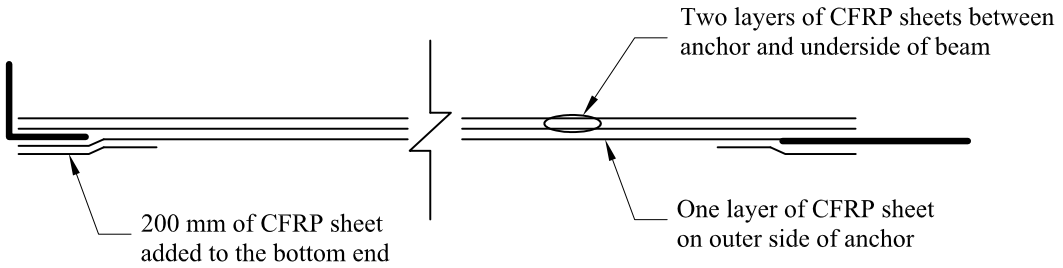

Figure 3.7 Different layers of laminate for the flat plate [16].

For the specimens with round and elliptical ends, only one continuous layer of laminate was used. For the round bar none, one or two additional layers were used at the anchorage zone. When one additional layer was used, a 150 mm long laminate was attached at the end. If two additional layers were used, a 200 mm long laminate was attached with a 150 mm long laminate on top of it. The laminate or laminates were rolled around the round anchorage three times and around the ellipse shaped anchorage three times. The additional layers resulted in an increased cross-section at the anchorage [16].

The results showed that the maximum strength was limited by the ultimate strength of the laminate. It was observed that the fracture occurred where the thickness of the laminate changed. This was interpreted as a result of the stress concentration due to change of cross-section area. The fracture started with breaking of fibres and ended in shear failure of the matrix [16].

All the tests had a linear elastic behaviour up to failure. For those specimens with additional layers, no failures were observed at the anchorage. In general, the flat plate gave the highest stresses. The flat plate with one layer of continuous laminate and an extra 200 mm laminate at anchorage gave the highest maximum stress, 1596 MPa, but the test with two layers of continuous laminate and an extra 200 mm laminate at anchorage gave the highest minimum stress, 1469 MPa. A joint behaviour for the specimens was that the additional layers at the anchorage moved the fracture away from the anchor zone. After the different shapes were analysed, their conclusion was that a flat plate anchor was simple and effective. A summary of the results can be found in Table 3.1 [16].

Table 3.1 Summary results of tension tests for CFRP-sheet anchors assembly[16].

Anchor type	Total number of tested specimens	Maximum stress[1] [MPa]	Minimum stress[1] [MPa]	Average stress[1] [MPa]	Layout of CFRP sheets
Round	5	1290	703	1029	1 layer
	2	1458	1354	1406	1 layer + 1 additional layer at each end
	2	1380	1145	1263	1 layer + 2 additional layers at each end
Ellipse	2	1414	1115	1265	1 layer
Flat plate	4	1543	1250	1408	1 layer
	2	1596	1303	1450	1 layer + 1 additional layer at each end
	3	1427	1331	1385	2 layers
	2	1517	1469	1493	2 layers + 1 additional layer at each end
	1	1234	1234	1234	3 layers + 1 additional layer at each end + wet epoxy[2]
	4	1387	905	1112	3 layers + 1 additional layer at each end
No anchor[3]	3	1520	1305	1412	1 single sheet

[1] Stress in sheet (calculated based on total area of sheet = fibre + resin).

[2] Epoxy was applied on sheet in last region between ends of additional layer.

[3] Both ends of sheet were held in testing machine by grips.

3.3.2 The Leoba-carboDur anchorage

One way of solving the anchorage problem in concrete structures is to use a double-lapped adhered connection. This solution is a combination of clamping and bonding [14].

The anchorage consists of a base plate, which is recessed into the concrete and attached by tilt up bolts that will take up the small tilt up moment. In between the concrete and the base plate there is a layer of adhesive mortar. On top of the base plate there is a clamping plate, and the CFRP is inserted in between the two plates. On both sides of the CFRP there is a layer of adhesive to create a double-sided adhered connection. The base plate and the clamping plate are pressed together by a clamping force and high tensile bolts will keep this force, see Figure 3.8.

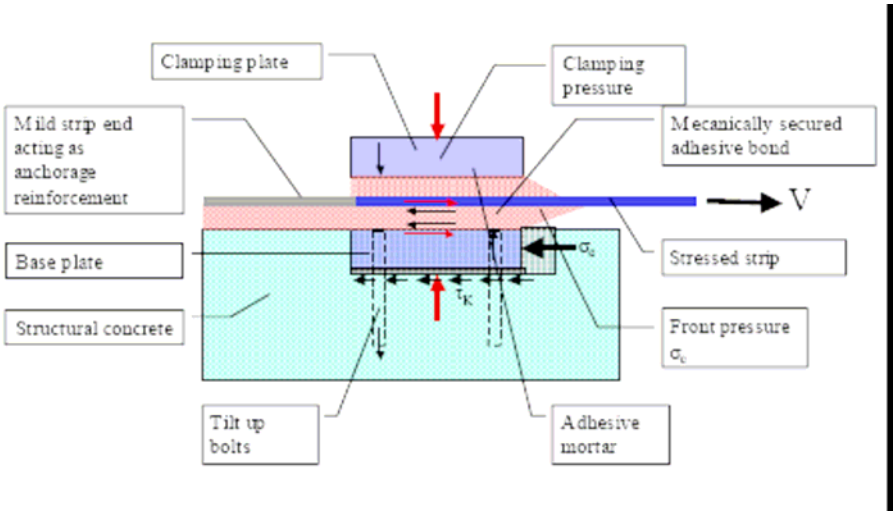

Figure 3.8 Double adhered clamping anchorage [14].

The force acting on the anchorage will be transferred into the concrete by front pressure of the plate and by bond of the adhesive mortar. The laminate continues through the anchorage device and works as an anchorage reinforcement [14].

The Leoba-carboDur anchorage will create an almost uniform stress distribution when the CFRP is close to fracture load and will provide an effective anchorage, which is required. This can be achieved because the prestressing force, V, will create high interfacial stresses in the rear of the anchorage and additional loading, ΔZ, will result in additional interfacial stresses in the front of the anchorage, see Figure 3.9 [14].

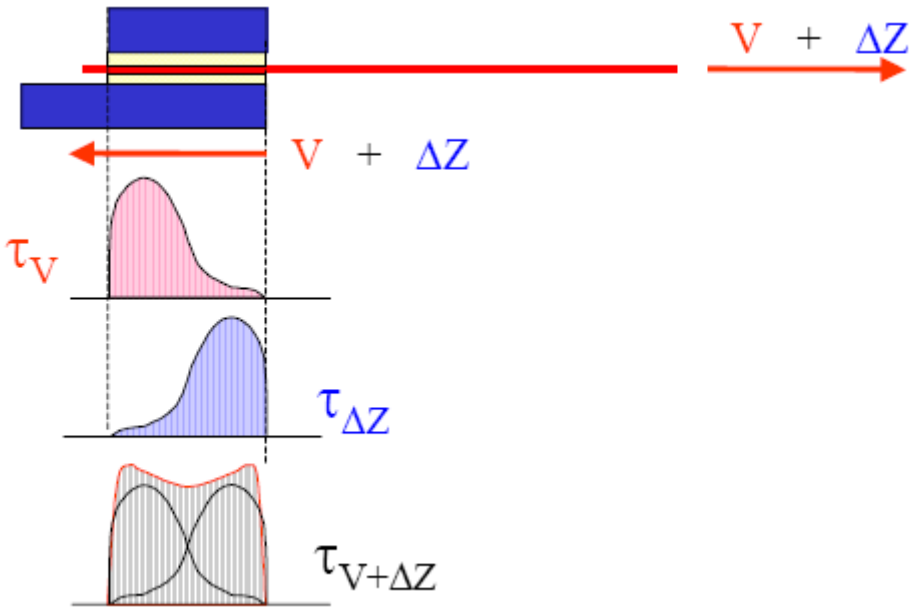

Figure 3.9 Shear stress distribution in anchorage for stresses due to prestressing and additional loading [14].

In order to test the behaviour of the anchorage the following arrangement was used, see Figure 3.10 [14]:

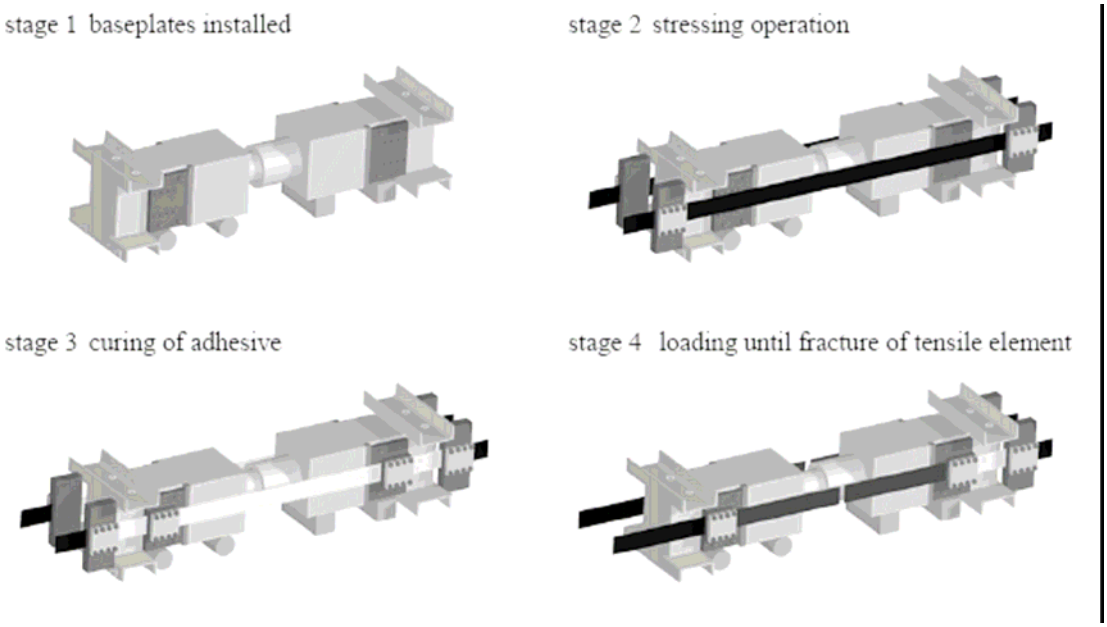

Figure 3.10 Test device for static load tests [14].

The device for stressing the laminates is of a "push-apart" model. The first stage consists of preparation of the base plate. In the second stage the laminate is pre-tensioned. During stage three, the adhesive is applied and the clamping plate is attached. When the adhesive has cured and the friction bolts have been tightened, the laminates can be loaded until failure, which is stage 4 [14].

Fatigue tests were also done. The same principle was used, and the laminates were tensioned with a force of 220 kN (stage 2). After the anchorages have reached their full capacity the load was increased up to 500 kN. With help of a pulsator, the system was loaded with the amplitude of 160 MPa and a constant upper load of 73 % of the laminate's characteristic strength. After 2.1 million cycles, the tests were interrupted and the laminates and the anchorage plate were loaded until failure. The two tests gave fracture load levels above the characteristic strength of the laminate and the fractures appeared in between the anchorage zones, which was a desired mode of failure. The load levels were 724 kN respectively 763 kN compared to the characteristic value of 706 kN [14].

This application was first used at strengthening the Gomadingen Bridge in Germany, in 1998. The CFRP tendons that were fastened to each anchorage zone had the dimensions 50 x 1.2 mm^2, and they were prestressed with a force of 60 kN, i.e. 1000 MPa [14].

In 2001, they managed to increase the size of the laminate to 90 x 1.4 mm and apply 165 kN, i.e. 1310 MPa, which was used at the Four-lane Koerschtal Bridge in Germany. This was a result due to development of what is called the second generation stressing system, see Figure 3.11, with a capacity to apply a prestressing force of 225 kN [14].

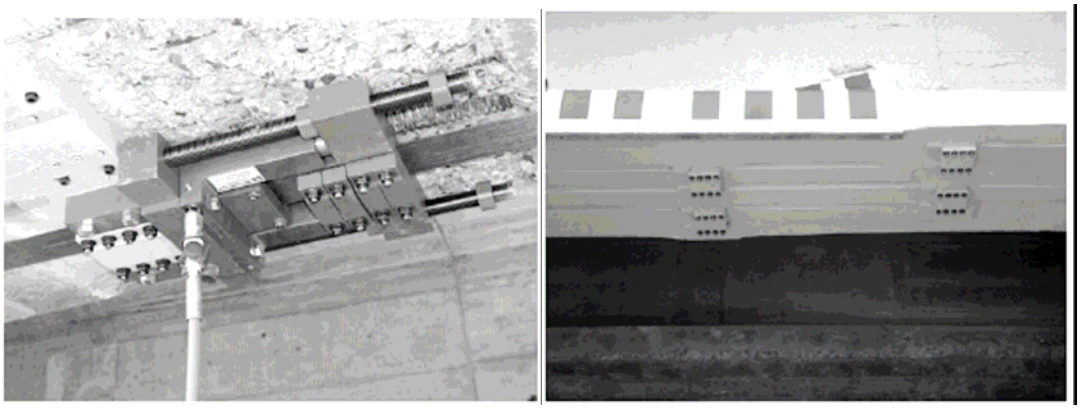

a) *b)*

Figure 3.11 a) Second generation stressing jack b) Final stage of prestressing [14].

3.3.3 Wedge-type anchor

Because of problems, such as creep, related to epoxy resins and cement, a wedge-type anchor was developed for FRP tendons. Earlier solution with a pre-cast wedge attached to the end of the tendon was not adjustable at site. An adjustable wedge system without resin was considered preferable as long as it did not cause premature failure [20].

The wedge type anchor developed consisted of a stainless steel barrel, four wedges of stainless steel, and a sleeve of copper or aluminium, see Figure 3.12 and Figure 3.13. The steel barrel had a conical socket and there was an angular differential of 0.1° between the socket and the wedges. This will make the wedges grip the tendon at the end of the barrel first and that will result in a more desirable stress distribution in the anchorage. The sleeve of copper or aluminium was used to distribute the stresses more evenly [20].

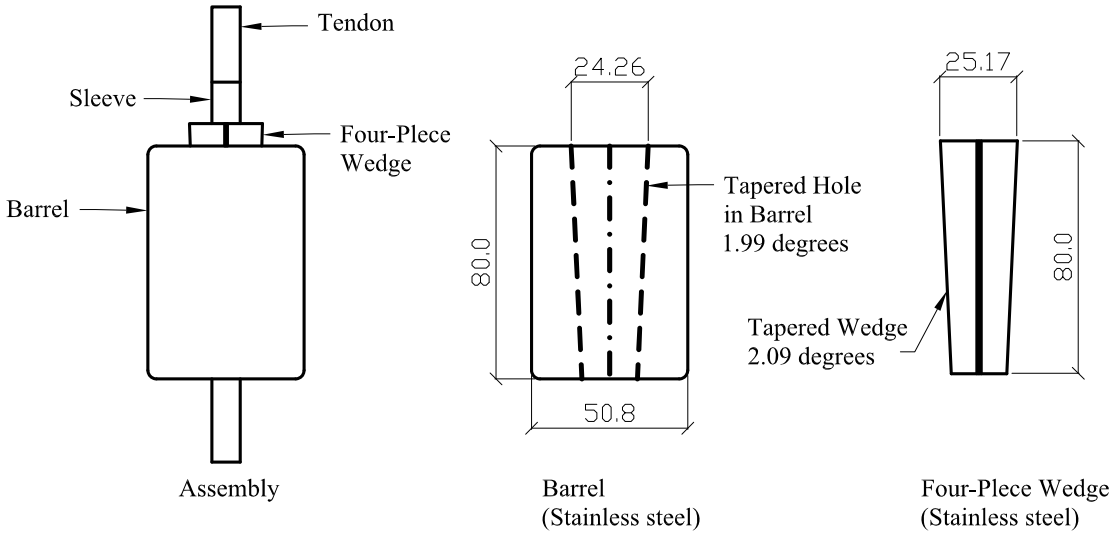

Figure 3.12 Detail of the wedge type anchor (all dimensions in mm) [20].

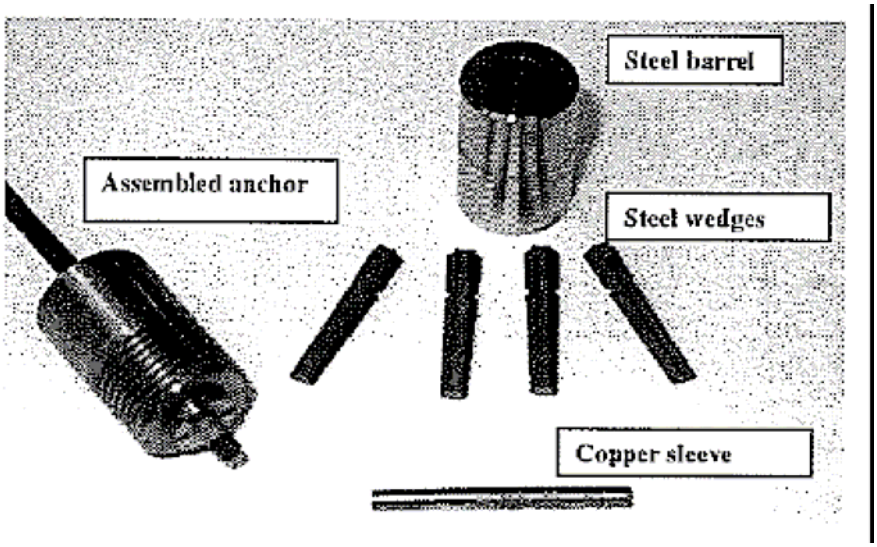

Figure 3.13 Wedge type anchor [20].

The first step in the evaluation of the new anchorage system was to create an FE-model to estimate the behaviour, see Figure 3.14 [20].

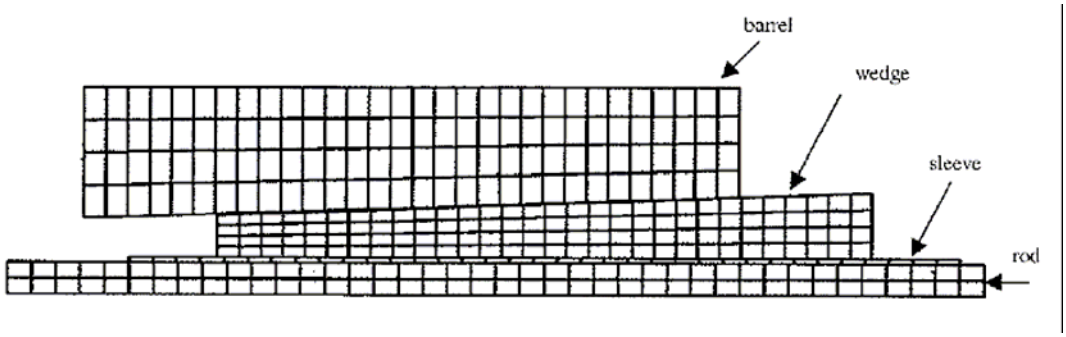

Figure 3.14 FE-model of wedge type anchor [20].

To investigate the influence of the angular differential, four different analyses were carried out. The friction coefficient between the barrel and the wedge was set to 0.2 and between the wedge and the tendon 0.4 was assumed. A high difference in slope resulted in high compressive stresses at the end of the barrel. With no difference in slope the compressive stresses were more evenly spread, see Figure 3.15. A desirable situation is to have zero compressive stresses in the front of the barrel to avoid the risk of a sudden and brittle failure of the tendon in the front of the barrel. An angular differential of 0.1° was considered as desirable in case of above named friction coefficients [20].

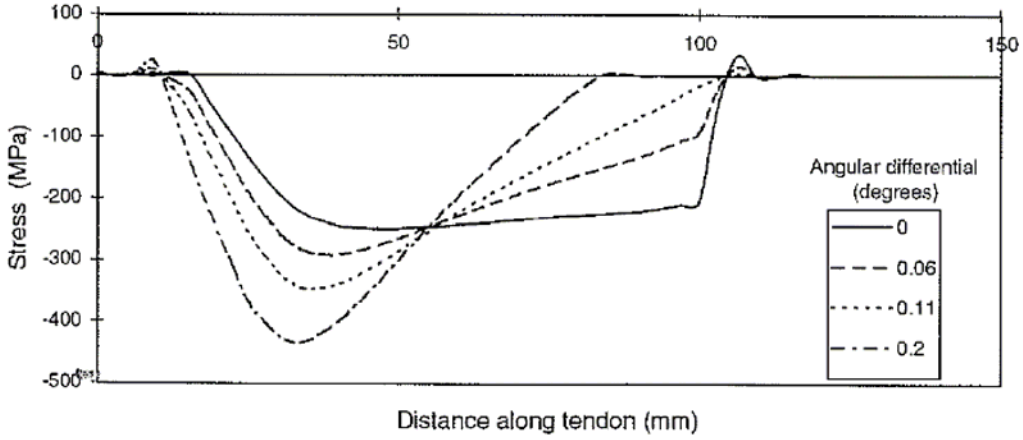

Figure 3.15 Variation of radial stress at the wedge-tendon interface with angular differential [20].

The next step was to conduct laboratory tests to investigate the real behaviour and to see how some parameters influenced the behaviour of the anchorage system. Furthermore, they investigated the behaviour in case of static and repeated loading.

The behaviour of the anchorage system, in case of static load, was investigated for both copper sleeve and aluminium sleeve. Two prestressing load levels were investigated; 50 and 100 kN. For the case of a prestressing level of 50 kN the anchorage could take loads up to approximately 35 kN for the copper sleeve and 40 kN for the aluminium sleeve. After that, the aluminium can take more loads with a more or less linear load displacement relationship, but the copper sleeve did not have this behaviour and cannot take further loading. For the other case with a 100 kN prestressing load, the static behaviour was better with small displacements. First at load levels above 75 kN could an increase of displacement be observed, see Figure 3.16 [20].

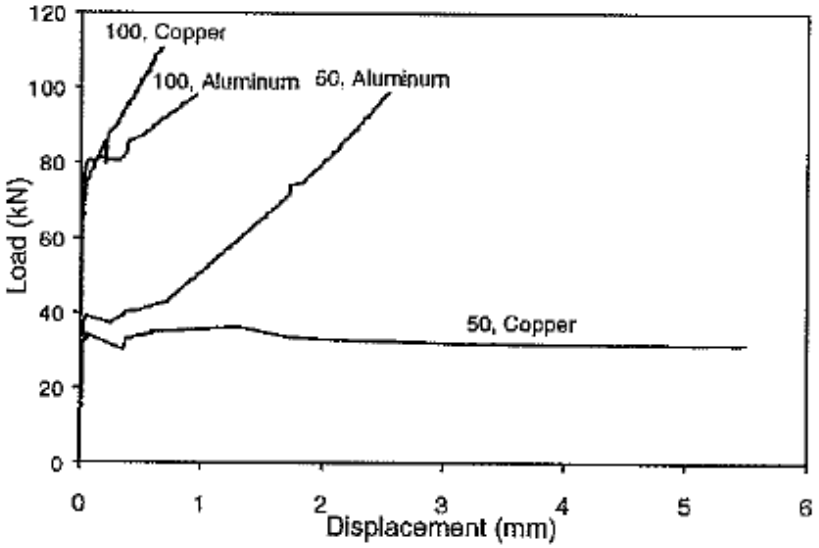

Figure 3.16 Load displacement graph for different prestressing levels and different sleeves [20].

To investigate the fatigue life, the pre-setting load was 80 kN, and three different load ratios and three different mean loads were investigated. The different R ratios ($R=\sigma_{min}/\sigma_{max}$) used were 0.65, 0.86, and 0.9. They found out that failure due to slipping was not a problem. Instead the failure appeared at the front of the barrel, which may be a result of slippage of the tendon in relation to the sleeve. Finally, they found out that no failure appeared after $2x10^6$ cycles for the ratios 0.86 and 0.9 in case of the maximum load 65 kN [20].

3.3.4 Test with different geometries of the anchorage

The interfacial stresses can be influenced by using a steel plate at the end of the laminate. Different shapes of the steel plate will give different values of the shear and peeling stresses.

Different geometries of steel plates as anchorages have been analysed by Butrooz et al. [17] with Finite Element analysis. They modelled different anchorage devices using a double-lap concept that involves adhesive bonding of the laminate between two steel plates. All the models consisted of one 1.4 mm thick CFRP-laminate with one steel plate on each side. A force of 134.4 kN was applied at the end of the laminate to simulate the prestressing force [17] [21].

In order to receive reference values, an anchorage with two steel plates with a thickness of 4 mm was analysed. The steel and laminate were bounded together by a 2 mm adhesive layer on each side of the laminate. The steel plates were 250 mm long and had a width of 80 mm, see Figure 3.17 [17].

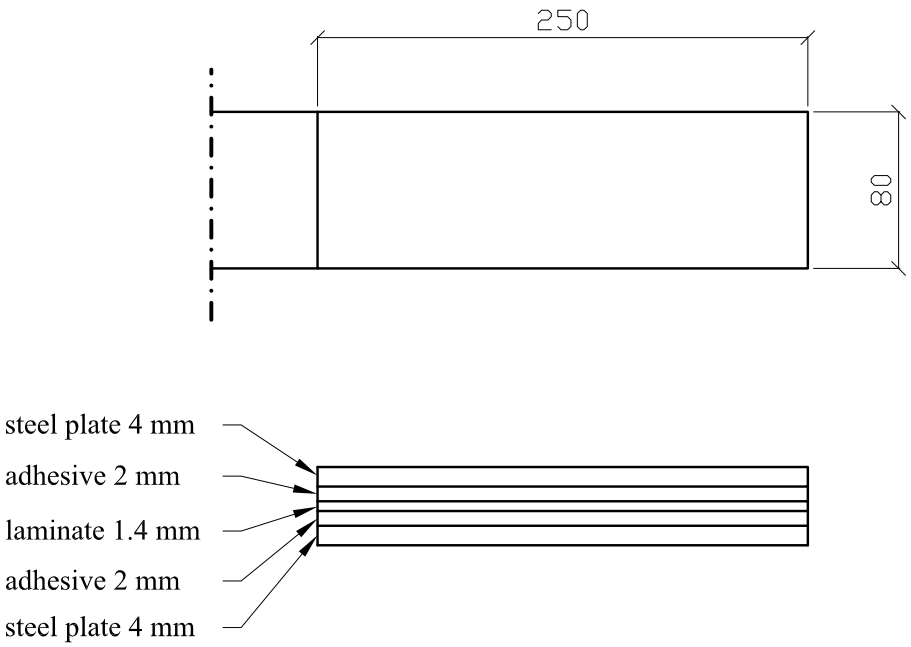

Figure 3.17 Rectangular anchorage plate [17].

The shear stress in the adhesive had a peak value of 63 MPa in the middle of the adhesive at the end of the steel plate [17].

In order to transfer the prestressing force more evenly, the steel plates were given triangular geometries, see Figure 3.18. The edge of the support follows the shape of the steel plate. The contact surface between them was applied with a friction coefficient of 0.5 [17].

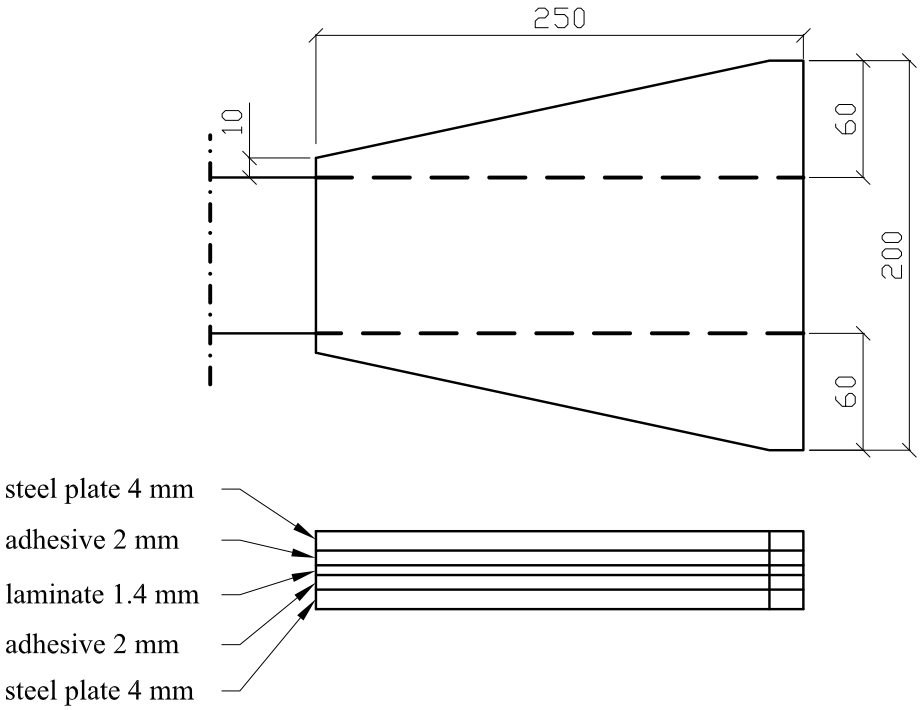

Figure 3.18 Triangular anchorage plate [17].

For the anchorage with a triangular geometry, the shear stress in the adhesive had a peak value of 52 MPa in the middle of the adhesive at the end of the steel plate [17].

The result of the shear force was improved, but not enough. In order to improve it further, a parabolic shape was used instead of the triangular and the support followed the shape of the steel plate, see Figure 3.19. This geometry was given in order to distribute the stresses to the narrow part more gradually, in order to reduce the peak values of the interfacial stresses [17].

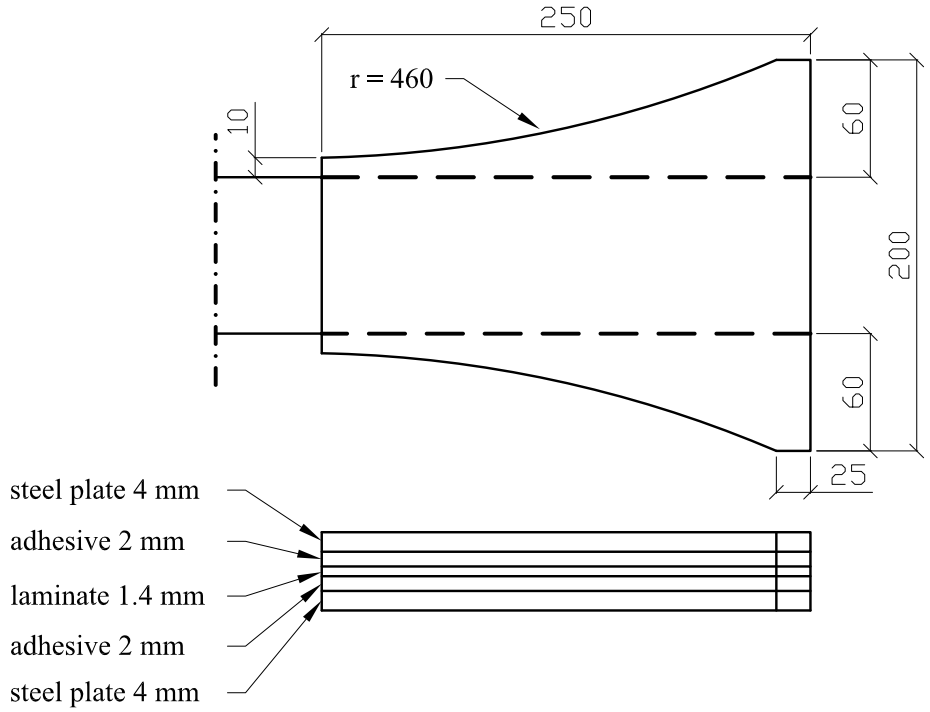

Figure 3.19 Parabolic anchorage plate [17].

No improvement was observed compared to triangular cross-section, and therefore other parameters had to be changed. The wider part of the steel plate was made thicker and also a parabolic shape of the steel plate's cross-section was initiated, see Figure 3.20. The plate still had the thickness of 4 mm at the narrower part. A new support that followed the new shape was also created [17].

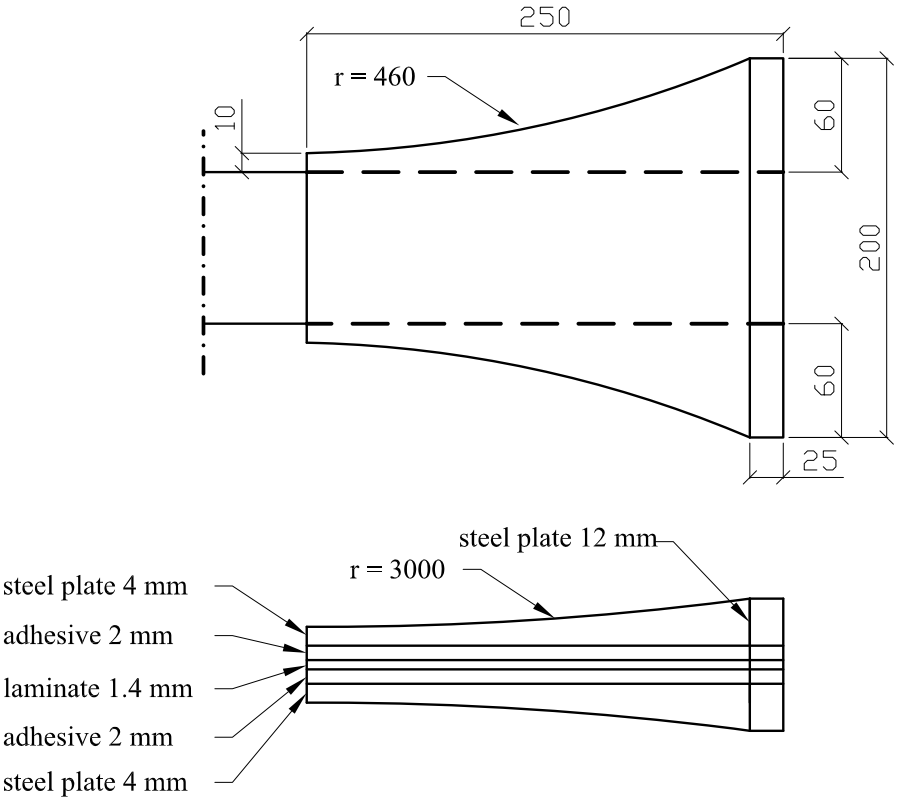

Figure 3.20 Parabolic anchorage plate with parabolic shape of the plate's cross-section [17].

A small improvement of the shear stress in the adhesive was obtained. The new geometry had a peak value of 50 MPa for the shear stresses [20].

The study showed reduced shear stresses if the thickness of the triangular and parabolic shaped anchorage were constant. If the parabolic shaped anchorage was tapered, see Figure 3.20, no significant improvements could be distinguished [20].

4 Examination of different methods to reduce the interfacial stresses

The first step in this master's thesis was to see how a steel beam behaves when it is strengthened with unprestressed CFRP-laminate and compare the behaviour to the case in which the CFRP-laminate is prestressed. This first step was divided into two parts. In the fist part the behaviour in the ultimate limit state is considered. The second part is concerned with the behaviour in the serviceability limit state. The next step was to see how different parameters influence the distribution and the values of the interfacial stresses in the adhesive. The parameters that will be discussed is loading, prestressing force, elastic modulus of the laminate and the adhesive, and the effect of the elastic plastic behaviour of the adhesive. Finally, methods and techniques that can be employed to reduce the high shear and peeling stresses will be presented.

To discuss the behaviour of a strengthened steel structure a double symmetric steel beam is used. Furthermore, this beam will also be used with regard to how different parameters, methods, and techniques are influencing the interfacial stresses. A double symmetric beam will also be used in the numerical analyses as well.

4.1 Global behaviour of prestressed steel beam

In this chapter the global behaviour of steel beams strengthened with prestressed and unprestressed CFRP-laminates will be discussed. All beams are strengthened with CFRP-laminate, but different elastic modulus of laminate and different prestressing forces are taken into account.

In general, apart of the strengthened beam itself, there are two factors that influence the global behaviour of a steel beam strengthened with bonded CFRP-laminate. The first is the properties of the materials used for strengthening. The second factor is the prestressing force introduced into the beam, if prestressing is used. It is of interest to see how these factors influence the global behaviour of a strengthened beam.

The global behaviour of a steel structure can be divided into two states. The first state is the elastic state, in which the material in the entire steel section is behaving linearly elastic. As long as the material is in this state there will be no plastic deformations when the structure is unloaded. In the second state the steel starts yielding. When the structure is unloaded in this state it will have some residual deformations.

By numerically analysing the global effects, such as deflection of the beam versus loading, the benefits of strengthening using bonded CFRP-laminates can be investigated.

4.1.1 Elastic state

In the elastic state the strains (or stresses) at any point in the cross-section will be below the elastic limit.

For a steel beam strengthened with unprestressed laminates the contribution to the increased load carrying capacity in the elastic state can be directly related to the increase in the moment of inertia of the beam resulting from the addition of the bonded CFRP-laminate.

For a beam strengthened with prestressed laminates the behaviour will be a little bit different. As mentioned in Section 2.2.1, by introducing a prestressing force to the lower flange of the steel beam, an initial compressive axial force and a negative moment are introduced to the beam. The applied moment depends on the distance between the centre of gravity of the beam and laminate, where the prestressing force is acting. Furthermore, the compressive stress in the beam depends on the cross-sectional area of the steel beam. The stresses, due to the initial compressive force and the moment, will influence the behaviour of the beam in the elastic state and also the load for which the steel beam will start to yield. For a prestressed beam the increase in the yielding load (moment) is because of the initiated moment generated by the prestressing. However, the normal stress acting on the cross-section will have a negative effect on the beams capacity.

With help of equation (2.1) - equation (2.4) in Section 2.2.1 the yielding moment can be derived for different beams. How the equations are derived can be found in Appendix A.

Unstrengthened beam:

$$M_{yielding} = \frac{\sigma_{yielding} \cdot I_s}{y_{G.C,uf}} \tag{4.1}$$

where

$M_{yielding}$ is the yielding moment

I_s is the moment of inertia of the steel section

$y_{G.C,uf}$ is the distance between the gravity centre of the steel beam and the outmost fibre in the upper flange

$\sigma_{yielding}$ is the yielding stress of the steel

Beam strengthened with unprestressed laminate:

$$M_{yielding} = \frac{\sigma_{yielding} \cdot I_{eff}}{y_{N.A,uf}} \tag{4.2}$$

where

I_{eff} is the effective moment of inertia for strengthened section

$y_{N.A,uf}$ is the distance between the neutral axis and outmost fibre in the upper flange

Beam strengthened with prestressed laminate:

$$M_{yielding} = F \cdot e \cdot \frac{I_{eff}}{I_s} \frac{y_{G.C,uf}}{y_{N.A,uf}} - \frac{F}{A_s} \cdot \frac{I_{eff}}{y_{N.A,uf}} - \frac{\sigma_{yielding} \cdot I_{eff}}{y_{N.A,uf}} \quad (4.3)$$

where

A_s is the cross-sectional area of the steel beam
F is the prestressing force introduced to the beam
e is the distance between the gravity centre and the middle of the laminate

With help of these formulas the expected yielding load can be calculated for different beams

To find out how the global behaviour in the elastic state is influenced by different elastic modulus of laminate and different prestressing forces different beams will be numerically analysed. The result will also be compared with the analytical solution. The beams will all have the same cross-section but the strengthening will be different.

4.1.2 Plastic state

When an unstrengthened steel beam reaches the plastic state the outmost fibres will start to yield. Theoretically, if the effect of strain hardening is ignored, the steel beam will lose its load bearing capacity after that half the cross-section has been yielding in tension and half yielding in compression. During the plastic deformation, an increased load will result in large deformations. For beams strengthened with a laminate, which is not prestressed, the behaviour will be different. When the load is increased in the plastic state the neutral axis will change its position and a larger part of the cross-section will be in compression, see Figure 4.1. Because of the high tensile strength and the linear elastic behaviour of the laminate, the latter can take all the tensile stresses, which means that the entire cross-section of the steel beam will yield in compression before failure. At failure, more or less, all compressive stresses are taken by the steel and all tensile stresses will be taken by the laminate. A corresponding increase in the moment capacity is thus obtained compared to the unstrengthened beam. Because of the fact that all tensile stresses are taken by the laminate there will be a difference in deflections between beams strengthen with high modulus and low modulus CFRP-laminates. The reason is that at the same moment larger deformation and thereby larger deflections are expected for high strength laminates due to its lower modulus of elasticity.

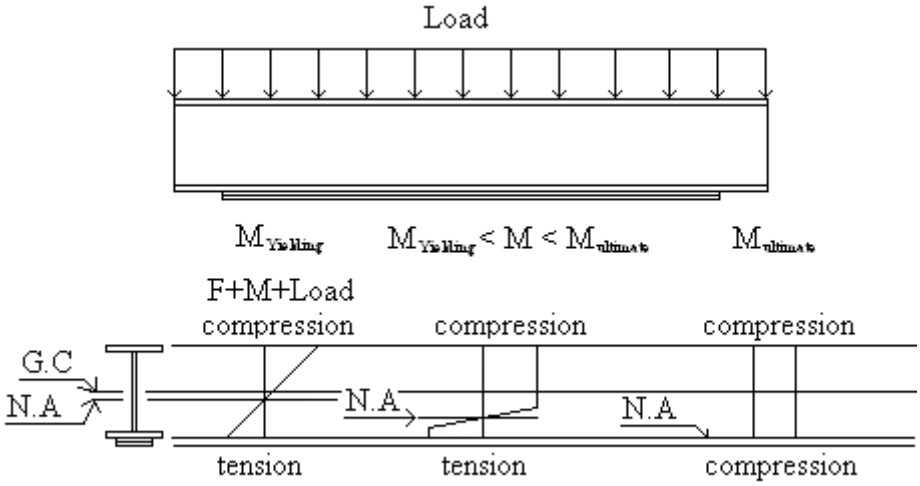

Figure 4.1 Stress distribution over the cross-section when the moment is increasing.

When it comes to prestressed laminates, the picture is not as clear. The reason why it is harder to predict the behaviour when the laminate is prestrssed is to the presence of the initial stresses that are introduced into the beam due to prestressing. These stresses will give the beam a more complex stress distribution over the height of the cross-section.

With help of numerical analyses the behaviour at ultimate limit state, for a steel beam strengthened with different laminates and different prestressing forces, will be investigated. Furthermore, how the value of the prestressing force affects the ultimate capacity of the beam will be studied.

4.2 Different parameter's influence on the interfacial stresses

In this section, the interfacial stresses between the laminate and the steel will be discussed along with how these stresses are influenced by material properties, loading, and prestressing. Different laminates and adhesives can be used when a steel beam is strengthened. Therefore, it is of interest to see how the interfacial stresses are influenced by different properties of the strengthening materials.

The bonded laminate will not only change the global behaviour of the beam. It also creates areas with stress raisers, as was discussed in Section 2.2.3. When a prestressed CFRP-laminate is attached by adhesive to a steel beam, interfacial stresses in the adhesive will be created upon releasing of the prestressing force. The magnitude and the distribution of the interfacial stresses are not only influenced by the magnitude of the prestressing force and loading but also by the stiffness of the laminate and the adhesive.

4.2.1 The effect of the prestressing force

According to equation (2.6) the shear stresses are proportional to the initial prestressing force. The shear stresses depend on the development of the axial force along the laminate. A lower initial prestressing force, P_0, will result in a lower residual prestressing force in the laminate. The axial force that will be transferred from the laminate to the beam will subsequently be smaller. Because of the lower axial force less stresses have to be transferred between the laminate and the steel beam, which will reduce the shear stresses.

By reducing the prestressing force the axial force at the end of the laminate is decreased. When the axial force is decreased the bending moment created by the eccentricity of the axial force will be decreased, see Section 2.2.3. This will result in reduced peeling stresses.

To be certain that the interfacial stresses are proportional to the initial prestressing force identical beams with different prestressing forces will be analysed.

4.2.2 The effect of external loading

It is of interest to find out how the interfacial stresses at the end of the laminate are influenced by the loading. For a beam strengthened with prestressed laminates there will be initial interfacial stresses due to the prestressing force. When beams strengthened with prestressed or unprestressed laminates it can be assumed that the additional stresses will have a different distributed. The reason is that the source of the additional stresses is the strain in the lower flange as a result of bending of the beam. Furthermore, the interfacial stresses due to loading will be relatively small, compared to interfacial stresses as a result of prestressing, towards the end of the laminate.

To investigate how the interfacial stresses at the end of the laminate are influenced by loading, one prestressed and one unprestressed laminate is numerically analysed. The unprestressed beam and the prestressed beam are compared to see how the interfacial stresses due to loading are influenced by the prestressing.

4.2.3 The effect of adhesive E-modulus

As has been mentioned in Section 2.2.4, if the elastic modulus of the adhesive is reduced, and thereby also the shear modulus, the shear stresses are reduced as well. A high modulus adhesive will carry over the force in the laminate in a shorter distance than a low modulus adhesive. Because of the lower elastic modulus, the displacements can take place and the development length of the prestressing force in the laminate will increase. This will result in a more distributed transfer of the axial force from the laminate into the steel structure. The result will be decreased shear stresses.

Because of the reduced axial force at the end of the laminate not only the shear stresses will be reduced but also the peeling stresses will be lowered. The reduction in

peeling stresses is obtained due to the lower bending moment at the end of the laminate because of the lower axial force there, see Section 2.2.3. The lower elastic modulus of the adhesive will also result in more evenly distributed peeling stresses. A less stiff adhesive will therefore result in smaller peeling stresses.

With help of equation (2.6) the influence of the elastic modulus of the adhesive was analysed analytically. The result showed that the shear stresses decreases when the elastic modulus of the adhesive is decreased. To see how the shear stresses vary along the laminate, see Appendix C, D, and E.

Table 4.1 Result from analytical analysis of a double symmetric steel beam strengthened with prestressed laminate. Different elastic modulus of the adhesive.

Elastic modulus [GPa]	Max. shear stresses [MPa]
1	75
5	167
9	224

To receive a more reliable results, FE-models with different modulus of elasticity, will be analysed and compared with each other.

4.2.4 The effect of laminate E-modulus

Prestressing the laminate will make it elongate. After bonding it to the steel beam the laminate wants to contract and this contraction is held back by the adhesive bond, see Figure 4.2.

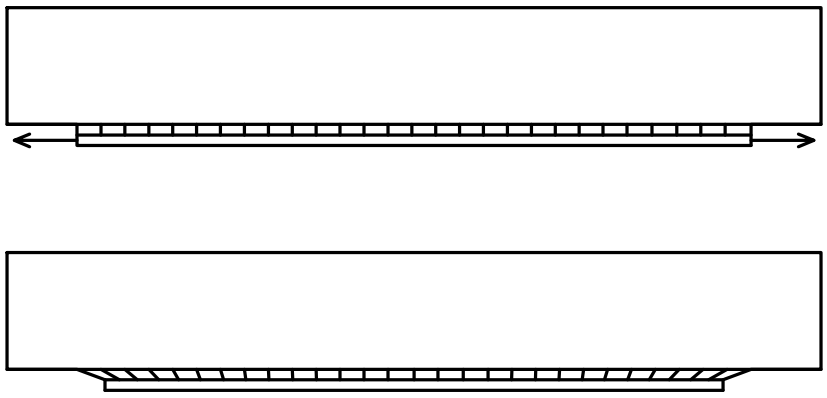

Figure 4.2 Contraction of the laminate after removing the prestressing device.

The contraction of the laminate is highest at the end of the laminate. Further away from the mid-span of the beam the laminate is more restrained. Equation (2.5) shows that the shear force in the laminate is a result of the difference between the deformation of the steel structure, δ_s, and the deformation of the laminate, δ_l, see also Figure 2.5. Furthermore, the deformation δ_l will be bigger for low modulus laminates than for high modulus laminates. Why the deformations will be smaller, and thereby the shear stress will be decreased, is because a stiffer laminate will transfer stresses with smaller deformations. That will result in more distributed stresses and reduced the peak values. More distributed stresses will increase the development length of the axial force in the laminate. A high modulus laminate will therefore also reduce the peeling stresses.

When equation (2.6) are analysed the following results were obtained for different elastic modulus of the laminate. To see how the interfacial stresses vary along the laminate see Appendix F, G, and H.

The result from the analytical solution shows what was expected. If a stiffer laminate can be used the shear stress will decrease, see Table 4.2.

Table 4.2 Result from analytical analysis of a double symmetric steel beam strengthened with prestressed laminate. Different elastic modulus of the laminate.

Elastic modulus [GPa]	Max. shear stresses [MPa]
100	252
200	181
300	150

To receive a more reliable result and also to see how the peeling stresses are influenced, FE-models with different laminates will be analysed and compared with each other.

4.2.5 Effects of the adhesive plastic behaviour

Adhesives are elastic-plastic materials, meaning that they have the ability to redistribute stresses at high loads through plastic deformation. The plastic redistribution is a result of non-linear stress-strain relationship of the adhesive. The non-linear behaviour will result in larger deformations when the stress is increased. The result is an improved distribution and lower peak values for the interfacial stresses.

The peeling stresses will also be influenced by the plastic behaviour of the adhesive. Due to the redistribution of stresses the axial force in the laminate will decrease towards the end of the laminate. Consequently, the peeling stress, which is a result of

the axial force in the laminate and the eccentricity, see Section 2.2.3, will also be decreased.

To find the effect of plastic redistribution an FE-model in which the adhesive is modelled as a linear elastic material will be compared with a similar model with an elastic plastic adhesive. The shear and peeling stresses in the adhesive will then be compared for the two models. One thing that has to be taken into account is the deformation capacity of the adhesive. With the intention of getting a comparable result the prestressing force is chosen in order to avoid exceeding the maximum deformation capacity of the adhesive.

4.3 Various techniques for controlling the interfacial stresses

The prestressing force in the laminate will have a development length before the fully prestressing force is achieved, see Figure 4.3.

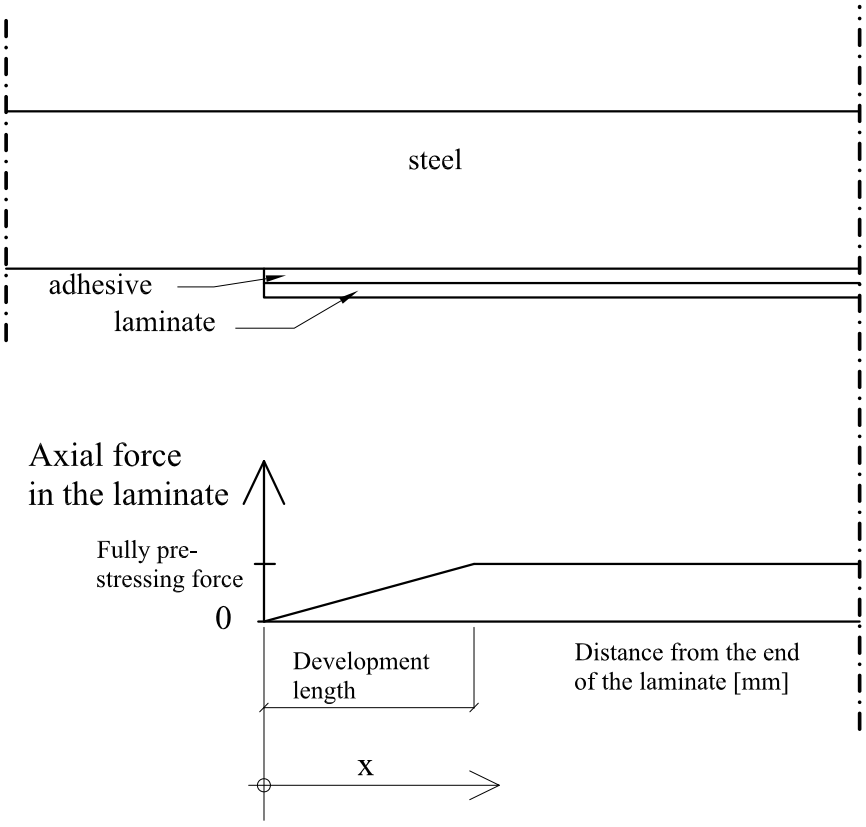

Figure 4.3 Schematic figure of how the axial force in the prestressed laminate is built up.

The interfacial stresses can be expressed as the variation of the axial force in the laminate, see equation (4.4). This expression is derived from equilibrium of a small segment of a strengthened beam.

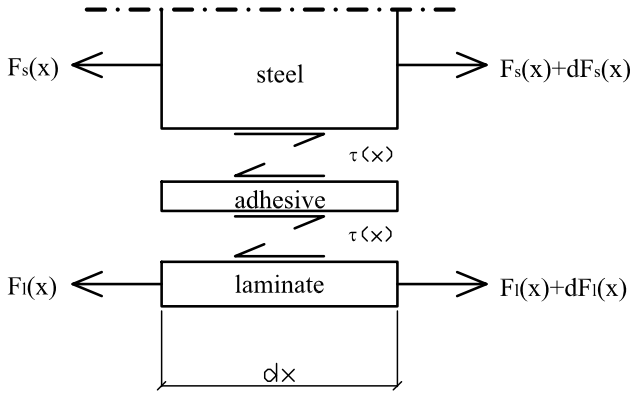

Figure 4.4 Horizontal forces in segment dx.

Equilibrium of the horizontal forces in segment dx will give equation (4.4).

$$F_l(x) + dF_l(x) - F_l(x) = \tau(x) \cdot dx \cdot b_l \Rightarrow$$

$$\tau(x) = \frac{dF_l(x)}{dx \cdot b_l} \tag{4.4}$$

where

F_l Axial force in the laminate

b_l Width of the laminate

As can be seen, the shear force depends on the variation of the axial force in the laminate.

Due to the fact that the interfacial shear stresses depend on the variation of the axial force in the laminate $dF_l(x)/dx$, theses stresses will be reduced if this variation is more gradual, see equation (4.4) and Figure 4.4. By introducing the axial force from the laminate to the steel beam more gradually, i.e. increasing the development length, the variation of the axial force, $dF_l(x)/dx$, will be decreased. Therefore, the main problem is the short distance where the axial force in the laminate is transferred into the steel beam, i.e. the short development length, see Figure 4.4. If this distance can be increased the shear stresses would be more uniformly distributed, which would result in reduced maximum shear stresses.

If the axial force in the laminate could be introduced into the beam more gradually it would also have a positive effect on the peeling stresses. The positive effect on the

maximum peeling stresses is a result of a lower bending moment that is created in the laminate due to the lower axial force in the laminate, see Section 2.2.3.

In this chapter different techniques and methods in order to increase the development length of the axial force is presented.

4.3.1 Shifting the prestressing position

If the end of the laminate can be left without being prestressed, an increased length can be utilized for distributing the shear stresses. Figure 4.5 shows schematically how the laminate is prestressed by a force F and how the axial force is constant over the length. With this method the zone with high interfacial stresses is moved away from the end of the laminate. The force F will be released when the adhesive between the laminate and the steel surface have been fully cured.

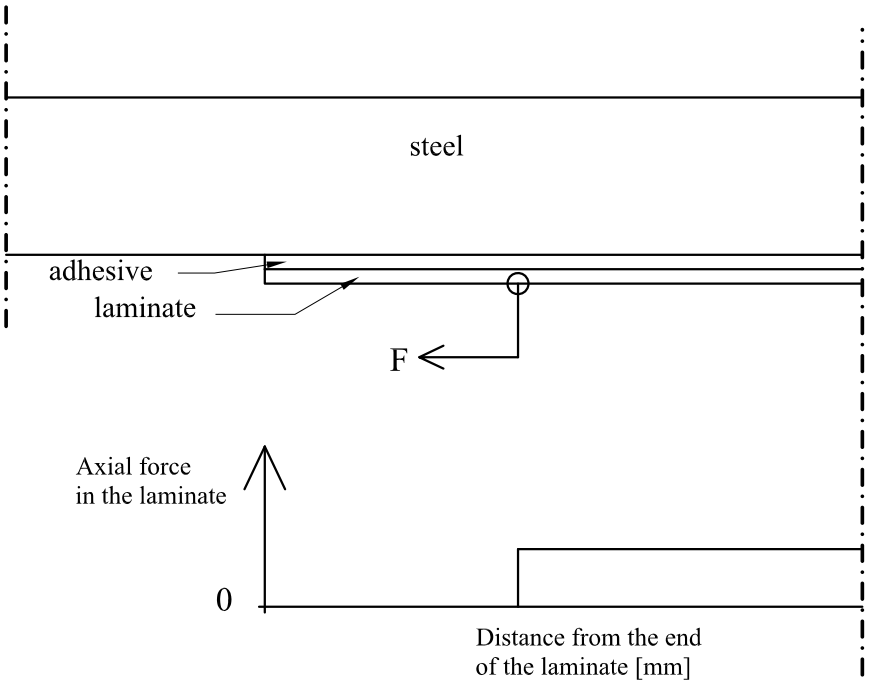

Figure 4.5 Schematic figure of unprestressed end of laminate. Prestressing force not released.

When the prestressing force is released the laminate wants to contract, which is held back by the unprestressed end. The axial force in the laminate is thereby introduced into the steel beam more gradually, see Figure 4.6. The gradual introduction of the force will result in a lower variation of the axial force dF(x)/dx. By reducing the differences of the axial force dF(x)/dx over the length, the maximum shear stress can be reduced and also be moved away from the end of the laminate.

The length of the unprestressed end influences the interfacial stresses at the end of the laminate. If the length of the unprestressed end is long enough, the interfacial stresses, due to prestressing at the end of the laminate can be reduced to almost zero.

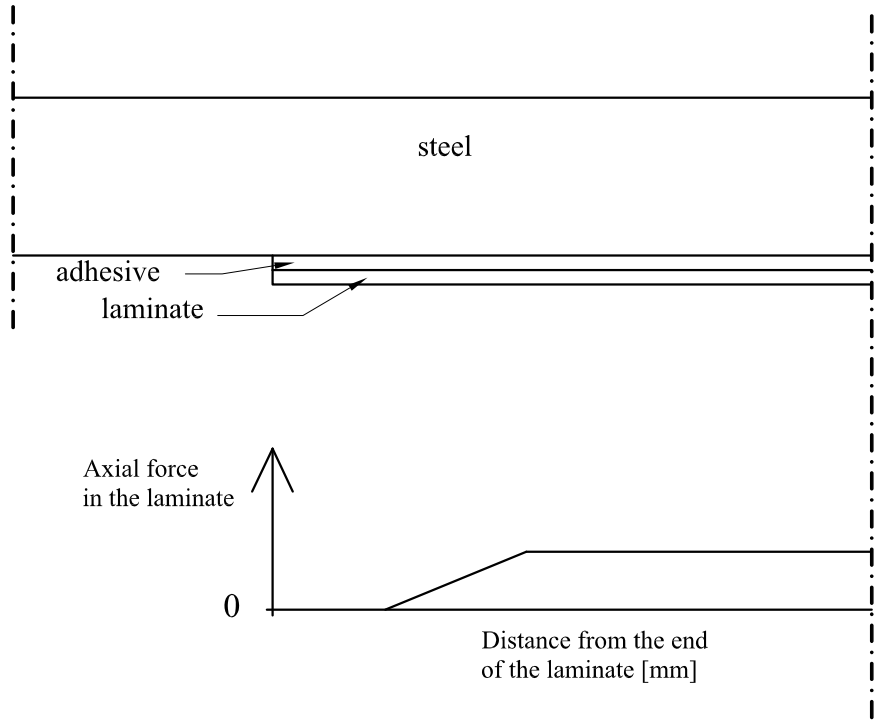

Figure 4.6 Schematic figure of unprestressed end of laminate. Prestressing force released.

Lower axial forces near the end of the laminate will also result in a lower bending moment acting on the laminate. This will result in lower peeling stresses in the adhesive at the end of the laminate. However, higher peeling stresses will appear at the zone of prestressing. These peeling stresses are due to the variation of the axial force in that region.

To study how the interfacial stresses change at the end of the laminate, when an unprestressed end is used, a numerical analysis will be performed. Different lengths of the unprestressed end will be analysed and compared with each other.

4.3.2 Step-releasing and gradual prestressing

Gradual prestressing and step-releasing are ways to gradually introduce the axial force into the laminate, see Figure 4.7. These two techniques are based on the theory that the interfacial stresses will decrease if the forces in the laminate decreases stepwise and gradually towards the end, i.e. the variation dF(x)/dx is reduced. This will result in a more evenly spread stress distribution and lower peak values of the interfacial stresses at the end of the laminate.

The shear stresses in the adhesive are dependent of the distribution of the axial force in the laminate. When the axial forces in the laminate vary drastically the shear stresses are higher. If the prestressing force is introduced gradually the maximum interfacial stresses will decrease. The ultimate situation would be if step-releasing and gradual prestressing could be carried out in a large number of steps over a long distance.

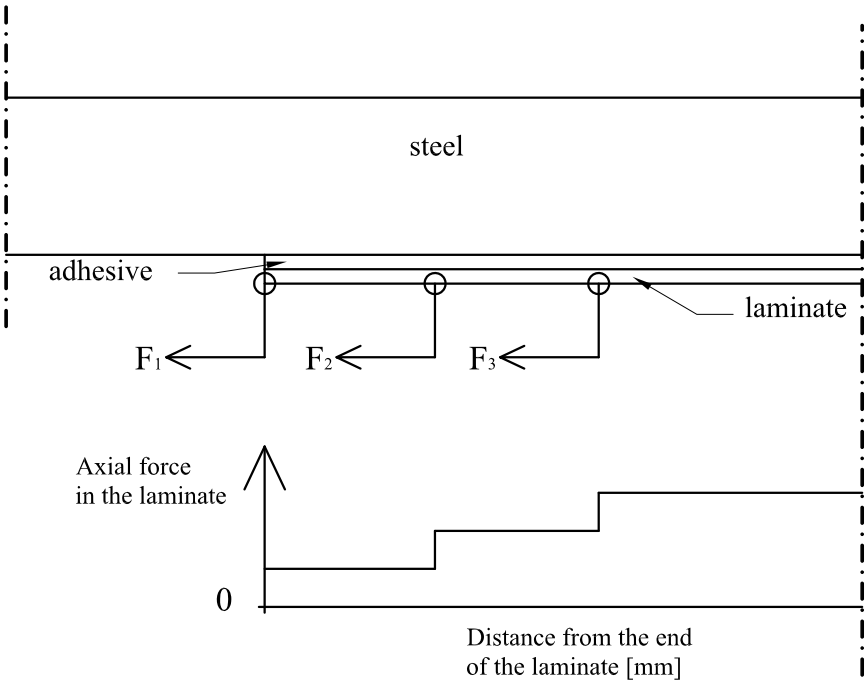

Figure 4.7 Schematic figure of step releasing/gradual prestressing of laminate. Prestressing force not released.

When the prestressing forces are released the development of the axial force is introduced into the steel beam in several steps, see Figure 4.8. This will result in an increased development length and the variation dF(x)/dx is reduced.

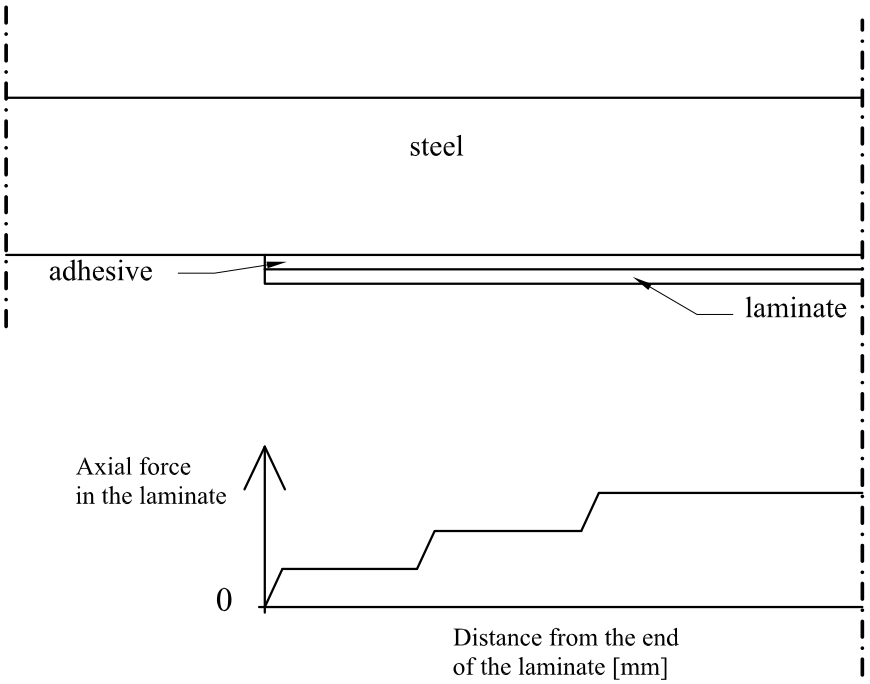

Figure 4.8 Schematic figure of step releasing/gradual prestressing of laminate. Prestressing force released.

A way of improving step-releasing and gradual prestressing is to use an unprestressed end, see Figure 4.9.

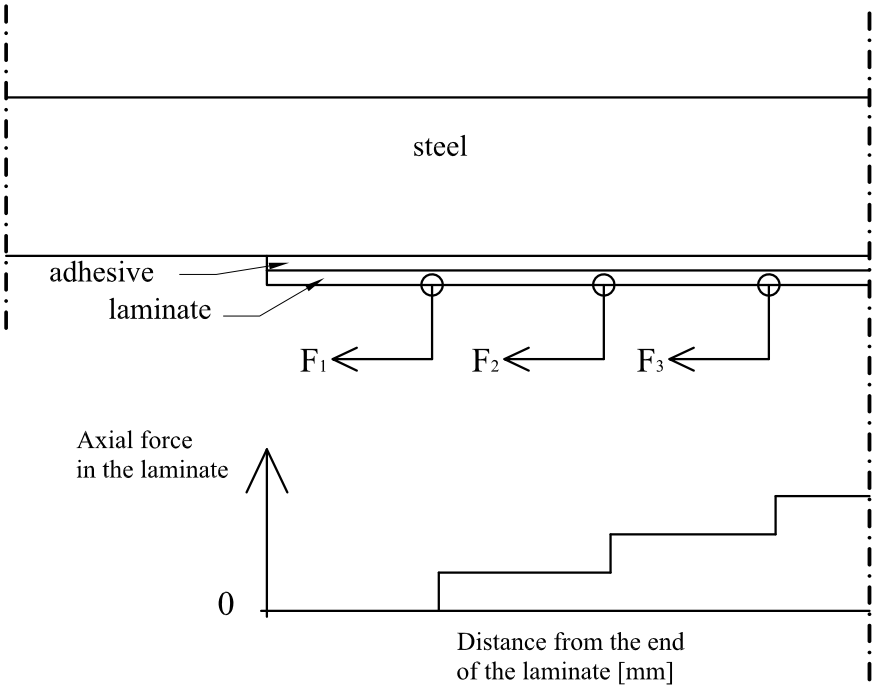

Figure 4.9 Schematic figure of step releasing/gradual prestressing of laminate with unprestressed end. Prestressing force not released.

After the provisional device has been removed the axial force in the laminate will have a long development length, see Figure 4.10. This will result in well distributed and very low interfacial stresses at the end of the laminate.

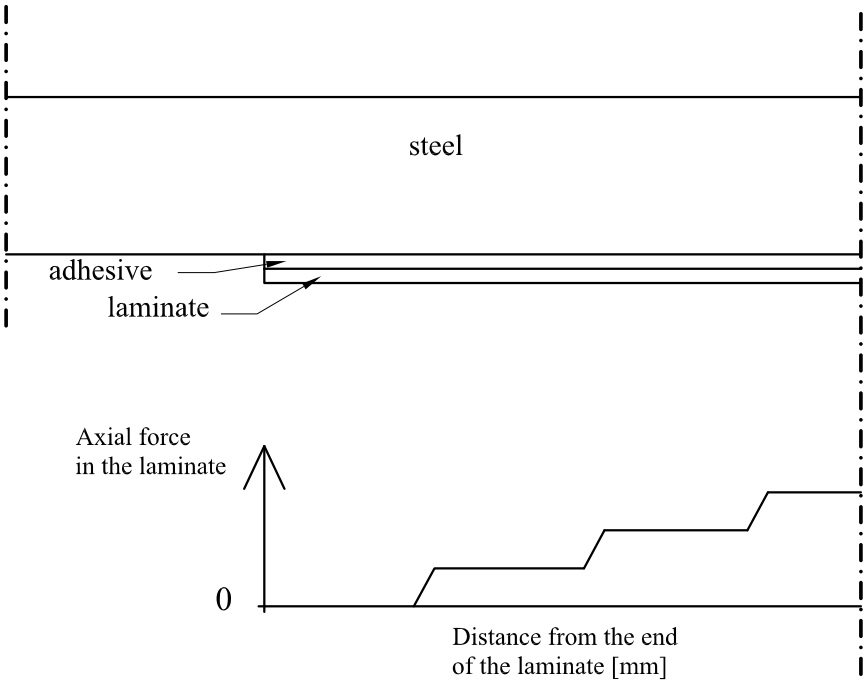

Figure 4.10 Schematic figure of step releasing/gradual prestressing of laminate with unprestressed end. Prestressing force released.

To examine the influence of step releasing and gradual prestressing analysis with different number of steps will be executed. Moreover, the step releasing / gradual prestressing in combination with an unprestressed end will be analysed numerically and the techniques influence on the interfacial stresses will be examined. For this study an arbitrary length of an unprestressed end will be used and the step releasing / gradual prestressing will be carried out in different number of step.

4.3.3 Tapering the laminate in width

By tapering the laminate in width, the area of the laminate is modified over the tapering length a, see Figure 4.11.

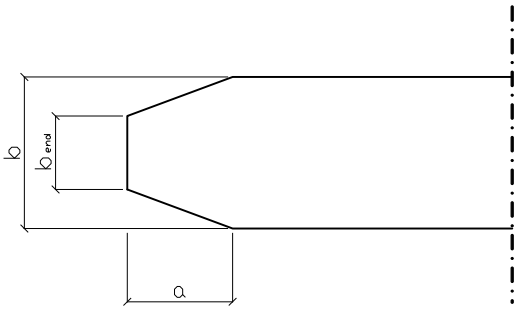

Figure 4.11 Tapered end of the width of the laminate. b is the width of the laminate at its end and a is the length of the taper.

The stiffness of the laminate is depending on the elastic modulus and the cross-section area. By slowly reducing the cross-section area of the laminate towards the end, the stiffness is slowly decreased. This will lead to a more distributed transfer of the prestressing force in the laminate into the beam. The shear stresses are decreased because the variation dF(x)/dx is reduced. The result is an increased development length and decreased maximum interfacial stresses.

The bending moment in the laminate is decreased due to a smaller axial force at the end of the laminate. This will result in lower peeling stresses.

To study the influence of the width of the taper several FE-models, with different widths of the tapered end, will be analysed and compared with each other. The next step is to evaluate how the length of the taper influences the interfacial stresses. To investigate how the length of the taper influences the interfacial stresses, FE-models with different lengths of tapers will be numerically analysed and compared.

4.3.4 Tapering the laminate in thickness

By tapering the laminate in thickness, the thickness and thereby also the cross-sectional will area vary over the tapering length a, see Figure 4.12. Because of the change of cross-section area the stiffness of the laminate will changes over the length. The stiffness of the laminate decreases towards the end and the transfer of the axial prestressing force from the laminate into the beam is more gradual, which will reduce the variation dF(x)/dx. This will decrease the shear stresses in the adhesive.

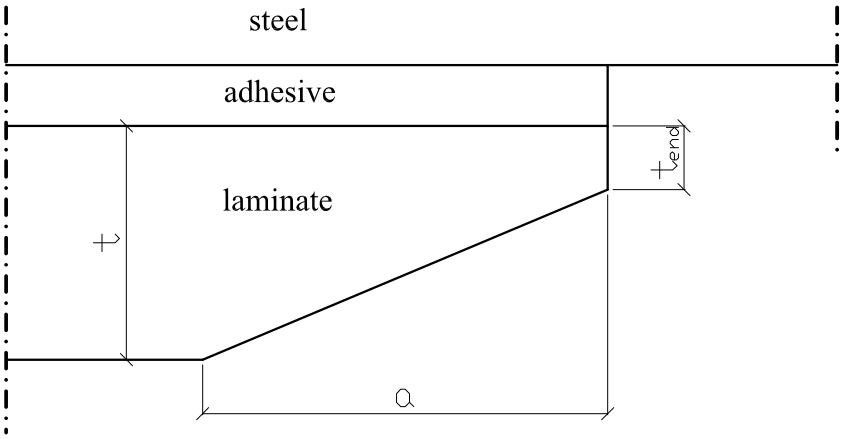

Figure 4.12 End of laminate tapered in thickness. t_{end} is the thickness and a is the length of the taper.

The peeling stresses are also reduced because the bending moment created by the eccentricity of the axial force is decreased. The bending moment is decreased due to a combination of a smaller axial force in the laminate and a shorter lever arm at the end. The lever arm is shorter because the thickness of the laminate at the end, t_{end}, is thinner. The peeling stresses will be more influenced by tapering the laminate in thickness compared to tapering in width, this is because of the change of the lever arm.

Both the thickness of the tapered end, t_{end}, and the length of the taper, a, will influence the change of stiffness and thereby the interfacial stresses. First the influence of the thickness of the tapered end will be analysed numerically and then the length of the taper.

4.3.5 Stepwise releasing at different curing times

When epoxies are curing they go from a stage of almost liquid to solid. Tests have been carried out for specimens at different curing times. The result shows that the modulus of elasticity changes over curing time, see Figure 4.13.

Theoretically, this behaviour is very beneficial. If some of the prestressing force could be released when the adhesive has a low modulus of elasticity the interfacial stresses will be more distributed. The influence of the elastic modulus of the adhesive is discussed in Section 2.2.4. The prestressing force is introduced over time until the entire force is initiated and the adhesive is fully cured. By doing this, the low elastic modulus in the first stage of curing can be utilized and this would result in well distributed interfacial stresses.

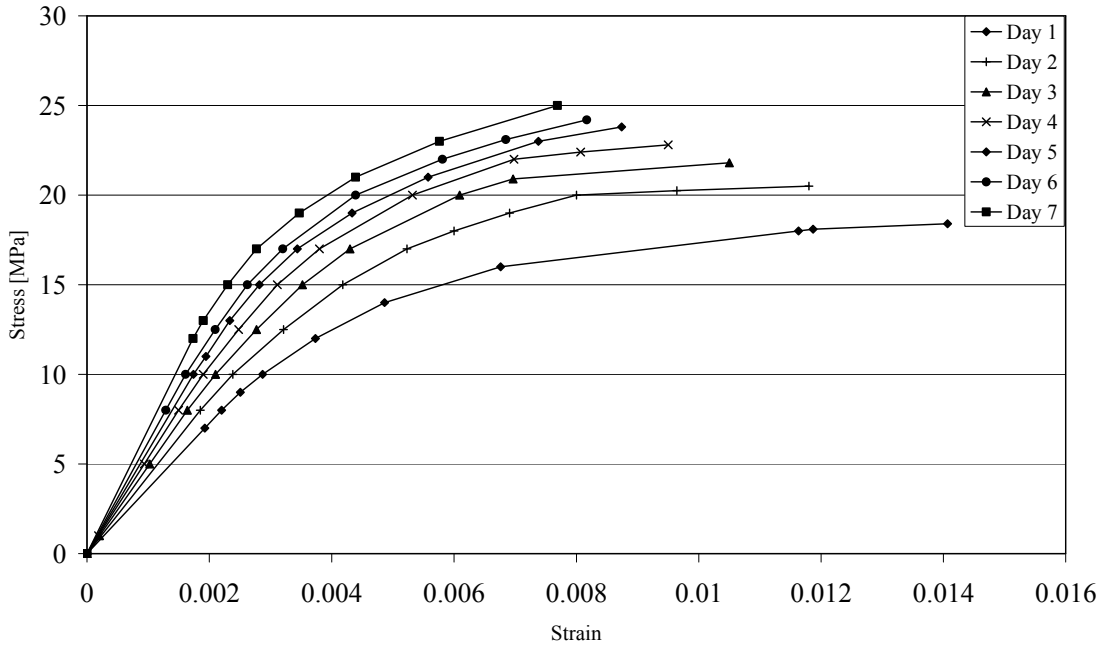

Figure 4.13 Stress and strain relationship for adhesive at different curing times.

However, there is a lack of knowledge when it comes to loading of adhesive when it is not fully cured. Because of the lack of knowledge, this technique will not be further investigated. Though, we want to discuss the problems and uncertainties with this method.

If this method is going to be used the adhesive must be able to be loaded up to a certain level when it is not fully cured and then cure fore another time period and then be loaded again. In order to introduce a high force from the laminate, this cycle must be carried out in many steps. The question is what happens to the adhesive. It can be assumed that a certain percent of the bond has been developed. What happens to these bonds when the adhesive is loaded over and over again?

In order to find the answer on these questions further investigations must be carried out and real laboratory tests should be executed due to its complex nature.

5 Structural model

To investigate the global and local behaviour of a beam strengthened with CFRP-laminate an FE-model will be used. This model is based on a structural model that have earlier been used for tests of steel beams loaded in bending at the Department of Structural Engineering at Chalmers University of Technology.

In this chapter the structural model will be presented.

5.1 Geometric properties

The steel beam chosen in the model is a hot-rolled beam with an HEA180 cross-section. The length of the beam is 2 m and the beam is simply supported with a span of 1.8 m, see Figure 5.1.

The cross-section, which is double-symmetric, has two flanges that are 180 mm wide and 9.5 mm thick, and a web that is 152 mm high with a thickness of 6 mm. In order to prevent local buckling in regions around concentrated loads, vertical stiffeners had to be used. These are welded to the beam underneath the points of load application and at the supports. The stiffeners are 120 mm high and 10 mm thick, made of the same steel as the steel beam.

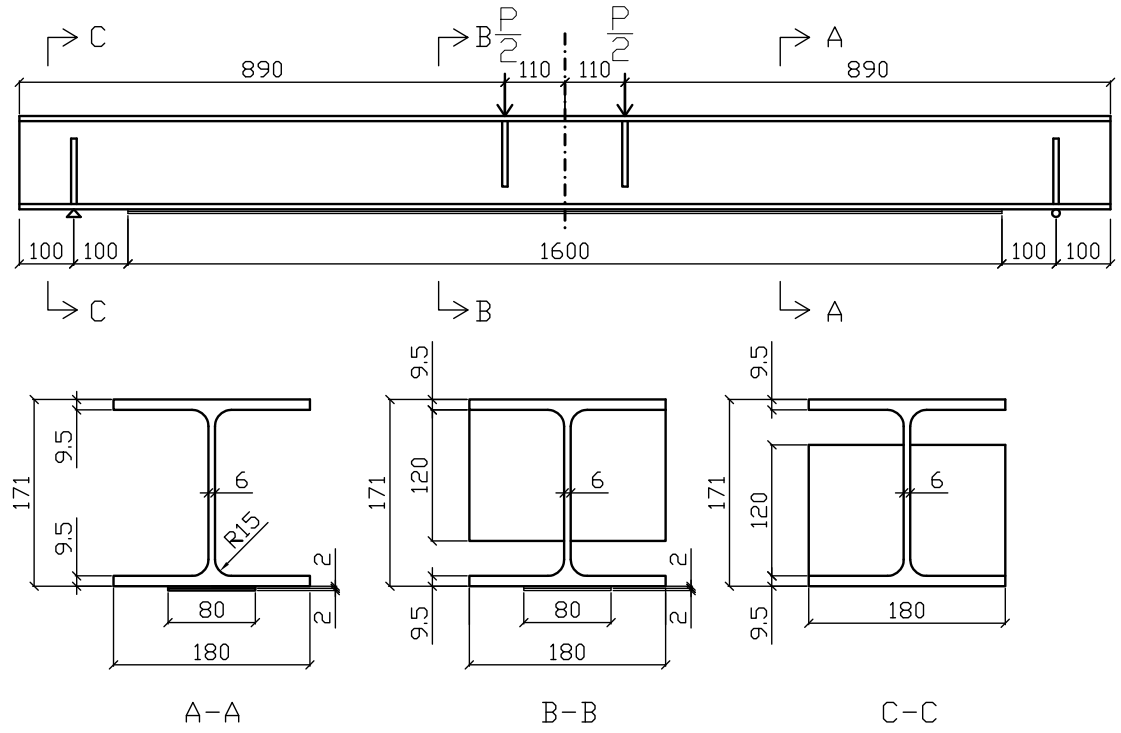

Figure 5.1 Dimensions of the structural model.

For strengthening the beam, an 80 mm wide and 2 mm thick laminate was bonded to the bottom flange with adhesive. The adhesive layer has a thickness of 2 mm and the same width as the laminate. The length of the laminate is 1600 mm.

5.2 Material properties

5.2.1 Steel

The steel in the beam and the stiffeners has an elastic modulus of 212 GPa and a yielding stress of 330 MPa. At 0.023 percent strain the steel is strain hardening and can take more load, see Figure 5.2.

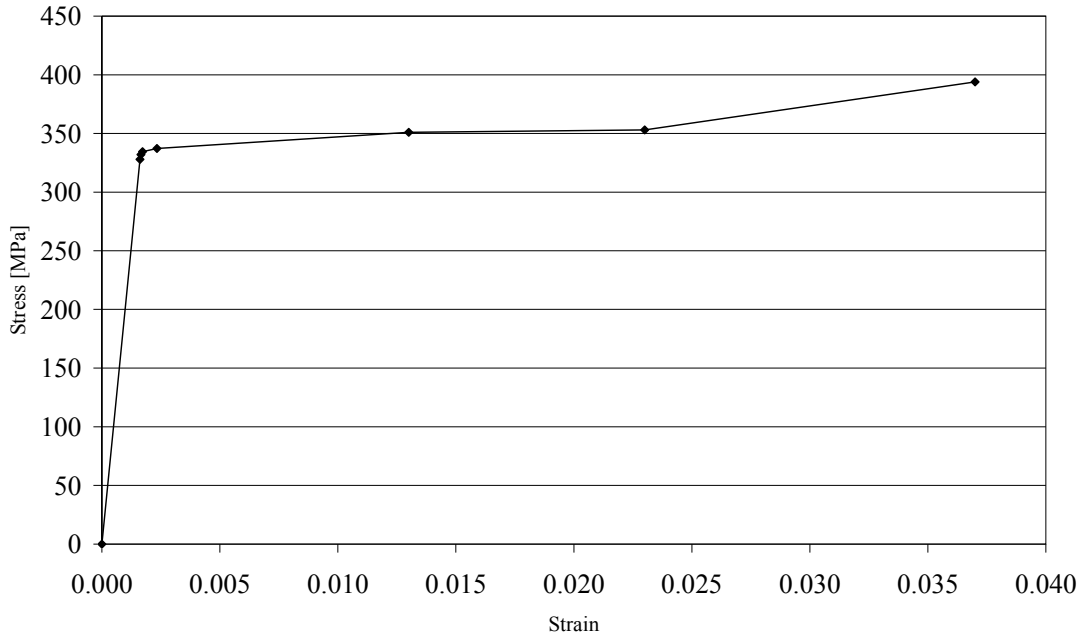

Figure 5.2 Stress and strain relationship for steel.

5.2.2 Adhesive

The adhesive used is an epoxy called BPE adhesive 567A/567B with an elastic modulus of 7 GPa. The poisson's ratio is 0.3 and the shear modulus is 2.69 GPa.

Figure 5.35.4 shows the stress-strain relationship of the epoxy used for bonding the laminate to the steel beam. For stresses below 12 MPa, the epoxy has an almost linear behaviour, but for higher stresses the behaviour is non-linear.

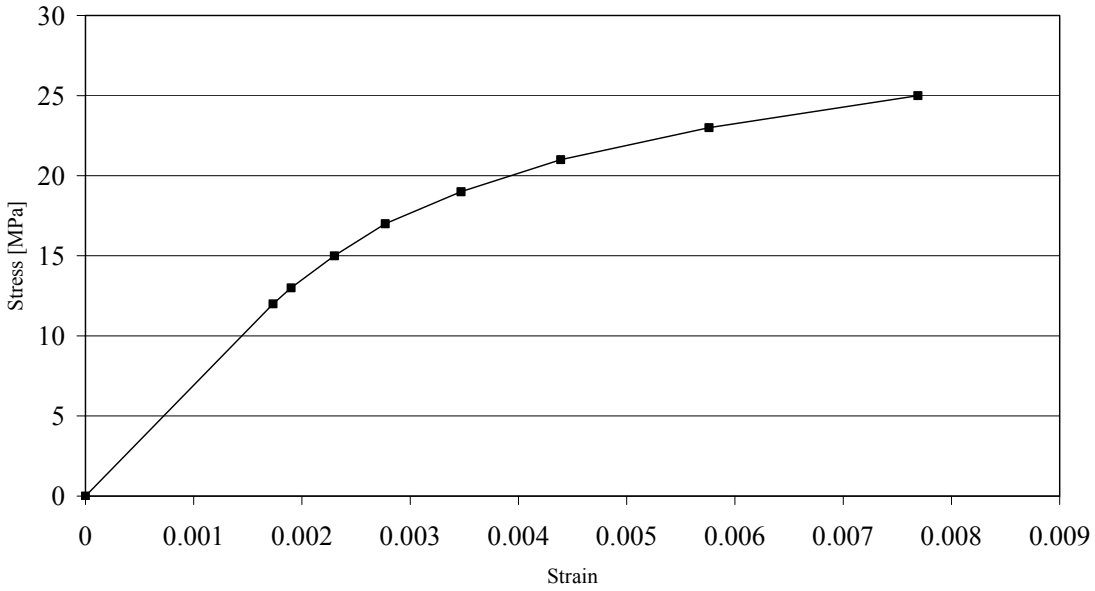

Figure 5.35.4 Stress and strain relationship for adhesive.

5.2.3 CFRP-laminate

The laminates used are one high modulus CFRP with elastic modulus of 400 GPa in the axial direction, and one high strength CFRP with elastic modulus of 165 GPa in the axial direction. The high modulus CFRP has a characteristic tensile strength of 1000 MPa, and the high strength CFRP has a characteristic tensile strength of 3000 MPa, see Table 5.1. Both laminates have all fibres arranged in the same direction, i.e. the material is unidirectional and isotropic. The CFRP-laminate is more or less linear elastic up to failure, and therefore a brittle failure can be expected.

Table 5.1 Material properties for CFRP-laminate

CFRP	E [GPa]	ft [MPa]
High modulus CFRP	400	1000
High strength CFRP	165	3000

5.3 Load

5.3.1 Prestressing

For prestressed beams, different prestressing forces are used depending on which parameter is analysed. In general, half the strength of the laminate is used to prestress the laminate. This means that high modulus CFRP is prestressed with 80 kN, and high strength CFRP is prestressed with 240 kN. However, models with other prestressing forces are also included in the analysis.

5.3.2 Loading

The beams are loaded in four-point bending. Two concentrated loads are applied symmetrically at the top flange of the beam. This will result in a constant bending moment and zero shear force in the middle of the beam, see Figure 5.5. The benefit of this loading is that the influence of a varying moment and shear force is small.

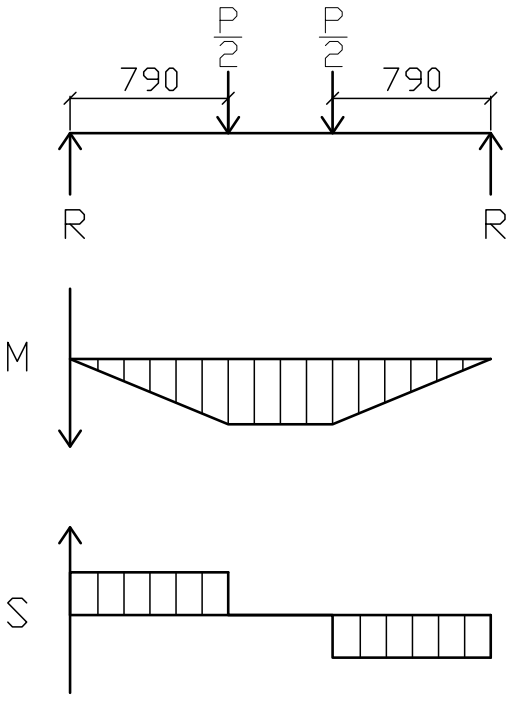

Figure 5.5 Schematically moment and shear force distribution.

The two concentrated loads, P/2, are acting on steel plates on the upper flange, see Figure 5.6. The area of the steel plates is 50x180mm^2 and its thickness is 10 mm. The concentrated loads are acting with a distance of 110 mm from the centre line of the beam, i.e. 790 mm from the supports.

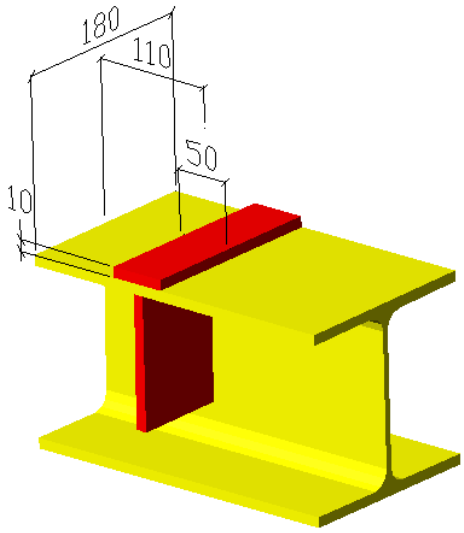

Figure 5.6 Steel plate where the concentrated force is acting.

6 Finite Element modelling

The FE-analyses are made using the commercial FEM software Abaqus version 6.5-1 and I-deas version 9. I-deas is superior to Abaqus when it comes to modelling and therefore all models were created in I-deas. The solving process will be performed in Abaqus or I-deas depending on the type of analysis (i.e. linear or non-linear). In addition some of the elements exist in I-deas but not in Abaqus and therefore a few models have to be analysed in I-deas.

The FE-model will be presented in this chapter.

6.1 Structural model

There are many ways to model a steel beam strengthened with CFRP-laminate. It was decided that modelling in two dimensions is appropriate the problem studied here. Because of the symmetry, only half the beam has to be modelled, see Figure 6.1.

The HEA beam was modelled with two flanges and a web. With the purpose of simplifying the model, the fillets between web and flange were neglected and no initial imperfects or residual stresses were included in the model.

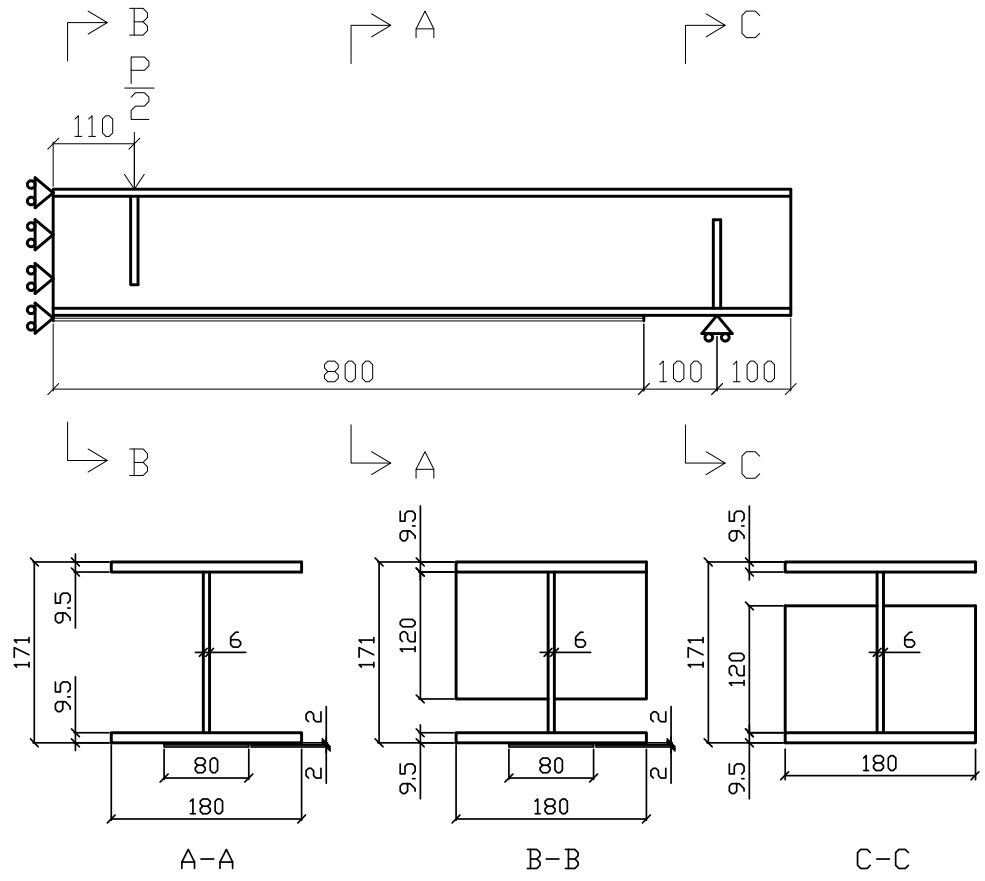

Figure 6.1 Dimensions of the FE-model.

6.2 Boundary conditions

Mechanical boundary conditions were applied to the regions where the displacements and the rotations were known. The degrees of freedom U1, U2, and U3 describe the axial displacement in each direction, see Figure 6.2. The degrees of freedom UR1, UR2, and UR3 describe the rotation around each direction.

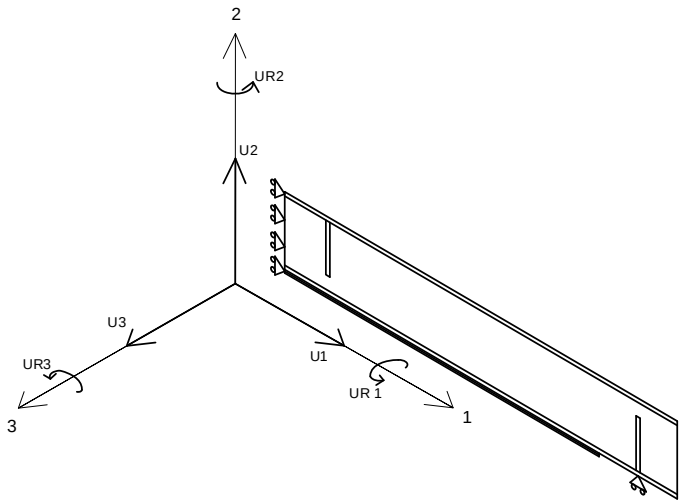

Figure 6.2 Degrees of freedom.

Due to symmetry, the mid-span of the beam will not be able to rotate and the only displacement along this section is in the vertical direction, i.e. the displacement in the 2-direction, see Figure 6.3.

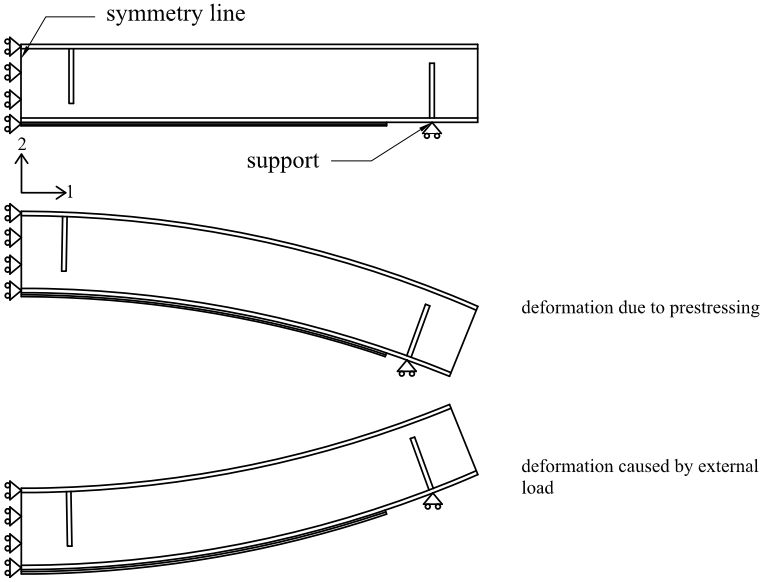

Figure 6.3 Degrees of freedom of the beam. Deformation due to prestressing and deformation caused by external load.

Along the symmetry line U1, U3. UR1, UR2 and UR3 were set to zero. At the support, the beam is able to rotate around its own axis, UR2, but is restricted to move in the vertical direction, U2. This will represent a simply supported roll-support.

6.3 Element type and mesh

The model has both two-dimensional plane stress elements and one-dimensional beam elements. The different elements will be described in the Sections below.

When meshing of the beam is executed, a number of parameters must be considered. A denser mesh will give better results, although the computational time will be longer. The interfacial stresses, at the end of the laminate, are influenced by the mesh density. In order to find an appropriate mesh, which ensures sufficiently accurate results, a convergence study was executed. With help of this study the mesh size in critical areas was chosen. After a convergence study, see Appendix I, an element size of 0.5x0.5 mm^2 was considered as appropriate for the adhesive at the end of the laminate. In areas where fine meshing is not needed, larger element sizes were used, see Figure 6.4.

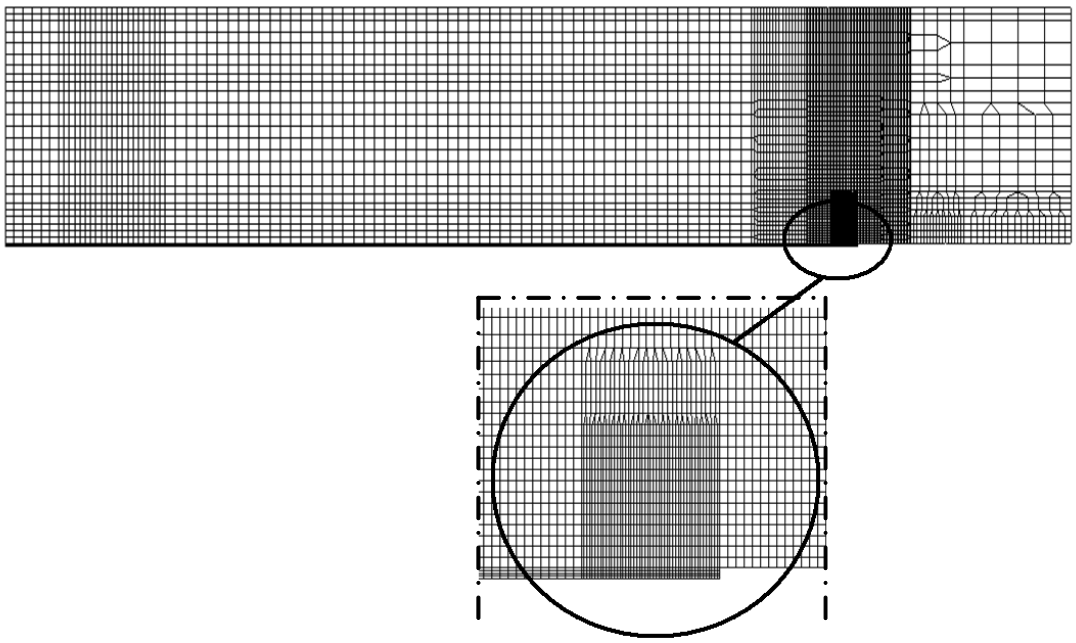

Figure 6.4 Mesh of the beam.

All elements were merged to each other by using the same nodes at the interfaces. This will give full interaction between the different parts of the structure.

6.3.1 HEA180-beam

The web and the flanges of the steel beam were modelled with two-dimensional plane stress elements, called 8-node bi-quadratic quadrilateral (see Figure 6.5) and 6-node quadratic triangle. Both element types have second-order, quadratic, interpolation. Plane stress elements are suitable for modelling thin structures. However, this is based on the assumption that there are no stresses in the out-of-plane direction.

The two-dimensional plane stress elements were assigned physical and material properties. In the physical properties the thickness of the element (web or the flange) was defined. The thicknesses of the flanges and the web were 180 mm respectively 6 mm. In the material properties the material model was defined.

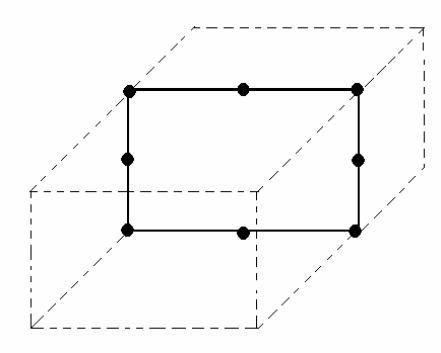

Figure 6.5 Two dimensional plane stress parabolic quadrilateral element.

6.3.2 Stiffeners

The stiffeners, at the support and at the points of load application, were modelled as one-dimensional beam elements. Beam elements are appropriate when the length of the structure is significantly greater than the size in the other two dimensions and the dominant stresses are in the direction of the axes, i.e. along the length of the stiffener.

The nodes will only be located along the length of the beam. The beam elements are one-dimensional line elements in three-dimensional space. The beam element used to model the stiffeners was 3-node parabolic beam, see Figure 6.6. They were given element properties, where cross-section and material properties were defined.

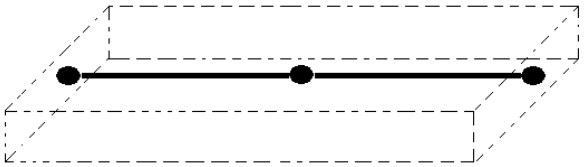

Figure 6.6 One dimensional beam element.

6.3.3 Adhesive

The adhesive was modelled with two-dimensional plane stress elements, called 8-node bi-quadratic quadrilateral, i.e. the same elements as for the HEA180-beam. The thickness was set to 80 mm, which is the width of the adhesive joint.

6.3.4 CFRP-laminate

The laminate was also modelled with beam elements. This is suitable because the length of the laminate is significantly greater than its width and thickness and the dominant stresses are in the direction of the axes, i.e. along the length of the laminate.

If beam elements are used it is easier to apply a prestressing force, which is applied with help of a negative temperature load and a thermal expansion factor. When beam elements are used, the expansion factor in the direction along the beam has to be added. If two- or three-dimensional elements were used it would be necessary to consider the contraction in different directions, which would make it more complicated.

In general, 3-nodes parabolic beam elements were used to model the laminate. In the models where laminates with tapered end are investigated, 2-nodes tapered beam elements and 2-nodes linear beams were used. By using the command offset, in I-deas, the nodes of the beam elements are moved. This is necessary because the nodes for the beam element are in the middle of the beam. If offset is not used the beam will overlap the adhesive, see Figure 6.7. With help of this command the nodes for the laminate can be moved half its thickness and receive its accurate position, see Figure 6.7.

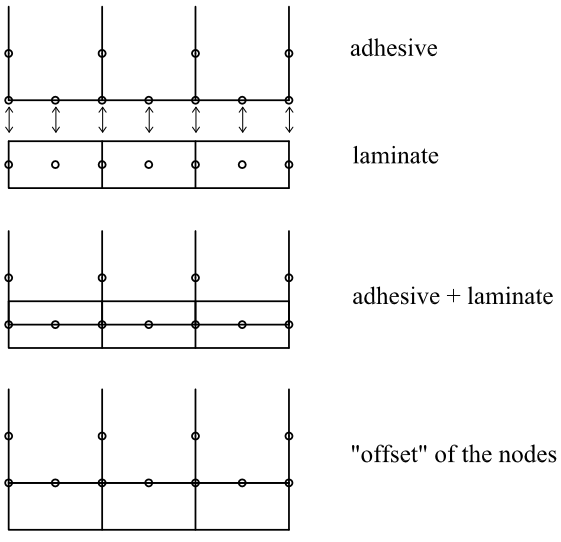

Figure 6.7 "Offset" of the nodes at the laminate.

6.4 Material models and data

The stress and strain received from tension tests on standard dog-bone specimens are called *engineering stress* or *nominal stress* (force per unit undeformed area) and *nominal strain* (length change per unit undeformed length). Abaqus requires values of the stress and strain that account for the changes in area during the finite deformations when the material is loaded. These values are called *true stress* and *true strain*. The nominal stress and the nominal strain that were obtained from tension tests performed at Chalmers were converted into true stress and true strain. A relationship between the true strain, the plastic strain and the elastic strain were needed to determine the plastic strains associated with the yield stress values.

The elastic modulus, the true stress, and the plastic strain were given as input for Abaqus. Abaqus then approximates the real smooth stress-strain relationship with straight lines between the values of the true stress and plastic strain that are given as input for the programme.

6.4.1 Steel

When only the effect of prestressing the steel beam is investigated, the steel material was modelled as a linear elastic material. When the beam was loaded, the steel was modelled as elastic-plastic material, this to be able to examine the behaviour when the steel is yielding. The nominal stress and the nominal strain from test specimens were given and true stress and plastic strain were calculated and used as input, see Table 6.1. The elastic modulus of the steel, as obtained from the tension tests, was 212 GPa and the true yield stress was 328.5 MPa.

Table 6.1 True stress and plastic strain of the steel.

Nom. Stress [MPa]	Nom. Strain	True Stress [MPa]	True Strain	Plastic Strain
0	0.00000	0.0	0.00000	
328.0	0.00161	328.5	0.00161	0.00000
332.0	0.00166	332.6	0.00165	0.00003
334.5	0.00172	335.1	0.00172	0.00008
337.2	0.00233	338.0	0.00233	0.00067
351.0	0.01300	335.6	0.01291	0.01117
335.0	0.02300	361.1	0.02274	0.02097
394.0	0.03700	408.6	0.03633	0.03433

6.4.2 Adhesive

The adhesive was modelled both as linear elastic up to failure and as elastic-plastic. When the adhesive was modelled as linear-elastic, an elastic modulus of 7 GPa was used. When the elastic-plastic behaviour of the adhesive was modelled it was assumed that the adhesive was elastic up to 12 MPa with an elastic modulus of 7 GPa. After 12 MPa the adhesive has a plastic behaviour. The poisson's ratio was 0.3 and the shear modulus was 2.69 GPa, as mention before. The nominal stress and the nominal strain were obtained from material tests performed at Chalmers (see Section 5.2.2) and true stress and plastic strain were calculated and used as input, see Table 6.2.

Table 6.2 True stress and plastic strain of the adhesive.

Nom. Stress [MPa]	Nom. Strain	True Stress [MPa]	True Strain	Plastic Strain
0	0.0000	0.0	0.0000	
12.0	0.0017	12.0	0.0017	0.0000
13.0	0.0019	13.0	0.0019	2.21E-05
15.0	0.0023	15.0	0.0023	1.32E-04
17.0	0.0028	17.0	0.0028	3.11E-04
19.0	0.0035	19.1	0.0035	7.18E-04
21.0	0.0044	21.1	0.0044	1.34E-03
23.0	0.0058	23.1	0.0057	2.41E-03
25.0	0.0077	25.2	0.0077	4.03E-03

6.4.3 CFRP-laminate

The CFRP-laminates were assumed to be linear elastic up to failure. The CFRP-laminate is an orthotropic material, but was modelled with beam elements. This is possible because only the stresses in the adhesive are of interest. In the models the laminate was modelled with one-dimensional beam elements for which only the material properties in the axial direction are required. An elastic modulus of 165 GPa was used for the high strength laminate and 400 GPa was used for the high modulus laminate.

6.5 Load

Two different loads are acting on the beam. The first one is the initial prestressing force acting on the laminate and the other one is the external loading. The self-weight of the materials were neglected.

6.5.1 Prestressing

The prestressing force was added to the structure by applying a negative temperature load, ΔT, to the beam elements which are representing the laminate. In order to receive a contraction of the laminate similar to the contraction after releasing the prestressing force, a thermal expansion coefficient, α, was assigned to the laminate. When the temperature is applied the laminate will contract according to equation (6.1). An initial axial stress is then received according to equation (6.2).

$$\varepsilon_0 = \Delta T \alpha \tag{6.1}$$

$$\sigma_0 = \varepsilon_0 \cdot E_l \tag{6.2}$$

where

E_l Elastic modulus of the laminate
ΔT Temperature load
α Thermal expansion coefficient
ε_0 Initial strain
σ_0 Initial stress

The axial force in the beam elements due to the axial stress will be gradually built up over the length of the laminate.

6.5.2 Loading

The external loading was applied as a four-point bending. The load was applied as a pressure on the upper flange, see Figure 6.8. The pressure was applied on a surface with the dimensions 50x180 mm^2. The load had its centre 110 mm from the symmetry line.

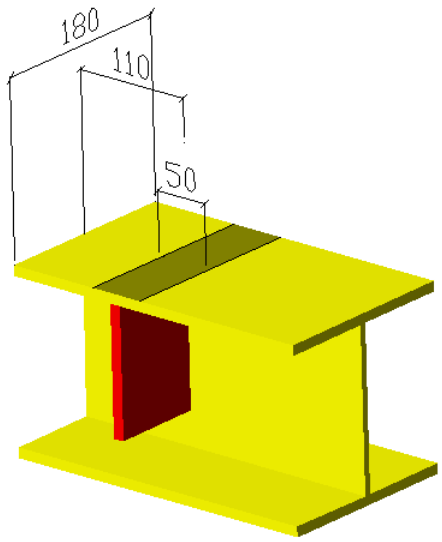

Figure 6.8 External load as pressure at the upper flange.

7 Compilation of Results from FEM-Analyses

In this chapter, the results from various FE-analyses are presented. The chapter is divided into three parts. In the first part the global behaviour of beams strengthened with prestressed and unprestressed laminate are compared with that of an unstrengthened beam. How prestressing, loading, and material properties influence the interfacial stresses is presented in the second part. In the last part, the effectiveness of different techniques and methods in reducing the interfacial stresses in the bondline is presented.

7.1 Global behaviour of prestressed beam

This first part presents the results from FE-analyses of the global behaviour of beams strengthened with different laminates. The steel beam used in the analyses of the global behaviour is presented in Chapter 5. The behaviour of the beam in the elastic phase and when the steel beam is yielding are presented.

Five different beams were analysed to investigate how the global behaviour will be affected when different laminates and different prestressing forces are used, see Table 7.1. Four beams were strengthened with CFRP-laminates and one was unstrengthened. The unstrengthened beam is used as a reference beam. Beam 1 and Beam 3 have high-strength CFRP-laminate and Beam 2 and Beam 4 have high-modulus CFRP-laminate. Beam 1 and Beam 2 were not prestressed. For Beam 3 and Beam 4 a prestressing force of half the tensile capacity of the laminate were applied to the beams. The resulting prestressing forces were 240 kN for Beam 3 and 80 kN for Beam 4.

Table 7.1 Beams used to investigate the global behaviour of strengthened beam.

	Modulus of elasticity CFRP-laminate [GPa]	Prestressing force [kN]
Reference beam	None	None
Beam 1	165	None
Beam 2	400	None
Beam 3	165	240
Beam 4	400	80

In general, two different limit states can be distingwished: elastic limit state and plastic limit state. For the elastic limit state the criterion is yielding of the outermost fibers of the beam cross-section at beam mid-span. When this limit was reached, the analysis was terminated. For the plastic limit state the “failure” criterion was 3.5

percent strain of the steel in compression. When the steel in the upper flange reached 3.5 percent strain the analyses were discontinued.

7.1.1 Elastic limit state

For many structures, such as railway bridges, plastic design is not allowed. Therefore, the behaviour in the elastic limit state has been analysed.

The results from the analyses are presented in Figure 7.1. What can be observed in this figure is that the deflection is negative for Beam 3 and Beam 4 before the load is applied. The negative deflection is a result of the prestressing force, which creates an initial moment. This deflection is 1.7 mm for Beam 3 and 0.6 mm for Beam 4. At this stage the upper flange is in tension and the lower flange in compression. However, at a certain level of applied external load the strain in the upper flange becomes zero for the prestressed beams. This appears at the load 15.1 kN for Beam 3 and 5.1 kN for Beam 4.

For Beam 1 and Beam 2, which are not prestressed, a stiffer behaviour than for the unstrengthened beam can be observed. Beam 1 is 3.6 % stiffer and Beam 2 is 8 % stiffer. Furthermore, Beam 1 and Beam 2 can take more load than the reference beam. The increase in yielding load is 2.4 kN for Beam 1 and 5.7 kN for Beam 2. That is an increase of 1.0 % for Beam 1 and 2.4 % for Beam 2 compared to the unstrengthened beam.

For Beam 3 the deflection of the mid-span is zero at the load 63 kN and for Beam 4 the deflection is zero at the load 22 kN. However, Beam 3 and Beam 4 cannot take 63 respectively 22 kN more load. This is due to the compressive normal force introduced into the beam. Instead, the increased capacities for the two beams are 17.5 kN respectively 10.3 kN, i.e. 7.3 % for respectively 4.4 %.

Therefore, for Beam 3 and Beam 4 the increase of load before the outmost upper fibre in the mid-section starts yielding is due to two effects. The first is the effect from the strengthening with laminate, which is 2.4 kN respectively 5.7 kN. The second is the effect of prestressing, which is 15.1 kN respectively 5.1 kN. The total effect is therefore 17.5 kN for Beam 3 and 10.8 kN for Beam 4.

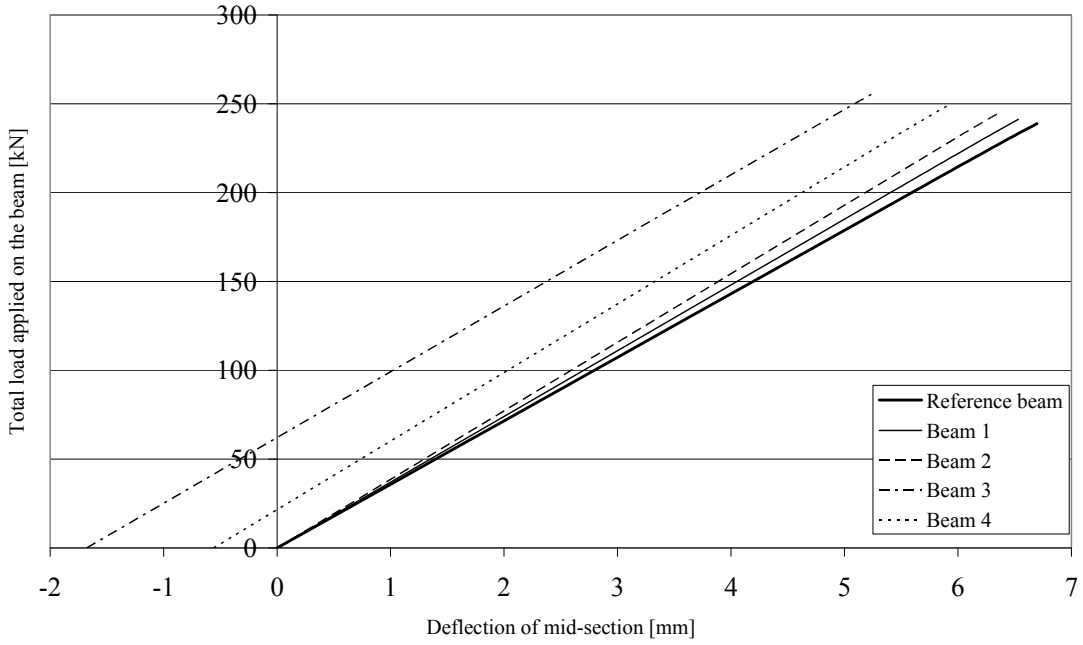

Figure 7.1 Load-deflection of unstrengthened and strengthened beams. Elastic limit state.

The loads and deflections for which the outmost fibre in the upper flange of the mid-section starts yielding can be found in Table 7.2. The effective deflection is the total deflection due to loading, i.e. from the deflection upwards due to the prestressing to the deflection downwards.

Table 7.2 The load and deflection when the steel in the mid-section, for Reference beam and Beam 1-4, starts yielding.

	Load when mid-section starts yielding [kN]	[%]	Deflection when mid-section starts yielding [mm]	Effective deflection [mm]
Reference beam	238.8	100	6.7	6.7
Beam 1	241.2	101.0	6.5	6.5
Beam 2	244.5	102.4	6.3	6.3
Beam 3	256.3	107.3	5.3	6.9
Beam 4	249.6	104.4	5.9	6.5

The increase in load at which the beam starts yielding is due to two factors. The first factor is the increase of moment of inertia for the cross-section. This effect is received

for all strengthened beams. The laminate will increase the effective moment of inertia and the neural axis will appear further away from the upper flange. The other factor is the effect of prestressing. This effect is of course only received for the two prestressed beams, i.e. Beam 3 and Beam 4.

With the equations in Section 4.1.1 the yielding load for the beams Beam 1-4 and the reference beam were analysed analytically, see Appendix J. The results from the analytical analyses were compared with the results from the FE-analyses, Table 7.3.

Table 7.3 Yielding load received from analytical analyses and the numerical analyses.

Beam	Analytical results [kN]	[%]	Numerical results [kN]	[%]
Reference beam	234.2	100	238.8	100
Beam 1	236.7	101.1	241.2	101.0
Beam 2	239.7	102.4	244.5	102.4
Beam 3	251.1	107.2	256.3	107.3
Beam 4	244.5	104.4	249.6	104.5

A difference between the yielding load for the analytical and the numerical analyses were observed. If instead the increase of yielding load is calculated the result will be similar, see Table 7.4.

Table 7.4 Increase of yielding load due to strengthening and prestressing.

	Increase of load due to (Analytical)		Increase of load due to (Numerical)	
	Strengthening [kN]	Prestressing [kN]	Strengthening [kN]	Prestressing[1] [kN]
Beam 1	2.5	-	2.4	-
Beam 2	5.4	-	5.7	-
Beam 3	2.5	14.4	2.4	15.1
Beam 4	5.4	4.9	5.7	5.1

[1] The effect of prestressing was found by observing the load when the strain in the outmost fibre in the upper flange was zero.

The increase of yielding load showed very similar results. The difference in the yielding load is a result of a disturbance near the mid-section. It is assumed that the mid-section has a constant moment and the stress distribution over the cross-section is linear. This is not true because of the two point loads acting only 110 mm away from the beam mid-span. And the stresses due to concentrated load will be spread down to the web and create local effects. For the reference beam the stresses will be larger in the lower flange than in the upper flange. This is a result of non-linear stress in the cross-section with higher stresses in the lower flange, see Figure 7.2. Therefore, all results from the FE-analyses were taken when the outmost upper fibre in the beam mid-span was yielding.

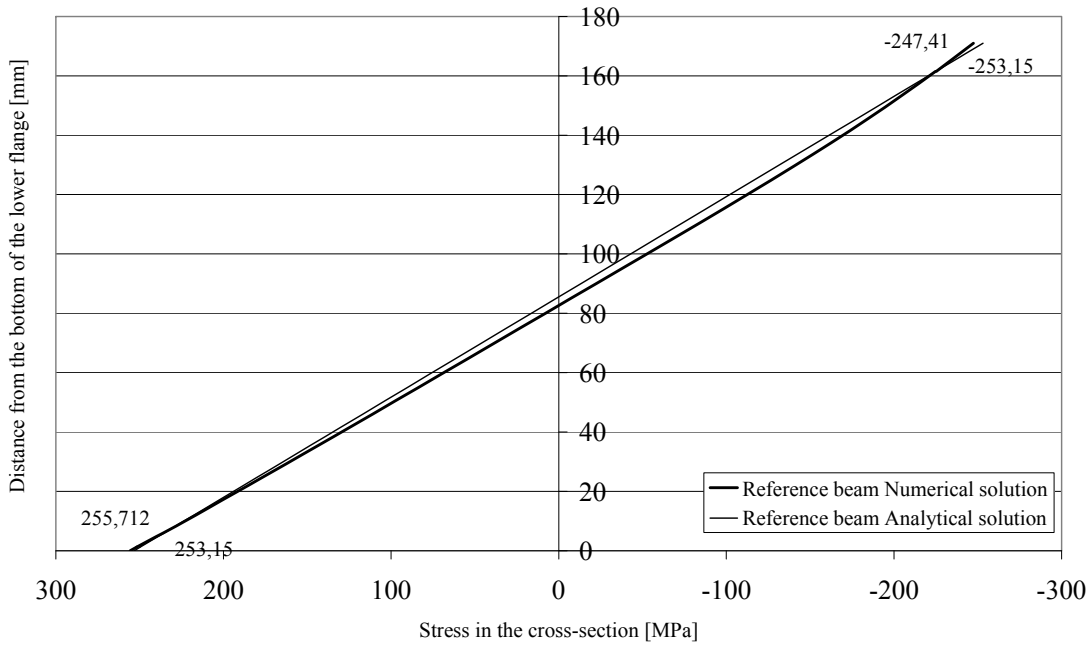

Figure 7.2 Stress distribution over the cross-section for the Reference beam at load P=180kN.

7.1.2 Plastic limit state

Figure 7.3 shows the behaviour of the five studied beams in the elastic and the plastic limit state. The different beams (see Table 7.1) were loaded until they reached 3.5 percent strain in the upper flange. The results show that an improved behaviour is obtained for the four strengthened beams compared to the unstrengthened beam. At the load 300 kN there is a large difference in deformation that can be observed for the different beams. However, when the load is further increased this difference tends to disappear.

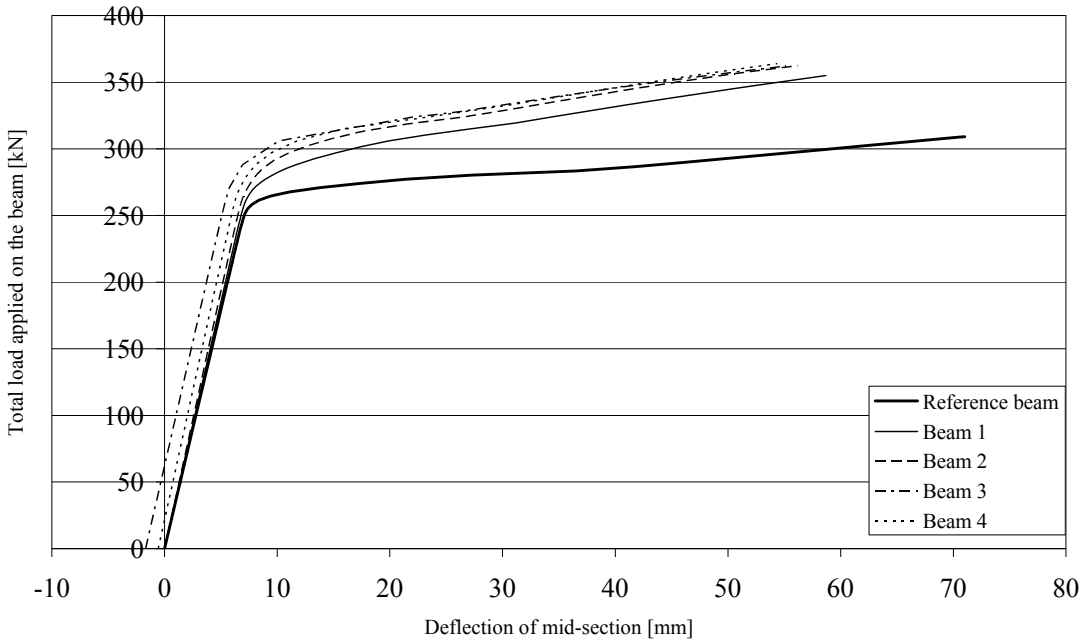

Figure 7.3 Load-deflection of unstrengthened and strengthened beams. Elastic and plastic state.

The ultimate moment capacity of the strengthened beams is increased with between 14.8 and 17.6 percent compared to unstrengthened beam, see Table 7.5. For Beam 2-4, 3.5 percent strain appears in the upper flange almost at the same load. The results show that the positive effects from the prestressing disappear when the beam is yielding. Observe that the only failure mode considered here is the strain in the steel beam.

Table 7.5 The load and deflection at failure for the Reference beam and Beam 1-4. The failure mode is 3.5 % strain in the upper flange of the beam mid-span.

	Load causing a strain of 3.5 % in the upper flange [kN]	[%]	Deflection at a strain of 3.5 % in the upper flange [mm]	[%]
Reference beam	309.1	100	71.1	100
Beam 1	355.0	114.8	58.7	82.6
Beam 2	362.5	117.3	56.2	79.0
Beam 3	362.2	117.2	55.2	77.6
Beam 4	364.0	117.6	54.4	76.5

In Table 7.5 the only failure criterion taken into account is the 3.5 percent strain in the upper flange. Table 7.6 also take the ultimate tensile capacity of the CFRP-laminate into account. The laminate in Beam 2 reaches its ultimate tensile strength already at a load of 291.6 kN. At this load the stress in the laminate is 1000 MPa. For Beam 4, which also has high-modulus laminate, the tensile failure will most likely appear already at a load of 175.5 kN. At this load the stress in the laminate is 1000 MPa, which is the ultimate tensile strength of the laminate. That means that the strengthening of Beam 2 would not increase the ultimate capacity and for Beam 4 the laminate will fail before the yielding load is reached.

Table 7.6 The load at failure for Reference beam and Beam 1-4. The failure mode is 3.5 % strain in the upper flange of the mid-section or tension failure of the laminate.

	Load at a strain of 3.5 % in the upper flange or capacity of laminate is reached [kN]	Failure mode	[%]
Reference beam	308.1	Steel	100
Beam 1	355.0	Steel	114.9
Beam 2	291.6	Laminate	95.4
Beam 3	362.2	Steel	117.8
Beam 4	175.5	Laminate	57.4

It was shown in the analyses of the global behaviour in the plastic state that the introduced prestressing force has no major influence on the ultimate capacity on a steel beam. Even if an increase of the ultimate capacity could be observed for the beam strengthened with prestressed laminate with an elastic modulus of 165 GPa. Instead, the main factor is the elastic modulus of the CFRP-laminate that influences the ultimate capacity. However, this is just true if the only failure mode is the strain in the steel. If all failure modes were taken into consideration, the result may be different.

7.2 The effect of various parameters on the interfacial stresses

There are many factors that can influence the magnitude of the interfacial stresses in the adhesive for beams strengthened with bonded prestressed composite plates. In this chapter the influence of prestressing, loading, and material properties is presented. The same double symmetric steel beam with a laminate bonded to the lower flange, as described in Section 5.1, is used in the analysis. The prestressing was carried out

according to Figure 7.4 and the results in this section show the behaviour after the adhesive has been fully cured and the prestressing force has been released.

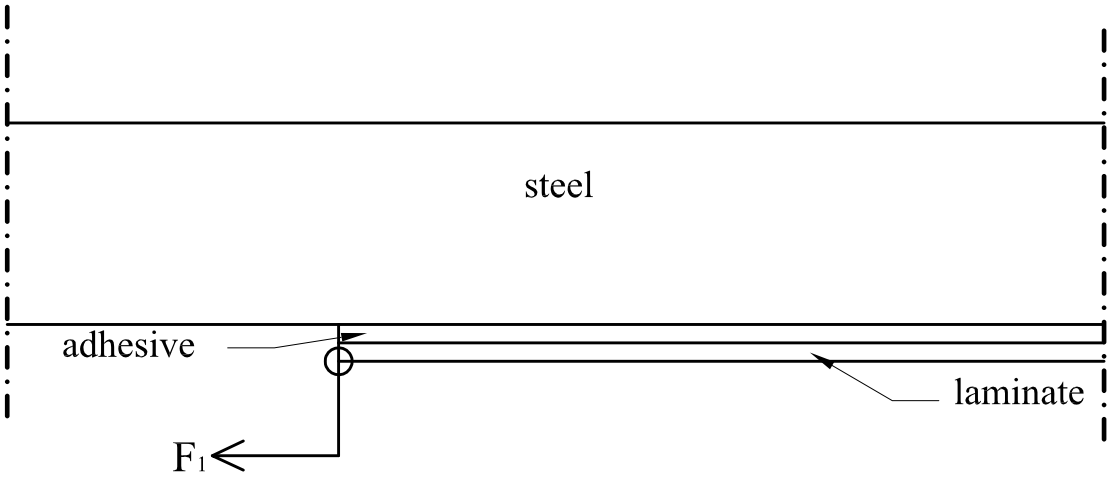

Figure 7.4 Prestressing of the laminate at the end of the laminate.

7.2.1 The effect of prestressing

To investigate how the interfacial stresses in the beam are influenced by the prestressing force a beam with a laminate with an elastic modulus of 165 GPa was used. By varying the prestressing force the influence can be examined. Five different prestressing forces were analysed. The different prestressing forces analysed were 0, 60, 120, 180, and 240 kN.

The distribution of the shear stresses at different prestressing forces can be found in Figure 7.5. The figure shows that the distance at which the shear stresses are acting does not increase. At the distance of 100 mm away from the end of the laminate the shear stresses are almost zero. This means that the prestressing force in the laminate is fully linked to the steel beam over a distance of 100 mm only. Therefore, the magnitude of the shear stresses at the end of the laminate will be increased. At a prestressing force of 240 kN the maximum shear stress is 159.2 MPa.

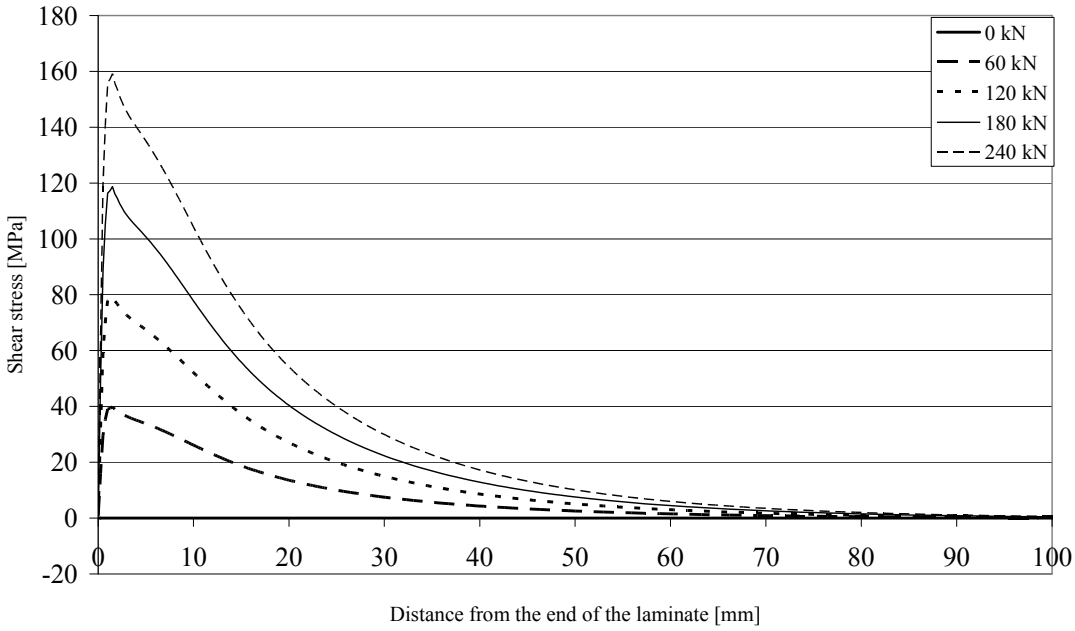

Figure 7.5 Shear stress distribution over a distance of 100 mm from the end of the laminate. Different prestressing forces.

In Figure 7.6 the distribution of the peeling stresses is plotted over a distance of 100 mm from the end of the laminate, for the five beams studied. What can be observed here is the point, approximately 4.5 mm away from the end of the laminate, where the peeling stresses are zero. This distance is not influenced by the prestressing force. When a prestressing force of 240 kN is applied the maximum peeling stress is 165.0 MPa.

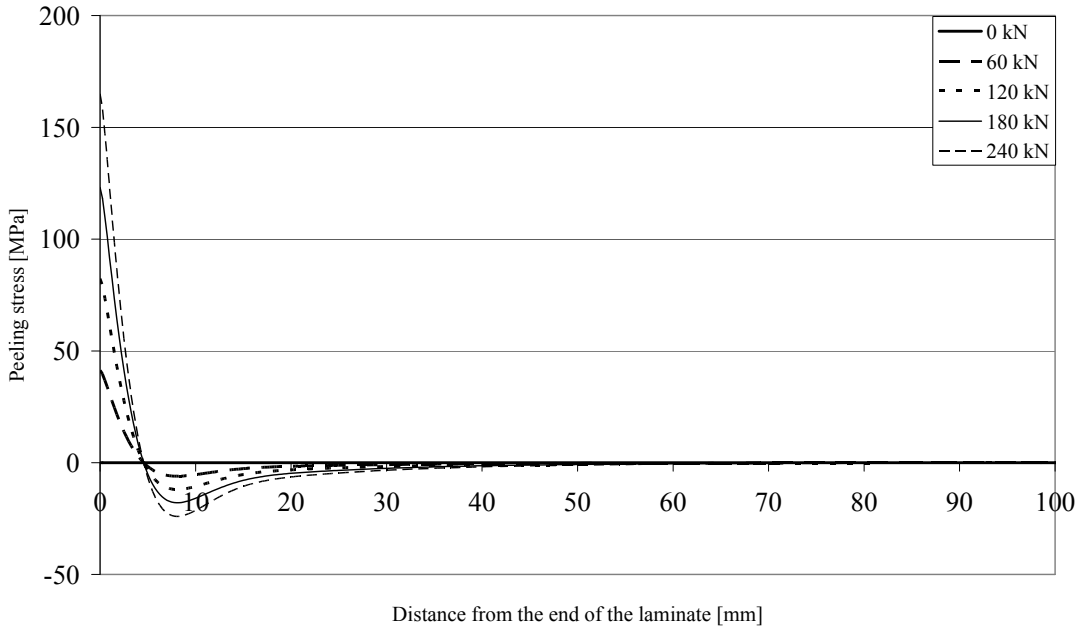

Figure 7.6 Peeling stress distribution over a distance of 100 mm from the end of the laminate. Different prestressing forces.

The result shows that the maximum shear and peeling stresses are proportional to the prestressing force. An increase of the prestressing force with 60 kN will increase the maximum shear stress with about 40 MPa and the maximum peeling stress with about 41 MPa, see Table 7.7.

Table 7.7 Maximum shear and peeling stresses. Different prestressing forces.

Prestressing force [kN]	Max. shear stress [MPa]	Max. peeling stress [MPa]
0	0	0
60	39.8	41.3
120	79.5	82.4
180	118.7	123.1
240	159.2	165.0

The prestressing force introduced into the beam will have a positive effect on the load for which the steel starts yielding. However, higher prestressing force will result in higher interfacial stresses in the adhesive.

The interfacial stresses are proportional to the prestressing force, see Figure 7.7. A higher prestressing force will result in higher interfacial stresses, as long as all other

parameters are kept constant. Therefore, it is important to not use a higher prestressing force in the laminate than necessary.

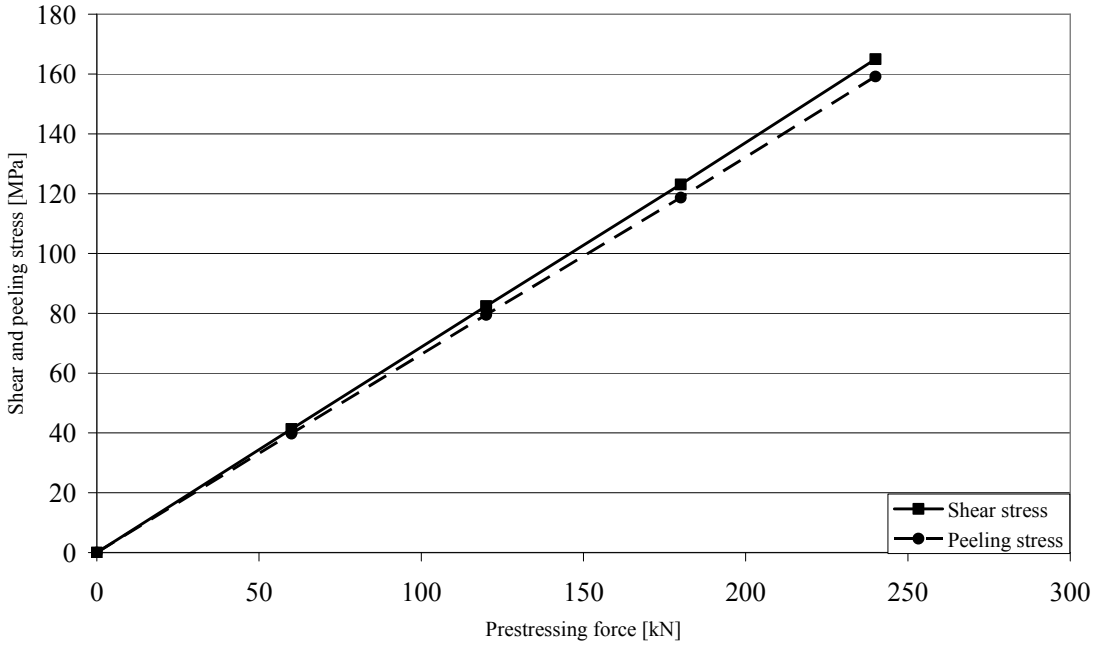

Figure 7.7 Maximum shear and peeling stress at different prestressing forces.

7.2.2 Interfacial stresses due to external loading

The interfacial stresses are influenced by the loading of the beam. Two steel beams were analysed to investigate how the stresses are influence by loading. The laminate is high-strength CFRP with an elastic modulus of 165 GPa. The adhesive used to bond the laminate to the steel beam has an elastic modulus of 7 GPa. The only difference between the two beams is that one is unprestressed and the other one is prestressed with 240 kN. The loading is in the elastic state of the beam, i.e. the steel in the cross-section do not reach yielding strain. The two beams were loaded with four points bending up to a total load of 234 kN and the result from five different loads were analysed. The loads are 0, 58.5, 117, 175.5, and 234 kN.

The first beam analysed is the beam strengthened with unprestressed laminate. The result from the first beam is presented in Figure 7.8. The results show that at a load of 234 kN the maximum shear stress in the laminate is 4.2 MPa. Furthermore, the shear stresses are increased by the increased load. At a distance of 100 mm away from the end of the laminate the stresses are approximately one sixth of the stresses compared to the maximum shear stress.

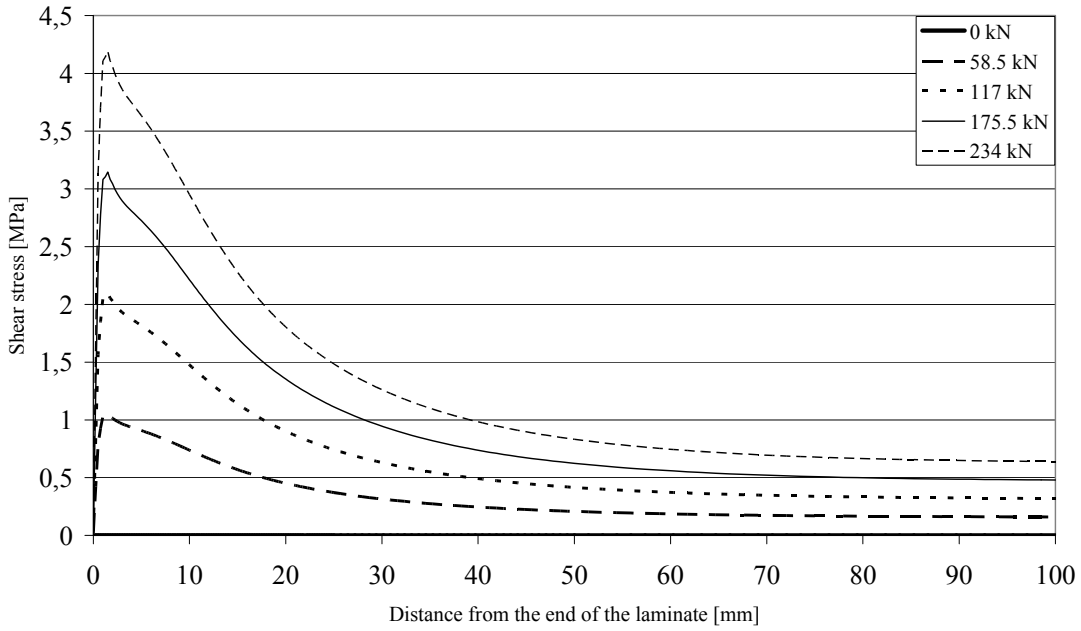

Figure 7.8 Shear stress distribution due to loading over a distance of 100 mm from the end of the laminate. Unprestressed laminate.

The peeling stresses due to loading are shown in Figure 7.9. The maximum peeling stress is 3.6 MPa. What can be observed is the point, approximately 4.5 mm away from the end of the laminate, where the peeling stresses are zero.

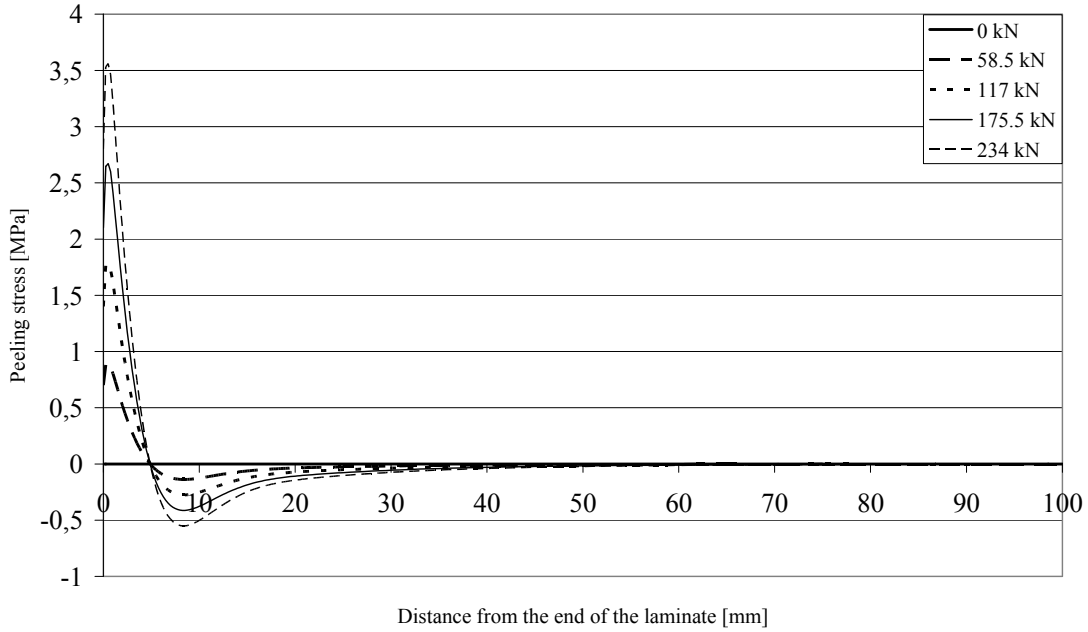

Figure 7.9 Peeling stress distribution due to loading over a distance of 100 mm from the end of the laminate. Unprestressed laminate

The maximum shear and peeling stresses and the maximum axial stress in the laminate at different loadings are presented in Table 7.8. The table shows how maximum shear stress, maximum peeling stress, and axial stress in the laminate are proportional to the loading.

Table 7.8 Axial stress in the laminate, maximum shear and peeling stress due to loading. Unprestressed laminate.

Loading [kN]	Max. shear stress [MPa]	Max. peeling stress [MPa]	Axial stress in the laminate [MPa]
0	0	0	0
58.5	1.0	0.9	62.8
117	2.1	1.8	125.6
175.5	3.1	2.7	188.4
234	4.2	3.6	251.3

The second beam that was analysed is the beam strengthened with prestressed laminate. The beam was prestressed with 240 kN and loaded up to 234 kN. The results for the five different loads are presented in Figure 7.10. At the load 234 kN the maximum shear stress in the adhesive is 163.4 MPa. The maximum shear and peeling stresses do not vary much due to loading of the beam. The high shear stresses are a result of prestressing.

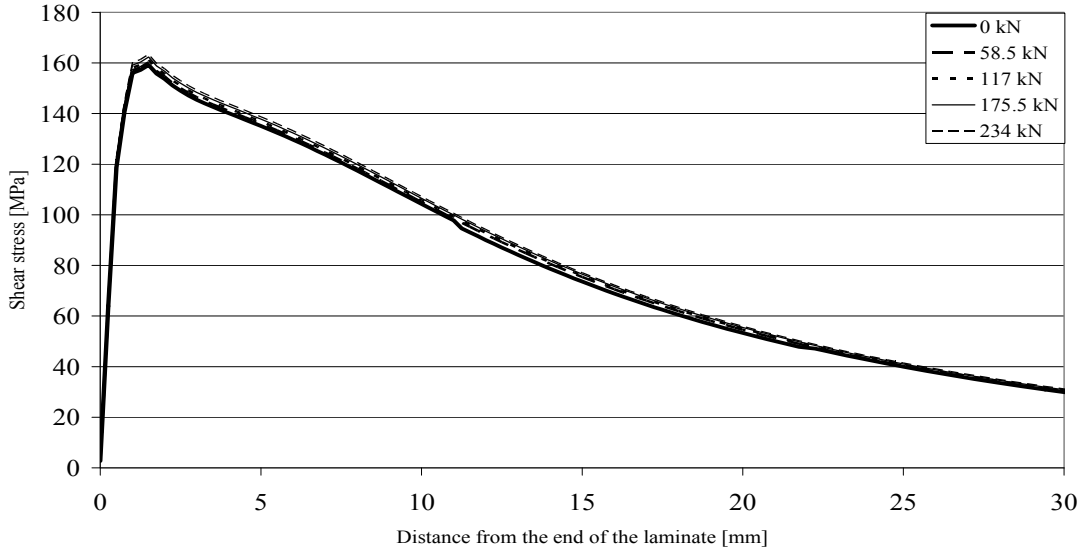

Figure 7.10 Shear stress distribution due to loading over a distance of 30 mm from the end of the laminate. Prestressed laminate.

How the peeling stresses increase with the load, for a beam strengthened with prestressed laminate, can be found in Figure 7.11. The increase of peeling stresses due to loading is small. The maximum peeling stress for the load 234 kN is 167.8 MPa. The maximum peeling stress due to prestressing, i.e. when the load is 0 kN, is 165 MPa. Even the prestressed beam has a point, approximately 4.5 mm away from the end of the laminate, where the peeling stresses are zero.

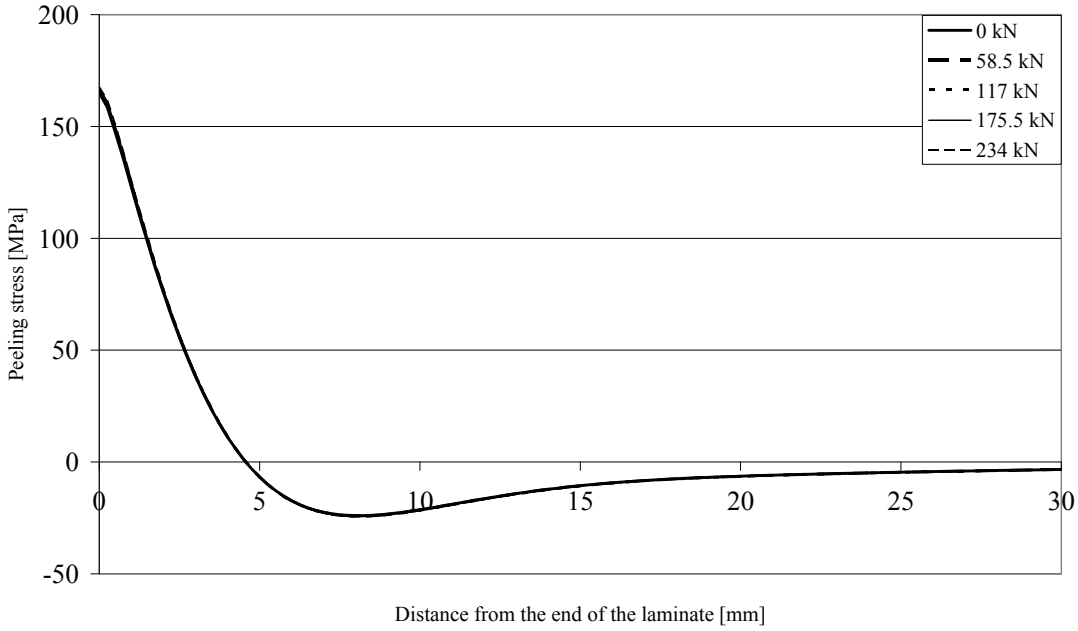

Figure 7.11 Peeling stress distribution due to loading over a distance of 30 mm from the end of the laminate. Prestressed laminate.

The high interfacial stresses in the laminate are the result of prestressing and not of loading. The maximum shear and peeling stresses are almost 40 respectively 46 times greater for a prestressed beam compared to an unprestressed beam at a load of 234 kN. However, the axial stress in the laminate is just 7 times greater.

The additional maximum shear and peeling stresses increase proportionally with the loading level, see Table 7.9. At the load 234 kN the maximum peeling stress in the laminate is 3.6 MPa. For each increase of the loading with 58.5 kN the maximum peeling stress increases with 0.9 MPa. Moreover, the same increase of load will increase the maximum shear stress with 1 MPa. A conclusion that can be drawn is that the additional maximum shear stress due to loading is not affected by the prestressing force. Table 7.9 shows that the additional maximum shear stress increases the same way as for the beam with unprestressed laminate. Delta max shear stress is the additional maximum shear stress due to loading.

The maximum peeling stress does not show the same behaviour. The increase of peeling stresses due to loading is less for the prestressed beam than the unprestressed

beam. The maximum peeling stress due to loading is 2.8 MPa for the prestressed laminate and 3.6 MPa for the unprestressed laminate.

Table 7.9 Axial stress in the laminate, maximum shear stress and maximum peeling stress due to loading. Prestressed laminate.

Loading [kN]	Max. shear stress [MPa]	Delta max. shear stress [MPa]	Max. peeling stress [MPa]	Delta max. peeling stress [MPa]	Axial stress in the laminate [MPa]	Delta axial stress in laminate [MPa]
0	159.2	0	165.0	0	1501.7	0
58.5	160.2	1.0	165.7	0.7	1564.5	62.8
117	161.3	2.1	166.4	1.4	1627.3	125.6
175.5	162.3	3.1	167.1	2.1	1690.5	188.8
234	163.4	4.2	167.8	2.8	1752.9	251.2

The interfacial stresses in the adhesive due to loading are because of the strain distribution in the cross-section. The strain is a result of the bending moment created by the load. As long as the steel is linear elastic the shear will be well distributed and follow the bending of the beam. Even though the bending moment is low at the end of the laminate the interfacial stresses are high compared to the stresses 100 mm away from the end. This is a result of the change of cross-section., which results in a stress-raiser. In that region the tensile stresses in the laminate have to be transferred into the steel beam. This will give higher interfacial stresses at the end of the laminate. However, these stresses have shown to be much lower than the interfacial stress due to prestressing.

Beams strengthened with prestressed and unprestressed laminates will have the same change of strain in the lower flange due to external loading as long as they have laminate with the same elastic modulus. The shear stresses in the adhesive due to loading will therefore be the same for unprestressed and prestressed laminates. However, there is a difference of the additional maximum peeling stress between the unprestressed beam and the prestressed beam. This can be a result of the deformation of the beam. An unprestressed beam will have a larger deflection compared to a prestressed beam. This can be the result of the small change of the maximum peeling stresses.

7.2.3 Effect of the adhesive E-modulus on interfacial stresses

To investigate how the interfacial stresses are influenced by different elastic modulus of the adhesive, five beams with adhesives having different E-modulus were analysed.

The beams were strengthened with high-strength CFRP-laminate which was prestressed with a prestressing force of 240 kN.

The result shows that the elastic modulus of the adhesive influences the maximum shear stresses and also the development length of the axial force in the laminate, see Figure 7.12. A stiff adhesive will result in a short development length and high maximum shear stresses. If instead an adhesive with low modulus of elasticity is used a more favourable distribution of the shear stresses can be obtained. An adhesive with an elastic modulus of 5 GPa will result in 20 MPa lower maximum shear stress compared to an adhesive with an elastic modulus of 7 GPa. How the maximum shear stress varies with different elastic modulus of the adhesive can be found in Table 7.10.

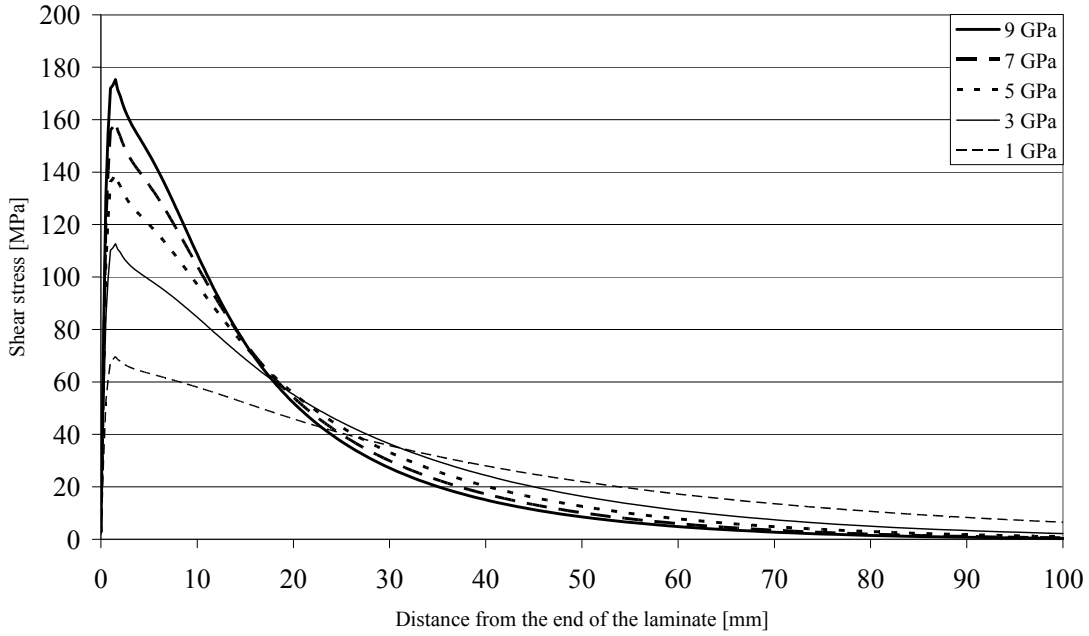

Figure 7.12 Sheer stress distribution over a distance of 100 mm from the end of the laminate. Different elastic modulus of the adhesive.

A stiffer adhesive will increase the peeling stresses, see Figure 7.13. If a less stiff adhesive is used, the peeling stresses decrease. An adhesive with an elastic modulus of 5 GPa will have 35 MPa lower peeling stresses than an adhesive with an elastic modulus of 7 GPa. Observe how the point where the peeling stresses are zero is moving away from the end of the laminate when the adhesive stiffness is reduced.

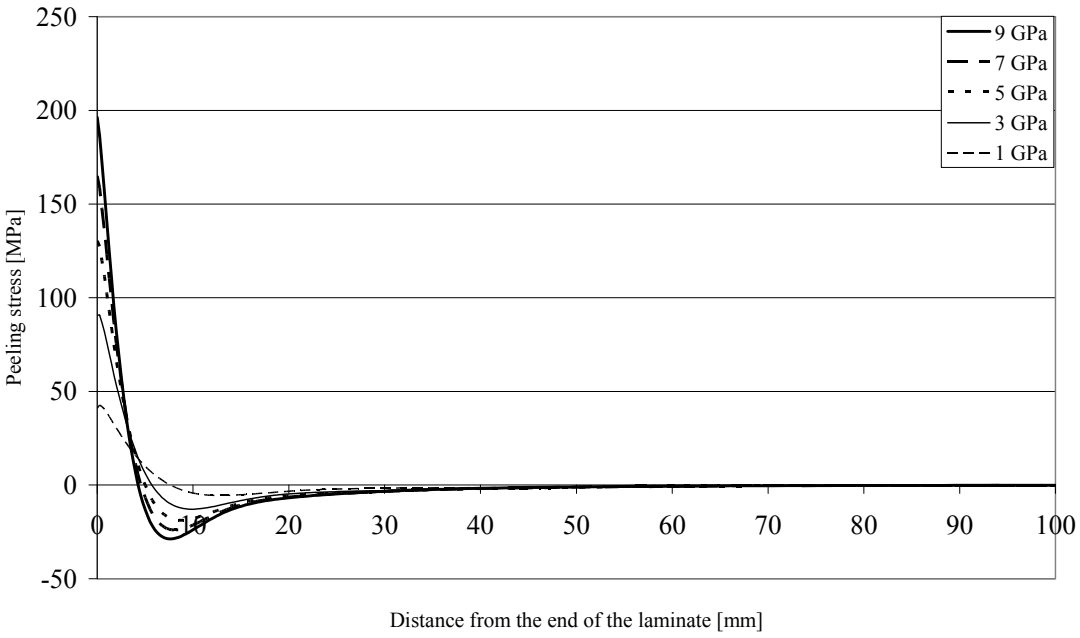

Figure 7.13 Peeling stress distribution over a distance of 100 mm from the end of the laminate. Different elastic modulus of the adhesive.

How the maximum shear and peeling stresses vary with different elastic modulus of the adhesive can be found in Table 7.10. In the table the values are compared with the maximum stresses obtained when the elastic modulus of the adhesive is 7 GPa.

Table 7.10 Maximum shear and peeling stresses. Different elastic modulus of the adhesive.

Modulus of elasticity [GPa]	Max. shear stress [MPa]	[%]	Max. peeling stress [MPa]	[%]
9	175.3	110	196.3	119
7	159.2	100	165.0	100
5	139.3	87.5	130.4	79.0
3	112.7	70.8	90.8	55.0
1	69.7	43.8	41.0	24.8

The elastic modulus of the adhesive has big effect on the interfacial stresses. The maximum shear stresses obtained from the FE-analyses was smaller than the results obtained from the analytical solution in Section 4.2.3. The difference was bigger for high modulus adhesive than for low modulus. However, both the FE-analyses and the

analytical analyses show that a reduction of the adhesive stiffness will reduce the maximum shear and peeling stresses.

The modulus of elasticity will affect the maximum value and the distribution of the interfacial stresses. Figure 7.14 shows how shear and peeling stresses vary at different elastic modulus of the adhesive. The maximum shear and peeling stresses change considerably for elastic modulus between 1 GPa and 9 GPa. An adhesive with an elastic modulus of 5 GPa instead of 7 GPa would reduce the peeling stress with 35 MPa, which is a reduction of 21%. The maximum shear stress would be decreased with 10 MPa, which is a decrease of 6.3%. This is because an adhesive with lower stiffness will allow a displacement of the laminate to take place without introducing high stresses in the adhesive. A less stiff adhesive results in a longer development length of the axial force in the laminate. The axial force in the zone at the end of the laminate is decreased, which will result in lower peeling stresses.

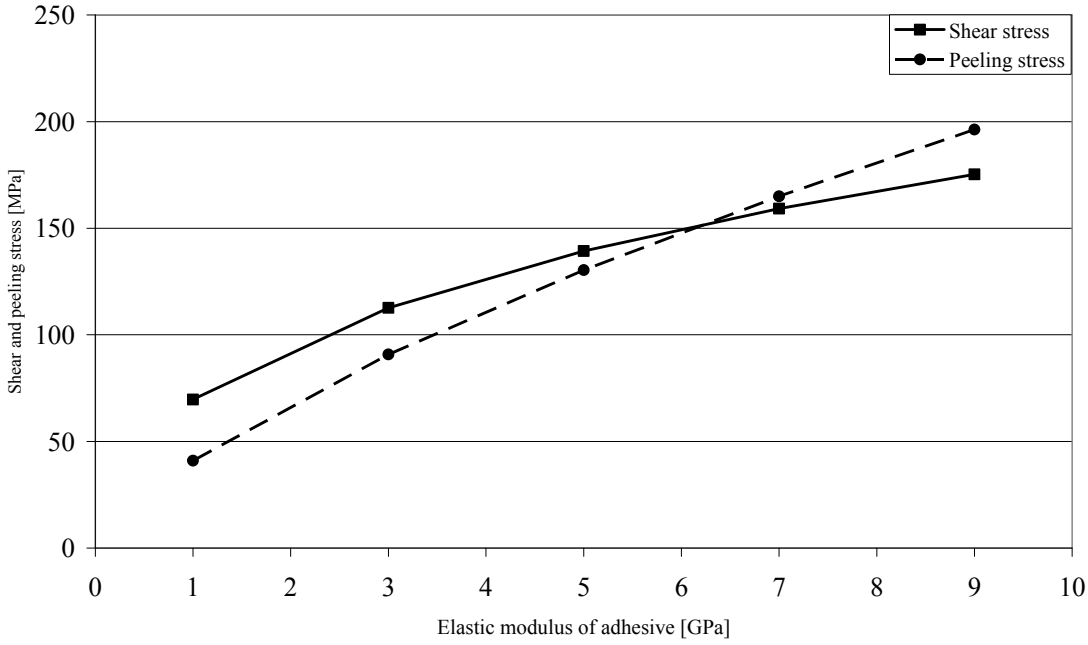

Figure 7.14 Maximum shear and peeling stress for different elastic modulus of the adhesive.

7.2.4 Effect of laminate E-modulus

To investigate how the interfacial stresses are influenced by the elastic modulus of the laminate, seven beams with different elastic modulus of the laminates were analysed. The laminates were prestressed with a prestressing force of 240 kN. All beams have the same cross-section and the same adhesive. The stiffest laminate has an elastic modulus of 1000 GPa and the least stiff laminate has an elastic modulus of 100 GPa.

The elastic modulus of the laminate influence the interfacial stresses. If a laminate with high modulus is used the maximum shear stress in the adhesive will decrease, see

Figure 7.15. This is of course true assuming that the prestressing force in the laminate is kept constant. By using a laminate with an elastic modulus of 200 GPa instead of a laminate with an elastic modulus of 165 GPa the maximum shear stress will decrease from 159.2 MPa to 148.3 MPa (i.e. a reduction with about 7%), see Table 7.11. Furthermore, a stiffer laminate will result in a further reduction of shear stresses.

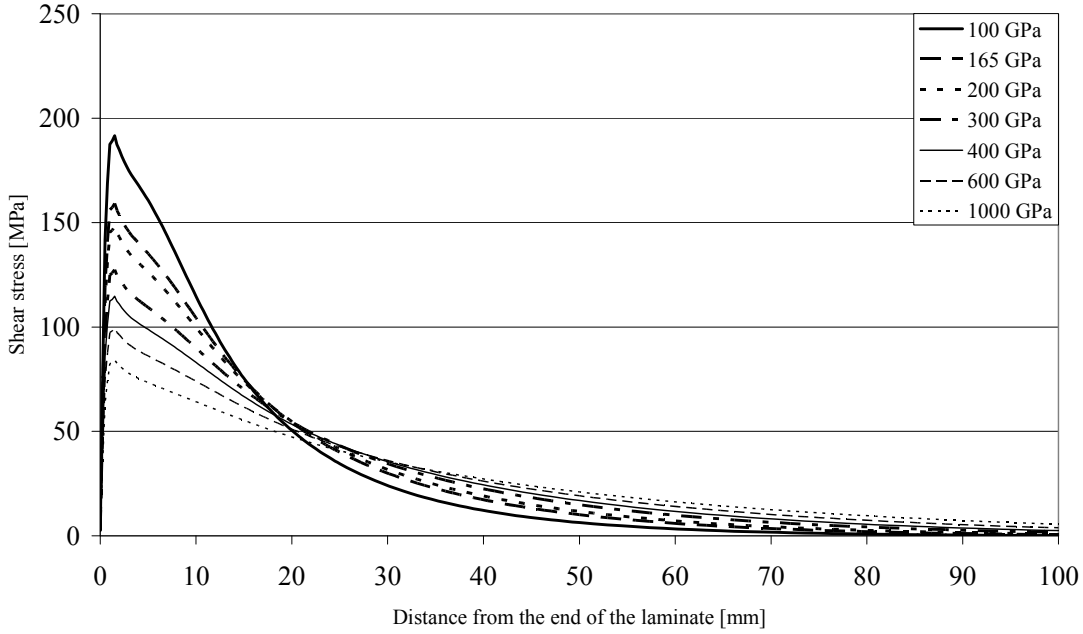

Figure 7.15 Sheer stress distribution over a distance of 100 mm from the end of the laminate. Different elastic modulus of the laminate.

An increased elastic modulus of the laminate has a positive effect on the peeling stresses as well, see Figure 7.16. By increasing the elastic modulus of the laminate the maximum peeling stress will be decreased. If the laminate has an elastic modulus of 200 GPa the maximum peeling stress will be 20 MPa lower compared to a laminate with an elastic modulus of 165 GPa, see Table 7.11. The point where the peeling stresses are zero is moving away from the end of the laminate.

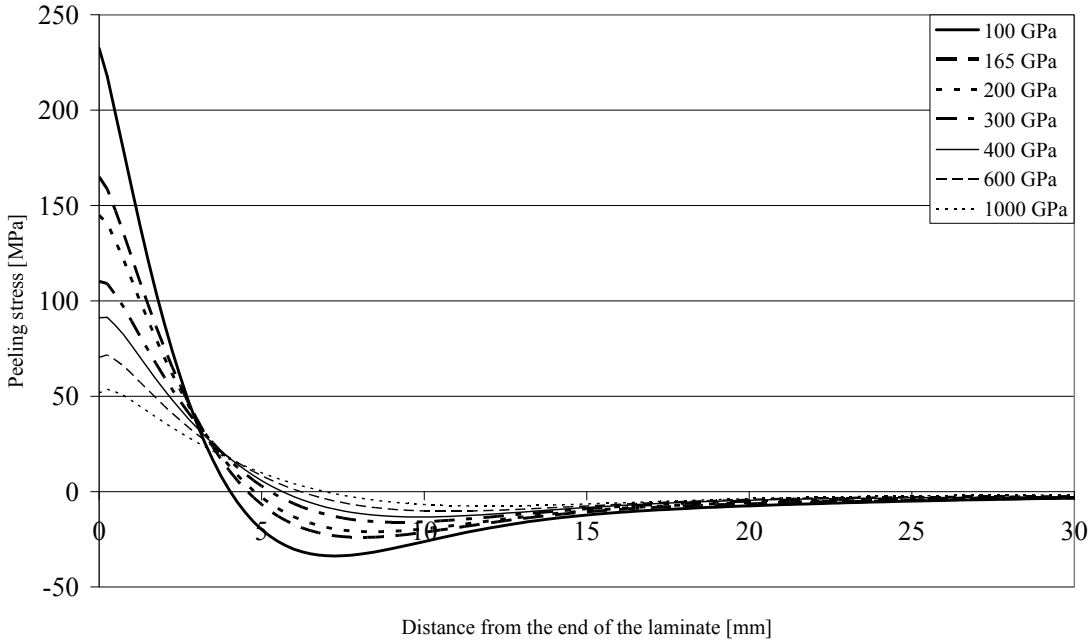

Figure 7.16 Peeling stress distribution over a distance of 30 mm from the end of the laminate. Different elastic modulus of the laminate.

The elastic modulus of the laminate will influence both the distribution and the maximum values of the shear and peeling stresses. This influence can be found in Table 7.11. The maximum shear and peeling stresses are also compared with the maximum shear and peeling stress obtained when the elastic modulus of the laminate is 165 GPa.

Table 7.11 Maximum shear and peeling stress. Different elastic modulus of the laminate.

Modulus of elasticity [GPa]	Max. shear stress [MPa]	[%]	Max. peeling stress [MPa]	[%]
100	191.6	120.4	232.4	140.8
165	159.2	100	165.0	100
200	148.2	93.1	144.8	87.8
300	127.4	80.0	110.2	66.8
400	114.7	72.0	91.2	55.3
600	99.4	62.4	70.3	42.6
1000	84.1	52.8	51.7	31.3

The elastic modulus of the laminate has shown to be another factor that influence the interfacial stresses considerably. However, FE-analyses showed lower maximum shear stresses than the analytical analyses in Section 4.2.4. The biggest difference can be observed for low modulus laminates.

In order to reduce the interfacial stresses in the adhesive due to prestressing, the laminate should be as stiff as possible. The stress in the laminate is a result of its elongation and for the same contraction a stiffer laminate will lose more stresses with the same displacement. That means a stiff laminate can transfer the axial force into the steel beam with a small displacement of the laminate itself. For that reason, a stiffer laminate needs smaller contractions of the laminate to reduce its axial force, which will result in more distributed shear stresses and a lower axial force at the end of the laminate. This means that a larger part of the axial force can be introduced into the beam further away from the end of the laminate. It will also result in reduced bending of the laminate and decreased axial force at the end of the laminate. The result will be an improved distribution of the shear stresses and lower peeling stresses. However, stiffer laminates have lower strength. For the beam analysed in this thesis, the high-modulus CFRP with the elastic modulus of 400 GPa did not have the accurate strength. As can be seen in Table 7.6, where both failure in the laminate and the steel is taken into account, the failure due to rapture of the laminate will most likely appear around a load of 175.5 kN. This can be compared with 364.0 kN, which is the theoretical ultimate capacity for the beam strengthen with prestressed high-modulus CFRP if only the failure due to strain of 3.5 percent in the steel is considered. However, if the strength of the laminate is overlooked it is favourable to use a stiff laminate. A stiff laminate will reduce the magnitude of the interfacial stresses due to prestressing, see Figure 7.17. It is however worth mentioning here that the situation is the opposite considering the effect of external loading. Here, stiffer laminate will result in substantially higher shear and peeling stresses. Figure 7.17 shows how the maximum shear and peeling stress are varying with different elastic modulus of the laminate.

The elastic modulus of the laminates, used in strengthening projects, range approximately between E = 100 GPa and E = 400 GPa. It is in this range the stress variation is the largest. If a laminate with an elastic modulus of 200 GPa is used instead of a laminate with an elastic modulus of 165 GPa the peeling stress would be decreased with 12 percent and the shear stress with 7 percent.

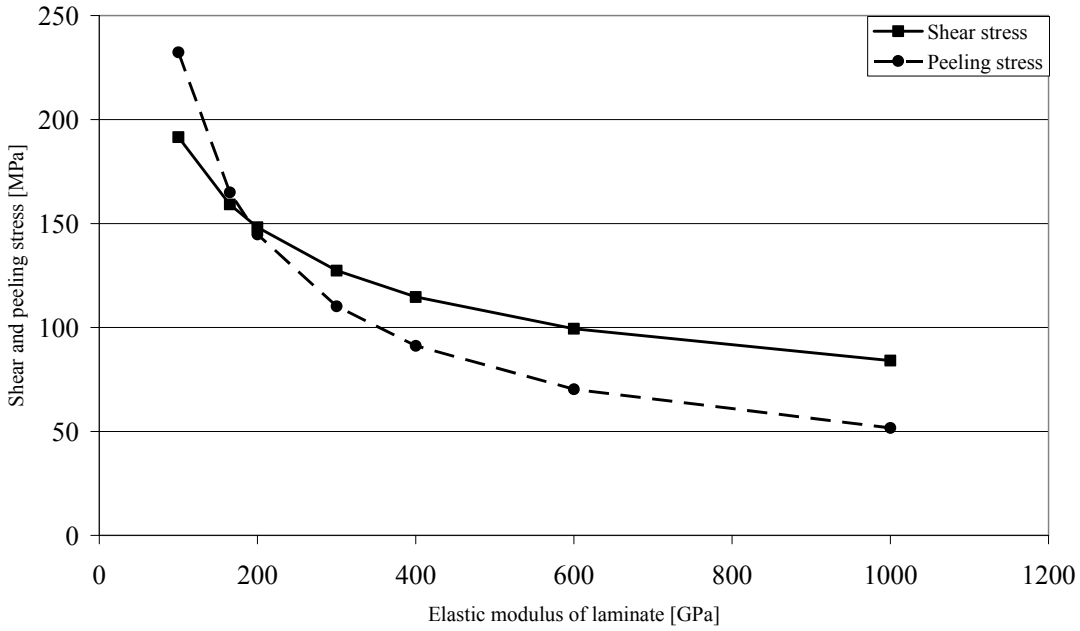

Figure 7.17 How maximum shear and peeling stress are varying with the elastic modulus of the laminate.

7.2.5 The effect of plastic behaviour of the adhesive

To investigate the effect of the plastic behaviour of the adhesive an FE-model with elastic plastic adhesive was compared with an FE-model with linear elastic adhesive. Taking the real behaviour of the adhesive, a smaller prestressing force of 20 kN was used in this investigation. If a higher prestressing force was used, the stresses in the adhesive would be higher than the strength of the adhesive used in the FE-model. The beams used were strengthened with a laminate with an elastic modulus of 165 MPa.

Figure 7.18 shows the result of plastic redistribution of the shear stresses. The high shear stresses at the end of the laminate will decrease and be more distributed. The maximum shear stress for linear elastic adhesive is 13.4 MPa and for elastic plastic adhesive the 10.7 MPa. This means that if the material is assumed to be linear elastic the maximum shear stress will be overestimated. The effect of plastic behaviour of the adhesive is therefore similar to the effect of the adhesive stiffness. However, the improved behaviour appears first when the stresses in the adhesive ecceed the linear limit of the material resulting in yielding.

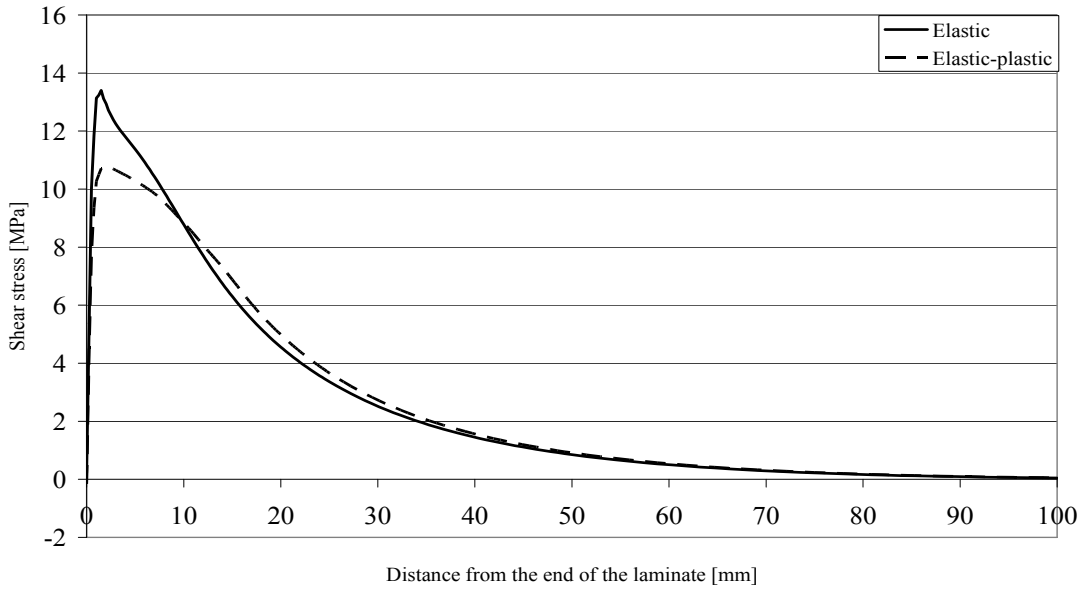

Figure 7.18 Sheer stress distribution over a distance of 100 mm from the end of the laminate. Linear elastic and elastic- plastic behaviour of the adhesive.

Also the peeling stresses will be influenced by the elastic plastic behaviour of the adhesive. Figure 7.19 shows how the maximum peeling stress decreases from 13.9 MPa for elastic adhesive to 10.1 MPa for elastic plastic adhesive. Due to the plastic behaviour, the distribution of the peeling stresses will be more uniform and the maximum peeling stress is reduced. The point where the peeling stress is zero will move away from the end of the laminate.

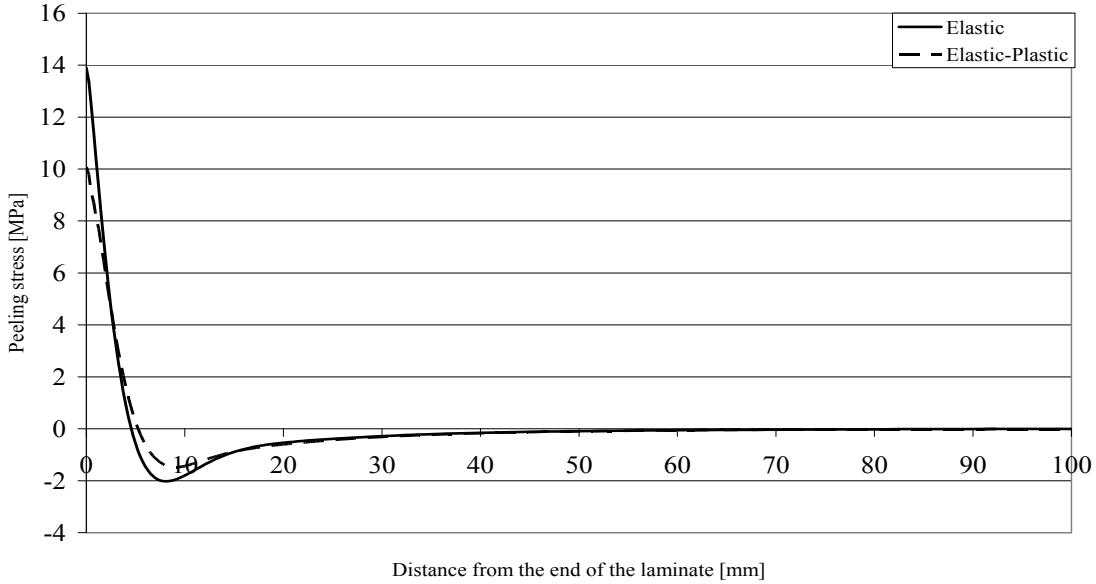

Figure 7.19 Sheer stress distribution over a distance of 100 mm from the end of the laminate. Linear elastic and elastic-plastic behaviour of the adhesive.

Since the stiffness of the adhesive influences the interfacial stresses, the material model used to analyse the stresses is important. In the other analyses performed, the adhesive is modelled as linear-elastic material. If the plastic behaviour is taken into account, the magnitude of the shear and peeling stresses will decrease. Because of the plastic behaviour the distribution length will be decreased and the axial force in the laminate will decrease at the end of the laminate, which results in reduced peeling stresses. Because of the plastic behaviour, the shear and the peeling stresses will be more uniformly distributed and lower maximum values of the stresses are achieved.

7.3 Techniques to decrease the interfacial stresses

Different techniques to decrease the interfacial stresses are presented in this section. The beams, used to examine how the interfacial stresses are influenced by these techniques and methods, have the same dimensions as described in Section 5.1. All beams are strengthened with prestressed laminate with elastic modulus of 165 GPa and the elastic modulus of the adhesive is 7 GPa. The introduced prestressing force is 240 kN.

7.3.1 Leaving the end of the laminate unprestressed

To study the effect of an unprestressed end, five models with five different lengths of the unprestressed part were analysed, see Figure 7.20. The shear and peeling stresses were then compared with a model with a prestressed end, see Figure 7.4. The five different lengths of the unprestressed part were 25, 50, 100, 150, and 200 mm.

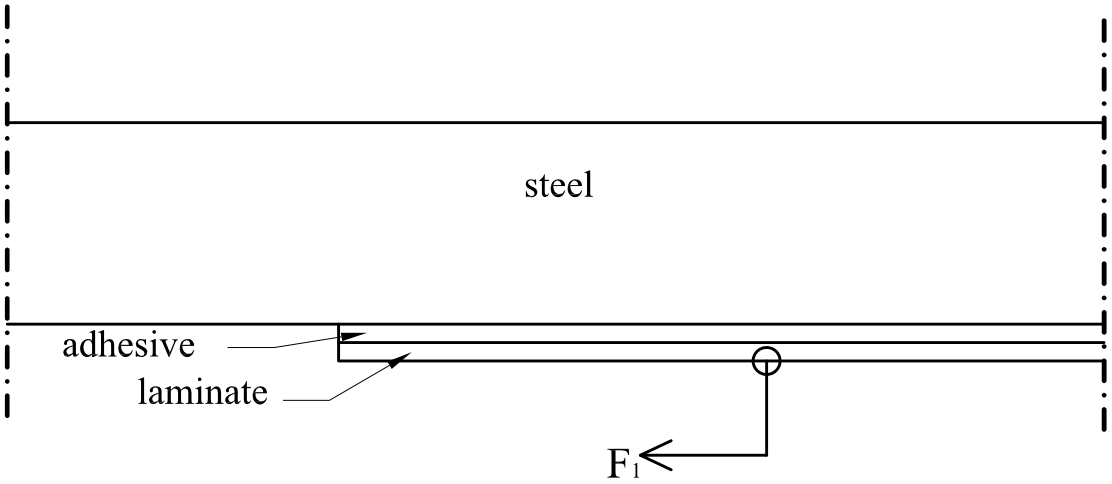

Figure 7.20 Prestressing of the laminate. Leaving the end of the laminate unprestressed.

Figure 7.21 shows the distribution of the shear stresses at the end of the laminate. What can be observed in this figure is that even a short length of the unprestressed

end will reduce the shear stresses significantly. An unprestressed end with a length of 25 mm reduces the maximum shear stress from 159.2 MPa to 89 MPa, see Table 7.12. The maximum shear stress appears at the border between prestressed and unprestressed, i.e. at a distance of 25 mm from the end of the laminate when the length of the unprestressed end is 25 mm. By leaving the end of the laminate unprestressed the maximum shear stress can be reduced by almost 50 percent, see Table 7.12.

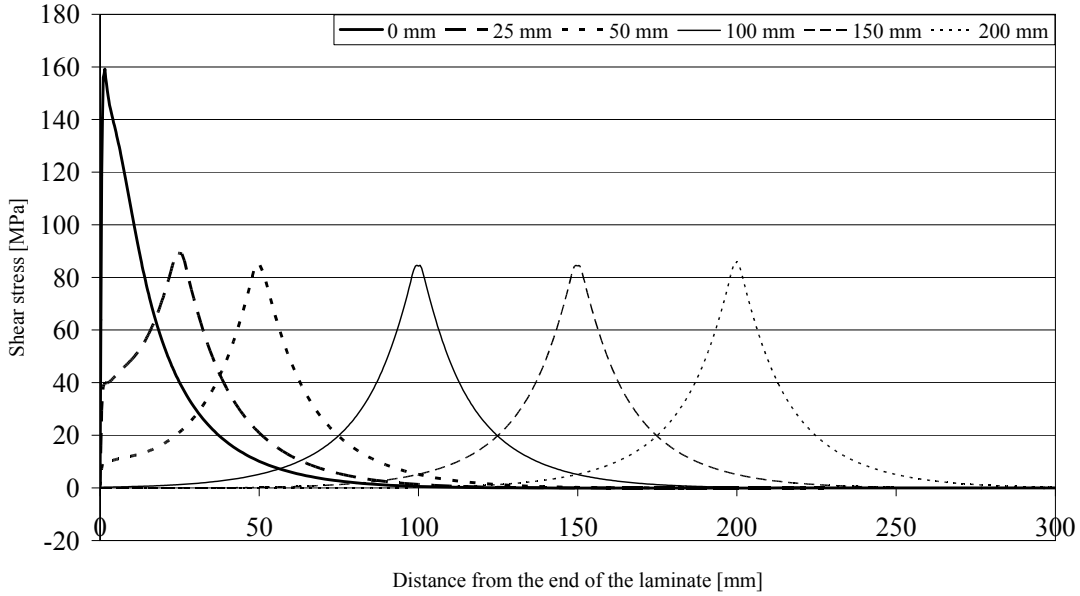

Figure 7.21 Shear stress distribution over a distance of 300 mm from the end of the laminate. Different lengths of the unprestressed end.

By prestressing the laminate and leave the end of the laminate unprestressed, there will be a very positive effect on the peeling stresses. By leaving 25 mm of the laminate unprestressed at the end the peeling stresses are reduced from 164.8 MPa to 37 MPa, see Figure 7.22.

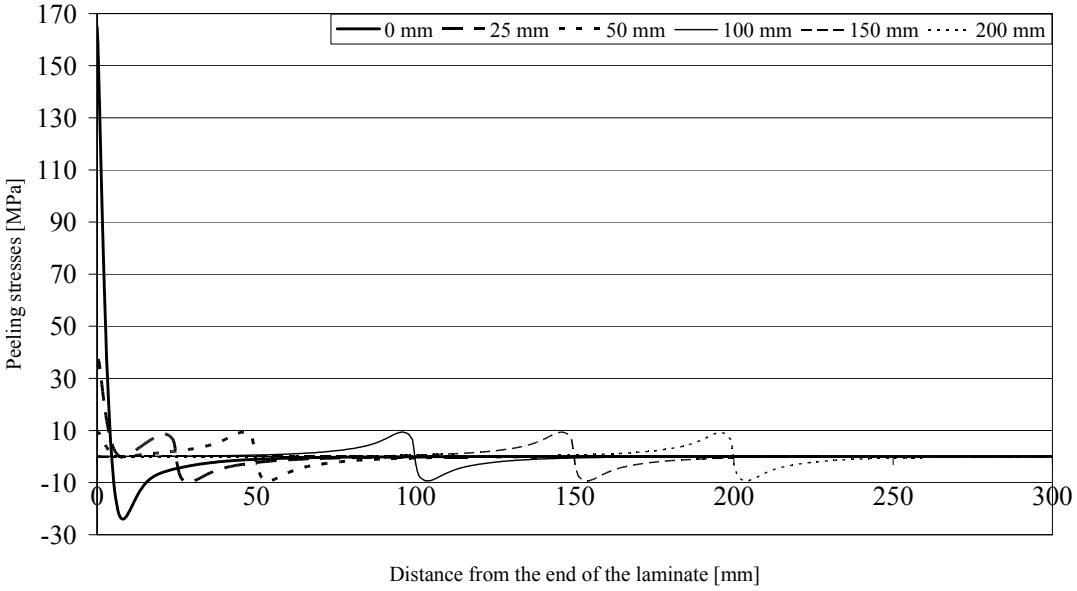

Figure 7.22 Peeling stress distribution over a distance of 300 mm from the end of the laminate. Different lengths of the unprestressed end of the laminate.

The influence of the different lengths of the unprestressed part of the laminate can be seen in Table 7.12. The results of the maximum shear and peeling stresses for different lengths of the unprestressed end are compared to the stresses obtained when the entire laminate is prestressed, i.e. the length of the unprestressed part is zero.

Table 7.12 Maximum shear and peeling stress. Different lengths of the unprestressed end of the laminate.

Unprestressed length [mm]	Max. shear stress [MPa]	[%]	Max. peeling stress [MPa]	[%]
0	159.0	100	164.8	100
25	89.0	56.0	37.0	22.4
50	85.2	53.6	9.2	5.6
100	84.6	53.2	9.4	5.7
150	84.6	53.2	9.4	5.7
200	86.1	54.2	9.4	5.7

Table 7.12 only consider the maximum shear and peeling stresses in the laminate. To investigate the effect at the end of the laminate of the unprestressed part a new table

was established, Table 7.13. In this table the maximum shear and peeling stresses at the last 10 mm are presented. The table shows that an unprestressed end with a length of 100 mm or longer will give almost no interfacial stresses at the end of the laminate due to prestressing.

Table 7.13 Maximum shear and peeling stress within 10 mm from the end of the laminate. Different lengths of the unprestressed end.

Unprestressed length [mm]	Max. shear stress within 10 mm away from the end of the laminate [MPa]	[%]	Peeling stress at the end of the laminate [MPa]	[%]
0	159.2	100	165.0	100
25	48.9	30.7	37.3	22.6
50	12.1	7.6	9.4	5.7
100	0.5	0.3	0.2	0.1
150	0.1	0.0	0	0.0
200	0	0.0	0	0.0

Besides reducing the maximum value of shear and peeling stresses, a benifitial effect of leaving the end of the laminate unprestressed is that the location of maximum shear and peeling is shifted away from the laminate end where the strength of the adhesive joint and the laminate is the lowest.

Figure 7.23 shows how the axial force increases gradually in the laminate. For the reference beam, where the whole laminate is prestressed, the axial force is introduced very fast. With an unprestressed end the axial force in the laminate is introduced more gradual. For the reference beam, with a prestressed end, the development length of the axial force is 100 mm. For an unprestressed end with a length of 100 mm the development length of the axial force is increased to approximately 200 mm.

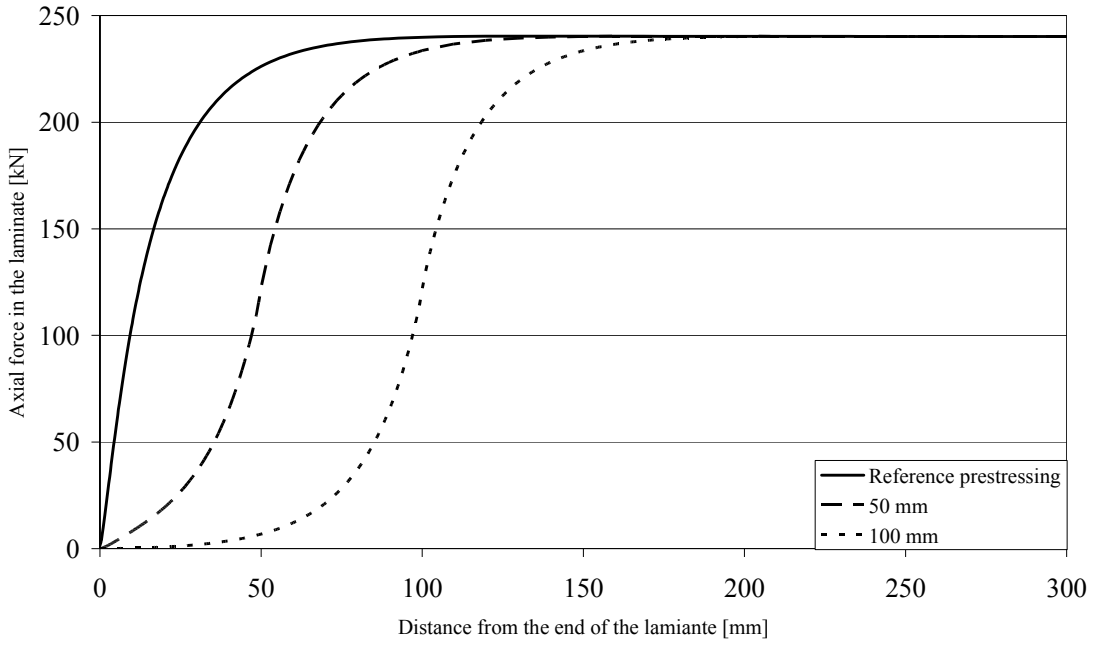

Figure 7.23 Axial force in the laminate over a distance of 300 mm from the end of the laminate. Different length of unprestressed end of the laminate.

By leaving the end of the laminate unprestressed the interfacial stresses can be reduced. The unprestressed part of the laminate will restrain the prestressed part of the laminate. The axial force in the laminate is thereby linked to the unprestressed part and this will reduce the slope of the axial force in the laminate, dF(x)/dx. This will result in a more distributed transfer of stresses between the steel beam and the laminate. However, the difference between the axial force in the prestressed laminate and the axial force in the unprestressed part is relatively big. The method decreases the stresses, but the stresses in the region between prestressed and unprestressed are still high. The maximum shear and peeling stresses are plotted for each length of the unprestressed end in Figure 7.24. The peeling stresses are more reduced than the shear forces. The reduction is due to two things. The first thing is that the difference of the axial force is smaller. The second thing is the contribution from the unprestressed part, which is reducing the bending of the laminate.

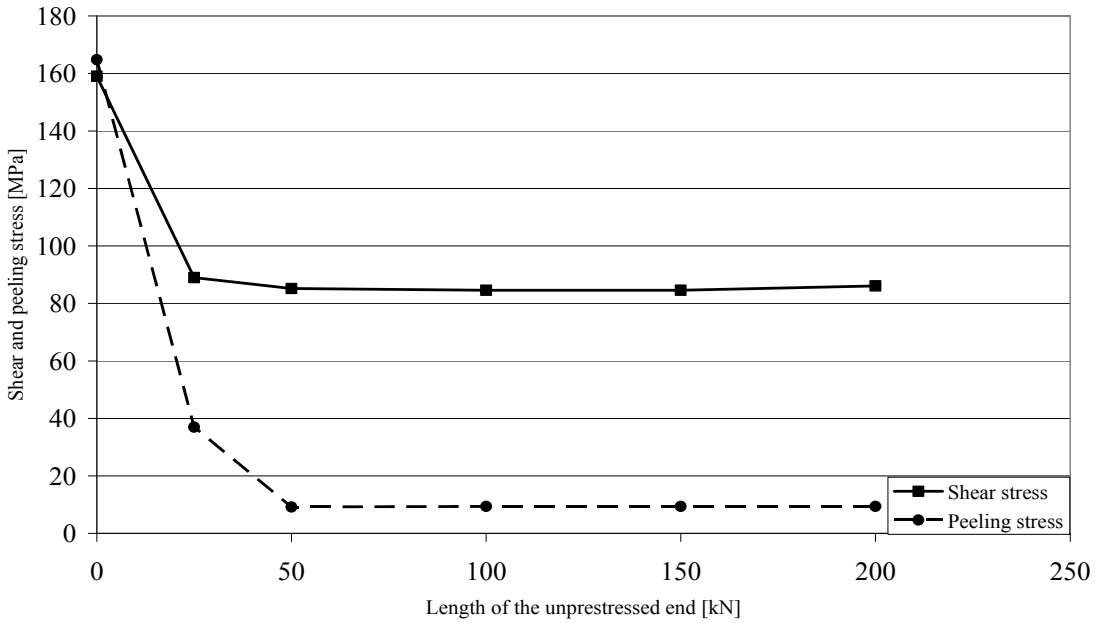

Figure 7.24 Maximum shear and peeling stresses for different lengths of the unprestressed end.

The largest improvement of an unprestressed end appears at the end of the laminate. With a 100 mm long unprestressed end the interfacial stresses at the end of the laminate are almost reduced to zero MPa, see Figure 7.25.

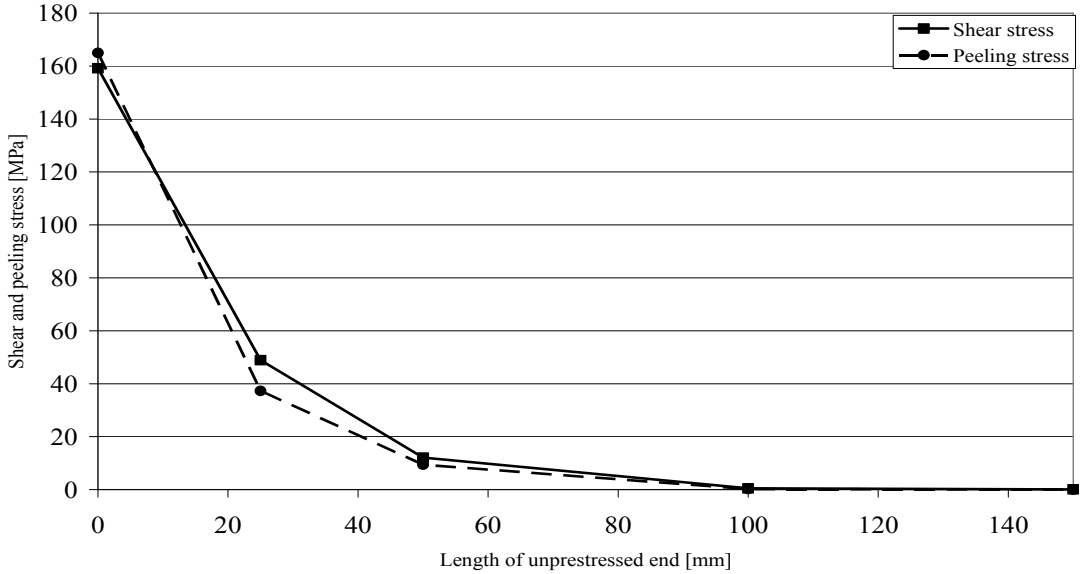

Figure 7.25 Maximum shear and peeling stresses at the end of the laminate. Different lengths of the unprestressed end.

7.3.2 Step releasing and gradual prestressing

In order to investigate the effect of step-releasing and gradual prestressing a beam with a laminate prestressed in 4 steps was analysed, see Figure 7.26. The effect of step releasing and gradual prestressing will give the same interfacial stresses. The only difference is the method used to introduce the prestressing force into the laminate. Therefore, the same analyses will be used for the both methods. The results from the analyses show the behaviour after the prestressing forces have been released. The beam used was a beam strengthened with prestressed laminate with an elastic modulus of 165 GPa. The prestressing force introduced into the beam was 240 kN. The distance between each step is 100 mm and at each step 60 kN was introduced into the laminate. Step releasing and gradual prestressing was compared to a reference prestressing. The reference prestressing is carried out in one step, see Figure 7.4.

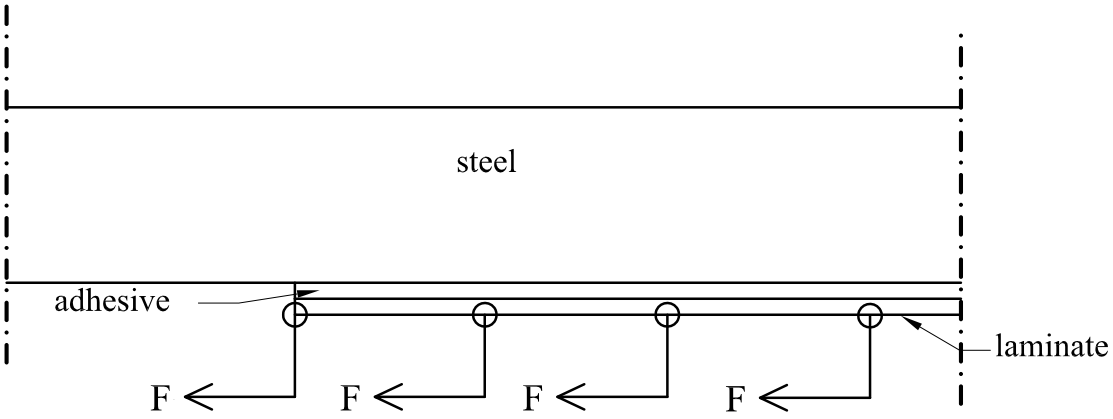

Figure 7.26 Step releasing and gradual prestressing in four steps.

Figure 7.27 and Figure 7.28 show the distribution of the shear and peeling stresses over a distance of 400 mm from the end of the laminate. The results show that both peeling and shear stresses were decreased. However, high interfacial stresses were observed at the end of the laminate. The maximum shear stress is 39.0 MPa at the end of the laminate and the maximum peeling stress is 41.3 MPa at the end of the laminate. Therefore, new analyses with step releasing and gradual prestressing in combination with an unprestressed end were performed.

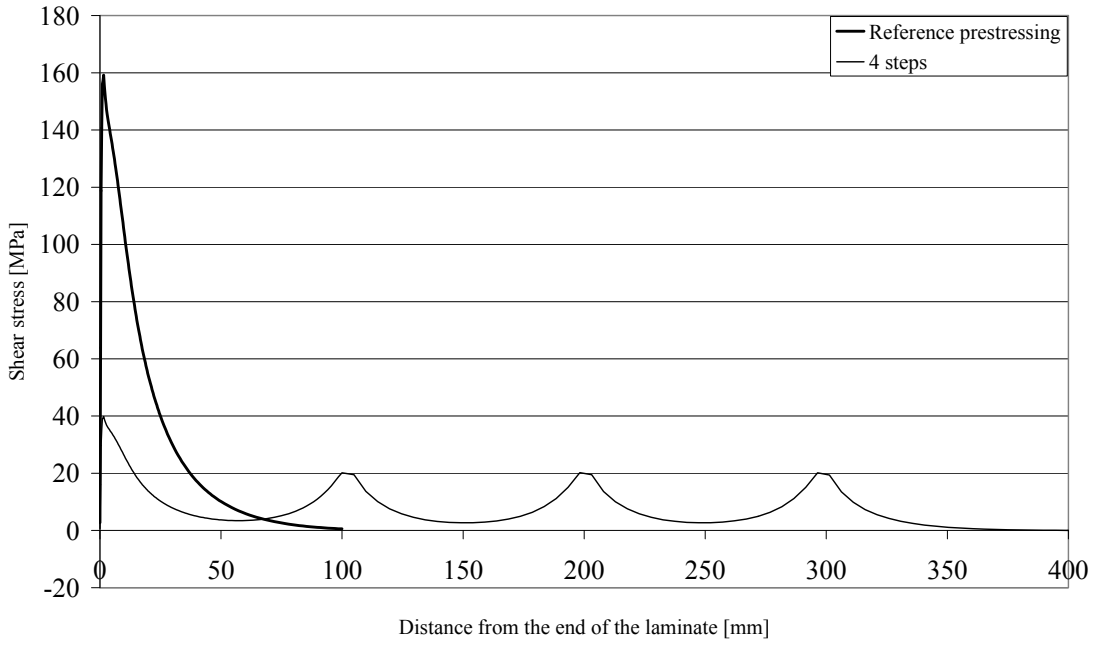

Figure 7.27 Sheer stress distribution over a distance of 400 mm from the end of the laminate. Step releasing or gradual prestressing with four steps.

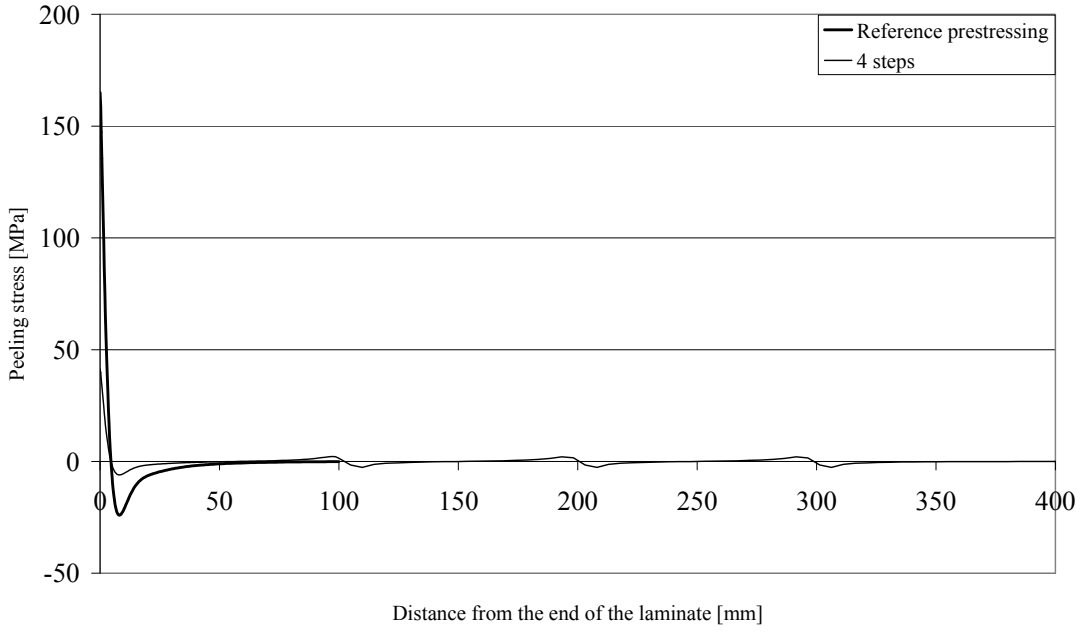

Figure 7.28 Peeling stress distribution over a distance of 400 mm from the end of the laminate. Step releasing or gradual prestressing with four steps.

To investigate the behaviour of step releasing and gradual prestressing in combination with unprestressed end four different models were analysed and compared with a reference beam. All five beams were strengthened with prestressed laminate with an elastic modulus of 165 GPa. The prestressing force introduced to the beam is 240 kN. All models except the reference beam have an unprestressed end with a length of 50 mm. Four different numbers of steps were considered. The different numbers of steps in the analyses were 1, 2, 4, and 8. For 2, 4, and 8 steps the distance between each step was 50 mm. The reference beam was prestressed in one step and with a prestressed end, see Figure 7.4.

The analysis of step-releasing and gradual prestressing in combination with an unprestressed end confirmed very good results. By leaving the end of the laminate unprestressed the shear stresses at the end of the laminate could be reduced. By introducing the prestressing force in several steps the interfacial stresses can be distributed over a larger area, see Figure 7.29. This will result in lower peak values of the shear stresses. If eight steps prestressing is performed instead of prestressing in one step the maximum shear stress can be reduced from 159.2 MPa to 11.8 MPa.

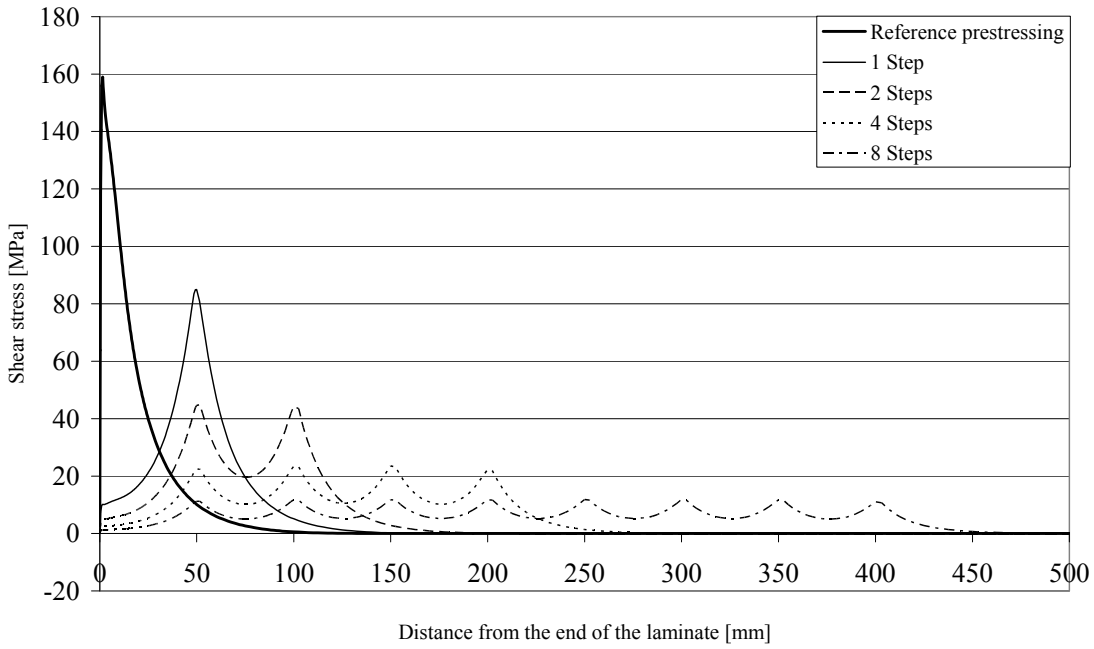

Figure 7.29 Sheer stress distribution over a distance of 500 mm from the end of the laminate. Step releasing or gradual prestressing with different numbers of steps and an unprestressed end with a length of 50 mm.

When it comes to the peeling stresses the greatest influence is from the unprestressed end. By combining four steps gradual prestressing or step releasing with a 50 mm long unprestressed end the maximum peeling stress decreases from 41.3 MPa to 2.3 MPa, see Figure 7.30. If step releasing or gradual prestressing is performed in eight steps the peeling stress can be reduced to 1.2 MPa.

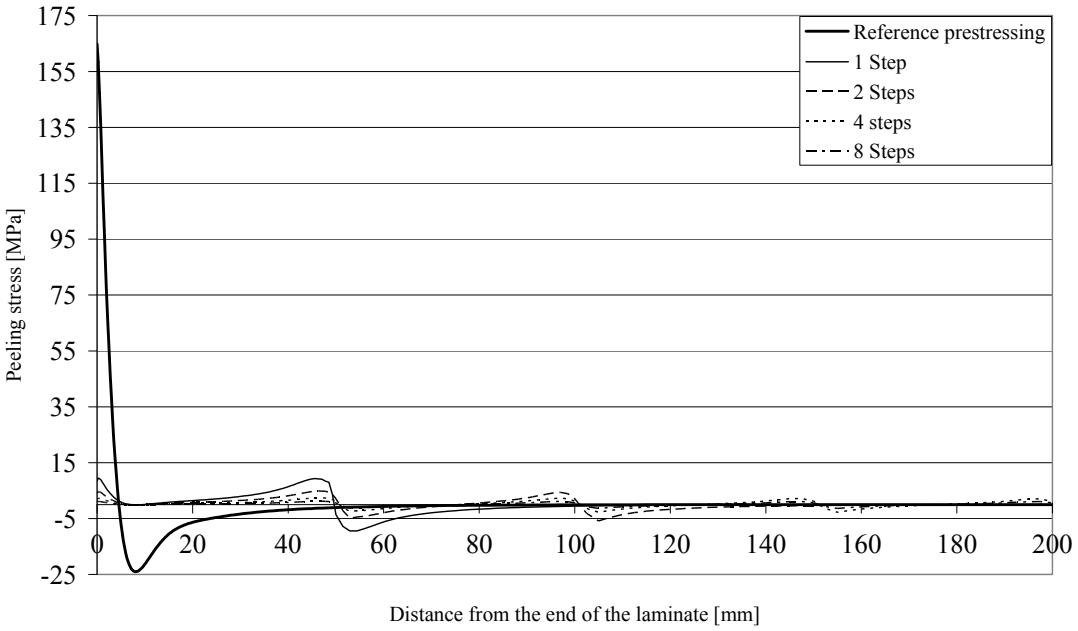

Figure 7.30 Peeling stress distribution over a distance of 200 mm from the end of the laminate. Step releasing or gradual prestressing with different steps and an unprestressed end of 50 mm.

How maximum shear and peeling stresses are influenced by the numbers of prestressing steps is presented in Table 7.14. The maximum shear and peeling stresses for different steps are compared with the reference beam. An increased number of prestressing steps will result in reduced maximum shear and peeling stresses. The number of steps will also decrease the stresses at the end of the laminate.

Table 7.14 Maximum shear and peeling stresses. Step releasing or gradual prestressing with different steps and an unprestressed end of 50 mm.

Number of steps [mm]	Max. shear stress [MPa]	[%]	Max. peeling stress [MPa]	[%]
0	159.0	100	164.8	100
1	85.2	53.6	9.2	5.6
2	44.8	28.2	4.9	3.3
4	23.4	14.7	2.3	1.6
8	11.8	7.4	1.2	0.8

Figure 7.31 demonstrates how the axial force in the laminate is decreasing towards the end of the laminate. For the reference beam the stresses are built up in the laminate

over a very short distance. The development length of the axial force is 100 mm for the reference beam. If step releasing or gradual prestressing is used this development can be increased. For 8 steps the development length is 450 mm.

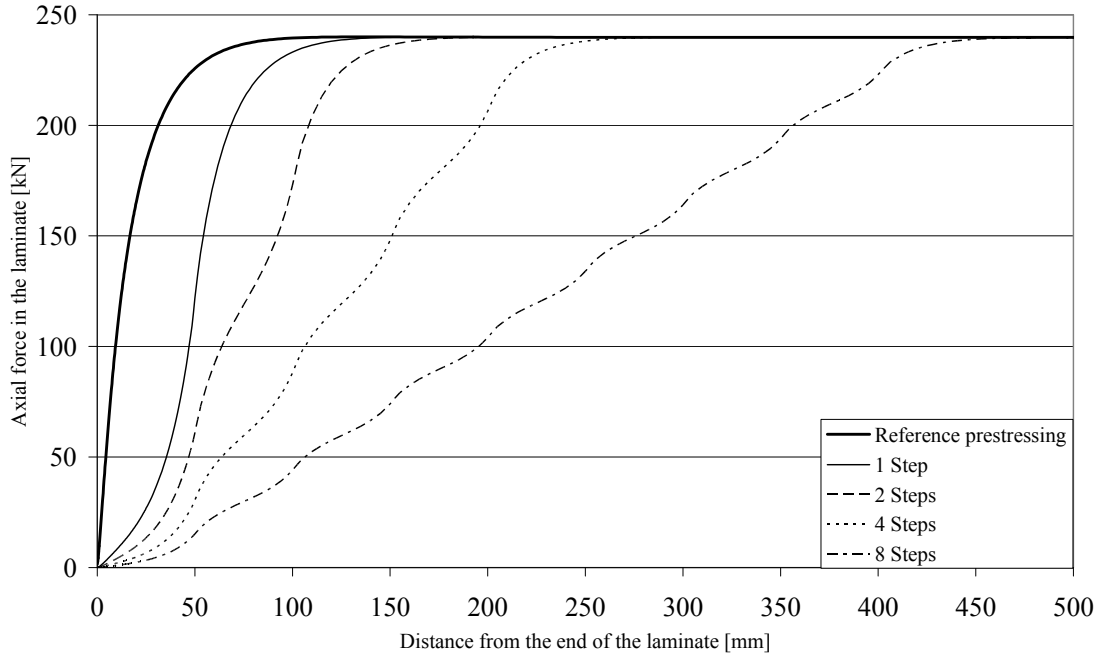

Figure 7.31 Axial force in the laminate over a distance of 500 mm from the end of the laminate. Step releasing or gradual prestressing with different steps.

Step releasing and gradual prestressing have shown to be excellent techniques to reduce the interfacial stresses in the adhesive. By prestressing in four steps instead of one, the maximum shear stress can be reduced to 25 percent of the maximum shear obtained with prestressing in one step. If the last 50 mm of the laminate is kept unprestressed the maximum shear stress will be reduced even further. If the step releasing and gradual prestressing is combined with unprestressed end the result will vary according to Figure 7.32. Figure 7.32 shows the maximum shear and peeling stresses for different numbers of steps and with 50 mm unprestressed at the end. The 0 step is the reference prestressing carried out according to Figure 7.4.

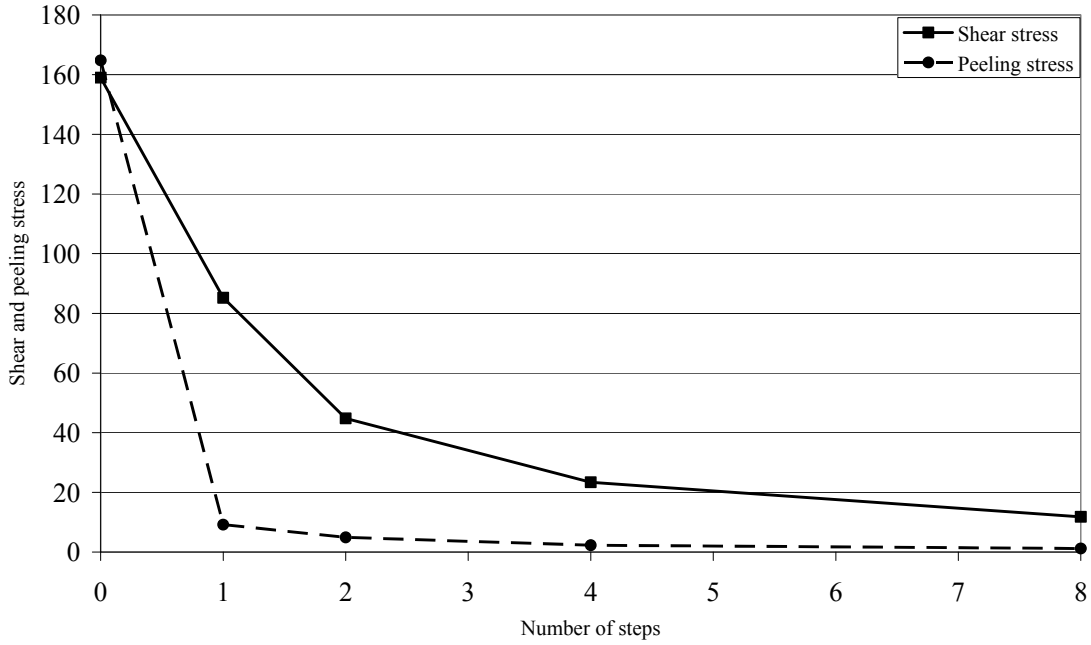

Figure 7.32 Maximum shear and peeling stress for different numbers of steps of step releasing or gradual prestressing. 0 steps is reference value for 1 step with prestressed end.

7.3.3 The effect of laminate tapered in width

The geometry of the laminate influences the interfacial stresses. To investigate how tapering in width, see Figure 7.33, will influence the interfacial stresses different tapers were analysed. In this section the effect of tapering in width is presented. The section is divided into two parts. In the first part the length of the taper is constant while different widths at the ends of the laminate are considered. In the second part the width at the end of the laminate is kept constant and the influence of the length of the taper is studied.

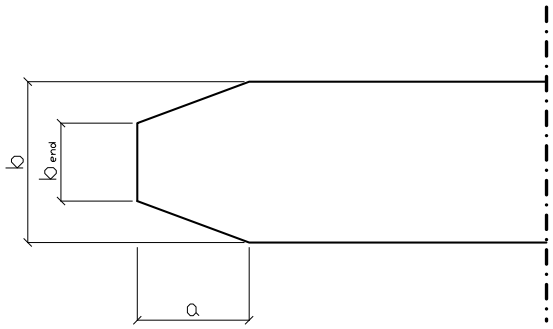

Figure 7.33 Laminate tapered in width.

The effect of tapering in width

The beams analysed here were strengthened with prestressed laminates with an elastic modulus of 165 GPa and the prestressing force was 240 kN. Three different widths of the tapered end were analysed and compared with an untapered end. The thickness of the different laminates was 2 mm and the widths were 50 mm, 30 mm, and 10 mm. The length of the tapers was 100 mm.

As can been observed in Figure 7.34, the shear stresses are increased when the laminate is tapered in width. If the laminate is tapered to 10 mm at the end the interfacial shear stresses will increase from 159 MPa to 206 MPa. That is an increase of about 30 percent.

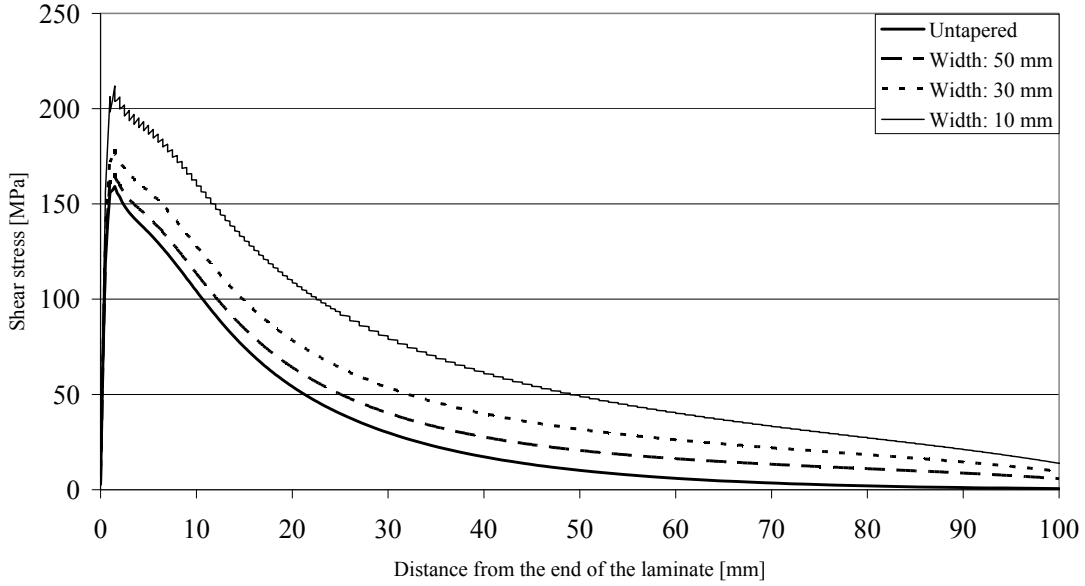

Figure 7.34 Sheer stress distribution over a distance of 100 mm from the end of the laminate. Different widths at the end of the taper. Constant thickness and length of the tapers.

Figure 7.35 shows how the peeling stresses are increasing when the width at the end of the laminate is reduced. For the taper with a width of 10 mm the maximum peeling stresses will increase from 165 MPa to 209 MPa. This is an increase of 27 percent.

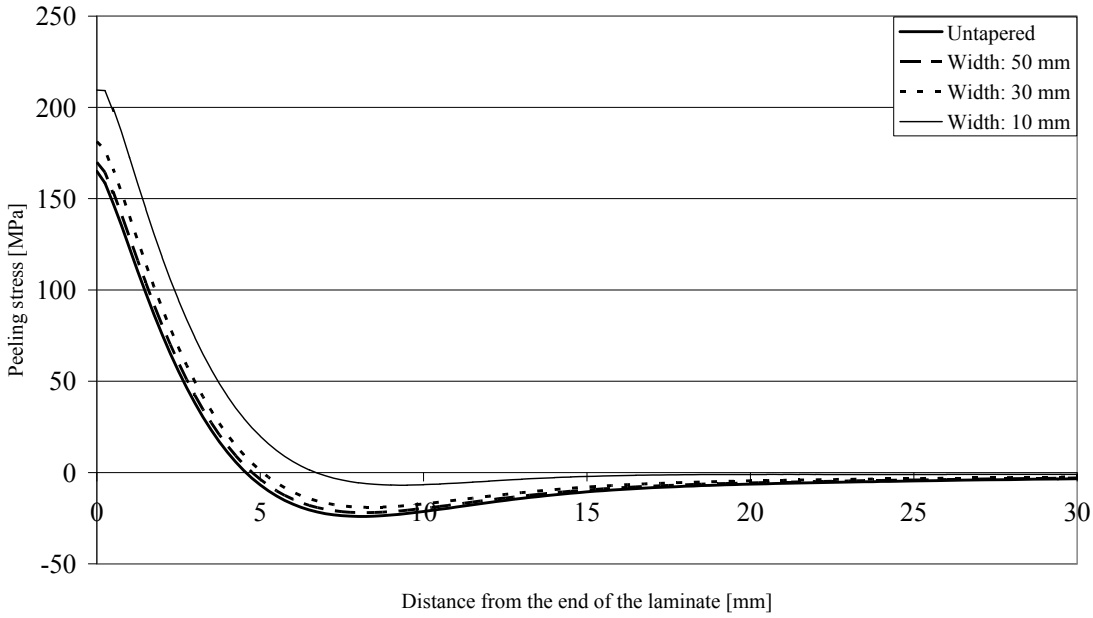

Figure 7.35 Peeling stress distribution over a distance of 30 mm from the end of the laminate. Different widths at the end of the taper. Constant thickness and length of the taper.

The maximum shear and peeling stresses that were attained for different widths are presented in Figure 7.15. The maximum shear and peeling stress is compared with the results of an untapered laminate. For a 100 mm long taper the interfacial stresses will increase when the width at the end of the laminate is decreasing.

Table 7.15 Maximum shear and peeling stresses. Different width of the taper. Constant thickness and length of the taper.

Width [mm]	Max. shear stress [MPa]	[%]	Max. peeling stress [MPa]	[%]
Untapered	159.2	100	165.0	100
50	166.3	104.5	170.0	103.0
30	179.2	112.6	181.3	109.9
10	206.4	129.6	209.5	127.0

Figure 7.36 shows how the axial force is introduced over the length of the laminate. The taper with a width of 10 mm at the end has a long development length and the increase of the axial force (dF(x)/dx) is very low.

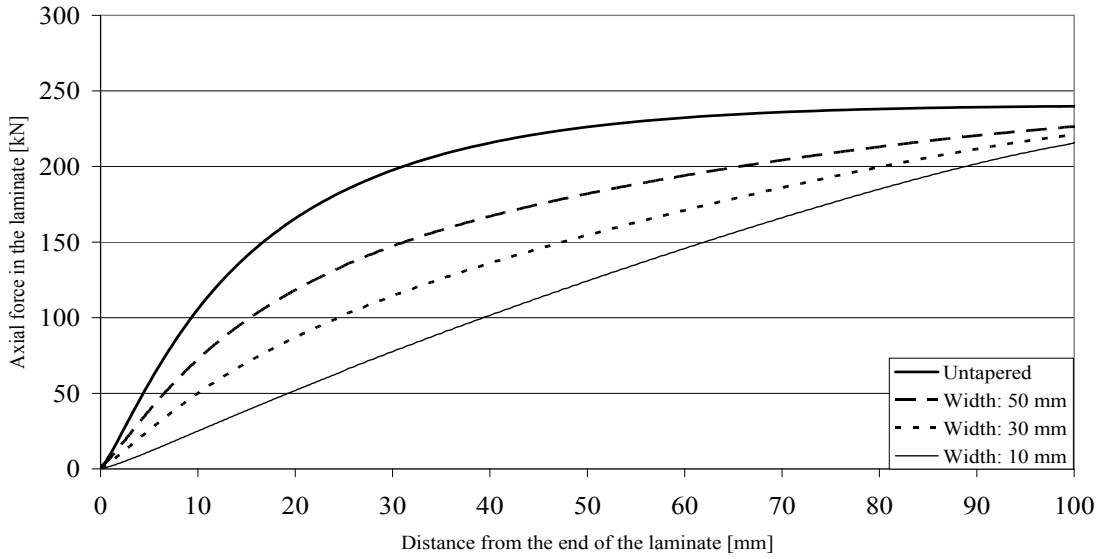

Figure 7.36 Axial force in the laminate over a distance of 100 mm from the end of the laminate. Different widths at the end of the taper. Constant length of 100 mm.

Figure 7.37 shows how the interfacial stresses are increased when the width of the end of the laminate is increased. Therefore, a smaller width at the end of the laminate will result in increased interfacial stresses even if the development length of the axial force is increased and the factor dF(x)/dx is reduced.

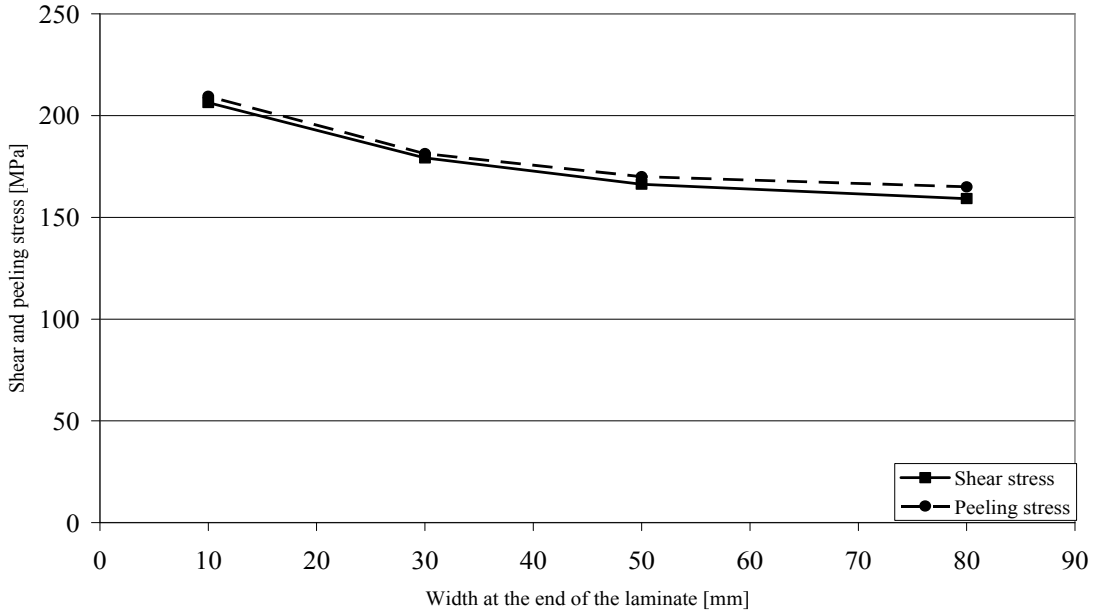

Figure 7.37 Maximum shear and peeling stresses influenced by the width of the taper. Constant length and a thickness of 2 mm at the end of the tapers.

The effect of different lengths of the tapered end

Different lengths were analysed to investigate how the length of the taper effect the interfacial stresses. The lengths analysed were 50, 100, and 150 mm long. The width at the end of the taper was kept constant with a width of 50 mm. The elastic modulus of the laminate is 165 GPa and the prestressing force introduced is 240 kN. The different analyses were compared with the analysis of an untapered end.

In Figure 7.38 the shear stresses for different lengths are plotted against the distance from the end of the laminate. No improvement of the result could be observed for the different tapers. For the 150 mm long taper the maximum shear stress is 164 MPa. That is 5 MPa higher than the maximum shear stresses obtained from the laminate without taper.

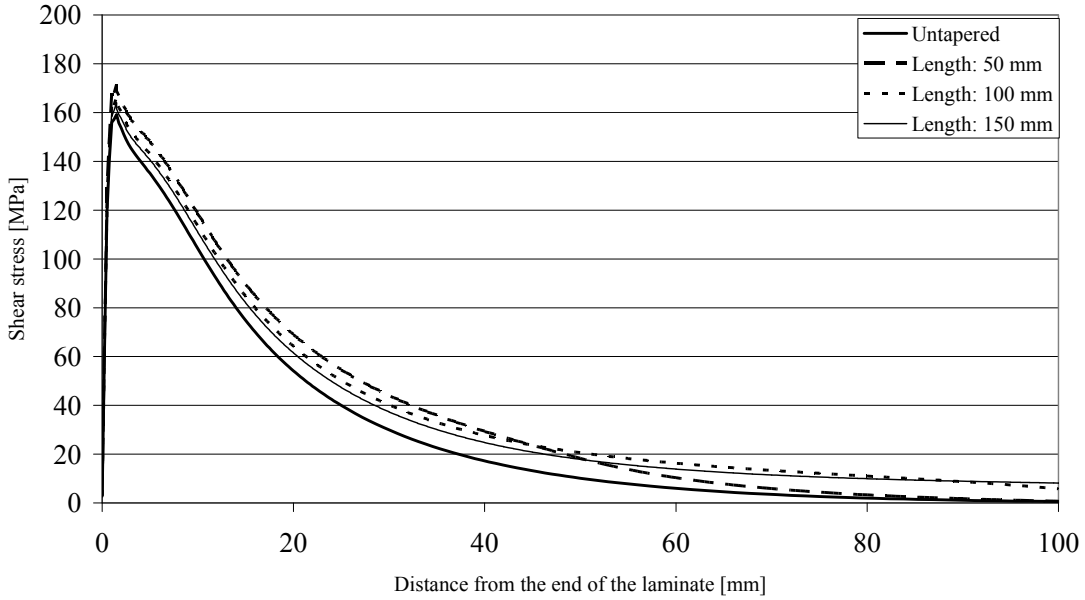

Figure 7.38 Shear stress distribution over a distance of 100 mm from the end of the laminate. Different lengths of the taper. Constant thickness of the taper and a width of 50 mm at the end of the taper.

Figure 7.39 shows the distribution of the peeling stresses. By tapering the laminate 150 mm the maximum peeling stress is increased from 165 MPa to 168 MPa, i.e. a decrease of 3 MPa compared to an untapered end. As can be observed, a 50 mm wide taper will increase the peeling stresses from 165 MPa to 174.3 MPa.

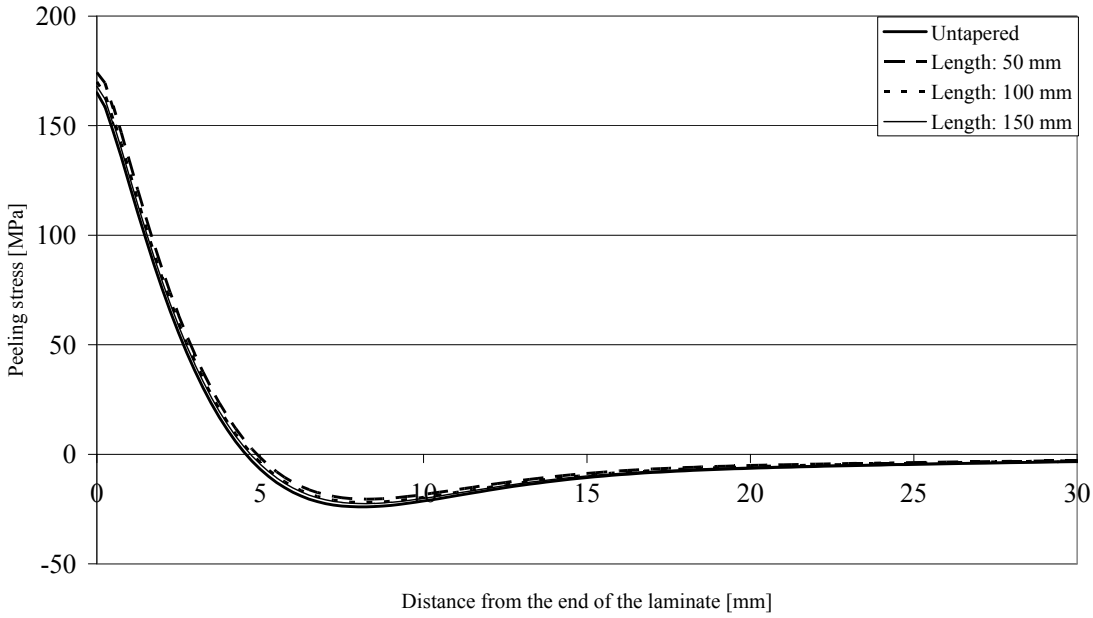

Figure 7.39 Peeling stress distribution over a distance of 30 mm from the end of the laminate. Different lengths of the taper. Constant thickness of the taper and a width of 50 mm at the end of the taper.

The maximum shear and peeling stresses for different lengths of a 50 mm wide tapered end is presented in Table 7.16. For the 50 mm wide taper the maximum shear and peeling stresses never get below the stresses obtained for an untapered end.

Table 7.16 Maximum shear and peeling stress. Different lengths of the taper. Constant thickness of the taper and a width of 50 mm at the end of the taper.

Length [mm]	Max. shear stress [MPa]	[%]	Max. peeling stress [MPa]	[%]
Untapered	159.2	100	165.0	100
50	171.6	107.8	174.3	105.6
100	166.3	104.5	170.0	103.0
150	164.1	103.1	168.0	102.0

Figure 7.40 shows how the axial force in the laminate is introduced into the laminate. If the length of the taper is increased the development length will increase. However, the factor dF(x)/dx will not be influenced much at the end of the laminate. That

indicates that the interfacial stresses will remain high when the length is further increased.

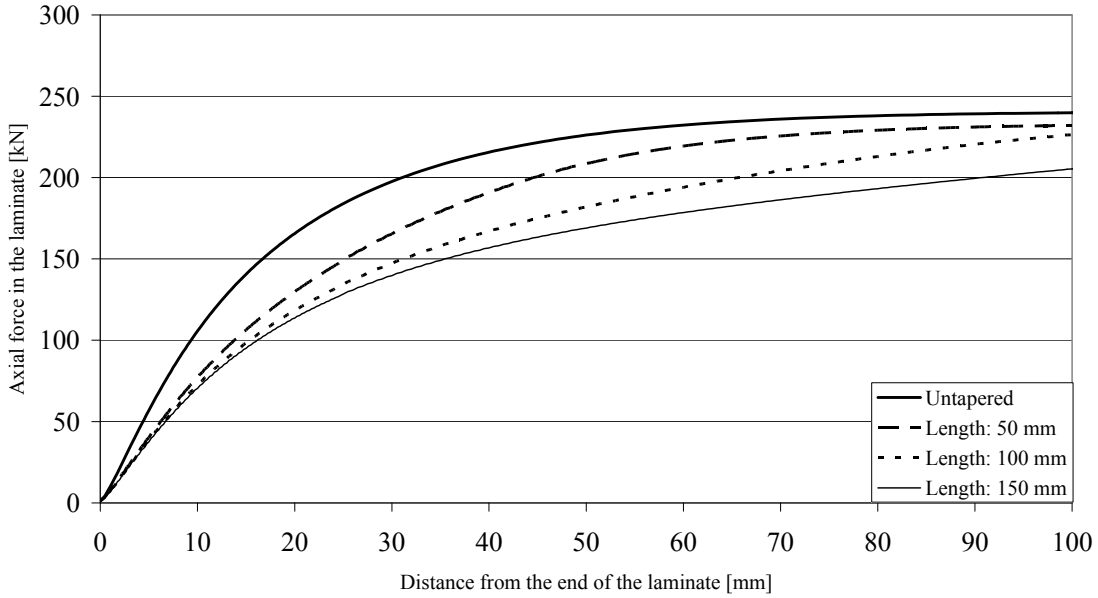

Figure 7.40 Axial force in the laminate over a distance of 100 mm from the end of the laminate. Different lengths of the taper. Constant width of 50 mm at the end of the laminate.

Figure 7.41 shows how the maximum shear and peeling stresses vary with different lengths of the taper. It can be observed that for short tapers the shear and peeling stresses have peak values between untapered and 100 mm long taper. For all tapers the maximum shear and peeling stresses were greater than the stresses for the untapered end.

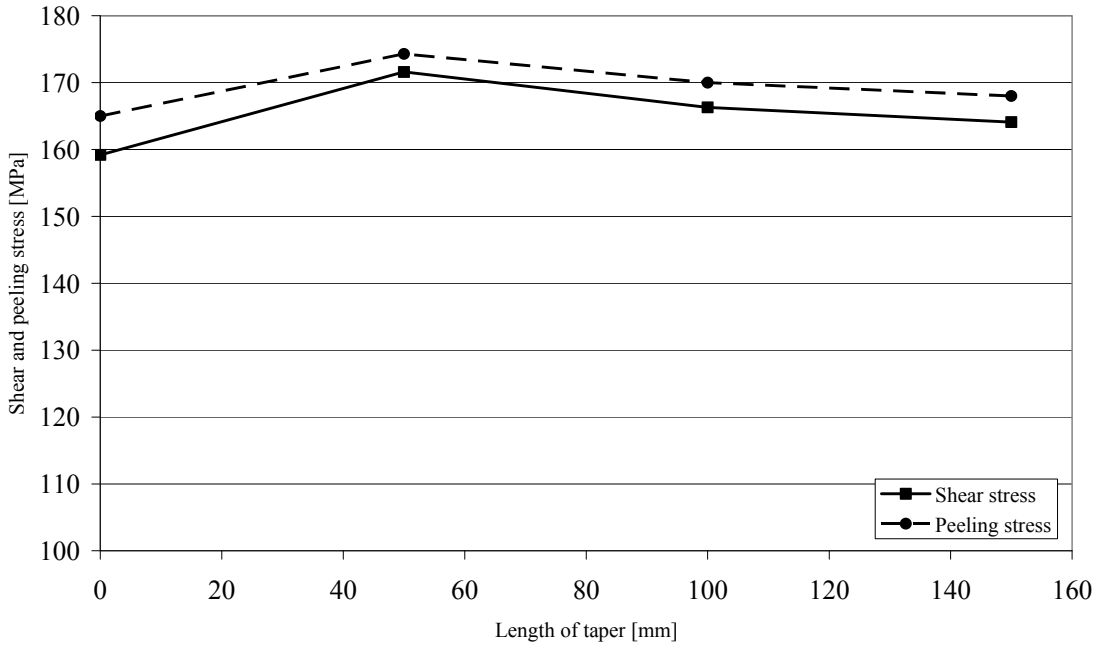

Figure 7.41 Maximum shear and peeling stresses influenced by the length of the taper. Constant width of 50 mm and constant thickness of 2 mm at the end of the tapers.

7.3.4 Tapering the laminate in thickness

The thickness of the laminate influences the interfacial stresses, as mentioned in Section 2.2.4. To investigate how tapering in thickness will affect the interfacial stresses different tapers were analysed. The analyses of the effect of tapering are divided into two parts. In the first part the length of the taper, a, is constant while the effect of different thicknesses, t_{end}, are analysed, see

Figure 7.42. In the second part the thickness, t_{end}, at the end of the laminate is constant and the effect of different lengths, a, of the taper were analysed.

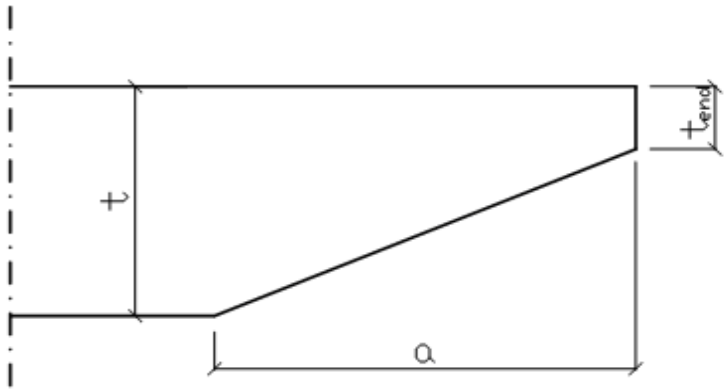

Figure 7.42 Laminate tapered in thickness.

The effect of different thicknesses

The remaing thickness at the ends of the tapered laminate was changed to see how the interfacial stresses are affected by this parameter. Two different thicknesses were analysed and compared with an untapered end. These were 1 mm and 0.001 mm. The length of the tapers was kept constant with a length of 100 mm. The laminate used has an elastic modulus of 165 kN and the prestressing force introduced to the beam was 240 kN.

In Figure 7.43 the shear stresses for different thicknesses are plotted against the distance from the end of the laminate. The lowest maximum shear stress was obtained for the laminate with the thickness of 0.001 mm at the end. This taper gave well distributed shear stresses with a maximum shear stress of 35 MPa. That is just 22 percent of the maximum shear stress for the untapered laminate, see Table 7.17. The maximum shear was 116 MPa for laminate with a thickness of 1 mm at the end.

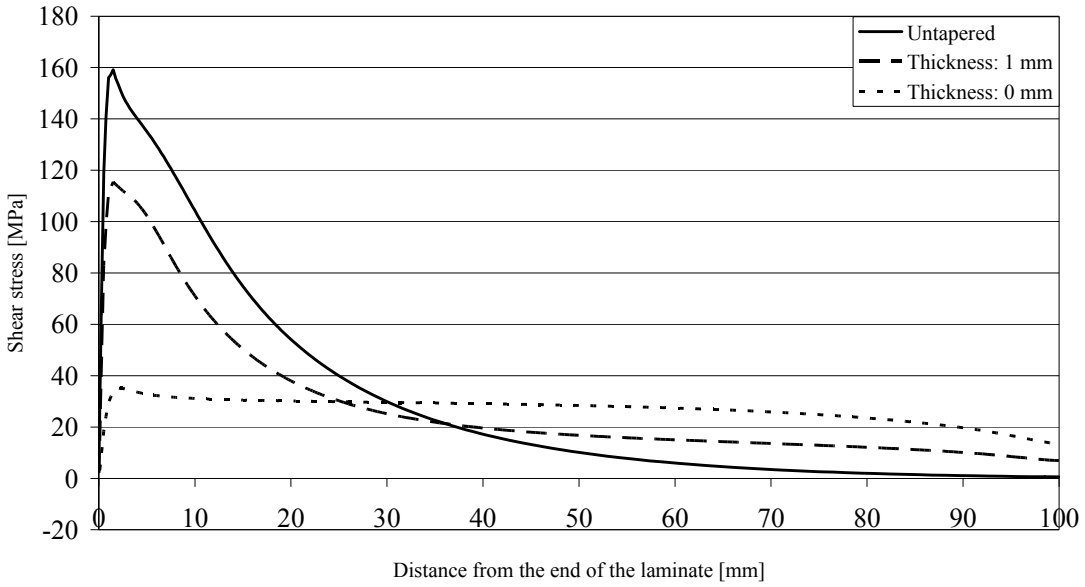

Figure 7.43 Shear stress distribution over a distance of 100 mm from the end of the laminate. Different thicknesses at the end of the taper. Constant width and length of the taper.

In Figure 7.44 the distribution of the peeling stresses are presented. The lowest maximum peeling stress is received for the laminate with the thickness of 0.001 mm. The maximum peeling stress could be reduced from 165 MPa to 46 MPa, see Table 7.17.

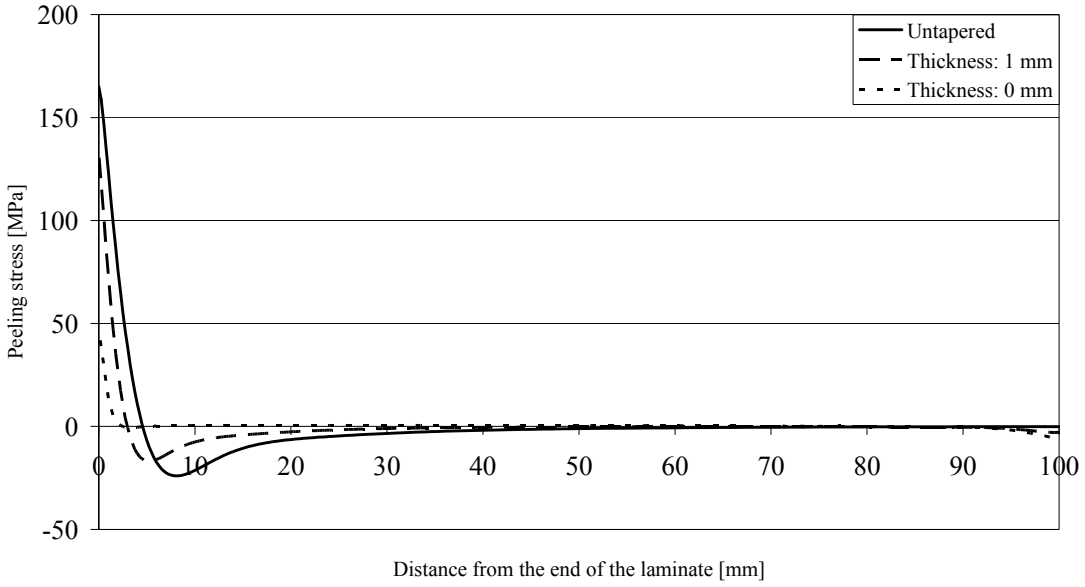

Figure 7.44 Peeling stress distribution over a distance of 100 mm from the end of the laminate. Different thicknesses at the end of the taper. Constant width and length of the taper.

By tapering the last 100 mm at the end of the laminate a more uniformly distributed shear stresses can be obtained. Also the peeling stresses will have a positive influence if the laminate is tapered the last 100 mm in thickness.

The best reduction of the maximum shear and peeling stress were obtained for the taper with a thickness of 0.001 mm. The maximum shear stress for a thickness of 0.001 mm was 124 MPa less compared to an untapered laminate. The peeling stresses were reduced by 119 MPa compared to the untapered laminate. The maximum shear and peeling stress is therefore only 22 percent respectively 28 percent compared to the maximum shear and peeling stress for the untapered end, see Table 7.17.

Table 7.17 Maximum shear and peeling stress. Different thicknesses at the end of the taper. Constant width and length of the taper.

Thickness [mm]	Max. shear stress [MPa]	[%]	Max. peeling stress [MPa]	[%]
Untapered	159	100	165	100
1.000	116	73	132	80
0.001	35	22	46	28

The effect of different lengths of the tapered end

As mentioned before, the length of the taper will influence the interfacial stresses. To investigate how the different lengths of the tapers influence the interfacial stresses, seven different lengths were analysed and compared to an untapered end. The lengths analysed were 2, 4, 10, 20, 40, 80, and 100 mm. The thicknesses at the end of the taper were kept constant with a thickness of 0.001 mm.

In Figure 7.45 the shear stresses at the end of the laminate for the different lengths of the tapers are presented. The lowest maximum shear stress was obtained for the longest taper, which has a length of 100 mm. The maximum shear stress was 35 MPa. That is 22 percent of the maximum shear stress for the untapered laminate, see Table 7.18.

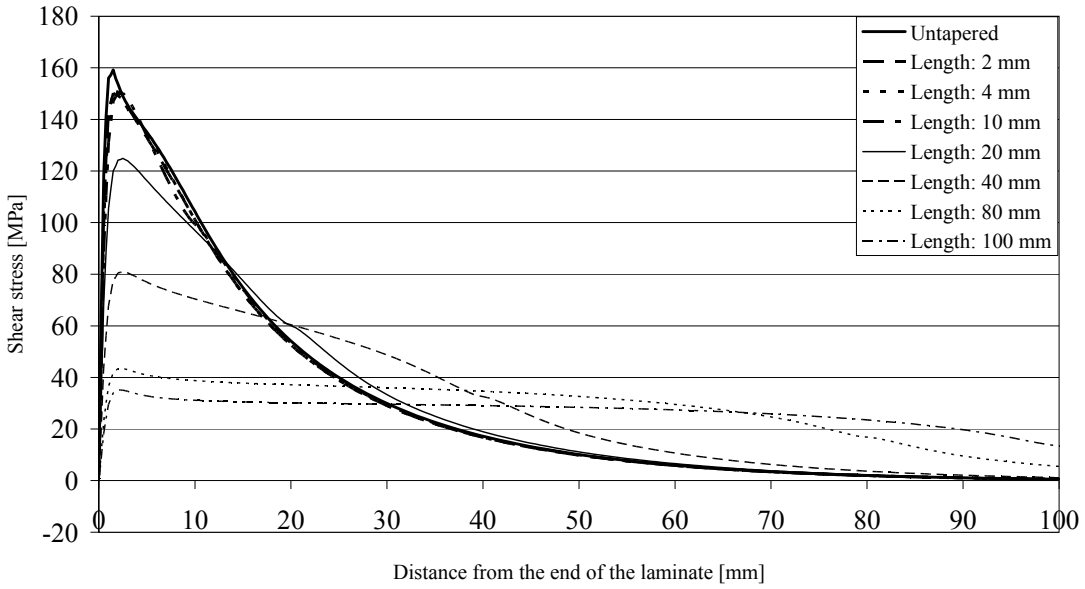

Figure 7.45 Shear stress distribution over a distance of 100 mm from the end of the laminate. Different lengths of the taper. Constant width of the taper and a thickness of 0.001 mm at the end of the laminate.

How peeling stresses vary with different lengths of the tapers can be found in Figure 7.46. By tapering the laminate from 2 mm to 0.001 mm over a length of 100 mm the maximum peeling stress would be reduced from 165 MPa to 46 MPa. This is 28 percent of the peeling stress for the untapered laminate, see Table 7.18. Observe that the maximum peeling stress was higher for the 2, 4, and 10 mm long tapers compared to the laminate with untapered end. For the laminate with a 4 mm long taper the peeling stress is 34 MPa higher than for an untapered laminate. Although, the 40 mm long taper there will be a reduction of 67 MPa. Furthermore, if the laminate is tapered with 80 mm or 100 mm the maximum peeling stress will be reduced from 165 MPa to

55 MPa for the 80 mm long taper and from 165 MPa to 46 MPa for the 100 mm long taper.

Figure 7.46 Peeling stress distribution over a distance of 50 mm from the end of the laminate. Different lengths of the taper. Constant width of the taper and a thickness of 0.001 mm at the end of the laminate.

The best reduction of the maximum shear and peeling stresses were obtained for a long taper with a thin end. The maximal shear stress obtained for the 100 mm long taper is 22 percent compared to an untapered laminate. The maximum shear stress for the 80 mm long taper is 28 percent compared to the maximum shear stress for an untapered laminate. In Table 7.18 it can be observed that the shear and peeling stresses are converging. At a certain length of the taper the maximum shear and peeling stresses will be more or less constant.

Table 7.18 Maximum shear and peeling stresses. Different lengths of the taper. Constant width of the taper and a thickness of 0.001 mm at the end of the laminate.

Length [mm]	Max. shear stress [MPa]	[%]	Max. peeling stress [MPa]	[%]
Untapered	159	100	165	100
2	150	94	188	114
4	152	96	199	121
10	151	95	187	113
20	125	79	151	92
40	81	51	98	59
80	43	27	55	33
100	35	22	46	28

The good result is due to the reduced stiffness in combination with constant area between the steel and the laminate (i.e. the area of the adhesive layer). If the laminate is tapered in thickness both shear and peeling stresses will decrease. If the last 100 mm of the laminate is tapered and the end of the taper is zero mm thick the maximum shear stress will be 22 percent compared to the untapered end and the maximum peeling stress will be 28 percent of the untapered end. How the maximum shear and peeling stresses vary with different thicknesses can be found in Figure 7.47.

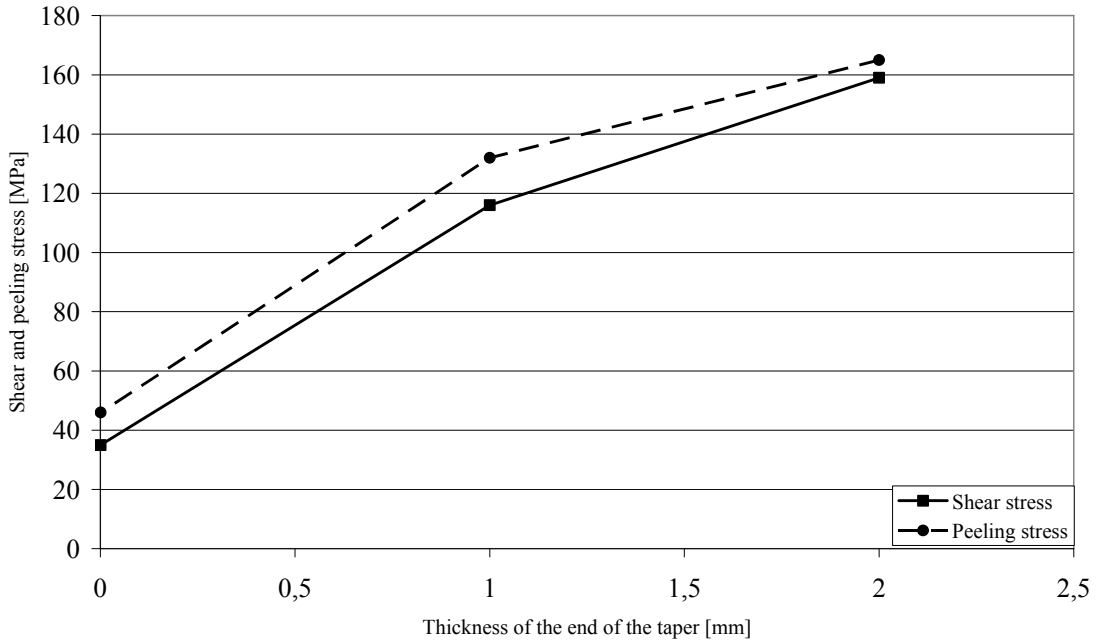

Figure 7.47 Maximum shear and peeling stresses for different thicknesses at the end of the taper. Constant width and length of the taper.

There are two effects that reduce the peeling stresses. The first factor is the decreased stiffness of the laminate. The decreased stiffness increases the development length of the axial force. This will reduce the axial force in the laminate at its end, which will decrease the peeling stresses. The other factor is the decreased eccentricity, see Section 2.2.3. Because of the tapering in thickness the distance between the force in the laminate and the steel beam will decrease (i.e. the lever arm causing bending at the laminate end). The combination of reduced axial force at the end of the laminate and the shorter level arm will reduce the maximum peeling stress. The increased development length will reduce the maximum shear stress.

The effect of the length of the taper was also investigated. In Figure 7.48 the maximum shear and peeling stresses are plotted for different lengths of the taper. The thickness at the end of the taper is 0.001 mm. The results show that by increasing the length of the taper the maximum shear and peeling stresses are reduced. The difference between the maximum shear and peeling stresses for an 80 mm long taper and a 100 mm long taper is relatively small. Therefore, a longer taper will not influence the results much.

It is interesting that the maximum peeling stress is higher for a taper with the length of 4 mm compare to the untapered laminate. The tapering is performed to reduce the stiffness and introduce the axial force in the laminate more gradually. But, the peeling stresses decrease when the elastic modulus of the laminate is increased. A stiffer laminate will result in smaller bending of the laminate due to the bending moment.

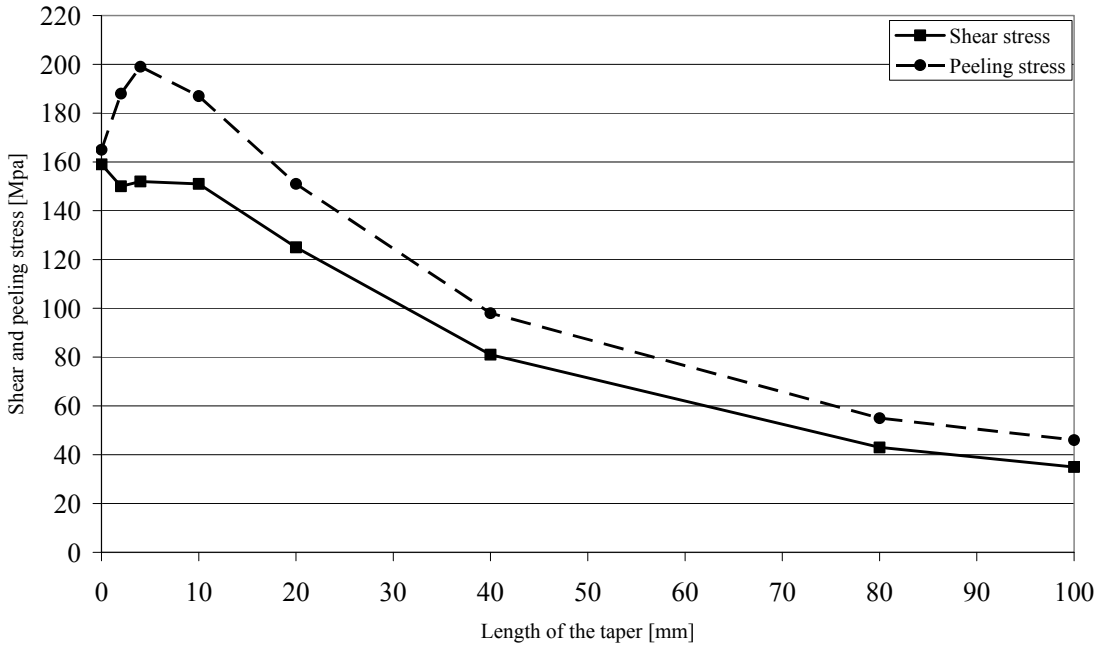

Figure 7.48 Maximum shear and peeling stresses influenced by the length of the taper. Constant width and a thickness of 0.001 mm at the end of the taper.

8 Discussion and suggestions on practical applications

Chapter 7 has shown that by strengthening a steel beam with laminate the behaviour is improved in both the elastic and the plastic state. Furthermore, the results have also shown that many parameters as well as the prestressing techniques influence the magnitude and the distribution of the interfacial stresses. In this chapter the result from chapter 7 and suggestions on how these parameters and techniques can be applied on practical applications will be discussed.

8.1 Global behaviour

It was shown in Section 7.1 that strengthening will improve the behaviour in both the linear-elastic state and the plastic state. However, prestressing will have a small effect on the ultimate load bearing capacity.

8.1.1 Elastic limit state

In order to increase the load for which the beam starts yielding a prestressing force is required. In order to obtain the same effect from just strengthening with unprestressed laminates a very stiff laminate or a large cross-sectional area of the laminate have to be used. This is not economical and therefore prestressing is preferable. To obtain the maximum effect from strengthening with laminate a stiff laminate and a high prestressing force should be used. However, a laminate with high elastic modulus have in general lower tensile strength than a laminate with low elastic modulus. It is therefore important to take the stresses in the laminate into account when steel structures are strengthened.

The increased yielding moment due to strengthening and prestressing can be estimated, for different prestressing levels and different elastic modulus of the laminate, with help of the equations in Section 4.1.1. The conclusion is that the analytical solution is a good approximation to find the increase of yielding load for different elastic modulus of laminates and different introduced prestressing forces.

8.1.2 Plastic limit state

The ultimate capacity is mainly due to the linear elastic behaviour of the laminate. A laminate with high elastic modulus have a higher ultimate capacity compared to a laminate with low elastic modulus if the failure mode is 3.5 percent strain in the outmost fibre in the upper flange. This is a result of the location of the neutral axis. However, high modulus laminates have in general lower strength than low modulus laminate.

8.2 The effect of different parameters

It has been discussed in Section 4.2 that there are many parameters that affect the interfacial stresses. The FE-analyses have shown that materials used to strengthening steel structures and also the applied prestressing force will affect the interfacial stresses. Furthermore, the loading will also affect the interfacial stresses. Finally, suggestions on practical applications will be presented.

The prestressing force

The prestressing force is proportional to the interfacial stresses. That means that a twice as high prestressing force will result in twice as high interfacial stresses.

The external loading

The interfacial stresses in the laminate due to loading are low compared to the interfacial stresses as a result of prestressing. However, there will be an increase of the interfacial stresses at the end of the laminate due to external loading. This increase must be taken into account in the design. In combination with the high interfacial stresses due to prestressing the stresses can be too high and failure may occur.

The adhesive E-modulus

The elastic modulus of the adhesive has a high effect on the interfacial stresses. By using an adhesive with a low elastic modulus the interfacial stresses can be reduced.

The laminate E-modulus

It is very important to choose an accurate laminate for strengthening of steel structures using prestressed laminates. An increased elastic modulus will increase the development length of the axial force in the laminate and reduces the axial force in the laminate at the end of the laminate. This will result in a more favourable distribution of shear stresses and decreased peeling stresses. However, a stiffer laminate is in general not as strong as less stiff laminate. Therefore, a laminate with a high elastic modulus should be chosen but the stresses in the laminate due to prestressing and loading must be taken into account. This is very important because CFRP-laminate has a brittle behaviour and failure due to tensile rapture will appear suddenly.

The influence of adhesive plastic behaviour

The results of the analysis show that the maximum peeling stress could be decreased from 13.9 to 10.1 and the maximum shear stress from 13.4 to 10.7 when the plastic behaviour of the adhesive was considered. This is a decrease with 27 percent respectively 20 percent. The effect from the plastic behaviour can not be taken advantage of in permanent constructions. However, the plastic behaviour can be of great use for provisional devices. Provisional devices will be discussed in Section 8.3.

8.3 The effect of various techniques

In this section the result from the FE-analyses of different techniques will be discussed. The techniques analysed were established in Section 4.3. In this section the practical applications of these techniques will be discussed. What have to be kept in mind is that the beams have not been exposed to external loading when the different techniques and parameters were analysed. Further analyses must be executed before field applications can be employed.

8.3.1 Unprestressed end

By using an unprestressed end the shear stresses can be reduced to 50 percent compared to a prestressed end. The peeling stresses can be reduced to 6 percent compared to a prestressed end. Furthermore, the interfacial stresses at the end of the laminate due to prestressing can be reduced to almost zero. One practical problem of leaving a part of the end of the laminate unprestressed is that the prestressing force needs to be held until the adhesive has cured. Moreover, the unprestressed part of the laminate has to be bonded to the steel at the same time as the prestressed part.

8.3.2 Step releasing and gradual prestressing

Because of the excellent results from the FE-analyses the step releasing and gradual prestressing was further analysed.

Step releasing and gradual prestressing give the same interfacial stresses in the adhesive after the provisional anchorage or prestressing device have been removed. The only difference is the technique used to receive the superior behaviour. To understand the problem with this method the different techniques will be explained. First the step releasing will be explained and then the gradual prestressing. In the last part of this section some results from FE-analyses will be presented.

Step releasing

This suggested application for step-releasing consists of one prestressing device and provisional anchorages. Before prestressing is applied the provisional anchorages are bonded by adhesive to the laminate. When the adhesive between the provisional anchorages and the laminate have been fully cured the laminate is prestressed with the prestressing device with the desirable force, see Figure 8.1. When the laminate has been prestressed the anchorage closest to the mid-span of the beam is attached to the beam. When that provisional anchorage has been attached to the steel beam the prestressing force will be partially released. Consequently, this decrease of prestressing force will be taken by the provisional anchorage. At step 3 the second provisional anchorage is attached and the rest of the prestressing is released. The unprestressed end will reduce the high shear and peeling stresses at the end of the laminate when the provisional anchorages have been released, see Section 7.4.1.

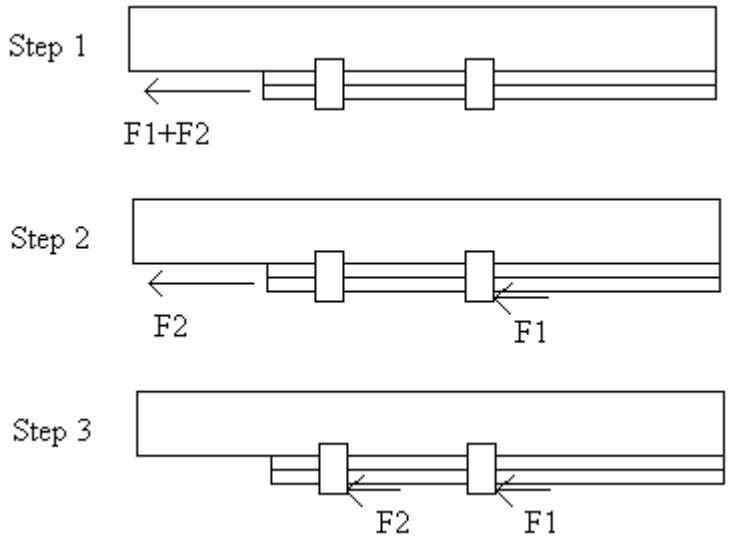

Figure 8.1 Schematic figure of step releasing with two provisional anchorages

As long as the provisional anchorages are attached to the beam the stresses in the laminate will be introduced into the beam through the provisional anchorages. At each anchorage there will be an increase of the force in the laminate.

When the adhesive between the laminate and the steel beam has cured the provisional anchorages can be removed. After removal of the provisional anchorages the force in the laminate will be built up gradually according to Figure 7.31 for 2 steps and the shear and peeling stresses in the adhesive will have a distribution according to Figure 7.29 and Figure 7.30 for 2 steps.

Gradual prestressing

The difference between gradual prestressing and step releasing is that in gradual prestressing the provisional anchorage devices also work as a prestressing device, see Figure 8.2. First the device closest to the end of the laminate will be loaded. In the next step the second device from the end of the laminate will be loaded. The stress in the laminate in between the two devices will be constant when the laminate is further prestressed. When the laminate is fully prestressed each and one of the prestressing devices should have the same amount of load. The prestressing is the sum of all loads taken by the provisional devices.

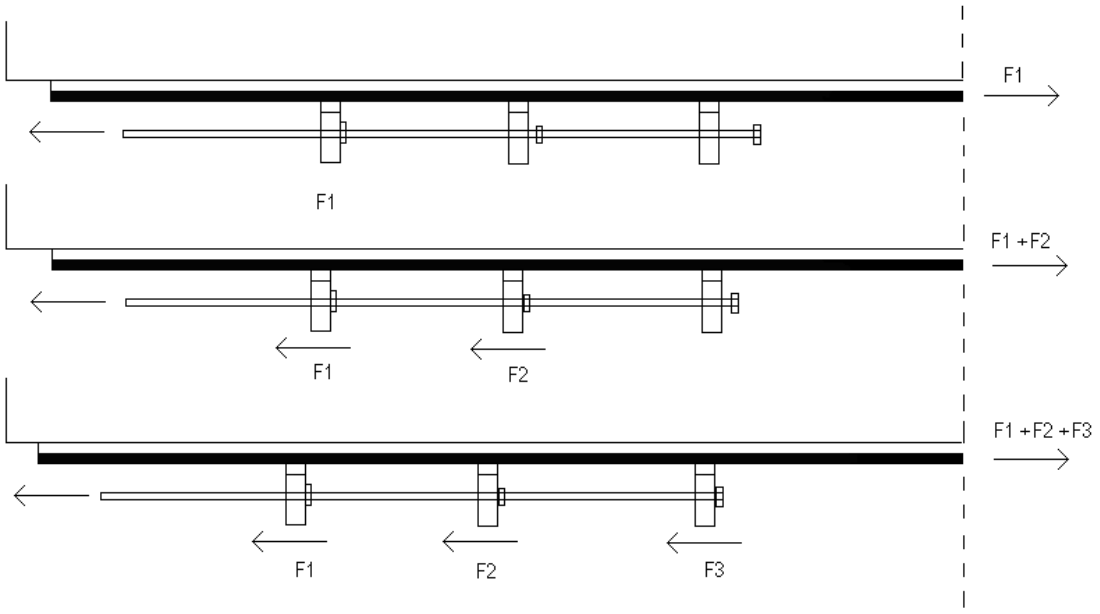

Figure 8.2 Schematic figure of gradual prestressing.

The prestressing is kept until the adhesive between the laminate and the steel has cured. After that the prestressing force can be released and the axial force in the laminate can be transferred through the adhesive into the steel beam.

FE-analyses of provisional device used for step-releasing and gradual prestressing

The problem with step-releasing and gradual prestressing is the high shear and peeling stresses that appear in the adhesive between the provisional anchorages or prestressing device and the laminate. In order to analyse these high interfacial stresses a provisional anchorage was used and the stresses were calculated numerically with ABAQUS. The FE-model was established according to Figure 8.3:

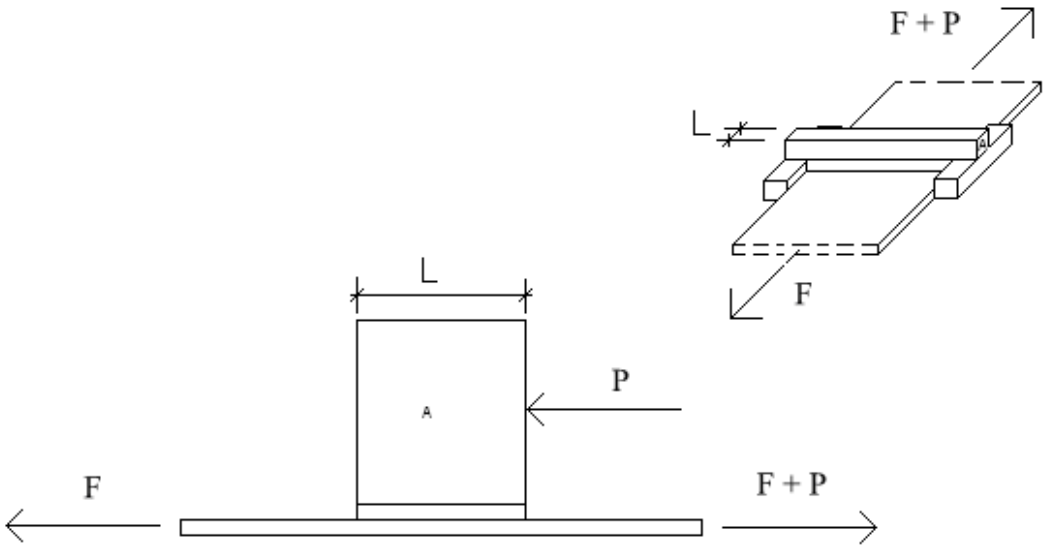

Figure 8.3 Provisional anchorage.

The force F+P is the applied prestressing force or the force in the laminate until next provisional device. The force F will continue to the next provisional anchorage and P is the load taken by the analysed anchorage. L is the length of the anchorage device, which was set to 10 mm. The laminate is 2 mm thick and 80 mm wide. The elastic modulus of the laminate is 165 GPa. The model is restricted from moving in vertical direction. This will prevent the device from rotating. All figures are showing the stresses in the middle of the adhesive.

In the first three analyses a 10 mm wide provisional device was used. In the first analysis the laminate is stressed with 240 kN (F=240 kN) and the device is loaded with 20 kN (P=20 kN). The result showed that very high interfacial stresses occur in the adhesive, see Figure 8.4.

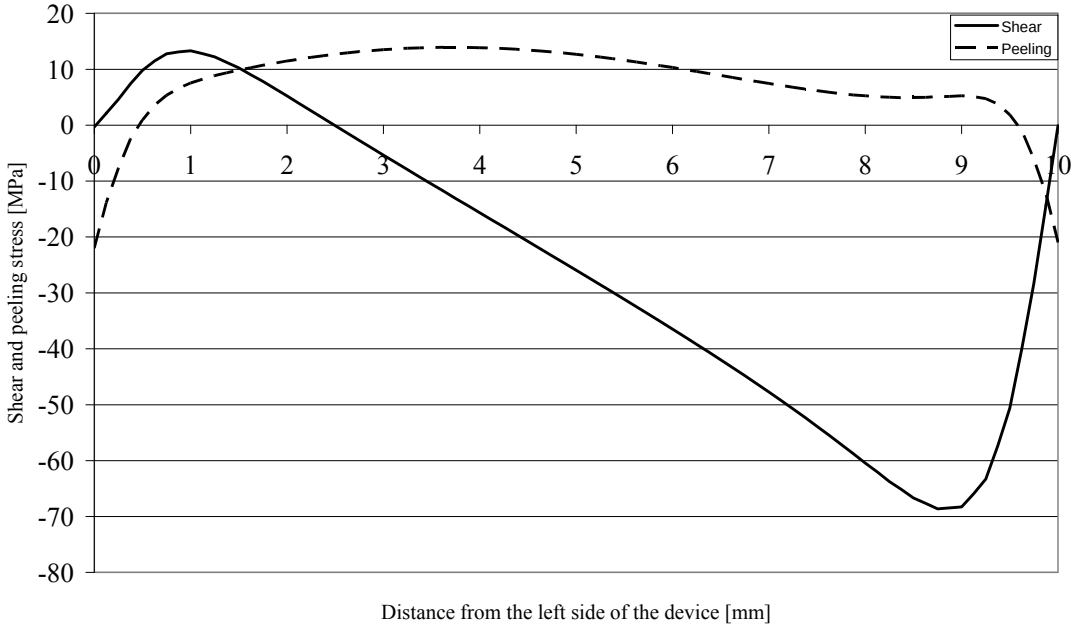

Figure 8.4 Shear and peeling stresses in the middle of the adhesive. F=240 kN P=20 kN

To examine how much of these stresses are coming from the stressing of the laminate the laminate was stressed with a force of F=260 kN while the reaction force was set to zero (P=0). The result from the analysis can be found in Figure 8.5. The figure shows that approximately 50 percent of the maximum shear stress is coming from the stressing of the laminate.

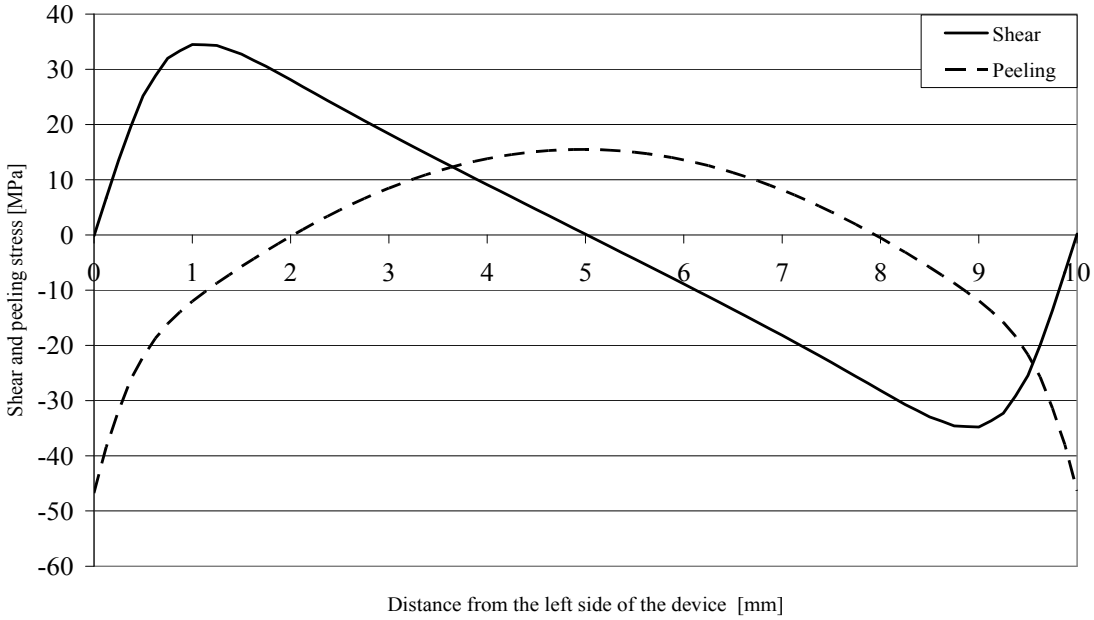

Figure 8.5 Shear and peeling stresses in the middle of the adhesive. F=260 kN, P=0 kN

In the last analysis of a 10 mm wide device the effect of the reaction force was investigated. The device was loaded with 20 kN (P=20 kN, F=0 kN) The result shows that approximately 50 percent of the maximum shear stress is a result of loading, see Figure 8.6.

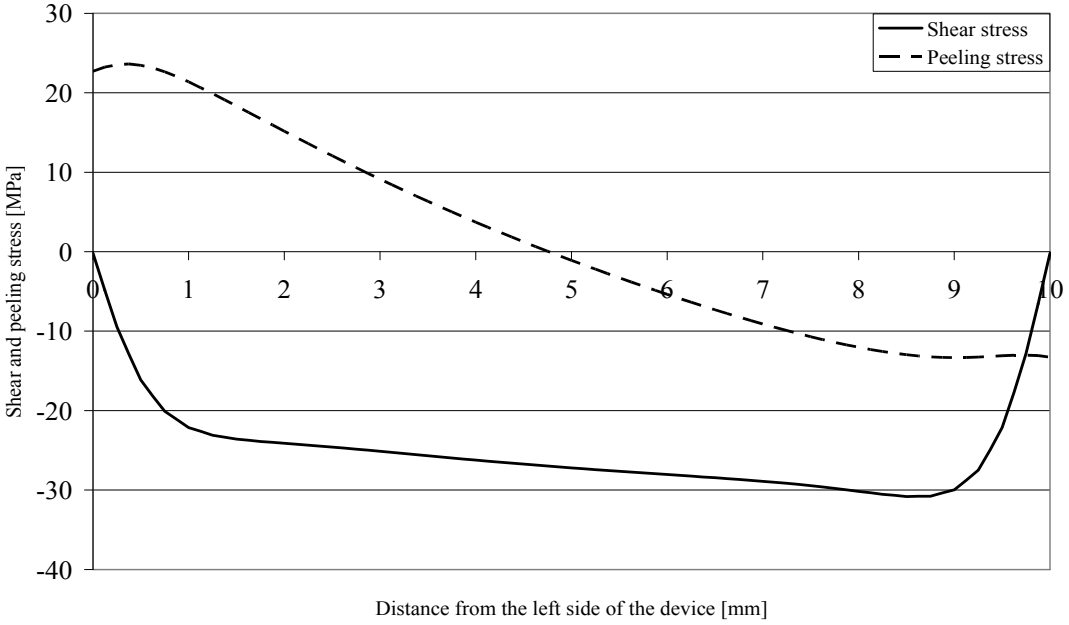

Figure 8.6 Shear and peeling stresses in the middle of the adhesive. P=20 kN F=0kN

A L=25 mm wide anchorage was analysed to see how that will effect the interfacial stresses. First the combination of load and stressing of the laminate was combined, i.e. F=240 kN and P=20 kN. The result shows that maximum shear stress is increased with 60 percent compared to the 10 mm wide anchorage, see Figure 8.7.

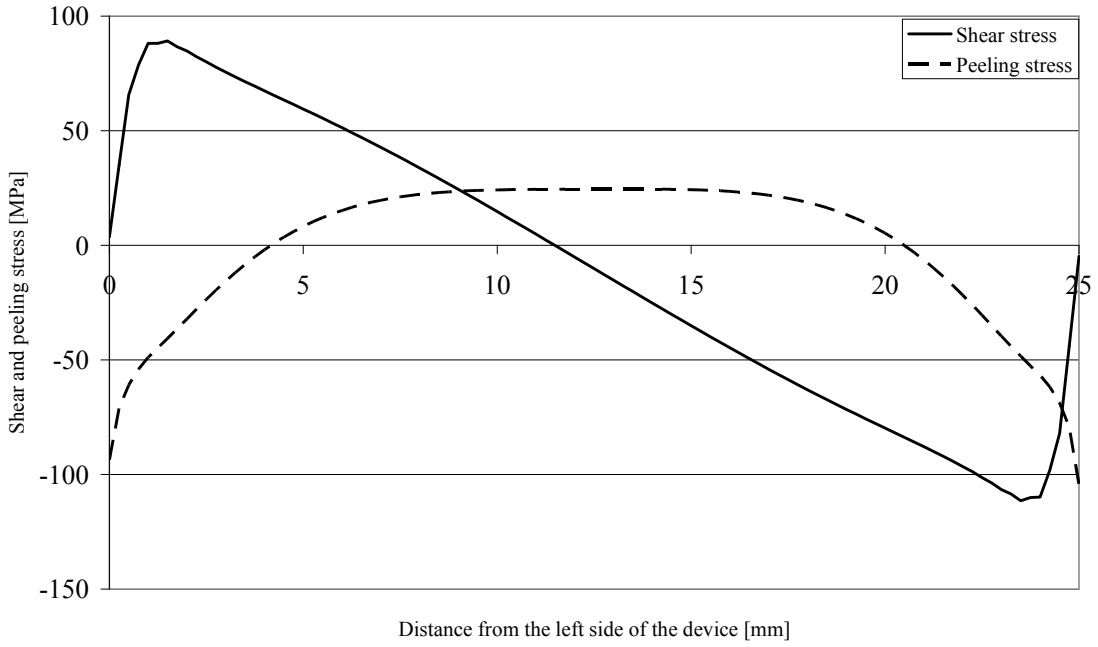

Figure 8.7 Shear and peeling stresses in the middle of the adhesive. F=240 kN P=20 kN

To examine how much of these stresses are coming from the stressing of the laminate the laminate was stressed with a force of 260 kN. The result from the analysis can be found in Figure 8.8. The figure shows that 100 MPa of the shear stresses are coming from the stressing of the laminate. By increasing the length of the device from 10 mm to 25 mm the maximum shear stresses were increased with almost 200 percent.

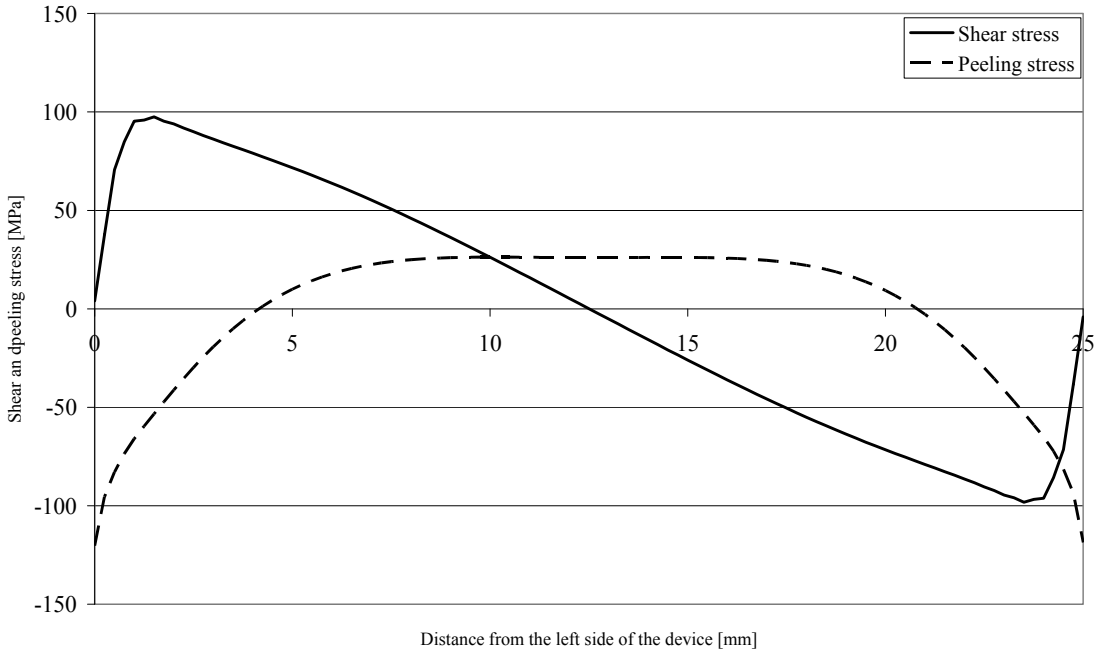

Figure 8.8 Shear and peeling stresses in the middle of the adhesive. F=260 kN P=0 kN

In the last analysis the effect from loading was investigated for the 25 mm wide device. Figure 8.9 shows how the maximum shear stresses are reduced from 30 MPa for the 10 mm wide device to 15 MPa for the 25 mm wide device, i.e. the stresses due to the reaction force is reduced with 50 %.

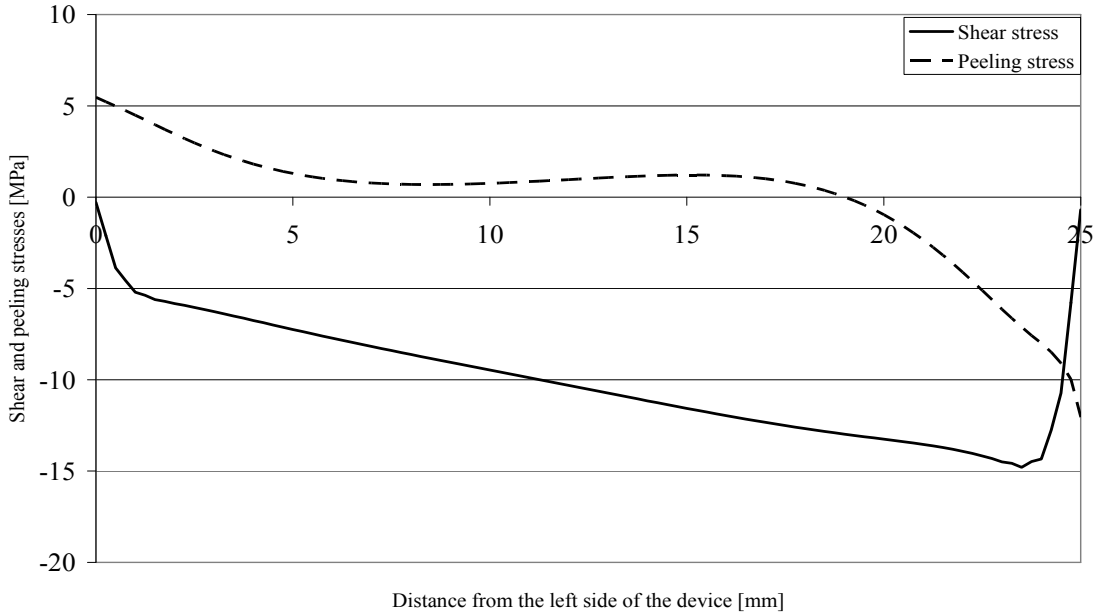

Figure 8.9 Shear and peeling stresses in the middle of the adhesive. P=20 kN F=0kN

The results from the analyses of the two types of provisional anchorages show that high interfacial stresses appear due to stressing of the laminate. By reducing the width of the anchorage the stresses due to prestressing of laminate can be reduced but the stresses as a result of the reaction force P will increase. However, by increasing the number of provisional devices the load can be decreased and with more devices there will be more steps, which have a positive effect on the interfacial stresses.

Our suggestion is to use many devices with small widths. That will reduce the stresses due to stressing of the laminate and the reaction force at each anchorage will be small. If many devices are used the shear stresses will be well distributed, which results in low peak values of the shear and peeling stresses.

8.3.3 Tapering of laminate

Tapering in width

Tapering the laminate in width has a negative effect on the interfacial stresses at the end of the laminate. A 100 mm long taper with a 10 mm wide end will increase the interfacial stresses with 30 percent. Even if a 150 mm long taper with a 50 mm tapered end is used the interfacial stresses at the end will increase. All the laminates tapered in width that are treated in this thesis will increase the interfacial stresses at the end and are therefore hazardous and should not be applied in field applications.

Tapering in thickness

Tapering in thickness has shown to be a good method theoretically if the taper is long enough. If the taper is shorter than 10 mm, i.e. 5 times the thickness of the laminate, the peeling stresses will be larger than for a laminate with an untapered end. Furthermore, for tapers shorter than 10 mm the shear stresses will not be decreased considerably. The increase of peeling stresses is a result of the change of cross-section, which creates forces perpendicular to the adhesive layer, see Figure 8.10.

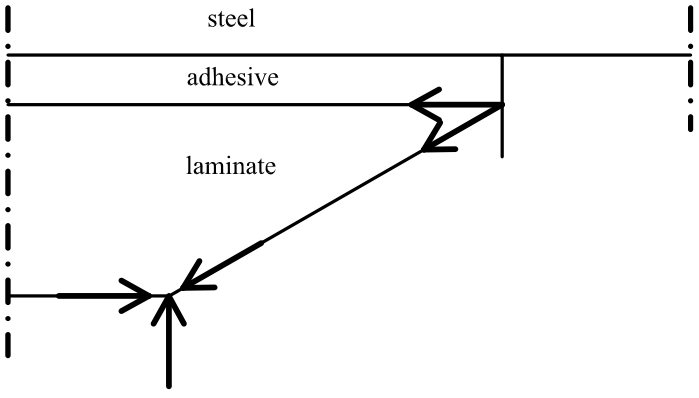

Figure 8.10 Forces due to tapering of the end of the laminate

These vertical forces will create a moment, which is bending the laminate. This can be illustrated by means of a beam on springs. When the concentrated forces are acting on the beam the beam end will rotate, see Figure 8.11.

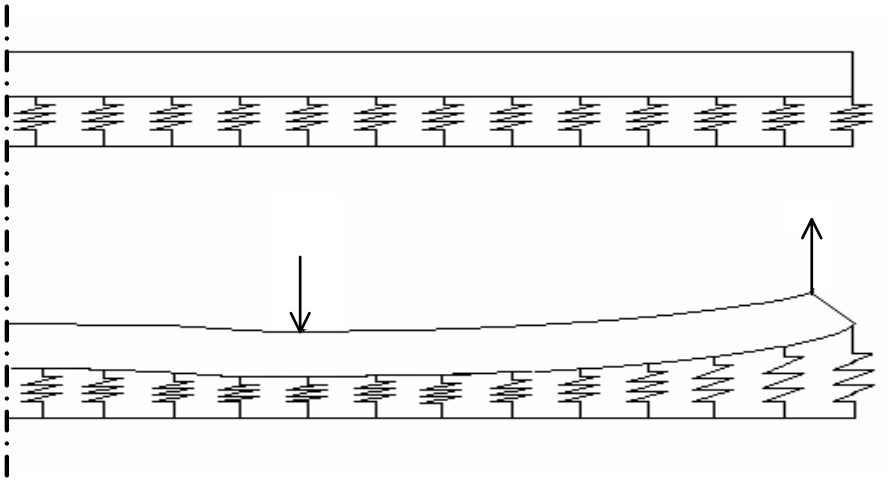

Figure 8.11 Schematic figure of the behaviour of the laminate with forces acting perpendicular to the adhesive

In the same way, for a laminate attached to the steel structure with adhesive bond, the peeling stresses at the end of the laminate will be larger if the taper is short, i.e. approximately 7 times the thickness, see Figure 8.12. If the change of cross-section is carried out over a large distance the vertical forces due to change of cross-section will be smaller.

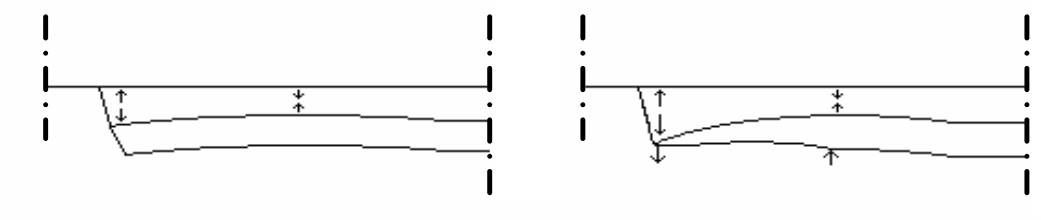

Figure 8.12 Untapered end and end tapered in thickness

One drawback with this method is the thickness of the laminate, which is very small. Due to the long taper required, there will be problems with regard to practical applications and geometrical properties. In this case the thickness is two millimetres and the tapering must be performed on a large area, see Figure 8.13 Due to the thin laminate and long taper there is a risk of defects and imperfections if the tapering is

executed manually. Therefore, a grinding machine with high accuracy is probably needed.

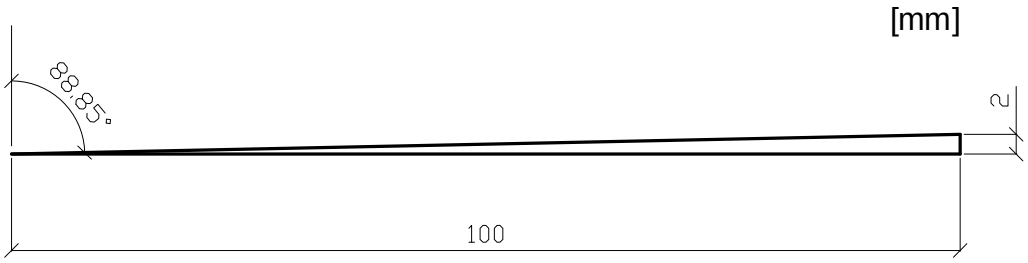

Figure 8.13 Laminate tapered in thickness.

9 Final Remarks

In this chapter the conclusion of the work conducted in this master's thesis will be brought up. Furthermore, suggestions on further research will be stated.

9.1 Conclusions

In the first part of this master's thesis the behaviour of a steel beam strengthened with bonded laminate was analysed. Both unprestressed and prestressed laminates were considered. The conclusion after these analyses is that the effect from strengthening and prestressing can easily be estimated with analytical calculations.

In the second part of the master's thesis the effects of various parameters, which were expected to influence the value of interfacial stresses in the bond-line were investigated. The result showed that the elastic modulus of the adhesive and the laminate have large influence on the interfacial stresses at the end of the laminate. By using a stiff laminate and low modulus adhesive the interfacial stresses can be reduced considerably. The magnitude of interfacial stresses at the ends of the laminate due to external loading was very low compared to those caused by prestressing. The prestressing is proportional to the interfacial stresses.

In the last part of the master's thesis the effect of various techniques were investigated. It was shown that by leaving a certain length of the end of the laminate unprestressed the interfacial stresses at the end can be reduced to zero. Also the value of maximum shear and peeling stress is reduced. Another technique that showed good results is to stress the laminate in different steps, i.e. introduce the axial force in the laminate stepwise. By doing so, the shear stresses will be more evenly distributed and the peak values of the shear and peeling stresses at the end of the laminate will de reduced. If the axial stress in the laminate is introduced stepwise and an unprestressed end is used the interfacial stresses can be reduced substantially. When it comes to tapering in thickness the maximum peeling stresses will be increased if the taper is shorter than five times the thickness of the laminate. The length of the taper for which a positive effect from tapering is achieved is between 10 and 20 mm, i.e. between five and ten times the thickness of the laminate. Tapering the laminate in width at the end has a negative effect on the interfacial stresses. Even if the length of the taper was increased the maximum shear and peeling stresses were larger than for an untapered end.

9.2 Suggestions on further research

In order to achieve the superior behaviour from unprestressed end, gradual prestressing, and step releasing further research have to be carried out. The research should focus on finding a device that can prestress the laminate stepwise or a provisional anchorage that can be released after the adhesive between the laminate and the steel has cured.

Earlier in this thesis it was mentioned that by releasing the prestressing force step-wise at different curing times the interfacial stresses can be decreased. More research is needed to fully understand the behaviour of a not fully cured adhesive.

Last but not least, it was observed that by tapering the thickness of the adhesive over a length shorter than 5 times the thickness of the laminate the peeling stresses were increased. For a taper twice the thickness of the laminate the peeling stresses were increased 21 %. By studying and fully understanding this phenomenon the risk of accidentally increasing the peeling stresses can be reduced. On the other hand, if a reverse taper is used a positive effect may achieved. A reverse taper is the same as tapering in thickness but with reverse taper the tapered side is facing the structure. This configuration has not been analysed and need to be studied in future work.

10 References

[1] Garden, H.N., Hollaway, L.C. (1998): An Experimental of the Influence of plate End Anchorage Carbon Fibre Composite Plates Used to Strengthen Reinforcement Concrete Beams. *Composite Structures*, Vol. 42, 1998, pp. 175-188.

[2] Hollaway, L.C., Cadie, J. (2002): Progress in the Technique of Upgrading Metallic Structures with Advanced Polymer Composites. *Prog. Struc. Engng Mater*, 2002; 4: 131-148 (DOI: 10.1002/pse.112), pp. 131-148.

[3] Nordin H. (2003): *Fibre Reinforced Polymers in Civil Engineering*. Lic. Thesis. Department of Civil and Mining engineering, Division of Structural Engineering, Luleå University of Technology, Publication no. 2003:25, Luleå, Sweden, 2003, 57 pp.

[4] Altenbach H., Altenbach J., Kissing W. (2003): *Mechanics of Composite Structural Elements*, Springer-Verlag, Heidelberg, 2004, pp. 1-6.

[5] Cadei J.M.C., Stratford T.J., Hollaway L.C., Duckett W.G. (2004): *Strengthening metallic structures using externally bonded fibre-reinforced polymers*, CIRIA, London, 2004, pp. 39-93.

[6] Shaat, A., Schnerch, D. Fam, A.; Rizkalla, S. (2003): *Retrofit of Steel Structures Using Fiber Reinforced Polymers (FRP): State-of-the-Art*, Research paper, 2003

[7] Al-Emrani M., Kliger R. (2006): Analysis of interfacial shear stresses in beams strengthened with bonded prestressed laminates. *Composites: Part B 37*, 2006, pp. 265-272.

[8] www.nationalbridgeinventory.com

[9] Sen, R., Liby, L., Mullins, G. (2001): Strengthening Steel Bridge Sections Using CFRP Laminates. *Composites: Part B 32*, 2001, pp. 309-322.

[10] Caroline, A., Täljsten, B. (2005): Concrete Beams Exposed to Live Loading during Carbon Fiber Reinforced Polymer Strengthening. *J. Compos. for Constr.,* Vol. 9, Issue 2, March/April 2005, pp. 178-186.

[11] El-Hacha, R., Wight, R. G., Green, M. F. (2001): Prestressed Fibre-Reinforced Polymer Laminates for Strengthening Structures. *Prog. Struc. Engng Mater*, 2001; 3: 111-121 (DOI: 10.1002/pse.76), pp. 111-121.

[12] Sustainable bridges (2004): *Strengthening and repair of metallic bridges using advanced composite materials, Literature Review, WP6*, Sustainable Bridges, 74 pp.

[13] Schnerch, D., Stanford, K., Sumner, E., Rizkalla, S. (2005): Bond Behaviour of CFRP Strengthened Steel Bridges and Structures, *Proceedings of International Symposium on Bond Bahaviour of FRP in Structures (BBFS 2005). International Institute for FRP in Construction,* 2005.

[14] Andrä, H.P., Maier, M., Poorbiazar, M. (2004): Carbon fibre composites for a new generation of tendons. *1st conference on application of FRP composites in construction and rehabilitation of structures*, Teheran, Iran, 2004. pp 29-37.

[15] Deng, J., Lee, M. M.K., Moy, S. S.J. (2004): Stress Analysis of Steel Beams Reinforced With a Bonded CFRP Plate. *Composite Structures*, Vol. 65, 2004, pp. 205-215.

[16] El-Hacha, R., Wight, R.G, Green, M.F. (2001): Innovative system for prestressing fiber-reinforced polymer sheets, *ACI Structural Journal*, No.3, May-June 2003, pp.305-313.

[17] Butrooz, F, Ruiz Miranda, F. (2004): *Prestressed Advanced Composites for Strengthening Steel Structures*. Master's Thesis. Department of Structural Engineering, Chalmers University of Technology, Publication no. 01:2, Göteborg, Sweden, 2004, 74 pp.

[18] Schnerch, D., Stanford, K., Sumner, E., Rizkalla, S. (2004): Strengthening Steel Structures and Bridges with High Modulus Carbon Fiber Reinforced Polymers: Resin Selection and Scaled Monopole Behaviour. *Transportation Resaéarch Record*, Vol. 1892, 2004, pp. 237-245.

[19] Nunziata V. (1999): Prestressed Steel Structures. *XVII Congresso C.T.A, Construire In Acciaio: Struttura e Architettura 1999 Napoli, Studio tecnico di Ingeeneria Civile, Palma Campania (NA)*, Napoli, 1999.

[20] Frauenberger, A., Liu, X., Meyyappan, L., Mata, J., Gupta, T., Silva, P.F., Dagli, C.H., Pottinger, H.J., Nanni, A. Marianos, W.N. Jr (2003): *FRP Repair and Health Monitoring of Railroad Steel Bridges.* Center for Infrastructure Engineering Studies 02-28, Rolla, USA, 2003, 213 pp.

[21] Campbell, T.I., Shrive, N.G., Soudki, K.A., Al-Mayah, A., Keatley, J.P., Reda, M.M. (1999): Design and evaluation of a wedge-type anchor for fibre reinforced polymer tendons. *Can. J. Civ. Eng*, Vol 27, 2000, pp. 985-992.

[22] Maravegias, S., Triantafillou, T.C. (1996): Numerical study of anchors for composite prestresses straps. *Composite Structures*, Vol. 35, 1996, pp. 323-330.

Appendix A

Yielding moment for strengthened beams

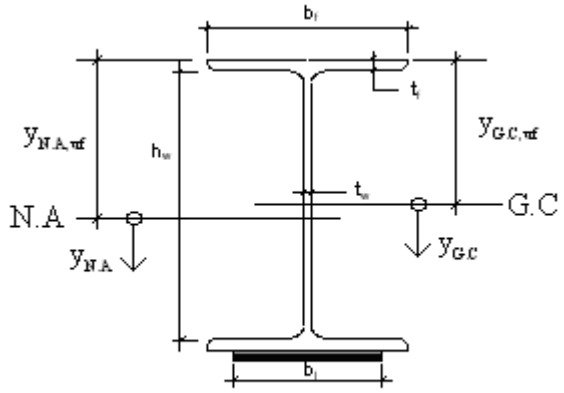

Figure A.1 Cross-section

Unstrengthened beam

For an unstrengthened beam the neutral axis coincide with the gravity centre. The stresses in the cross-section can be expressed with the following equation:

$$\sigma_{M_l}(y_{G.C}) = \frac{M_l}{I_s} \cdot y_{G.C} \tag{A.1}$$

where

σ_{M_l} is the stresses in the cross-section due to loading

M_l is the moment in the beam due to loading

I_s is the moment of inertia for the steel cross-section

$y_{G.C}$ is the distance from the gravity centre, positive downwards

To find the moment M_l for which the steel beam starts yielding the stress in the outmost upper fibre is used. Instead of a variable ($y_{G.C}$) a fixed distance ($y_{G.C,uf}$) is used, see Figure A.1. The yielding moment is the moment for which the outmost fibre

in the upper (or lower) flange is yielding. Therefore, the stress at the distance of $y_{G.C,uf}$ from the gravity centre is set to the yielding stress, $\left|\sigma_{M_l}(y_{G.C})\right| = \sigma_{yielding}$ for $\left|y_{G.C}\right| = y_{G.C,uf}$.

This will give

$$\sigma_{yielding} = \frac{M_l}{I_s} \cdot y_{G.C,uf} \tag{A.2}$$

And thereby an expression of the yielding load is received.

$$M_l = \frac{\sigma_{yielding} \cdot I_s}{y_{G.C,uf}} \tag{A.3}$$

Strengthened beam

A beam strengthened with CFRP-laminate the elastic modulus of the laminate will be different than the elastic modulus of the steel. Therefore, instead of using the moment of inertia the effective moment of inertia is used. For this cross-section the neutral axis will not coincide with the gravity centre. Instead the neutral axis will be further away from the upper flange. For a strengthened beam the stresses in the cross-section can be expressed with the following equation:

$$\sigma_{M_l}(y_{N.A}) = \frac{M_l}{I_{eff}} \cdot y_{N.A} \tag{A.4}$$

where

σ_{M_l} is the stresses in the cross-section due to loading

M_l is the moment due to loading

I_{eff} is the effective moment of inertia for the steel cross-section

$y_{N.A}$ is the distance from the neutral axis, positive downwards

The neutral axis is calculated by weighting the area of the laminate with a factor $\alpha = E_l/E_s$. For example, if the laminate has a larger elastic modulus the effective area will be α times larger.

To find the moment M_l for which the steel beam starts yielding the stress in the outmost upper fibre is used. Instead of a variable ($y_{N.A}$) a fixed distance ($y_{N.A,uf}$) is used, see Figure A.1. The yielding moment is the moment for which the outmost fibre in the upper (or lower) flange is yielding. Therefore, the stress at the distance of $y_{N.A,uf}$ above the neutral axis is set to the yielding stress, $\left|\sigma_{M_l}(y_{N.A})\right| = \sigma_{yielding}$ for $\left|y_{N.A}\right| = y_{N.A,uf}$.

This will give

$$\sigma_{yielding} = \frac{M_l}{I_{eff}} \cdot y_{N.A,uf} \tag{A.5}$$

And thereby an expression of the yielding load is received.

$$M_l = \frac{\sigma_{yielding} \cdot I_{eff}}{y_{N.A,uf}} \tag{A.6}$$

Prestressed strengthened beam

There are three different effects that influence the behaviour of a prestressed beam. The first factor is the normal stresses created by the prestressing:

$$\sigma_F = -\frac{F}{A_s} \tag{A.7}$$

where

A_s is the area of the steel cross-section

F is the prestressing force introduced to the beam

σ_F is the stresses in the cross-section due to the compressive prestressing force

The second factor is the introduced initial moment due to prestressing.

$$\sigma_M(y_{G.C}) = -\frac{F \cdot e}{I_s} \cdot y_{G.C} \tag{A.8}$$

where

e is the distance from the gravity centre to the middle of the laminate

σ_M is the stresses in the cross-section due to the initial moment

The last factor is the same as for just strengthening. The laminate will increase the effective moment of inertia and the change the position of the neutral axis.

$$\sigma_{M_l}(y_{N.A}) = \frac{M_l}{I_{eff}} \cdot y_{N.A} \tag{A.9}$$

To find the maximum moment for which the outmost fibre in the upper flange starts to yield there will be some changes. Due to the fact that we are only considering the outmost fibre in the upper flange the variable distance $y_{N.A}$ is replaced by the fixed distance $y_{N.A,uf}$ and the variable distance $y_{G.C}$ is replaced by the fixed distance $y_{G.C,uf}$. The positive direction is downwards and equation (A.8) will therefore be positive. This will give the following stress in the outmost fibre in the upper flange:

$$\sigma = \frac{F \cdot e}{I_s} \cdot y_{G.C,uf} - \frac{F}{A_s} - \frac{M_l}{I_{eff}} \cdot y_{N.A,uf} \tag{A.10}$$

By introducing $\sigma = \sigma_{yielding}$ the moment for which the outmost fibre in the upper flange starts yielding can be expressed.

$$M_{l.} = M_{yielding} = F \cdot e \cdot \frac{I_{eff}}{I_s} \frac{y_{G.C,uf}}{y_{N.A,uf}} - \frac{F}{A_s} \cdot \frac{I_{eff}}{y_{N.A,uf}} - \frac{\sigma_{yielding} \cdot I_{eff}}{y_{N.A,uf}} \tag{A.11}$$

Appendix B

Derivation of shear stresses in the middle of adhesive between laminate and steel beam

The following derivation is for a CFRP-laminate bonded to a steel beam with adhesive, see Figure B.1. The cross-section is an I-section, see Figure B.2.

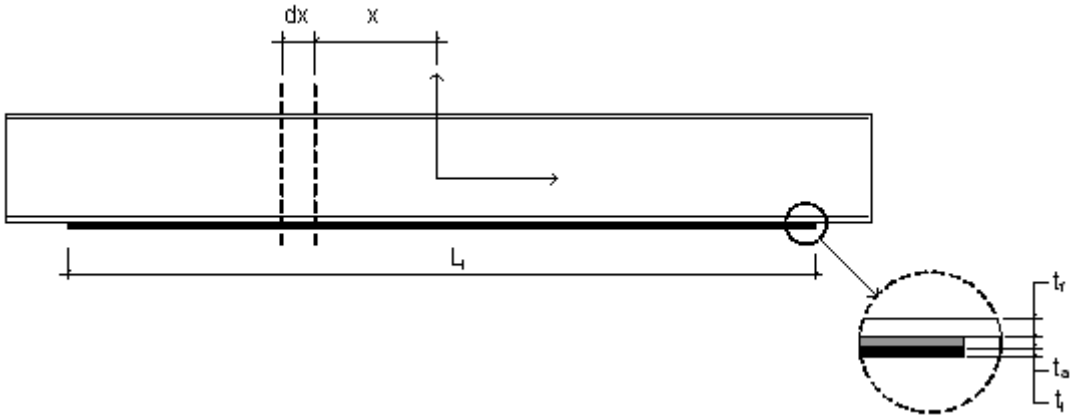

Figure B.1 A steel beam strengthened with bonded prestressed laminate

Assumptions:

1. Linear elastic materials
2. Isotropic adhesive
3. Adhesive is only subjected to shear
4. CFRL is only subjected to tension

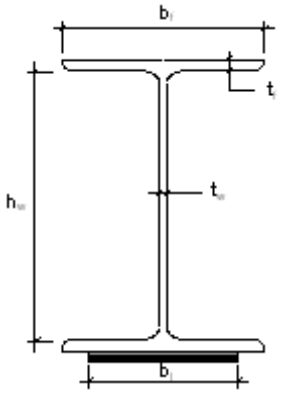

Figure B.2 Cross-section

Notations

A_l Cross-sectional area of the laminate
A_s Cross-sectional area of the beam
C_1 Constant
C_2 Constant
E_l Modulus of elasticity of the laminate
E_s Modulus of elasticity of the beam
G_a Shear modulus of the adhesive
I_s Moment of inertia of the steel beam
L Laminate length
M_s Bending moment in the beam due to prestressing
P_0 Initial prestressing force in the laminate
P_l Prestressing force in the laminate after bonding and releasing
P_s Axial force in the beam due to prestressing
b_l Width of the laminate
h Height of the beam
t_a Thickness of the adhesive layer
t_l Thickness of the laminate
δ_l Displacement in the laminate
δ_s Displacement in the outmost fibres of the beam lower flange
ε_l Strain in the laminate
ε_s Strain in the outmost fibres of the beam lower flange
τ Shear stress in the adhesive layer
ω Constant

Deformation compatibility

The shear stress in the adhesive is related to the difference of the deformations in the lower flange of the steel beam and in the laminate, see Figure B.3.

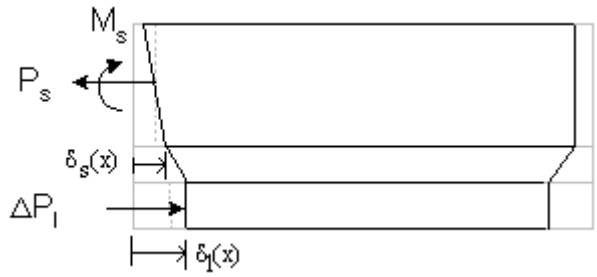

Figure B.3 Sectional forces and deformations in a section of the composite beam at a distance x from the mid-span of the beam

$$\gamma(x) = \frac{\delta_l(x) - \delta_s(x)}{t_a}$$

But

$$\gamma(x) = \frac{\tau(x)}{G_a}$$

$$\Rightarrow$$

$$\tau(x) = \frac{G_a}{t_a} \cdot \left(\delta_1(x) - \delta_s(x)\right) \tag{B.1}$$

$$\frac{d}{dx}\delta_s(x) = \varepsilon_s(x) = \frac{-P_s(x)}{A_s \cdot E_s} + \frac{-M_s(x)}{I_s \cdot E_s} \cdot \frac{h}{2} \tag{B.2}$$

$$\frac{d}{dx}\delta_1(x) = \Delta\varepsilon_1(x) = \frac{\Delta P_1(x)}{A_1 \cdot E_1} = \frac{P_0 - P_1(x)}{A_1 \cdot E_1} \tag{B.3}$$

Deriving equation (B.1) with respect to x

$$\frac{d}{dx}\tau(x) = \frac{G_a}{t_a} \cdot \left(\frac{d}{dx}\delta_1(x) - \frac{d}{dx}\delta_s(x)\right)$$

$$\Rightarrow$$

$$\frac{d}{dx}\tau(x) = \frac{G_a}{t_a} \cdot \left(\frac{P_0}{A_1 \cdot E_1} - \frac{P_1(x)}{A_1 \cdot E_1} + \frac{P_s(x)}{A_s \cdot E_s} + \frac{M_s(x)}{I_s \cdot E_s} \cdot \frac{h}{2}\right) \tag{B.4}$$

Equilibrium

Equilibrium of the horizontal forces and the moments in segment dx at a distance x from the mid-span of the beam, see Figure B.4, gives:

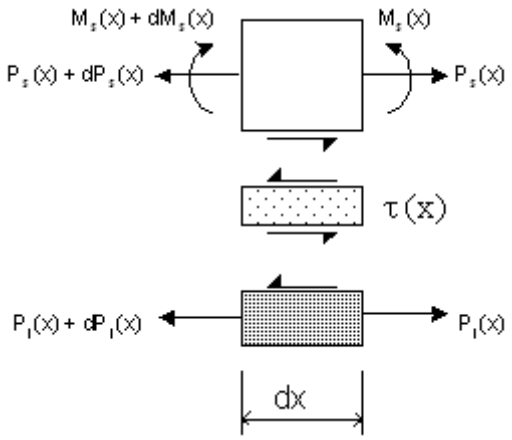

Figure B.4 Equilibrium of forces in a segment dx at a distance x from the mid-span of the beam

H :

$$\frac{d}{dx}P_s(x) = b_1 \cdot \tau(x) \tag{B.5}$$

$$\frac{d}{dx}P_l(x) = -b_1 \cdot \tau(x) \tag{B.6}$$

M :

$$\frac{d}{dx}M_s(x) = b_1 \cdot \frac{h}{2} \cdot \tau(x) \tag{B.7}$$

Deriving equation (B.4) yields:

$$\frac{d^2}{dx^2}\tau(x) = \frac{G_a}{t_a}\cdot\left(\frac{-1}{A_l \cdot E_l}\cdot\frac{d}{dx}P_l(x) + \frac{1}{A_s \cdot E_s}\cdot\frac{d}{dx}P_s(x) + \frac{h}{2I_s \cdot E_s}\cdot\frac{d}{dx}M_s(x)\right) \tag{B.8}$$

Inserting the equilibrium conditions (B.5) - (B.7) in (B.4) results:

$$\frac{d^2}{dx^2}\tau(x) = \frac{G_a}{t_a}\cdot\left(\frac{b_1}{A_l \cdot E_l} + \frac{b_1}{A_s \cdot E_s} + \frac{b \cdot h^2}{4I_s \cdot E_s}\right)\cdot\tau(x) \tag{B.9}$$

or:

$$\frac{d^2}{dx^2}(\tau(x)) = \omega^2 \cdot \tau(x) \tag{B.10}$$

In which:

$$\omega^2 = \frac{G_a}{t_a}\cdot\left(\frac{b_1}{A_1\cdot E_1} + \frac{b_1}{A_s\cdot E_s} + \frac{b\cdot h^2}{4I_s\cdot E_s}\right)$$

Equation (B.5) has the following general solution:

$$\tau(x) = C_1\cdot e^{\omega x} + C_2\cdot e^{-\omega x} \tag{B.11}$$

C1 and C2 are to be determined from boundary conditions.

Boundary conditions

Due to symmetry, all displacements at the middle of the composite beam are zero:

1)

$$\delta_1(x = 0) = \delta_s(x = 0) = 0$$

Together with equation (B.1), this gives:

$$\tau(x = 0) = 0$$

$$C_1 = -C_2$$

At the end of the laminate, the forces and moment are zero:

2)

$$P_1\left(x = \frac{L}{2}\right) = P_s\left(x = \frac{L}{2}\right) = M_s\left(x = \frac{L}{2}\right) = 0$$

$$M(x = 0) = P_0\cdot\frac{h}{2}$$

Inserting in (B.4) gives:

$$\frac{d}{dx}\tau(x) = \frac{G_a\cdot P_0}{t_a\cdot A_1\cdot E_1}$$

$$\frac{d}{dx}\tau(x) = \frac{G_a\cdot P_0}{t_a\cdot A_1\cdot E_1} = \omega\cdot C_1\cdot e^{\frac{\omega L}{2}} - \omega\cdot C_2\cdot e^{\frac{-\omega L}{2}}$$

$$C_1 = -C_2 = \frac{G_a \cdot P_0}{t_a \cdot A_1 \cdot E_1} \cdot \frac{1}{2 \cdot \omega \cdot \cosh\left(\frac{\omega \cdot L}{2}\right)}$$

Substituting in (B.11) gives equation (B.12). Equation (B.12) describes the distribution of the shear stresses in the adhesive layer along the bond line:

$$\tau(x) = \frac{G_a \cdot P_0}{t_a \cdot A_1 \cdot E_1} \cdot \frac{\sinh(\omega \cdot x)}{\omega \cdot \cosh\left(\frac{\omega \cdot L}{2}\right)} \tag{B.12}$$

Deriving (B.12) and equating with (B.4) after substituting:

$$\frac{G_a \cdot P_0}{t_a \cdot A_1 \cdot E_1} \cdot \frac{\cosh(\omega \cdot x)}{\cosh\left(\omega \cdot \frac{L}{2}\right)} = \frac{G_a}{t_a} \cdot \left(\frac{P_0}{A_1 \cdot E_1} - \frac{P_1(x)}{A_1 \cdot E_1} - \frac{P_1(x)}{A_s \cdot E_s} - \frac{P_1(x)}{I_s \cdot E_s} \cdot \frac{h^2}{4} \right)$$

$$M_s(x) = -P_1(x) \cdot \frac{h}{2}$$

$$\left(\frac{h}{2} > t_a, t_1 \right)$$

$$P_1(x) = -P_s(x)$$

$$\frac{d}{dx}\tau(x) = \frac{G_a}{t_a} \cdot \left(\frac{P_0}{A_1 \cdot E_1} - \frac{P_1(x)}{A_1 \cdot E_1} - \frac{P_1(x)}{A_s \cdot E_s} - \frac{P_1(x)}{I_s \cdot E_s} \cdot \frac{h^2}{4} \right) = \frac{G_a \cdot P_0}{t_a \cdot A_1 \cdot E_1} \cdot \frac{\cosh(\omega \cdot x)}{\cosh\left(\omega \cdot \frac{L}{2}\right)}$$

The distribution of the axial force in the laminate can be expressed as:

$$P_1(x) = \frac{P_0}{A_1 \cdot E_1} \cdot \left(1 - \frac{\cosh(\omega \cdot x)}{\cosh\left(\omega \cdot \frac{L}{2}\right)} \right) \cdot \frac{1}{\frac{1}{A_1 \cdot E_1} + \frac{1}{A_s \cdot E_s} + \frac{h^2}{4 \cdot E_s \cdot I_s}} \tag{B.13}$$

The equilibrium requires that:

$$P_s(x) = -P_1(x) \tag{B.14}$$

It is assumed that the thickness of the laminate is very small compared to the height of the beam. Therefore, the thickness of the laminate is neglected when the bending moment is calculated.

The distribution of the bending moment along the length of the strengthened beam becomes:

$$M_s(x) = -P_0 \cdot \frac{h}{2} \cdot \frac{1 - \dfrac{\cosh(\omega \cdot x)}{\cosh\left(\omega \cdot \dfrac{L}{2}\right)}}{1 + \dfrac{A_1 \cdot E_1}{A_s \cdot E_s} + \dfrac{A_1 \cdot E_1 \cdot h^2}{4 \cdot E_s \cdot I_s}} \qquad \text{(B.15)}$$

Appendix C

Shear stresses in adhesive when the elastic modulus of the adhesive is 1 GPa

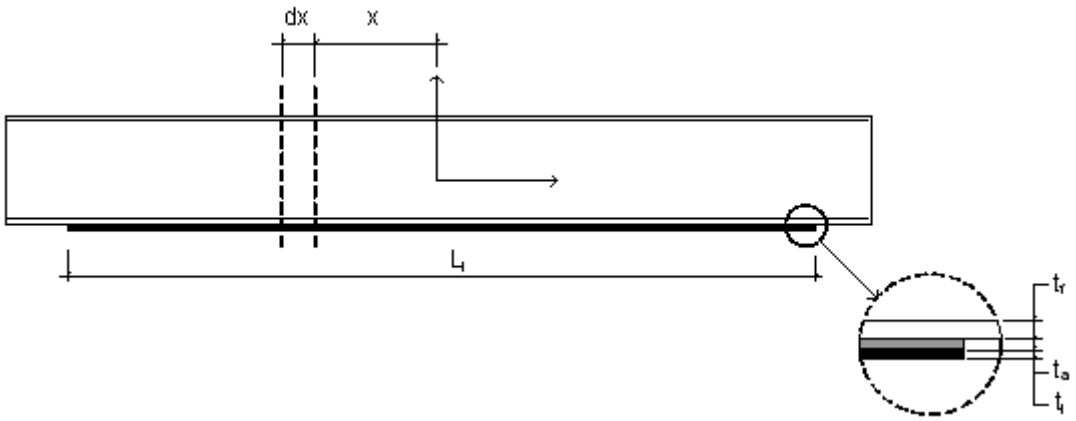

Figure C.1 Steel beam strengthened with bonded prestressed laminate

Adhesive

$E_a := 1GPa$

$t_a := 2mm$

$\upsilon_a := 0.3$

$$G_a := \frac{E_a}{2\cdot(1+\upsilon_a)}$$

Laminate

$E_1 := 165\cdot10^3\cdot MPa$

$t_1 := 2mm$

$b_1 := 80mm$

$A_1 := b_1\cdot t_1$

$L := 1.6m$

Steel beam

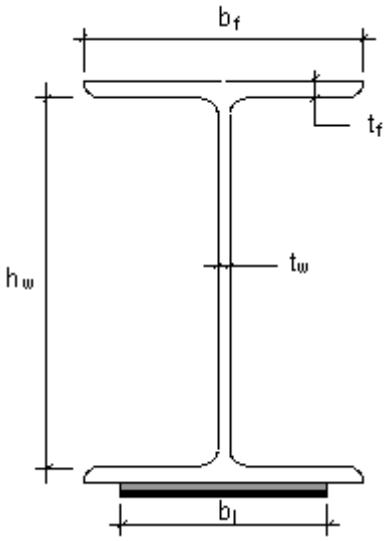

Figure C.2 Cross-section of steel beam strengthened with bonded prestressed laminate

$E_s := 212 \cdot 10^3 MPa$

$b := 180mm$

$h := 171mm$

$hw := 152mm$

$t_f := 9.5mm$

$t_w := 6mm$

$A_s := 2 \cdot (b \cdot t_f) + hw \cdot t_w$

$$I_s := \frac{t_w \cdot hw^3}{12} + 2 \cdot b \cdot t_f \left(\frac{hw}{2} + \frac{t_f}{2} \right)^2 + 2 \cdot b \cdot \frac{t_f^3}{12}$$

$I_s = 2.408 \times 10^{-5} m^4$

$$W_s := \frac{I_s}{\frac{h}{2}}$$

Prestressing

$\sigma_0 := 1605\text{MPa}$

$P_0 := \sigma_0 \cdot t_l \cdot b_l$

$P_0 = 256.8\,\text{kN}$

Prestressing force in the laminate after bonding and releasing, P_l, is 240 kN.

The distribution of the shear stresses in the adhesive layer along the bond line, x, is the distance from the mid-span of the beam.

$$\tau(x) := \frac{G_a \cdot P_0}{t_a \cdot A_l \cdot E_l} \cdot \frac{\sinh(\omega \cdot x)}{\omega \cdot \cosh\left(\frac{\omega \cdot L}{2}\right)}$$

Maximum shear stress will appear at the end of the laminate:

$\tau\left(\frac{L}{2}\right) = 75.034\,\text{MPa}$

The distribution of the shear stresses in the adhesive along the bond line, see Figure C.3.

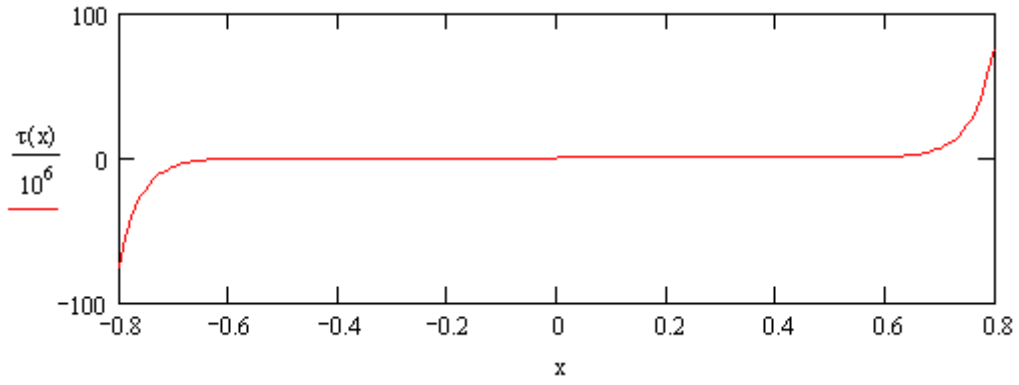

Figure C.3 Shear stresses at the distance x from the mid-span of the beam

Appendix D

Shear stresses in adhesive when the elastic modulus of the adhesive is 5 GPa

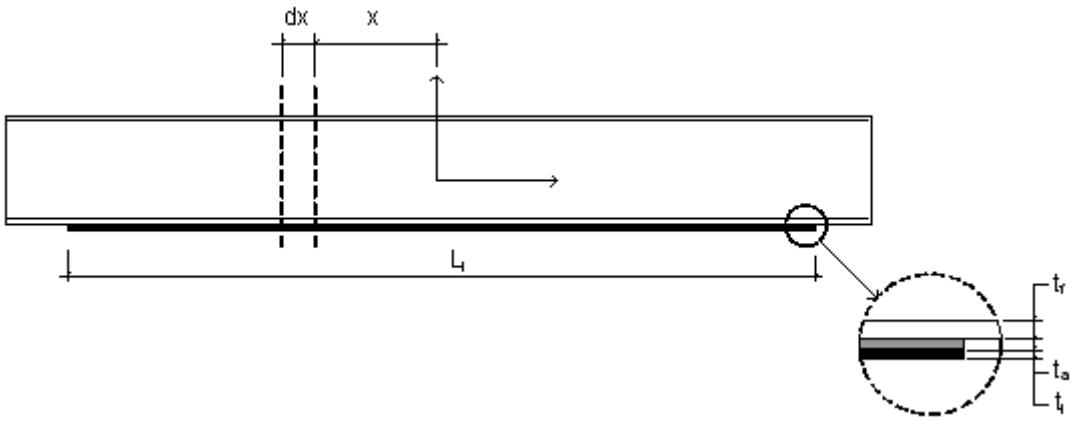

Figure D.1 Steel beam strengthened with bonded prestressed laminate

Adhesive

$E_a := 5GPa$

$t_a := 2mm$

$\upsilon_a := 0.3$

$$G_a := \frac{E_a}{2\cdot(1+\upsilon_a)}$$

Laminate

$E_1 := 165\cdot10^3\cdot MPa$

$t_1 := 2mm$

$b_1 := 80mm$

$A_1 := b_1\cdot t_1$

$L := 1.6m$

Steel beam

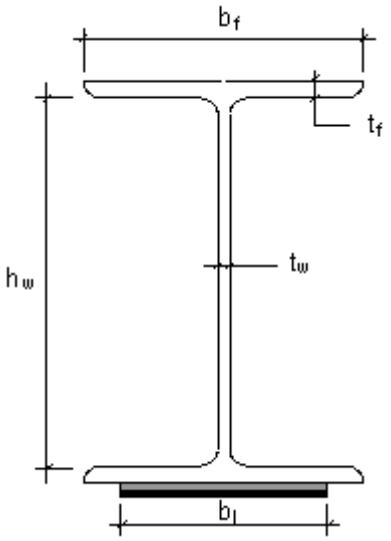

Figure D.2 Cross-section of steel beam strengthened with bonded prestressed laminate

$E_s := 212 \cdot 10^3 MPa$

$b := 180mm$

$h := 171mm$

$hw := 152mm$

$t_f := 9.5mm$

$t_w := 6mm$

$A_s := 2 \cdot (b \cdot t_f) + hw \cdot t_w$

$$I_s := \frac{t_w \cdot hw^3}{12} + 2 \cdot b \cdot t_f \left(\frac{hw}{2} + \frac{t_f}{2} \right)^2 + 2 \cdot b \cdot \frac{t_f^3}{12}$$

$I_s = 2.408 \times 10^{-5} m^4$

$$W_s := \frac{I_s}{\frac{h}{2}}$$

Prestressing

$\sigma_0 := 1605MPa$

$P_0 := \sigma_0 \cdot t_1 \cdot b_1$

$P_0 = 256.8\,kN$

Prestressing force in the laminate after bonding and releasing, P_l, is 240 kN.

The distribution of the shear stresses in the adhesive layer along the bond line, x, is the distance from the mid-span of the beam.

$$\tau(x) := \frac{G_a \cdot P_0}{t_a \cdot A_1 \cdot E_1} \cdot \frac{\sinh(\omega \cdot x)}{\omega \cdot \cosh\left(\frac{\omega \cdot L}{2}\right)}$$

Maximum shear stress will appear at the end of the laminate:

$$\tau\left(\frac{L}{2}\right) = 167.78\,MPa$$

The distribution of the shear stresses in the adhesive along the bond line, see Figure D.3.

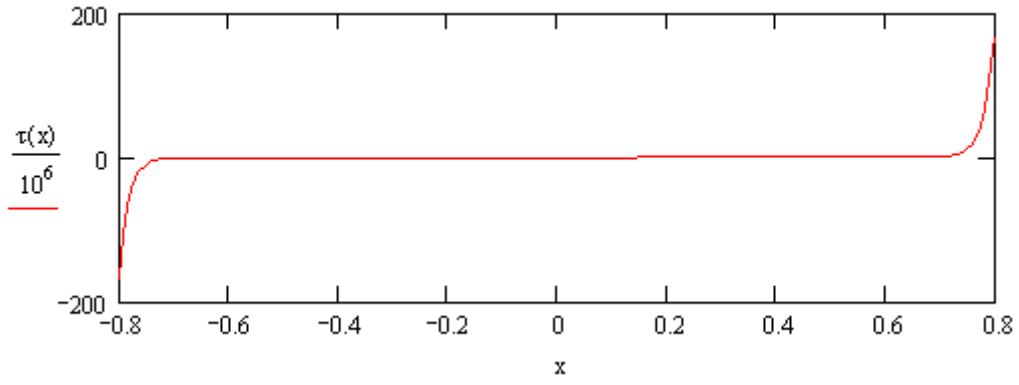

Figure D.3 Shear stresses at the distance x from the mid-span of the beam

Appendix E

Shear stresses in adhesive when the elastic modulus of the adhesive is 9 GPa

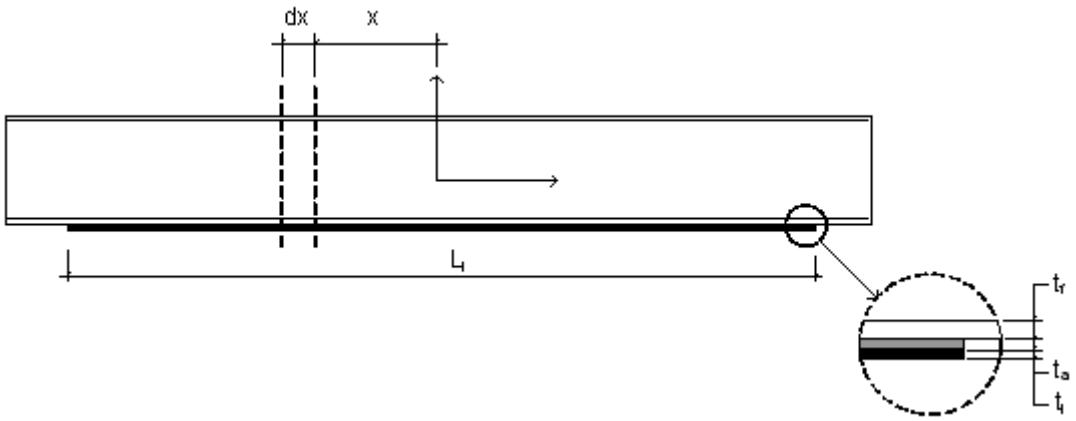

Figure E.1 Steel beam strengthened with bonded prestressed laminate

Adhesive

$E_a := 9GPa$

$t_a := 2mm$

$\upsilon_a := 0.3$

$$G_a := \frac{E_a}{2\cdot(1+\upsilon_a)}$$

Laminate

$E_1 := 165\cdot10^3\cdot MPa$

$t_1 := 2mm$

$b_1 := 80mm$

$A_1 := b_1\cdot t_1$

$L := 1.6m$

Steel beam

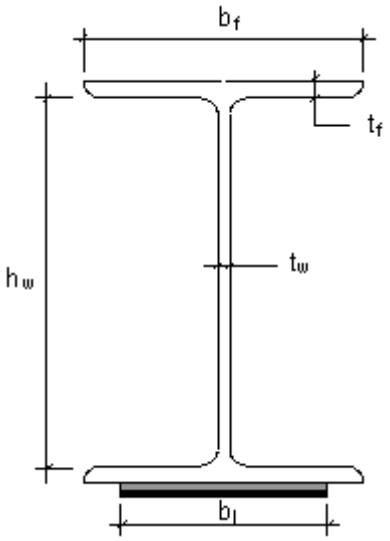

Figure E.2 Cross-section of steel beam strengthened with bonded prestressed laminate

$E_s := 212 \cdot 10^3 MPa$

$b := 180mm$

$h := 171mm$

$hw := 152mm$

$t_f := 9.5mm$

$t_w := 6mm$

$A_s := 2 \cdot (b \cdot t_f) + hw \cdot t_w$

$$I_s := \frac{t_w \cdot hw^3}{12} + 2 \cdot b \cdot t_f \left(\frac{hw}{2} + \frac{t_f}{2} \right)^2 + 2 \cdot b \cdot \frac{t_f^3}{12}$$

$I_s = 2.408 \times 10^{-5} m^4$

$$W_s := \frac{I_s}{\frac{h}{2}}$$

Prestressing

$\sigma_0 := 1605\text{MPa}$

$P_0 := \sigma_0 \cdot t_l \cdot b_l$

$P_0 = 256.8\,\text{kN}$

Prestressing force in the laminate after bonding and releasing, P_l, is 240 kN.

The distribution of the shear stress in the adhesive layer along the bond line, x, is the distance from the mid-span of the beam.

$$\tau(x) := \frac{G_a \cdot P_0}{t_a \cdot A_l \cdot E_l} \cdot \frac{\sinh(\omega \cdot x)}{\omega \cdot \cosh\left(\frac{\omega \cdot L}{2}\right)}$$

Maximum shear stress will appear at the end of the laminate:

$$\tau\left(\frac{L}{2}\right) = 225.101\,\text{MPa}$$

The distribution of the shear stresses in the adhesive along the bond line, see Figure E.3.

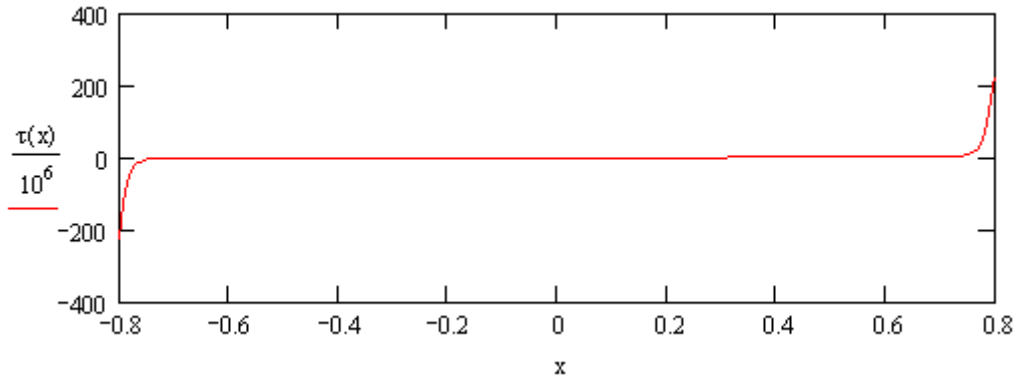

Figure E.3 Shear stresses at the distance of x from the mid-span of the beam

Appendix F

Shear stresses in adhesive when the elastic modulus of the laminate is 100 GPa

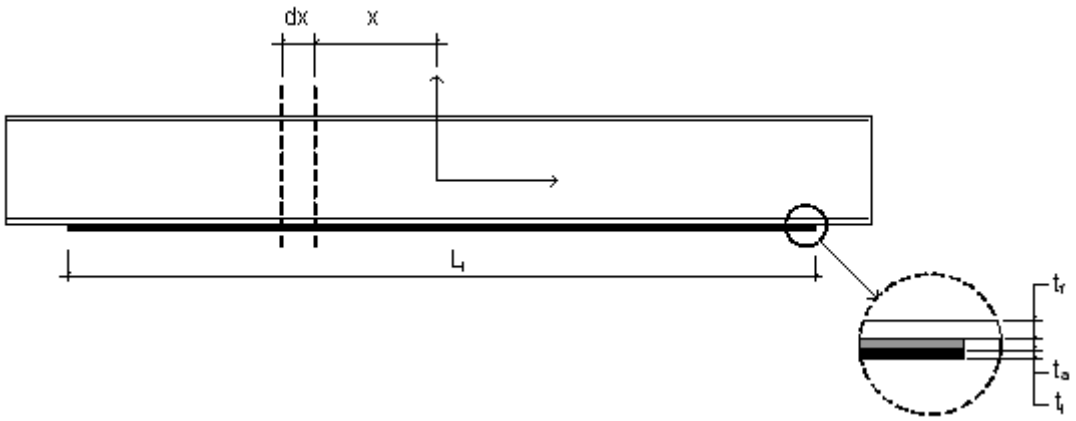

Figure F.1 Steel beam strengthened with bonded prestressed laminate

Adhesive

$E_a := 7GPa$

$t_a := 2mm$

$\upsilon_a := 0.3$

$$G_a := \frac{E_a}{2\cdot(1+\upsilon_a)}$$

Laminate

$E_1 := 100\cdot10^3\cdot MPa$

$t_1 := 2mm$

$b_1 := 80mm$

$A_1 := b_1\cdot t_1$

$L := 1.6m$

Steel beam

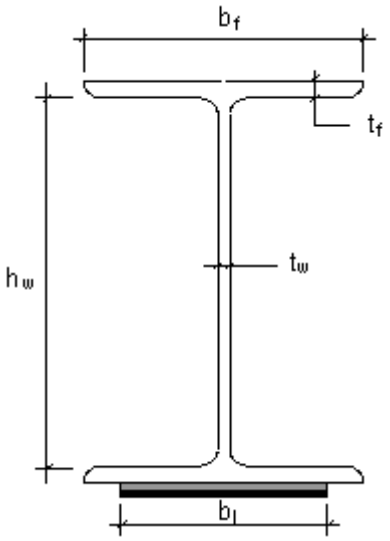

Figure F.2 Cross-section of steel beam strengthened with bonded prestressed laminate

$E_s := 212 \cdot 10^3 MPa$

$b := 180mm$

$h := 171mm$

$hw := 152mm$

$t_f := 9.5mm$

$t_w := 6mm$

$A_s := 2 \cdot (b \cdot t_f) + hw \cdot t_w$

$$I_s := \frac{t_w \cdot hw^3}{12} + 2 \cdot b \cdot t_f \left(\frac{hw}{2} + \frac{t_f}{2} \right)^2 + 2 \cdot b \cdot \frac{t_f^3}{12}$$

$I_s = 2.408 \times 10^{-5} m^4$

$$W_s := \frac{I_s}{\frac{h}{2}}$$

Prestressing

$\sigma_0 := 1567\text{MPa}$

$P_0 := \sigma_0 \cdot t_l \cdot b_l$

$P_0 = 250.72\,\text{kN}$

Prestressing force in the laminate after bonding and releasing, P_l, is 240 kN.

The distribution of the shear stresses in the adhesive layer along the bond line, x, is the distance from the mid-span of the beam.

$$\tau(x) := \frac{G_a \cdot P_0}{t_a \cdot A_l \cdot E_l} \cdot \frac{\sinh(\omega \cdot x)}{\omega \cdot \cosh\left(\frac{\omega \cdot L}{2}\right)}$$

Maximum shear stress will appear at the end of the laminate:

$$\tau\left(\frac{L}{2}\right) = 252.084\,\text{MPa}$$

The distribution of the shear stresses in the adhesive along the bond line, see Figure F.3.

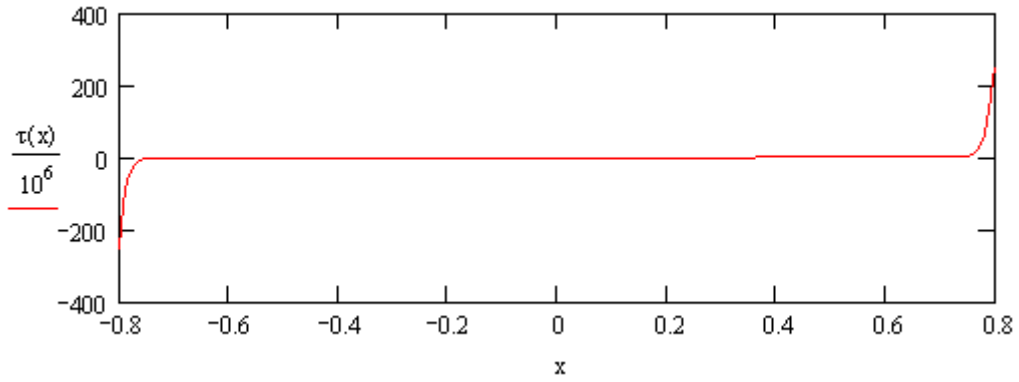

Figure F.3 Shear stresses at the distance x from the mid-span of the beam

Appendix G

Shear stresses in adhesive when the elastic modulus of the laminate is 200 GPa

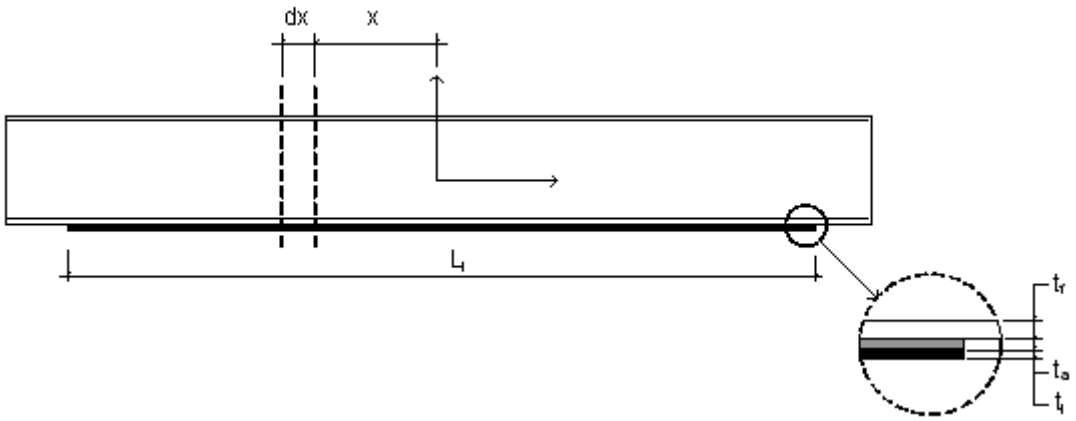

Figure G.1 Steel beam strengthened with bonded prestressed laminate

Adhesive

$E_a := 7GPa$

$t_a := 2mm$

$\upsilon_a := 0.3$

$$G_a := \frac{E_a}{2\cdot(1+\upsilon_a)}$$

Laminate

$E_1 := 200\cdot10^3\cdot MPa$

$t_1 := 2mm$

$b_1 := 80mm$

$A_1 := b_1\cdot t_1$

$L := 1.6m$

Steel beam

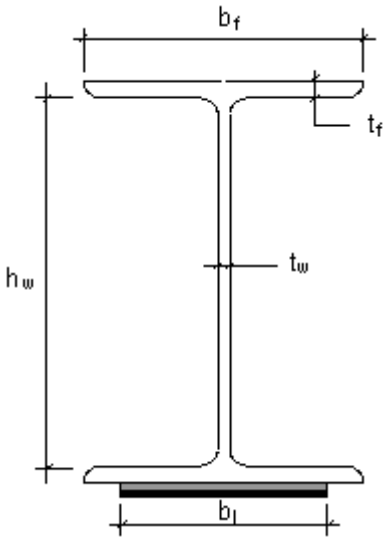

Figure G.2 Cross-section of steel beam strengthened with bonded prestressed laminate

$E_s := 212 \cdot 10^3 MPa$

$b := 180mm$

$h := 171mm$

$hw := 152mm$

$t_f := 9.5mm$

$t_w := 6mm$

$A_s := 2 \cdot (b \cdot t_f) + hw \cdot t_w$

$$I_s := \frac{t_w \cdot hw^3}{12} + 2 \cdot b \cdot t_f \left(\frac{hw}{2} + \frac{t_f}{2} \right)^2 + 2 \cdot b \cdot \frac{t_f^3}{12}$$

$I_s = 2.408 \times 10^{-5} m^4$

$$W_s := \frac{I_s}{\frac{h}{2}}$$

Prestressing

$\sigma_0 := 1625\text{MPa}$

$P_0 := \sigma_0 \cdot t_l \cdot b_l$

$P_0 = 260\,\text{kN}$

Prestressing force in the laminate after bonding and releasing, P_l, is 240 kN.

The distribution of the shear stress in the adhesive layer along the bond line, x, is the distance from the mid-span of the beam.

$$\tau(x) := \frac{G_a \cdot P_0}{t_a \cdot A_l \cdot E_l} \cdot \frac{\sinh(\omega \cdot x)}{\omega \cdot \cosh\left(\frac{\omega \cdot L}{2}\right)}$$

Maximum shear stress will appear at the end of the laminate:

$$\tau\left(\frac{L}{2}\right) = 181.366\,\text{MPa}$$

The distribution of the shear stresses in the adhesive along the bond line, see Figure G.3.

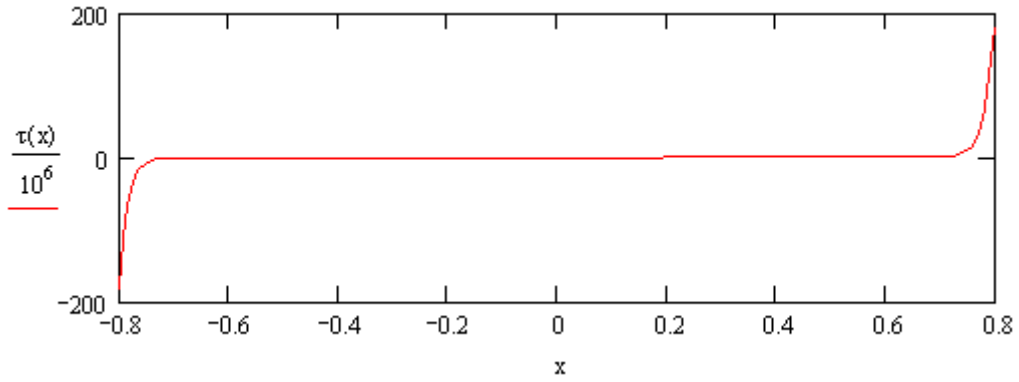

Figure G.3 Shear stresses at the distance x from the mid-span of the beam

Appendix H

Shear stresses in adhesive when the elastic modulus of the laminate is 300 GPa

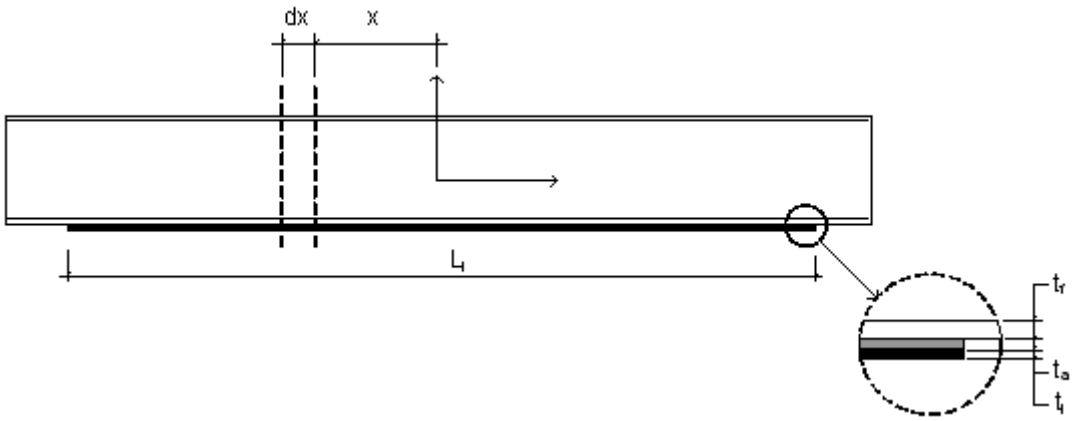

Figure H.1 Steel beam strengthened with bonded prestressed laminate

Adhesive

$E_a := 7GPa$

$t_a := 2mm$

$\upsilon_a := 0.3$

$$G_a := \frac{E_a}{2\cdot(1+\upsilon_a)}$$

Laminate

$E_l := 300\cdot10^3\cdot MPa$

$t_l := 2mm$

$b_l := 80mm$

$A_l := b_l\cdot t_l$

$L := 1.6m$

Steel beam

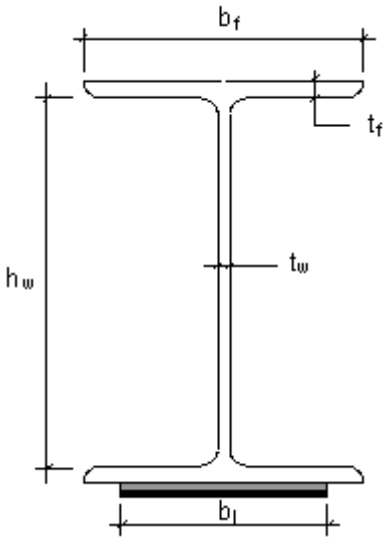

Figure H.2 Cross-section of steel beam strengthened with bonded prestressed laminate

$E_s := 212 \cdot 10^3 MPa$

$b := 180mm$

$h := 171mm$

$hw := 152mm$

$t_f := 9.5mm$

$t_w := 6mm$

$A_s := 2 \cdot (b \cdot t_f) + hw \cdot t_w$

$$I_s := \frac{t_w \cdot hw^3}{12} + 2 \cdot b \cdot t_f \left(\frac{hw}{2} + \frac{t_f}{2} \right)^2 + 2 \cdot b \cdot \frac{t_f^3}{12}$$

$I_s = 2.408 \times 10^{-5} m^4$

$$W_s := \frac{I_s}{\frac{h}{2}}$$

Prestressing

$\sigma_0 := 1676MPa$

$P_0 := \sigma_0 \cdot t_l \cdot b_l$

$P_0 = 268.16\,kN$

Prestressing force in the laminate after bonding and releasing, P_l, is 240 kN.

The distribution of the shear stresses in the adhesive layer along the bond line, x, is the distance from the mid-span of the beam.

$$\tau(x) := \frac{G_a \cdot P_0}{t_a \cdot A_l \cdot E_l} \cdot \frac{\sinh(\omega \cdot x)}{\omega \cdot \cosh\left(\frac{\omega \cdot L}{2}\right)}$$

Maximum shear stress will appear at the end of the laminate:

$$\tau\left(\frac{L}{2}\right) = 149.959\,MPa$$

The distribution of the shear stresses in the adhesive along the bond line, see Figure H.3.

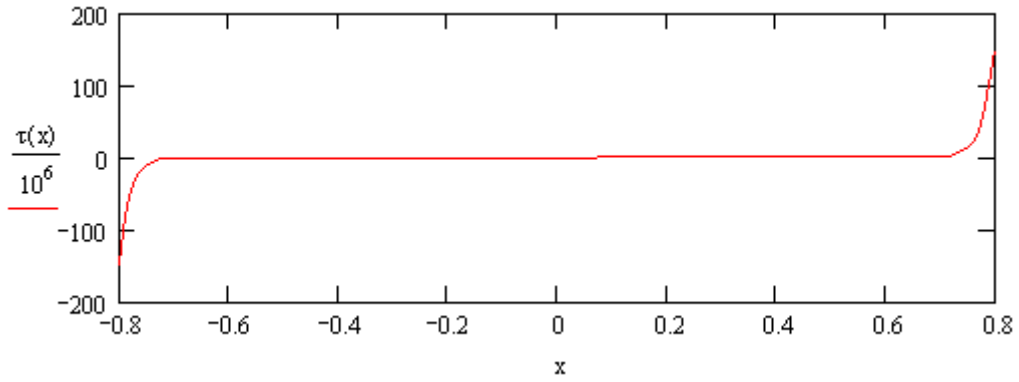

Figure H.3 Shear stresses at the distance x from the mid-span of the beam

Appendix I

Convergence study

A convergence study was performed in order to find an appropriate mesh. With help of this study the mesh size in critical areas was chosen, see Figure I.1.

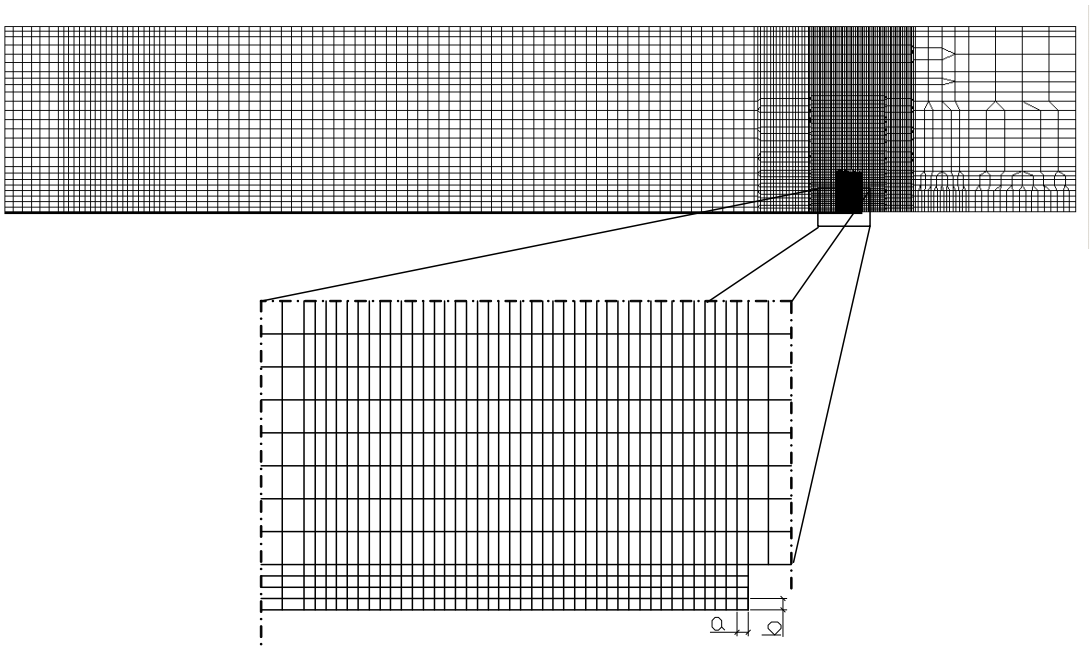

Figure I.1 *Mesh of the adhesive at the end of the laminate. a is the width of the elements and b is the height of the elements*

Shear and peeling stresses for different meshes were plotted in order to find out if the model converge, see Figure I.2 and Figure I.3. After studying how the maximum shear and peeling stresses are varying by changing the mesh density, appropriate values of a and b were chosen. To ensure sufficiently accurate results the values a = 0.5 mm and b = 0.5 mm were chosen.

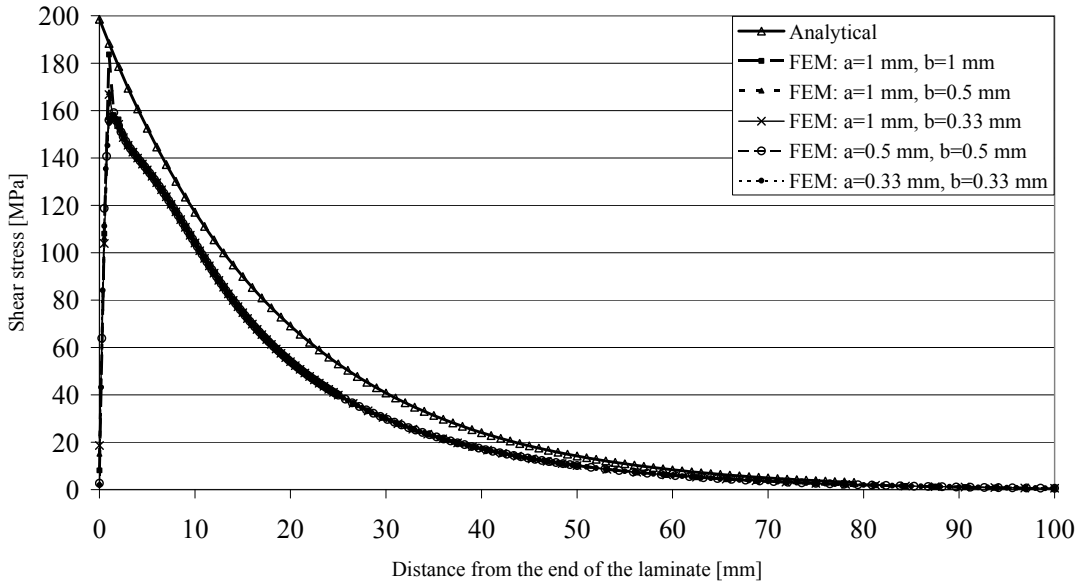

Figure I.2 Convergence study of shear stresses

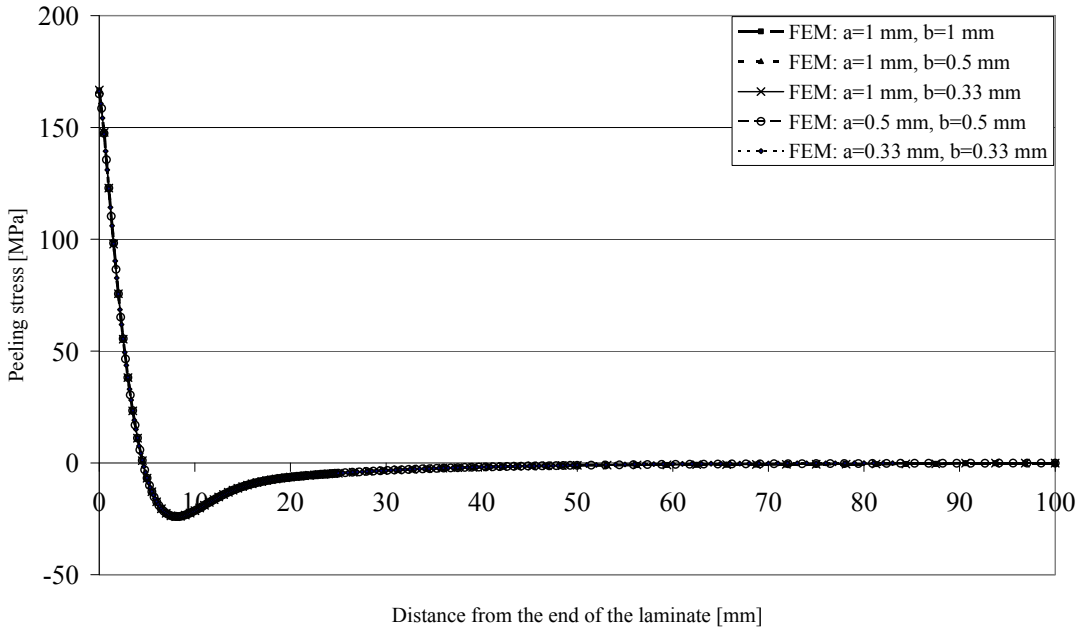

Figure I.3 Convergence study of peeling stresses

Appendix J

Calculations of yielding loads

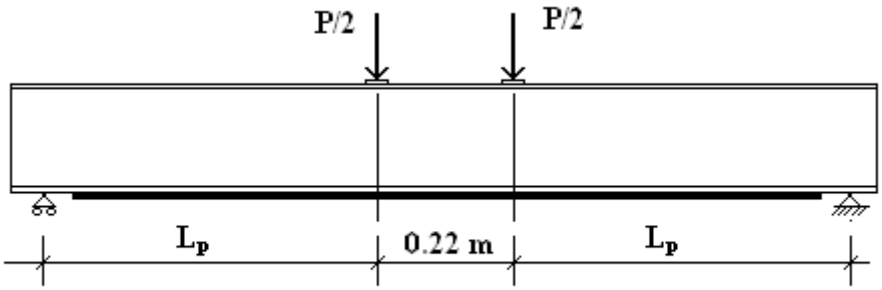

Figure J.1 A steel beam strengthened with bonded laminate

The moment in the mid-section is:

$$M_l = \frac{P}{2} \cdot L_p \qquad L_p := 0.79m$$

where

M_l is the moment in the mid-section

P is the total load

L_p is the distance between the concentrated load and the support

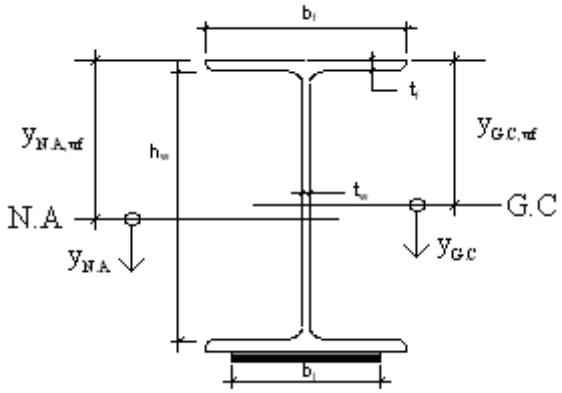

Figure J.2 Cross-section

Stresses in the cross-section, moment capacity:

1. Unstrengthened beam

$$\sigma(y_{G.C}) = \frac{M_1}{I_s} \cdot y_{G.C}$$

$$M_{yielding} = \frac{\sigma_{yielding} \cdot I_s}{y_{G.C,uf}}$$

where

I_s is the moment of inertia for steel cross-section
$M_{yielding}$ is the moment for which the beam starts yielding
$y_{G.C}$ is the distance away from the gravity centre, positive direction downwards
$y_{G.C,uf}$ is the distance from the gravity centre to the outmost fibre in the upper flange
$\sigma(y_{G.C})$ is the stress distribution in the cross-section
$\sigma_{yielding}$ is the stress for which the steel starts yielding

2. Strengthened beam, unprestressed

$$\sigma(y_{N.A}) = \frac{M_1}{I_{eff}} \cdot y_{N.A}$$

$$M_{yielding} = \frac{\sigma_{yielding} \cdot I_{eff}}{y_{N.Auf}}$$

where

I_{eff} is the effective moment of inertia

$Y_{N.A}$ is the distance from the neutral axis, positive direction downwards
$Y_{N.Auf}$ is the distance between the neutral axis and the outmost fibre in the upper flange

3. Prestressed beam

$$\sigma(y_{G.C}, y_{N.A}) = -\frac{N_p \cdot e}{I_s} \cdot y_{G.C} - \frac{N_p}{A_s} + \frac{M_1}{I_{eff}} \cdot y_{N.A}$$

$$M_{yielding} = N_p \cdot e \cdot \frac{y_{G.Cuf}}{y_{N.Auf}} \cdot \frac{I_{eff}}{I_s} - \frac{N_p \cdot I_{eff}}{A_s \cdot y_{N.Auf}} - \frac{\sigma_{yielding} \cdot I_{eff}}{y_{N.Auf}}$$

where

A_s is the cross-sectional area of the steel beam
N_p is the prestressing force introduced into the beam
e is the distance between the gravity centre and the middle of the adhesive

1. Unstrengthened beam

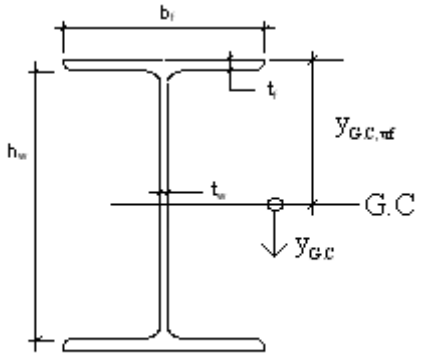

Figure J.3 Cross-section of unstrengthened beam

Steel beam

$E_s := 212 \cdot 10^3 MPa$ $b_f := 180mm$ $h_w := 152mm$

$t_f := 9.5mm$ $t_w := 6mm$ $h = 0.171\ m$

$A_s := 2 \cdot (b_f t_f) + h_w \cdot t_w$ $A_s = 4.332 \times 10^{-3}\ m^2$

$$I_s := \frac{t_w \cdot h_w^3}{12} + 2 \cdot b_f t_f \left(\frac{h_w}{2} + \frac{t_f}{2}\right)^2 + 2 \cdot b_f \frac{t_f^3}{12} \qquad I_s = 2.408 \times 10^{-5}\ m^4$$

$y_{G.Cuf} := \frac{-171}{2} \cdot mm$ $\quad y_{G.Cuf} = -0.086\ m$

$\sigma_{yielding} := -328.5MPa$

Yielding moment:

$M_{yielding} := \frac{\sigma_{yielding} \cdot I_s}{y_{G.Cuf}}$ $\quad M_{yielding} = 92.525\ kN \cdot m$

Yielding load:

$P_1 := \frac{2M_{yielding}}{L_p}$ $\quad P_1 = 234.241\ kN$

2.A Strengthened beam with laminate E=165 GPa

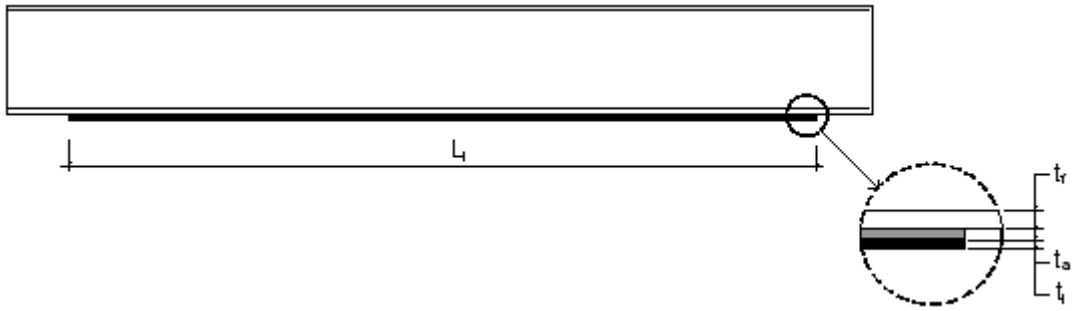

Figure J.4 Thickness of flange, adhesive, and laminate

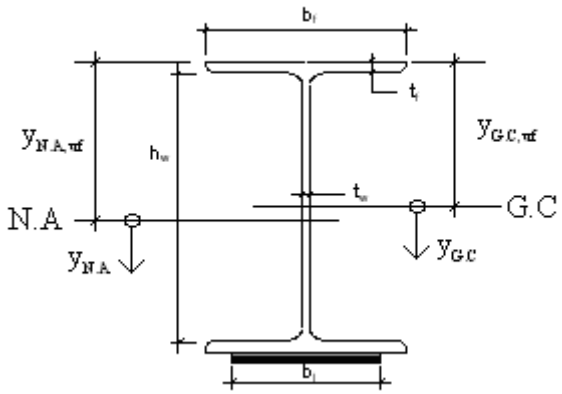

Figure J.5 Cross-section of strengthened beam

Steel beam	Adhesive	Laminate
$E_s := 212 \cdot 10^3 MPa$	$E_a := 7GPa$	$E_l := 165 \cdot 10^3 \cdot MPa$
$b_f := 180mm$	$ba := 80mm$	$b_l := 80mm$
$h_w := 152mm$	$t_a := 2mm$	$t_l := 2mm$
$t_f := 9.5mm$	$A_a := ba \cdot t_a$	$A_l := b_l \cdot t_l$
$t_w := 6mm$	$A_a = 1.6 \times 10^{-4}\ m^2$	$A_l = 1.6 \times 10^{-4}\ m^2$
$h = 0.171\ m$	$A_{aeff} := A_a \cdot \frac{E_{adh}}{E_s}$	$A_{leff} := A_l \cdot \frac{E_l}{E_s}$
$A_s := 2 \cdot (b_f t_f) + h_w \cdot t_w$	$A_{aeff} = 5.283 \times 10^{-6}\ m^2$	$A_{leff} = 1.245 \times 10^{-4}\ m^2$
$A_s = 4.332 \times 10^{-3}\ m^2$		
$I_s := \frac{t_w \cdot h_w^3}{12} + 2 \cdot b_f t_f \left(\frac{h_w}{2} + \frac{t_f}{2}\right)^2 + 2 \cdot b_f \frac{t_f^3}{12}$		$I_s = 2.408 \times 10^{-5}\ m^4$

The location of the neutral axis:

$$NA := \frac{b_f t_f \frac{t_f}{2} + h_w \cdot t_w \left(\frac{h_w}{2} + t_f\right) + b_f t_f \left(t_f + h_w + \frac{t_f}{2}\right) + A_{aeff} \left(2 \cdot t_f + h_w + \frac{t_a}{2}\right) + A_{leff} \left(2 \cdot t_f + h_w + t_a + \frac{t_l}{2}\right)}{b_f t_f 2 + h_w \cdot t_w + A_{aeff} + A_{leff}}$$

$NA = 0.088\ m$

$y_{N.Auf} := -NA$	$y_{N.Auf} = -0.088\ m$

Effective moment of inertia:

$$I_{effflange} := 2 \cdot \frac{b_f t_f^3}{12} + b_f t_f \left(Na - \frac{t_f}{2}\right)^2 + b_f t_f \left(h_w + 2 \cdot t_f - \frac{t_f}{2} - Na\right)^2$$

$$I_{effweb} := \frac{t_w \cdot h_w^3}{12} + t_w \cdot h_w \left(Na - \frac{h_w + 2 \cdot t_f}{2}\right)^2$$

$$I_{effadhesive} := A_{aeff}\left(2 \cdot t_f + h_w + \frac{t_a}{2} - Na\right)^2$$

$$I_{efflaminate} := A_{leff}\left(2 \cdot t_f + h_w + t_a + \frac{t_l}{2} - Na\right)^2$$

$$I_{eff} := I_{effflange} + I_{effweb} + I_{effadhesive} + I_{efflaminate} \qquad I_{eff} = 2.507 \times 10^{-5}\ m^4$$

Yielding moment:

$$M_{yielding} := \frac{\sigma_{yielding} \cdot I_{eff}}{y_{N.Auf}} \qquad M_{yielding} = 93.498\ kN \cdot m$$

Yielding load:

$$P := \frac{2M_{yielding}}{L_p} \qquad P = 2.367 \times 10^5\ N$$

2.B Strengthened beam with laminate E=400 GPa

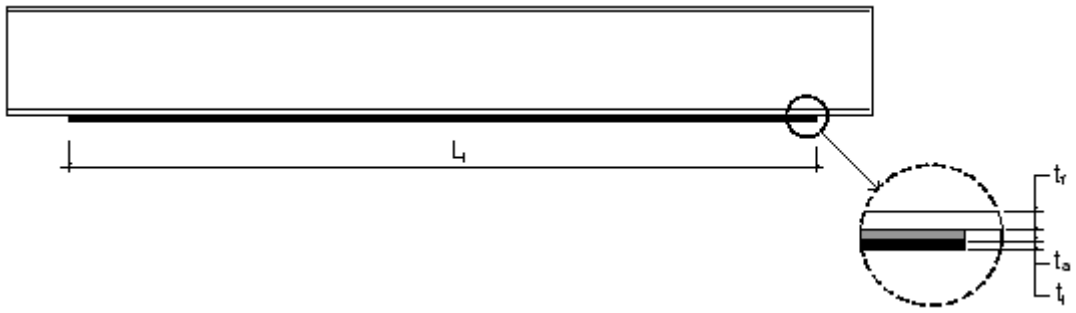

Figure J.6 Thickness of flange, adhesive, and laminate

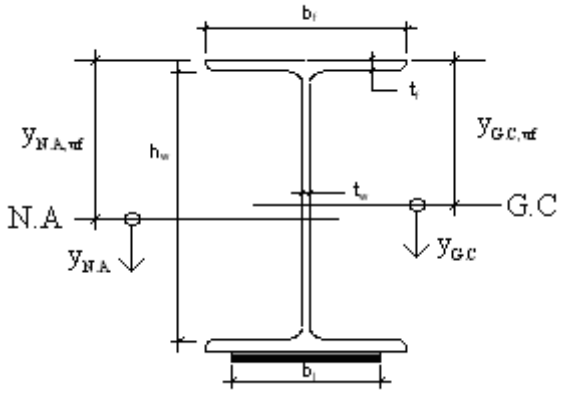

Figure J.7 Cross-section of strengthened beam

Steel beam	Adhesive	Laminate
$E_s := 212 \cdot 10^3 MPa$	$E_a := 7GPa$	$E_l := 400 \cdot 10^3 \cdot MPa$
$b_f := 180mm$	$ba := 80mm$	$b_l := 80mm$
$h_w := 152mm$	$t_a := 2mm$	$t_l := 2mm$
$t_f := 9.5mm$	$A_a := ba \cdot t_a$	$A_l := b_l \cdot t_l$
$t_w := 6mm$	$A_a = 1.6 \times 10^{-4}\ m^2$	$A_l = 1.6 \times 10^{-4}\ m^2$
$h = 0.171\ m$	$A_{aeff} := A_a \cdot \frac{E_{adh}}{E_s}$	$A_{leff} := A_l \cdot \frac{E_l}{E_s}$
$A_s := 2 \cdot (b_f t_f) + h_w \cdot t_w$	$A_{aeff} = 5.283 \times 10^{-6}\ m^2$	$A_{leff} = 3.019 \times 10^{-4}\ m^2$
$A_s = 4.332 \times 10^{-3}\ m^2$		
$I_s := \frac{t_w \cdot h_w^3}{12} + 2 \cdot b_f t_f \left(\frac{h_w}{2} + \frac{t_f}{2}\right)^2 + 2 \cdot b_f \frac{t_f^3}{12}$		$I_s = 2.408 \times 10^{-5}\ m^4$

Location of neutral axis:

$$N.A := \frac{b_f t_f \frac{t_f}{2} + h_w \cdot t_w \cdot \left(\frac{h_w}{2} + t_f\right) + b_f t_f \left(t_f + h_w + \frac{t_f}{2}\right) + A_{aeff} \cdot \left(2 \cdot t_f + h_w + \frac{t_a}{2}\right) + A_{leff} \left(2 \cdot t_f + h_w + t_a + \frac{t_l}{2}\right)}{b_f t_f 2 + h_w \cdot t_w + A_{aeff} + A_{leff}}$$

$N.A = 0.091\ m$

$y_{N.Auf} := -N.A$ $\quad y_{N.Auf} = -0.091\ m$

Effective moment of inertia:

$$I_{effflange} := 2\cdot\frac{b_f t_f^3}{12} + b_f t_f\left(Na - \frac{t_f}{2}\right)^2 + b_f t_f\left(h_w + 2\cdot t_f - \frac{t_f}{2} - Na\right)^2$$

$$I_{effweb} := \frac{t_w\cdot h_w^3}{12} + t_w\cdot h_w\cdot\left(Na - \frac{h_w + 2\cdot t_f}{2}\right)^2$$

$$I_{effadhesive} := A_{aeff}\cdot\left(2\cdot t_f + h_w + \frac{t_a}{2} - Na\right)^2$$

$$I_{efflaminate} := A_{leff}\cdot\left(2\cdot t_f + h_w + t_a + \frac{t_l}{2} - Na\right)^2$$

$$I_{eff} := I_{effflange} + I_{effweb} + I_{effadhesive} + I_{efflaminate}$$

$I_{eff} = 2.633\times 10^{-5}\ m^4$

Yielding moment:

$$M_{yielding} := \frac{\sigma_{yielding}\cdot I_{eff}}{y_{N.Auf}}$$ $\quad M_{yielding} = 94.665\ kN\cdot m$

Yielding load:

$$P := \frac{2M_{yielding}}{L_p}$$ $\quad P = 2.397\times 10^5\ N$

3.A Strengthened beam with prestressed laminate E=165 GPa

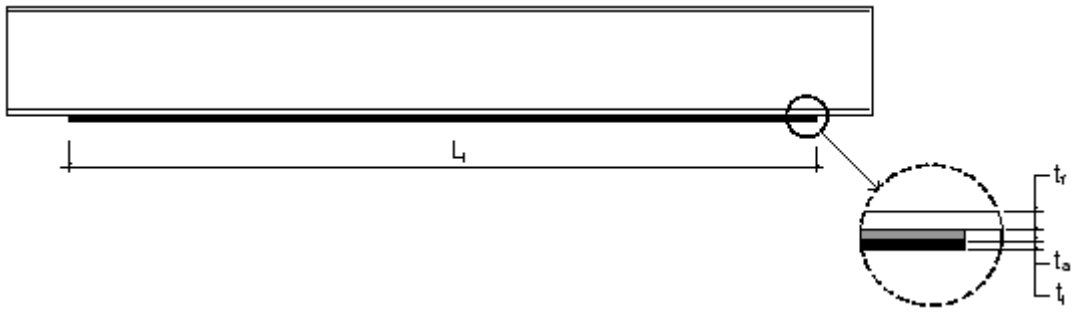

Figure J.8 Thickness of flange, adhesive, and laminate

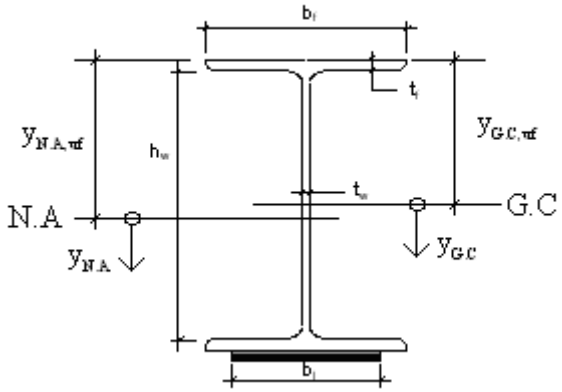

Figure J.9 Cross-section of strengthened beam

Prestressing force introduced to the beam:

P_l=240 kN

Eccentricity of the force:

$$e := \frac{2 \cdot t_f + h_w}{2} + t_a + \frac{t_l}{2} \qquad e = 0.089\ m$$

Steel beam	Adhesive	Laminate
$E_s := 212 \cdot 10^3 MPa$	$E_a := 7GPa$	$E_l := 165 \cdot 10^3 MPa$
$b_f := 180mm$	$b_a := 80mm$	$b_l := 80mm$
$h_w := 152mm$	$t_a := 2mm$	$t_l := 2mm$

$t_f := 9.5mm$ $A_a := ba \cdot t_a$ $A_1 := b_1 \cdot t_1$

$t_w := 6mm$ $A_a = 1.6 \times 10^{-4}\ m^2$ $A_1 = 1.6 \times 10^{-4}\ m^2$

$A_{aeff} := A_a \cdot \frac{E_{adh}}{E_s}$ $A_{1eff} := A_1 \cdot \frac{E_1}{E_s}$

$h = 0.171\ m$

$A_s := 2 \cdot (b_f t_f) + h_w \cdot t_w$ $A_{aeff} = 5.283 \times 10^{-6}\ m^2$ $A_{1eff} = 1.245 \times 10^{-4}\ m^2$

$A_s = 4.332 \times 10^{-3}\ m^2$

$$I_s := \frac{t_w \cdot h_w^3}{12} + 2 \cdot b_f t_f \left(\frac{h_w}{2} + \frac{t_f}{2}\right)^2 + 2 \cdot b_f \frac{t_f^3}{12} \qquad I_s = 2.408 \times 10^{-5}\ m^4$$

The location of the neutral axis:

$$N.A := \frac{b_f t_f \frac{t_f}{2} + h_w \cdot t_w \cdot \left(\frac{h_w}{2} + t_f\right) + b_f t_f \left(t_f + h_w + \frac{t_f}{2}\right) + A_{aeff} \cdot \left(2 \cdot t_f + h_w + \frac{t_a}{2}\right) + A_{1eff} \left(2 \cdot t_f + h_w + t_a + \frac{t_1}{2}\right)}{b_f t_f 2 + h_w \cdot t_w + A_{aeff} + A_{1eff}}$$

$N.A = 0.088\ m$

$y_{N.Auf} := -N.A$ $y_{N.Auf} = -0.088\ m$

Effective moment of inertia:

$$I_{effflange} := 2 \cdot \frac{b_f t_f^3}{12} + b_f t_f \left(Na - \frac{t_f}{2}\right)^2 + b_f t_f \left(h_w + 2 \cdot t_f - \frac{t_f}{2} - Na\right)^2$$

$$I_{effweb} := \frac{t_w \cdot h_w^3}{12} + t_w \cdot h_w \cdot \left(Na - \frac{h_w + 2 \cdot t_f}{2}\right)^2$$

$$I_{effadhesive} := A_{aeff} \cdot \left(2 \cdot t_f + h_w + \frac{t_a}{2} - Na\right)^2$$

$$I_{efflaminate} := A_{1eff} \cdot \left(2 \cdot t_f + h_w + t_a + \frac{t_1}{2} - Na\right)^2$$

$I_{eff} := I_{effflange} + I_{effweb} + I_{effadhesive} + I_{efflaminate}$ $I_{eff} = 2.507 \times 10^{-5}\ m^4$

Yielding moment:

$$M_{yielding} = N_p \cdot e \cdot \frac{y_{G.Cuf}}{y_{N.Auf}} \cdot \frac{I_{eff}}{I_s} + \frac{N_p \cdot I_{eff}}{A_s \cdot y_{N.Auf}} + \frac{\sigma_{yielding} \cdot I_{eff}}{y_{N.Auf}} \qquad M_{yielding} = 99.193\,kN \cdot m$$

Yielding load:

$$P_{yielding} := \frac{2M_{yielding}}{L_p} \qquad P_{yielding} = 251.121\,kN$$

3.B Strengthened beam with prestressed laminate E=400 GPa

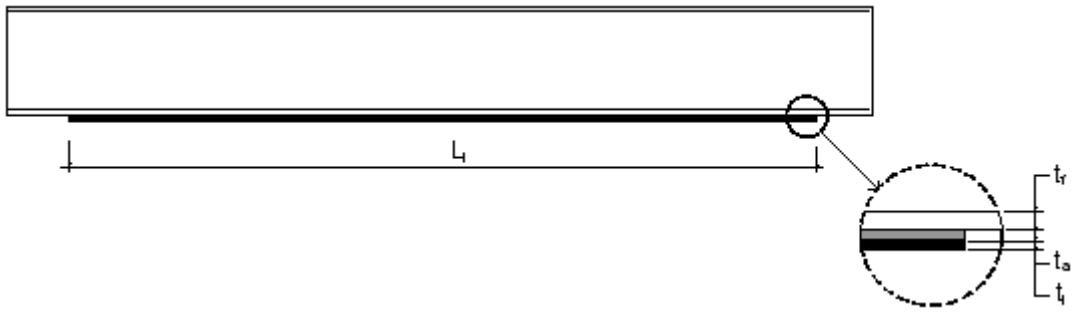

Figure J.10 Thickness of flange, adhesive, and laminate

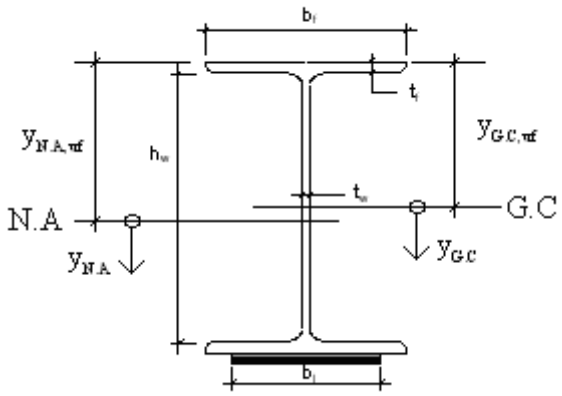

Figure J.11 Cross-section of strengthened beam

Prestressing force introduced into the beam:

N_p=80 kN

Eccentricity of the force:

$$e := \frac{2 \cdot t_f + h_w}{2} + t_a + \frac{t_1}{2} \qquad e = 0.089\ m$$

Steel beam	Adhesive	Laminate
$E_s := 212 \cdot 10^3 MPa$	$E_a := 7GPa$	$E_1 := 400 \cdot 10^3 \cdot MPa$
$b_f := 180mm$	$ba := 80mm$	$b_1 := 80mm$
$h_w := 152mm$	$t_a := 2mm$	$t_1 := 2mm$
$t_f := 9.5mm$	$A_a := ba \cdot t_a$	$A_1 := b_1 \cdot t_1$
$t_w := 6mm$	$A_a = 1.6 \times 10^{-4}\ m^2$	$A_1 = 1.6 \times 10^{-4}\ m^2$
$h = 0.171\ m$	$A_{aeff} := A_a \cdot \frac{E_{adh}}{E_s}$	$A_{1eff} := A_1 \cdot \frac{E_1}{E_s}$
$A_s := 2 \cdot (b_f t_f) + h_w \cdot t_w$	$A_{aeff} = 5.283 \times 10^{-6}\ m^2$	$A_{1eff} = 3.019 \times 10^{-4}\ m^2$

$$A_s = 4.332 \times 10^{-3}\ m^2$$

$$I_s := \frac{t_w \cdot h_w^3}{12} + 2 \cdot b_f t_f \left(\frac{h_w}{2} + \frac{t_f}{2} \right)^2 + 2 \cdot b_f \frac{t_f^3}{12}$$

$$I_s = 2.408 \times 10^{-5}\ m^4$$

Location of neutral axis:

$$NA := \frac{b_f t_f \frac{t_f}{2} + h_w \cdot t_w \cdot \left(\frac{h_w}{2} + t_f \right) + b_f t_f \left(t_f + h_w + \frac{t_f}{2} \right) + A_{aeff} \cdot \left(2 \cdot t_f + h_w + \frac{t_a}{2} \right) + A_{1eff} \left(2 \cdot t_f + h_w + t_a + \frac{t_1}{2} \right)}{b_f t_f 2 + h_w \cdot t_w + A_{aeff} + A_{1eff}}$$

$$N.A = 0.091\ m$$

$y_{N.Auf} := -N.A$ $\quad y_{N.Auf} = -0.091\ m$

Windows Media Player.lnk

Effective moment of inertia:

$$I_{effflange} := 2\cdot\frac{b_f t_f^{3}}{12} + b_f t_f\left(Na - \frac{t_f}{2}\right)^2 + b_f t_f\left(h_w + 2\cdot t_f - \frac{t_f}{2} - Na\right)^2$$

$$I_{effweb} := \frac{t_w\cdot h_w^{3}}{12} + t_w\cdot h_w\cdot\left(Na - \frac{h_w + 2\cdot t_f}{2}\right)^2$$

$$I_{effadhesive} := A_{aeff}\cdot\left(2\cdot t_f + h_w + \frac{t_a}{2} - Na\right)^2$$

$$I_{efflaminate} := A_{leff}\cdot\left(2\cdot t_f + h_w + t_a + \frac{t_l}{2} - Na\right)^2$$

$$I_{eff} := I_{effflange} + I_{effweb} + I_{effadhesive} + I_{efflaminate}$$

$$I_{eff} = 2.633\times 10^{-5}\ m^4$$

Yielding moment:

$$M_{yielding} = N_p\cdot e\cdot\frac{y_{G.Cuf}}{y_{N.Auf}}\cdot\frac{I_{eff}}{I_s} + \frac{N_p\cdot I_{eff}}{A_s\cdot y_{N.Auf}} + \frac{\sigma_{yielding}\cdot I_{eff}}{y_{N.Auf}} \qquad M_{yielding} = 96.587\ kN\cdot m$$

Yielding load:

$$P_{yielding} := \frac{2M_{yielding}}{L_p} \qquad P_{yielding} = 244.523\ kN$$